DOE/NE/32134-T1-Vol.3-Bk.2

NUS 5126
Rev. 1

FINAL SAFETY ANALYSIS REPORT FOR THE GALILEO MISSION

VOLUME III (BOOK 2) NUCLEAR RISK ANALYSIS DOCUMENT APPENDICES

January 25, 1989

GENERAL PURPOSE HEAT SOURCE
RADIOISOTOPE THERMOELECTRIC GENERATOR
PROGRAM
CONTRACT DE-AC01-87NE32134

Prepared for
U.S. Department of Energy

DISCLAIMER

DOE/NE/32134--T1-Vol.3-Bk.2

DE89 007273

FINAL SAFETY ANALYSIS REPORT FOR THE GALILEO MISSION

VOLUME III (BOOK 2) NUCLEAR RISK ANALYSIS DOCUMENT APPENDICES

January 25, 1989

GENERAL PURPOSE HEAT SOURCE RADIOISOTOPE THERMOELECTRIC GENERATOR PROGRAM CONTRACT DE-AC01-87NE32134

Prepared for
U.S. Department of Energy

NUS CORPORATION

TABLE OF CONTENTS

This Final Safety Analysis Report, Volume III, Nuclear Risk Analysis Document was prepared by NUS Corporation under Contract DE-AC01-87NE32134 with the U.S. Department of Energy.

When Government drawings, specifications, or other data are used for any purpose other than in connection with a definitely Government-related procurement, the United States Government incurs no responsibility or any obligation whatsoever. The fact that the Government may have formulated or in any way supplied the said drawings, specifications, or other data, is not to be regarded by implication, or otherwise in any manner construed, as licensing the holder, or any other person or corporation; or as conveying any rights or permission to manufacture, use, or sell any patented invention that may in any way be related thereto.

This report has been authored by a contractor of the United States Government. Accordingly, the United States Government retains a nonexclusive, royalty-free license to publish or reproduce the material contained herein, or allow others to do so, for the United States Government purposes.

APPENDIX A

RISK ASSESSMENT METHODOLOGY

A.1 INTRODUCTION

This appendix describes the methods used in evaluating the radiological consequences presented in FSAR, Volume III, Nuclear Risk Analysis Document (NRAD), Book I, based on the postulated accidents and associated probabilities and source terms described in FSAR, Volume II, Accident Model Document (AMD). Information is provided below on potential exposure pathways, measures of radiological consequence, and the approach taken to radiological consequence assessment.

A.1.1 Development of Accident Cases

Each mission phase is analyzed separately. This is because the location of an accident having a release is important to the type of accidents that are possible, the amount of release, and to the consequences of that release. Mission Phases 0 and 1, are on the launch pad or during early ascent in the Cape Canaveral area. Consequence analyses during these phases make use of meteorological, demographic, and land use data for the Kennedy Space Center (KSC) and environs. Phase 2 involves the possibility of a failure during later ascent with a reentry and impact along an African ground track. An accident during Phases 3 and 4 can result in a reentry anywhere within the 33° north to 33° south latitude bands. A Venus-Earth Earth Gravity Assist (VEEGA) failure could result in a reentry and impact anywhere on the Earth's surface. A worldwide data base has been used for the accident consequence analyses for mission Phases 3, 4, and 5. The specific data used for these analyses are contained in appendices C, E, F, and G of NRAD Book II.

The range of radiological accident consequences starts from zero since most occurrences of any accident considered would not result in a release of fuel. At the upper limit, any accident release with a probability associated with it less than one in ten million (10^{-7}) has been deemed to be not credible. This probability criterion defines a set of AMD source terms called maximum source terms in each mission phase for the accident scenarios considered in the phase.

A maximum consequence accident scenario is selected from the set of maximum source terms for each mission phase. The maximum consequence case may not be the same as the maximum source term case. For example, the maximum source term in mission Phase 1 occurs at 148,000 feet altitude, several miles down range, while the maximum consequence case is essentially on or near the launch pad. The lower altitude release and the proximity of people to the launch pad area cause the calculated consequences to be greater in the second instance. Radiation doses to people (collective dose) is the measure of consequence used to define the maximum consequence cases.

The AMD also provides average source terms for each accident scenario. This is the arithmetic average of all the analyses

for that scenario that have a source term. The average source term for the accident scenario having the highest probability of a release is designated as the most probable case (given a source term) for each mission phase.

Finally, the AMD quantifies a probability weighted source term, considering all the accident scenarios, for each mission phase. Mathematically, this case (called the expectation case) can be represented as:

$$<Q> = \frac{\sum_{i=1}^{n} P_i Q_i}{\sum_{i=1}^{n} P_i}$$

where:

<Q> = expectation source term

i = i^{th} accident scenario

n = number of scenarios in the mission phase

P_i = total probability of a source term for the i^{th} scenario

Q_i = average source term for the i^{th} scenario

The three cases just described, maximum, most probable, and expectation, are analyzed in this NRAD for each phase.

A.1.2 Measures of Radiological Consequences

The radiological hazards associated with 238-PuO_2 are described in Appendix B, Biomedical Aspects of 238-PuO_2. Measures of radiological consequences considered in the NRAD include population exposure to radiation (doses) and environmental contamination, as summarized in Figure A-1.

Consequences have been quantified in terms of radiation doses to persons, and in areas of ground deposition relating to EPA and DOE dose criteria for radioactive materials in the environment, intended to protect the general population. Radiation dose results are expressed as the numbers of persons receiving doses above selected dose levels and as total population dose, also known as collective dose to the exposed population.

Doses to individuals are expressed in units of rem or millirem (mrem) committed effective dose equivalent. This dose is constructed by calculating doses to the affected body organs and

POPULATION EXPOSURE	ENVIRONMENTAL CONTAMINATION
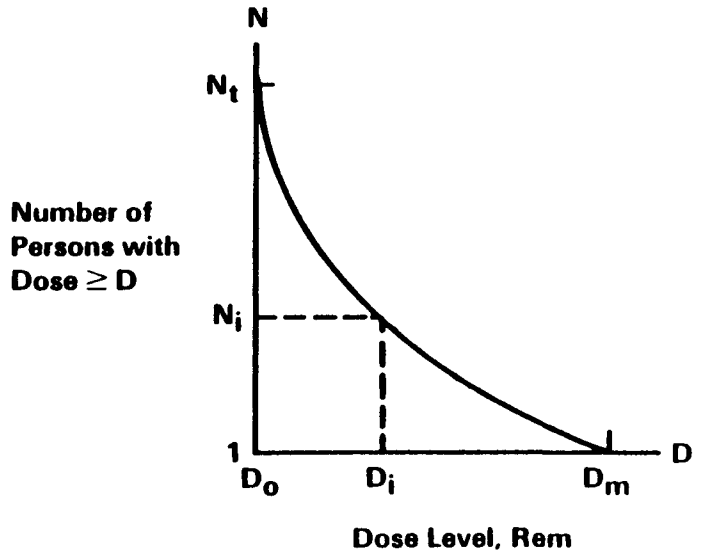	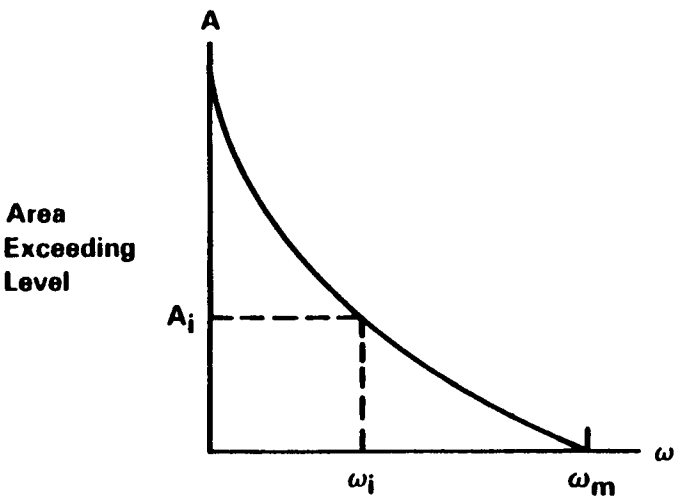
• Maximum Individual Dose, D_m • De Minimis Dose, D_o • Number of Persons, N_i, with Dose $\geq D_i$ • Total Population Dose $PD = \int_{D_o}^{D_m} NdN$ • Population Health Effects $H = k \times PD$	• Surface Area, A_i, with Levels $\geq \omega_i$ — Dry Land — Swamp — Inland Water — Ocean

Figure A-1
MEASURES OF RADIOLOGICAL CONSEQUENCES

combining those organ doses with weighting factors which reflect their individual susceptibility to cancer induction by radiation.

The word "committed" means that dose delivered by the radioactive material taken into the body is accounted for over the period of its residence in the body. The commitment period is taken to be 70 years. The 70-year dose commitment period has been used to account for the age span of the population and because the internal dosimetry model used in the analysis is not age dependent.

Two periods of time are accounted for in terms of exposure period. The first period of time is that during which radioactive material is being dispersed by winds immediately after the accident. The dose from this exposure can be avoided simply by getting out of the way of the down wind directions of the release. It can be reduced by sheltering during cloud passage. This has been termed the "short-term" dose. The population groups accounted for in the calculation of short-term dose include onsite workers, spectators, and offsite residential population.

The second period of time is that following cloud passage and it accounts for dose delivered to those offsite Kennedy Space Center (KSC) and worldwide populations by means of atmospheric resuspension of material deposited from the initial cloud passage and for dose delivered through food pathways (vegetables and seafood) and by external radiation. This is called an "environmental dose commitment" and it accounts for the continuing exposure to the radioactive material if it is left in the environment over long periods of time. The environmental dose commitment period is also taken as 70 years. This has been termed the "long term" dose. It can be reduced by cleaning up heavily contaminated areas, if any, by restrictions on consumption of contaminated food, or by other administrative controls. The rate of delivery of dose is greatest during the first two years following an accident, so administrative controls can be effective. In addition to the general population, long term doses are calculated to KSC workers due to inhalation of resuspended material, assuming an exposure period of 35 years based on a 40 hour work week.

The summation of all doses to exposed individuals is called the collective dose, and has units of person-rem. This collective dose can be converted to a calculated incidence of fatal cancers over the lifetime of the exposed population using the linear dose response hypothesis. A health effects estimator of 1.85×10^{-4} excess cancer fatality per person-rem has been used in this calculation. The bases for this health effects estimator are discussed in Appendix B.

For the purpose of calculating fatal cancers from collective dose, the recommendations of NCRP Report No. 91 regarding a

"Negligible Individual Risk Level" (NIRL) of 1 x 10^{-7} annual risk, corresponding to a dose rate of one millirem per year, have been followed (Reference A-1). The recommendation is that doses below one millirem per year should be excluded from assessments of collective dose since they imply negligible risk. This has also been called a de minimis dose, adopted from a legal term referring to "trifling matters." Related to a de minimis dose level as applied in the FSAR in calculating health effects is a dose level "below regulatory concern", below which no regulatory action would be deemed appropriate. NRC and DOE are considering proposed dose levels "below regulatory concern" in the range of 1 to 10 mrem/yr.

If an accident occurs that releases RTG fuel, deposition of that material on the ground will eventually occur since its physical form is particles. This deposition can be a source of continuing impact to people, as quantified by the long term dose.

EPA has under development, and DOE has criteria which relate to the possibility of limiting this impact (References A-2 through A-4). The object is to ensure that administrative controls on land use are not required over periods of time in order to limit individual risk when they cannot be assured. The basic dose limit for individuals in the general population is an annual dose commitment of 100 mrem. This is supplemented with a general policy that all radiation exposures should be limited to levels that are as low as reasonably achievable (ALARA). This implies that when annual dose commitments are as high as 100 mrem, some remedial action might be indicated. A level of 25 mrem per year has been selected to correspond to a level characterized as ALARA, based on DOE FUSRAP (Formerly Utilized Sites Remedial Action Program) experience (Reference A-4).

Results relating to ground deposition issues are displayed in tables showing areas within which annual radiation dose commitments might exceed 100 mrem, 25 mrem, and 10 mrem. Also shown is the area outside of which deposition density is less than a 0.2 $\mu Ci/m^2$ screening level. This is a level below which EPA has proposed as appropriate for unrestricted use with no requirement for continuing surveillance.

In summary, each of the mission phases are analyzed for accidents characterized as maximum, most probable and expectation (probability weighted). Analyses results are expressed in terms of radiation dose commitments at various reference dose levels to persons (number of people exceeding reference levels) and to populations (collective dose) for both the initial accident exposure (short term dose) and extended exposure to material in the environment (long term dose). For the expectation case, these doses are converted to numbers of potential fatal cancers over the lifetimes of the exposed population. This number is used to quantify risk, defined as the product of probability and consequence. Average individual

risk and the number of potential fatal cancers can then be compared to bench marks such as other societal risks, including total cancer rate in the general population.

A.1.3 Radiological Consequence Assessment Approach

The evaluation of the radiological consequences of fuel release to the environment for a postulated accident includes the following steps:

1. Identification of the postulated accident, fuel release probability, and release location.

2. Source term characterization in terms of quantity, particle size distribution, and volume distribution.

3. Analysis of the dispersion of the released fuel in the environment to determine concentrations in environmental media (air, soil, and water) as functions of time and space.

4. Analysis of the interaction of environmental radioactive concentrations and people through inhalation, ingestion, and external exposure pathways.

5. Evaluation of resulting radiological consequences in terms of population doses and contaminated environmental media.

The implementation in the NRAD of the radiological consequence and risk analysis outlined above is shown diagrammatically in Figure A-2.

The information developed in FSAR, Volume II related to accident scenarios and associated source terms and probabilities, represented by the Failure Abort/Sequence Trees (FASTs), is used as initial input to the radiological consequence and risk analysis. These inputs are in terms of the most probable, maximum, and expectation release cases as identified in NRAD, Book I.

For each mission phase the radiological consequences were calculated for each release case type using the KSC-EMERGE, LOPAR, and HIPAR computer models. Releases in the troposphere were treated using KSC-EMERGE. High altitude releases were treated using LOPAR (for particles less than 10 microns in diameter) and HIPAR (for particles greater than 10 microns in diameter). The results for the maximum and most probable release cases identify specific accident scenarios, while the results for the expectation cases are used in the calculation of risk.

The remainder of this appendix summarizes the methods utilized to implement the above steps. Section 2.0 Volume III, Book 1,

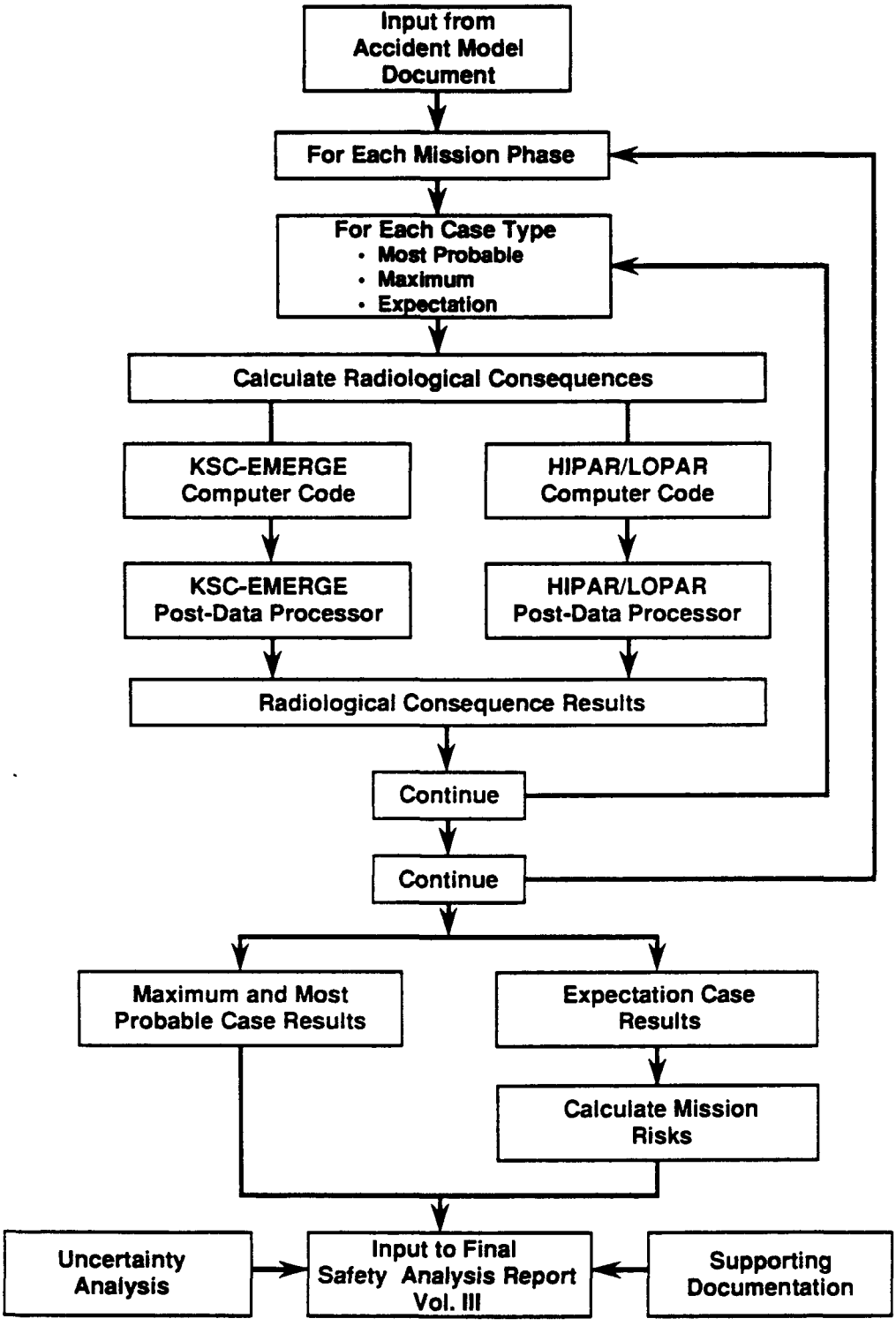

Figure A-2
INTEGRATED RISK ASSESSMENT METHODOLOGY

describes how the information developed in FSAR, Volume II is used in establishing the inputs to the radiological consequence analysis as included in Steps 1 and 2 above. Section A.2 of this appendix describes the environmental dispersion models used to evaluate radioactive concentrations in time and space, and interactions with population through exposure pathways, as included in Steps 3 and 4. Section A.3 of this appendix reviews the internal dosimetry model that relates population exposure to radiological consequences in terms of total body burden and dose. Finally, Section A.4 describes the model used in establishing the plume configuration for launch pad area releases.

A.2 ATMOSPHERIC DISPERSION MODELS

The radiological consequences of fuel released to the atmosphere have been evaluated using models appropriate to the regimes of release altitude and particle size range characteristic of the release scenario. These models include KSC-EMERGE, HIPAR, and LOPAR whose basic characteristics and regimes of applicability are summarized in Table A-1 and Figure A-3. Additional information on key features of these models relevant to the NRAD analyses is presented below.

A.2.1 KSC-EMERGE

A.2.1.1 KSC-EMERGE Model Features

The KSC-EMERGE model utilizes a three-dimensional, variable trajectory, Gaussian puff model to simulate atmospheric transport and diffusion (References A-5 and A-7). The model accounts for time-varying meteorological conditions (in 15-minute time steps) and variations in meteorological conditions with altitude. Atmospheric transport and diffusion of a given release is modeled by EMERGE by first developing a three-dimensional wind field based on the input meteorological data. The initial source term, particle size distributions, and vertical plume configurations are modeled by a series of Gaussian puff releases that are tracked individually in time and space. Particle-size-dependent deposition and source depletion are modeled, with the deposition rate determined by the gravitational settling velocities of the particles along with turbulent diffusion due to puff growth.

The presence of a sea-breeze recirculation cell, shown schematically in Figure A-4, could significantly affect the radiological consequences, depending on the point of release. A release within the thermal internal boundary layer (TIBL) would be expected to be recirculated by the return flow field. A release in the stable inflow layer would be expected to be mixed rapidly down to ground level should the release intersect the TIBL, resulting in so-called fumigation conditions and leading to high ground concentrations.

Table A-1

Summary Description of Atmospheric Dispersion Models

Description	KSC-EMERGE	HIPAR	LOPAR
1. Purpose	Calculates radiological consequences from atmospheric releases of Pu-238 oxide particulates near the launch pad during mission Phases 0 and 1 within the troposhere.	Calculates trajectories and ground concentrations of particulates (greater than 10 microns) released at high altitude.	Calculates time-integrated air and ground concentrations of vapor and small particles (less than or equal to 10 microns) released at high altitude
2. Developer	NUS Corporation	NUS Corporation (Modification of Travelers Research Corporation Model B).	NUS Corporation (based on weapons fallout data)
3. References	A-5, A-6	A-7	A-7
4. Inputs			
a. Source characterization	For each source (up to 4): total quantity (Curies), particle size distribution, particle density, release height, and cloud dimensions.	Total quantity (Curies), particle size distribution, particle density, release height, and release latitude and longitude.	Total quantity (Curies) and release latitude
b. Meteorological conditions	Accounts for time and space (vertical) variation in meteorological conditions including sea-breeze recirculation. Uses a 24-hour sequence of historical meteorological data for each run.	Vertical profile of wind speed and direction as functions of altitude latitude and longitude.	Redistribution of material as a function of release latitude based on weapons fallout data, as determined by global atmospheric circulation patterns

Table A-1 (continued)

Summary Description of Atmospheric Dispersion Models

Description	KSC-EMERGE	HIPAR	LOPAR
5. Method of calculation	Gaussian puff-trajectory model that accounts for time and space varying meteorological conditions; and particle-size-dependent transport, deposition, plume depletion, resuspension and internal dosimetry. Exposure pathways include inhalation, ingestion (vegetables and sea food) and external. A polar coordinate receptor grid out to 100 kilometers is used in the calculations. Outputs include number of persons versus dose distribution, population dose, and areas of surface-types (dry land, swamp, inland water, and ocean) exceeding specified contamination levels.	Trajectories of mass elements are determined on the rate of change of latitude, longitude, and altitude using local wind speed components and the particle terminal fall velocities. Based on the release altitude, latitude, and longitude the model predicts ground concentration as a function of affected area.	The redistribution of material into each latitude band as a function of release latitude based on weapon fallout data as determined by global atmospheric circulation pattern. Calculates resulting time integrated air and ground concentrations.

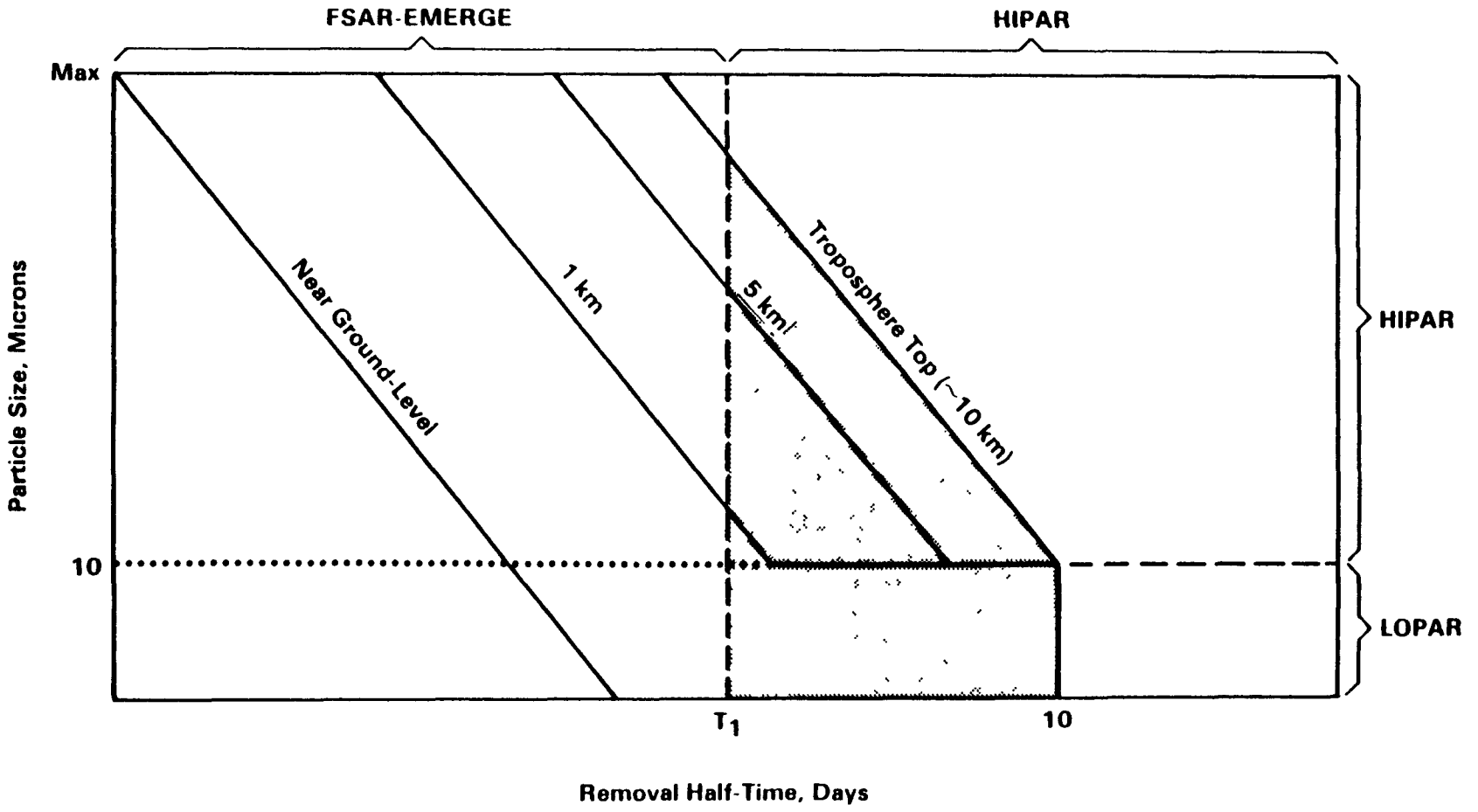

T_1 — Time required to transport beyond 100 km FSAR-EMERGE grid.

□ — Material released within troposphere transported outside 100 km FSAR-EMERGE grid.

Figure A-3
MODEL REGIMES OF APPLICABILITY

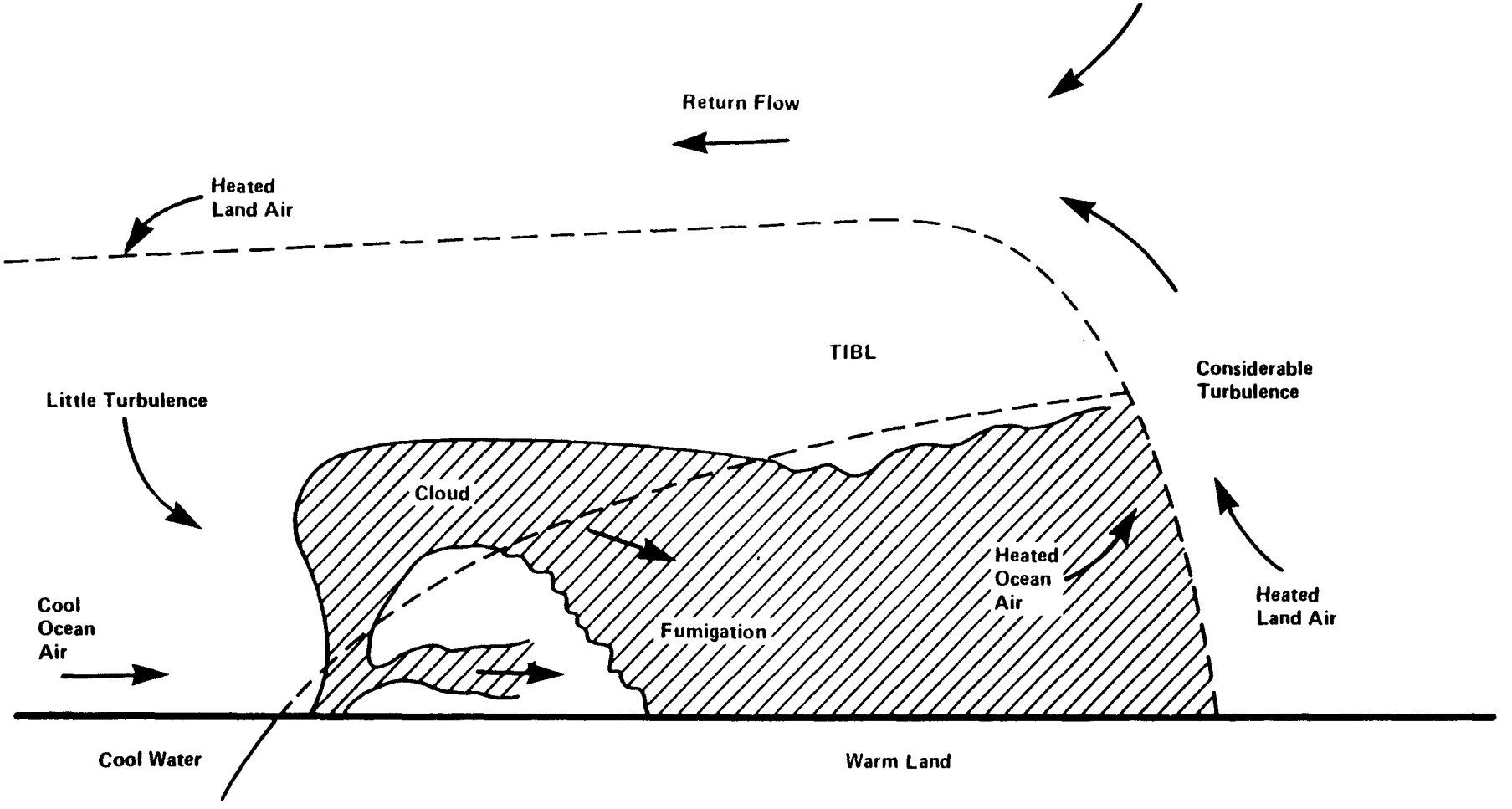

Figure A-4
SEA-BREEZE CIRCULATION AND FUMIGATION CONDITIONS

In order to account for these conditions, KSC-EMERGE models coastal circulations by simulating TIBL growth, wind flow recirculation aloft, and the time- and space-variations of the sea/land-breeze frontal positions. The presence of a sea/land breeze recirculation are detected by KSC-EMERGE through an algorithm that uses input data on ocean temperature, land temperature, and vertical variation in winds. The wind field, including that associated with a sea breeze recirculation cell, is modeled using the grid shown in Figure A-5. The lower grid extends from the surface to a height of 800 meters and is divided into eight (8) 100 meter high cells. The gradient wind/return flow layer extends from 800 meters to a user-defined level. A maximum of five (5) user-defined upper wind layers can also be utilized.

In performing the calculations of dose and deposition, KSC-EMERGE uses a basic polar receptor grid extending to a radius of 100 km with 8960 receptor locations (56 concentric rings with 160 equidistance receptors per ring). This receptor grid interfaces with the population grid and surface type (dry land, inland water, swamp, and ocean) grid presented in Appendix E.

Releases are modeled by KSC-EMERGE using up to four initial source terms to simulate the vertical plume configuration by the superposition of Gaussian puffs. In addition, each source term is independently defined by the position of its center-of-mass, an initial size in the horizontal and vertical directions, a total activity, and up to 15 particle size groups representing a particle size distribution which is defined by the fraction of the source term in each size range. This results in KSC-EMERGE independently tracking 4 sources times 15 particle size groups, or 60 puffs in time and space.

The output of KSC-EMERGE is provided in tabular and graphic forms, both showing radiation dose and surface contamination levels. The radiological consequences calculated by KSC-EMERGE correspond to the measures of short- and long-term doses and surface contamination as identified in Section A.1.2. Particle-size-dependent internal dose conversion factors developed in accordance with the internal dosimetry model described in Section A.3 are utilized.

The EMERGE model has been evaluated against four other atmospheric dispersion models for selected release cases. The models used in the comparison included the NUS Corporation ATMOS model (Reference A-7), the Savannah River Laboratory PFPL model (Reference A-8), the Sandia National Laboratory DIFOUT model (Reference A-9), and the Lawrence Livermore National Laboratory ARAC MATHEW/ADPIC model (References A-10 and A-11). The results of this comparison, presented in Reference A-12, indicated reasonably good agreement among the models, and any differences in results were explainable.

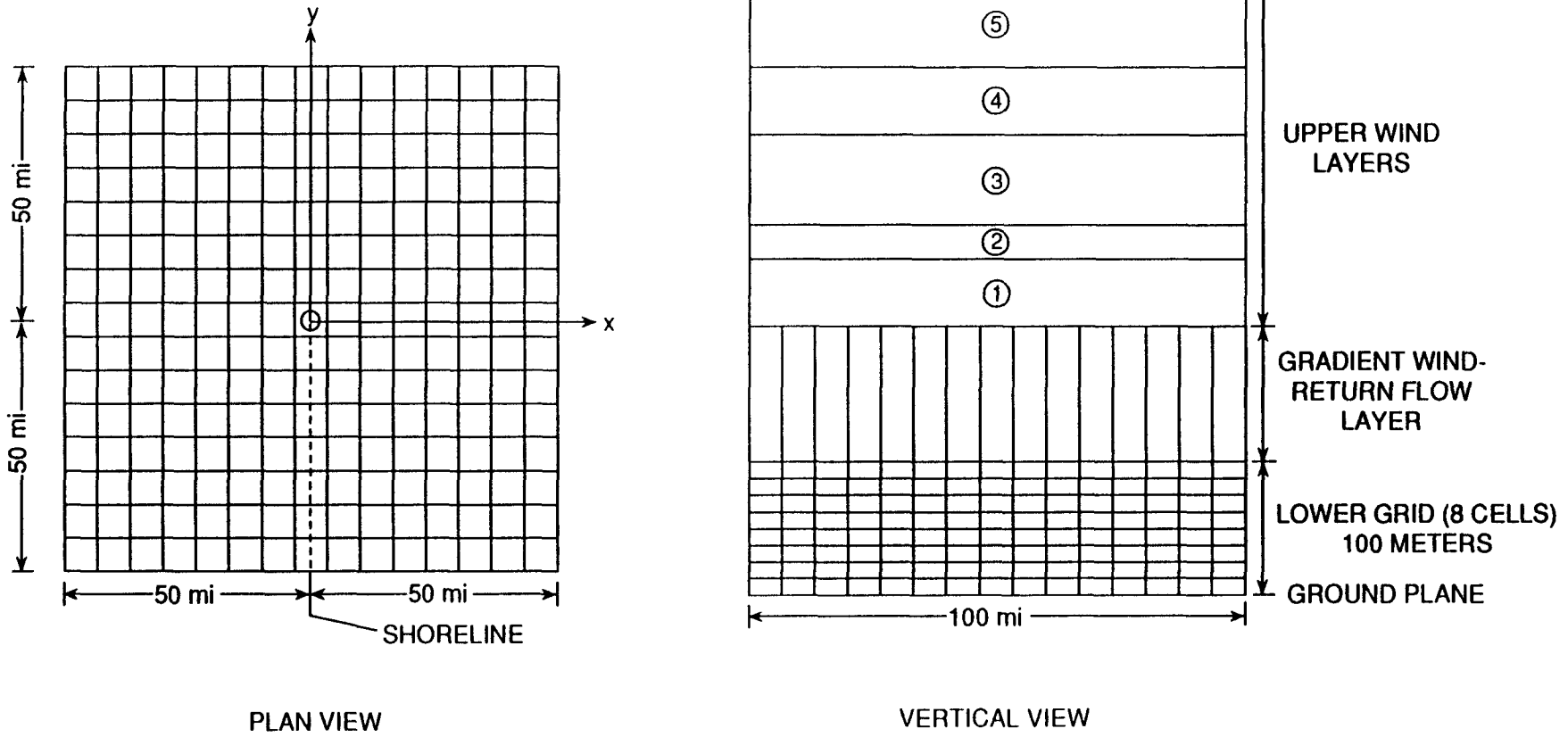

Figure A-5
EMERGE WIND FLOW-STABILITY GRID

A.2.1.2 Application of KSC-EMERGE

The KSC-EMERGE model was used in the NRAD risk analysis to evaluate radiological consequences of PuO_2 releases in the troposhere, including elevated and/or ground level releases near the launch pad in Phases 0 and 1, and ground level releases at worldwide locations in Phases 2 through 5.

In applying KSC-EMERGE to releases in Phase 0 and 1, historical meteorological data were reviewed and 42 sets of 24-hour historical meteorological data sequences were selected as being representative of the 50-day launch window during October-November, shown in Figure A-6. The selection of the 42 data sequences was such that the launch window was uniformly sampled by hour and by day over the entire 50 day launch window. Each 24-hour data sequence was selected to cover the period from T-8 hours prior to launch on a given day to T+16 hours following launch, with T-0 centered on the launch window time cutoffs for that day. (Details on the meteorological conditions prevailing during the October-November launch window at KSC as well as the meteorological data sources are presented in Appendix C, KSC Meteorology.)

The expectation case source term for each of Phases 0 and 1 was modeled using KSC-EMERGE and each of the 42 sequential data sets (i.e., 42 KSC-EMERGE runs for each expectation case). In all runs, the most probable vertical plume configuration was used (See Section A.4). Each run consisted of KSC-EMERGE processing the 24-hour sequential data set in 15-minute time steps, using the data from T-8 hours to T-0 to determine whether a sea/land breeze recirculation cell exists. The release occurs at T-0, with time-varying meteorological conditions updated every 15-minute time step until T+16 hours, thus affecting atmospheric transport and dispersion of the release in a time-varying manner. The results of these runs for Phases 0 and 1 are presented in Tables A-2 and A-3, respectively. These results represent the distribution of radiological consequences for a fixed source term and vertical plume configuration due to variations in meteorological conditions.

The radiological consequences for the expectation cases (in Phases 0 and 1) were then determined from the average of the result for the 42 runs. The radiological consequences for the most probable cases (in Phases 0 and 1) were calculated using the most probable vertical plume configuration, and that sequential data set corresponding to a 50th percentile condition (50 percent of the 42 cases yielded higher results). The radiological consequences for the maximum cases were calculated using a lower, tighter vertical plume configuration (see Section A.4) and that sequential data set (of the 42 sets) which maximized the radiological consequences.

Accidents involving the GPHS-RTGs in Phases 2, 3, 4, and 5 can lead to rock impacts of Aeroshell modules (Phases 2, 3, and 4)

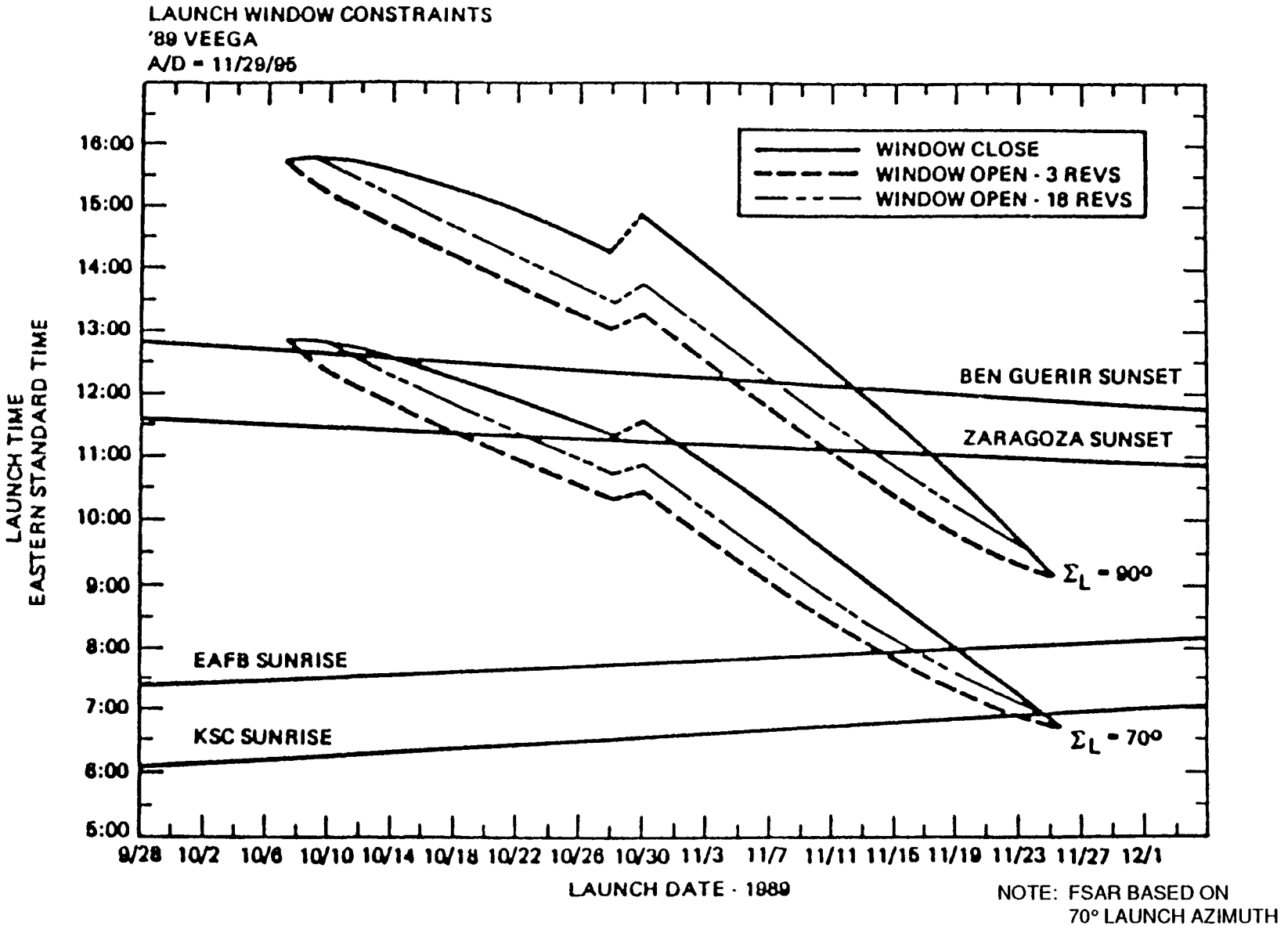

Figure A-6
GALILEO LAUNCH WINDOW VS. LAUNCH DATE

Table A-2 (Page 1 of 2)
SUMMARY OF SELECTED DATA FOR ALL PHASE 0 EXPECTATION CASES

**	1	2	3	4	5	6	7	8	9	10	11	12
1	2.11E-04	5.46E-07	4.84E+00	4.21E+01	0.00E+00	0.00E+00	1.42E+01	1.54E+00	4.72E+00	0.00E+00	4.69E+01	0.00E+00
2	7.01E-04	1.35E-03	5.63E+00	3.96E+01	0.00E+00	0.00E+00	7.50E+00	9.64E-01	4.37E+00	0.00E+00	4.52E+01	0.00E+00
4	3.11E-04	3.92E-03	3.66E+00	7.86E+01	0.00E+00	0.00E+00	2.59E+00	7.04E+00	1.21E+00	4.27E+01	0.00E+00	
6	1.99E-04	3.62E-03	1.31E+00	2.47E+01	0.00E+00	0.00E+00	1.71E+01	2.00E+00	5.77E+00	0.00E+00	2.60E+01	0.00E+00
7	3.11E-04	2.80E-05	3.98E-01	3.94E-01	0.00E+00	0.00E+00	5.15E+00	1.46E+00	4.09E+00	6.99E+00	7.92E-01	0.00E+00
8	0.00E+00	0.00E+00	0.00E+00	1.50E-05	0.00E+00	0.00E+00	2.45E-02	0.00E+00	0.00E+00	1.37E+00	1.50E-05	0.00E+00
10	1.69E-04	8.46E-06	1.84E-01	2.45E-02	0.00E+00	0.00E+00	6.76E+00	1.54E+00	3.88E+00	1.71E+00	2.08E-01	0.00E+00
11	5.67E-04	4.14E-03	7.02E+00	1.87E+01	0.00E+00	0.00E+00	6.15E+00	5.45E-01	2.03E+00	0.00E+00	2.53E+01	0.00E+00
12	2.33E-04	7.19E-03	3.64E+00	6.41E+01	0.00E+00	0.00E+00	9.31E+00	4.87E-01	3.13E+00	0.00E+00	6.77E+01	0.00E+00
13	2.60E-04	1.95E-03	2.34E+00	3.97E+01	0.00E+00	0.00E+00	7.46E+00	6.19E-02	3.14E+00	2.96E+00	4.20E+01	0.00E+00
15	6.40E-05	1.48E-03	5.57E-01	4.76E+00	0.00E+00	0.00E+00	4.42E+00	0.00E+00	1.35E+00	1.04E+00	5.31E+00	0.00E+00
16	7.51E-04	2.62E-03	2.80E+00	2.96E+01	0.00E+00	0.00E+00	6.08E+00	1.03E+00	3.91E+00	0.00E+00	3.24E+01	0.00E+00
17	2.74E-04	2.77E-03	1.65E+00	4.61E+01	0.00E+00	0.00E+00	1.44E+01	4.12E-02	3.76E+00	0.00E+00	4.78E+01	0.00E+00
18	1.59E-04	7.53E-04	1.44E+00	7.17E+00	0.00E+00	0.00E+00	9.68E+00	2.61E+00	7.10E+00	8.72E+00	8.61E+00	0.00E+00
19	2.15E-04	4.87E-03	1.49E+00	1.97E+01	0.00E+00	0.00E+00	8.11E+00	2.53E+00	4.14E+00	0.00E+00	2.12E+01	0.00E+00
20	2.20E-04	3.52E-04	3.85E+00	3.87E+00	0.00E+00	0.00E+00	5.07E+00	1.57E+00	4.76E+00	1.40E+00	7.72E+00	0.00E+00
22	2.46E-04	2.74E-03	2.01E+00	2.52E+01	0.00E+00	0.00E+00	6.96E+00	1.23E+00	4.45E+00	0.00E+00	2.73E+01	0.00E+00
23	5.23E-04	1.50E-03	6.30E+00	3.84E+01	0.00E+00	0.00E+00	6.37E+00	9.28E-02	2.62E+00	9.33E+00	4.47E+01	0.00E+00
24	3.49E-04	1.97E-03	2.65E+00	2.58E+01	0.00E+00	0.00E+00	9.06E+00	1.48E-01	2.79E+00	1.67E+00	2.84E+01	0.00E+00
25	2.81E-04	5.49E-03	2.75E+00	2.60E+01	0.00E+00	0.00E+00	1.01E+01	1.68E+00	4.47E+00	0.00E+00	2.88E+01	0.00E+00
26	3.84E-04	1.10E-03	1.31E+00	1.34E+01	0.00E+00	0.00E+00	7.51E+00	6.19E-02	2.67E+00	2.21E+00	1.47E+01	0.00E+00
27	3.87E-04	6.42E-03	4.21E+00	2.51E+01	0.00E+00	0.00E+00	5.14E+00	1.53E+00	5.24E+00	4.29E+00	2.93E+01	0.00E+00
28	9.52E-08	3.13E-07	3.34E-04	1.13E-03	0.00E+00	0.00E+00	7.36E-02	0.00E+00	0.00E+00	1.46E+00	1.46E-03	0.00E+00
30	1.68E-04	2.53E-04	9.80E-01	2.81E+00	0.00E+00	0.00E+00	6.45E+00	1.80E+00	5.03E+00	2.72E+00	3.79E+00	0.00E+00
31	1.49E-04	2.27E-05	4.43E-02	1.79E-02	0.00E+00	0.00E+00	6.20E+00	1.17E+00	3.26E+00	1.82E+00	6.22E-02	0.00E+00
32	2.26E-04	2.76E-03	2.68E+00	3.53E+01	0.00E+00	0.00E+00	7.63E+00	2.49E+00	7.53E+00	0.00E+00	3.80E+01	0.00E+00
33	2.33E-04	4.71E-03	2.55E+00	4.83E+01	0.00E+00	0.00E+00	7.43E+00	1.46E+00	5.24E+00	0.00E+00	5.08E+01	0.00E+00
34	2.40E-04	2.48E-03	2.32E+00	3.21E+01	0.00E+00	0.00E+00	5.17E+00	1.14E+00	4.47E+00	0.00E+00	3.44E+01	0.00E+00
35	7.25E-04	5.41E-03	7.72E+00	8.16E+01	0.00E+00	0.00E+00	3.30E+00	2.27E-01	2.49E+00	0.00E+00	8.93E+01	0.00E+00
36	1.75E-04	3.84E-03	1.65E+00	3.38E+01	0.00E+00	0.00E+00	1.25E+01	1.63E+00	4.57E+00	0.00E+00	3.55E+01	0.00E+00
38	1.00E-05	3.76E-05	1.11E-01	7.69E-01	0.00E+00	0.00E+00	2.96E-01	0.00E+00	4.91E+00	1.67E+00	8.80E-01	0.00E+00
39	4.55E-04	5.17E-04	3.52E+00	8.24E+00	0.00E+00	0.00E+00	2.87E+00	1.93E+00	3.95E+00	6.73E+00	1.18E+01	0.00E+00
40	1.63E-04	4.12E-04	2.41E+00	5.92E+00	0.00E+00	0.00E+00	7.24E+00	2.07E+00	6.05E+00	1.36E+00	8.33E+00	0.00E+00
41	1.23E-03	1.06E-05	5.23E-02	1.05E-01	0.00E+00	0.00E+00	1.61E+00	0.00E+00	5.30E+00	1.65E+00	1.57E-01	0.00E+00
42	1.17E-04	7.77E-04	7.67E-01	8.10E+00	0.00E+00	0.00E+00	1.12E+01	0.00E+00	7.20E+00	1.73E+00	8.46E+00	0.00E+00
43	2.11E-04	2.61E-04	5.90E-01	1.84E+00	0.00E+00	0.00E+00	2.66E+00	0.00E+00	5.57E+00	8.46E+00	2.43E+00	0.00E+00
44	2.76E-04	1.98E-03	3.66E+00	4.12E+01	0.00E+00	0.00E+00	4.51E+00	2.23E+00	6.77E+00	4.05E+00	4.49E+01	0.00E+00
45	2.66E-04	2.99E-05	3.67E-01	2.23E-01	0.00E+00	0.00E+00	3.22E+00	1.05E+00	3.18E+00	1.33E+00	5.90E-01	0.00E+00
46	1.76E-04	3.99E-03	1.81E+00	3.70E+01	0.00E+00	0.00E+00	8.51E+00	2.79E+00	4.35E+00	0.00E+00	3.88E+01	0.00E+00
47	2.12E-04	2.38E-03	3.00E+00	2.84E+01	0.00E+00	0.00E+00	6.22E+00	1.64E+00	6.28E+00	0.00E+00	3.14E+01	0.00E+00
49	1.62E-04	4.78E-03	1.99E+00	6.60E+01	0.00E+00	0.00E+00	1.63E+01	2.92E+00	8.32E+00	0.00E+00	6.80E+01	0.00E+00
50	3.32E-04	2.26E-03	3.15E+00	3.74E+01	0.00E+00	0.00E+00	5.55E+00	1.74E+00	6.31E+00	0.00E+00	4.05E+01	0.00E+00
no.	4.20E+01	4.20E+01	4.20E+01	4.20E+01	4.20E+01	4.20E+01	4.20E+01	4.20E+01	4.20E+01	4.20E+01	4.20E+01	4.20E+01
avg	2.74E-04	2.20E-03	2.35E+00	2.39E+01	0.00E+00	0.00E+00	6.97E+00	1.16E+00	4.43E+00	1.80E+00	2.62E+01	0.00E+00
std	2.07E-04	1.91E-03	1.97E+00	2.07E+01	0.00E+00	0.00E+00	3.96E+00	9.15E-01	1.86E+00	2.60E+00	2.20E+01	0.00E+00
min	0.00E+00	0.00E+00	0.00E+00	1.50E-05	0.00E+00	0.00E+00	2.45E-02	0.00E+00	0.00E+00	0.00E+00	1.50E-05	0.00E+00
max	1.27E-03	6.42E-03	7.72E+00	8.16E+01	0.00E+00	0.00E+00	1.71E+01	2.92E+00	8.32E+00	9.37E+00	8.93E+01	0.00E+00
at	41	27	35	35	1	1	6	49	49	27	35	1

Maximum Individual Dose, rem
- Column 1 - Short Term
- Column 2 - Long Term

Population Dose, person-rem
- Column 3 - Short Term (w/o D1 Minimus)
- Column 4 - Long Term (w/o D1 Minimus)
- Column 5 - Short Term (w D1 Minimus)
- Column 6 - Long Term (w D1 Minimus)

Area Exceeding Surface Contamination of 0.2 uCi/m2, km2
- Column 7 - on Dry Land
- Column 8 - on Swamp
- Column 9 - on Inland Water
- Column 10 - on Ocean

Total Population Dose, person-rem
- Column 11 - Short and Long Term (w/o D1 Minimus)
- Column 12 - Short and Long Term (w D1 Minimus)

Total Population Dose by Population Groups, person-rem
- Column 13 - Workers (w/o D1 Minimus)
- Column 14 - Spectators (w/o D1 Minimus)
- Column 15 - Residents (w/o D1 Minimus)

Total Population Dose Fraction to Each Pathway
- Column 16 - Direct Inhalation by Workers
- Column 17 - Re-Suspension by Workers
- Column 18 - Direct Inhalation by Residents
- Column 19 - Re-Suspension by Residents
- Column 20 - Vegetable Consumption by Residents
- Column 21 - Seafood Consumption by Residents

Dry Land Area Exceeding Long Term Dose of 25 mrem, km2
- Column 22 - On-Site 0-70 year Time Interval
- Column 23 - Off-Site 0-70 year Time Interval
- Column 24 - On-Site 0-1 year Time Interval
- Column 25 - Off-Site 0-1 year Time Interval
- Column 26 - On-Site 1-2 year Time Interval
- Column 27 - Off-Site 1-2 year Time Interval
- Column 28 - On-Site 2-3 year Time Interval
- Column 29 - Off-Site 2-3 year Time Interval

Table A-2 (Page 2 of 2)
SUMMARY OF SELECTED DATA FOR ALL PHASE 0 EXPECTATION CASES

	13	14	15	16	17	18	19	20	21	22	23	24	25	26	27	28	29
1	6.72E-02	9.95E-01	4.59E+01	5.51E-01	4.47E-01	8.30E-02	1.58E-01	7.59E-01	1.72E-09	0.00E+00	0.00E+00	0.00E+00	0.00E+00	0.00E+00	0.00E+00	0.00E+00	0.00E+00
2	2.91E-01	1.44E+00	4.35E+01	8.75E-01	1.23E-01	9.04E-02	1.61E-01	7.48E-01	5.78E-09	0.00E+00	0.00E+00	0.00E+00	0.00E+00	0.00E+00	0.00E+00	0.00E+00	0.00E+00
4	1.84E-01	2.12E+00	3.99E+01	5.69E-01	4.30E-01	3.61E-02	9.10E-02	8.73E-01	3.44E-08	0.00E+00	0.00E+00	0.00E+00	0.00E+00	0.00E+00	0.00E+00	0.00E+00	0.00E+00
6	5.72E-02	2.75E-01	2.56E+01	9.78E-01	1.18E-02	3.80E-02	1.03E-01	8.59E-01	2.82E-09	0.00E+00	0.00E+00	0.00E+00	0.00E+00	0.00E+00	0.00E+00	0.00E+00	0.00E+00
7	1.87E-01	2.90E-01	3.16E-01	5.38E-01	4.61E-01	2.43E-02	8.22E-02	8.93E-01	2.21E-05	0.00E+00	2.80E+00	0.00E+00	2.77E+00	0.00E+00	0.00E+00	0.00E+00	0.00E+00
8	5.04E-11	0.00E+00	1.50E-05	0.00E+00	0.00E+00	0.00E+00	0.00E+00	0.00E+00	1.00E+00	0.00E+00	2.45E-02	0.00E+00	2.45E-02	0.00E+00	0.00E+00	0.00E+00	0.00E+00
10	7.04E-02	1.35E-01	2.84E-03	6.70E-01	3.28E-01	5.79E-01	2.91E-01	1.24E-01	5.56E-03	0.00E+00	2.47E+00	0.00E+00	2.20E+00	0.00E+00	0.00E+00	0.00E+00	0.00E+00
11	2.55E-01	1.02E+00	2.41E+01	8.02E-01	1.95E-01	2.41E-01	3.36E-01	4.23E-01	1.66E-09	0.00E+00	0.00E+00	0.00E+00	0.00E+00	0.00E+00	0.00E+00	0.00E+00	0.00E+00
12	7.12E-02	6.50E-01	6.70E+01	5.84E-01	4.14E-01	4.39E-02	1.94E-01	7.62E-01	7.66E-10	0.00E+00	0.00E+00	0.00E+00	0.00E+00	0.00E+00	0.00E+00	0.00E+00	0.00E+00
13	2.52E-02	5.93E-01	4.14E+01	9.82E-01	1.44E-02	4.16E-02	1.11E-01	8.47E-01	6.88E-09	0.00E+00	6.00E-01	0.00E+00	5.18E-01	0.00E+00	0.00E+00	0.00E+00	0.00E+00
15	2.08E-04	4.49E-04	5.32E+00	7.75E-01	2.21E-01	1.04E-01	2.07E-01	6.89E-01	2.24E-06	0.00E+00	3.80E+00	0.00E+00	3.72E+00	0.00E+00	0.00E+00	0.00E+00	0.00E+00
16	2.45E-01	9.99E-01	3.11E+01	6.90E-01	3.08E-01	5.24E-02	1.20E-01	8.28E-01	2.16E-09	0.00E+00	0.00E+00	0.00E+00	0.00E+00	0.00E+00	0.00E+00	0.00E+00	0.00E+00
17	5.58E-03	7.04E-02	4.77E+01	8.58E-01	1.30E-01	3.29E-02	1.54E-01	8.13E-01	1.16E-09	0.00E+00	0.00E+00	0.00E+00	0.00E+00	0.00E+00	0.00E+00	0.00E+00	0.00E+00
18	8.37E-02	9.38E-01	7.59E+00	5.09E-01	4.89E-01	6.06E-02	6.48E-01	2.91E-01	1.19E-06	0.00E+00	2.89E+00	0.00E+00	2.71E+00	0.00E+00	0.00E+00	0.00E+00	0.00E+00
19	3.58E-01	6.22E-01	2.02E+01	4.99E-01	4.98E-01	3.47E-02	1.19E-01	8.47E-01	2.90E-09	0.00E+00	0.00E+00	0.00E+00	0.00E+00	0.00E+00	0.00E+00	0.00E+00	0.00E+00
20	8.01E-02	2.09E+00	5.55E+00	5.26E-01	4.74E-01	3.08E-01	5.24E-01	1.68E-01	1.90E-06	0.00E+00	2.80E+00	0.00E+00	2.76E+00	0.00E+00	0.00E+00	0.00E+00	0.00E+00
22	6.21E-01	1.08E+00	2.56E+01	3.50E-01	6.49E-01	2.79E-02	1.26E-01	8.46E-01	2.70E-09	0.00E+00	0.00E+00	0.00E+00	0.00E+00	0.00E+00	0.00E+00	0.00E+00	0.00E+00
23	7.27E-02	1.03E+00	4.36E+01	6.49E-01	3.50E-01	1.20E-01	2.61E-01	6.19E-01	3.75E-09	0.00E+00	1.87E-01	0.00E+00	1.67E-01	0.00E+00	0.00E+00	0.00E+00	0.00E+00
24	2.65E-02	3.47E-01	2.81E+01	6.69E-01	3.29E-01	8.13E-02	3.13E-01	6.06E-01	7.95E-09	0.00E+00	2.21E-01	0.00E+00	2.11E-01	0.00E+00	0.00E+00	0.00E+00	0.00E+00
25	6.05E-02	1.20E+00	2.75E+01	6.60E-01	3.35E-01	5.52E-02	1.34E-01	8.10E-01	2.90E-09	0.00E+00	0.00E+00	0.00E+00	0.00E+00	0.00E+00	0.00E+00	0.00E+00	0.00E+00
26	7.21E-02	1.32E-01	1.45E+01	4.66E-01	5.33E-01	7.90E-02	4.66E-01	4.55E-01	1.03E-07	0.00E+00	4.99E-01	0.00E+00	4.89E-01	0.00E+00	0.00E+00	0.00E+00	0.00E+00
27	4.29E-01	1.83E+00	2.70E+01	7.06E-01	2.94E-01	7.66E-02	1.80E-01	7.43E-01	1.40E-08	0.00E+00	7.08E-01	0.00E+00	6.64E-01	0.00E+00	0.00E+00	0.00E+00	0.00E+00
28	0.00E+00	0.00E+00	1.46E-03	0.00E+00	0.00E+00	2.28E-01	3.43E-01	4.18E-01	1.02E-02	0.00E+00	7.36E-02	0.00E+00	6.38E-02	0.00E+00	0.00E+00	0.00E+00	0.00E+00
30	9.55E-02	6.12E-01	3.08E+00	4.79E-01	5.20E-01	1.04E-01	7.97E-01	9.88E-02	5.48E-06	0.00E+00	2.96E+00	0.00E+00	2.91E+00	0.00E+00	0.00E+00	0.00E+00	0.00E+00
31	2.62E-02	3.19E-02	4.06E-03	4.32E-01	5.66E-01	2.62E-01	5.38E-01	1.97E-01	3.50E-03	0.00E+00	3.77E+00	0.00E+00	3.68E+00	0.00E+00	0.00E+00	0.00E+00	0.00E+00
32	5.56E-01	1.17E+00	3.62E+01	4.98E-01	5.01E-01	3.40E-02	2.12E-01	7.54E-01	2.73E-08	0.00E+00	1.18E-01	0.00E+00	8.84E-02	0.00E+00	0.00E+00	0.00E+00	0.00E+00
33	7.60E-01	5.49E-01	4.96E+01	5.73E-01	4.26E-01	3.16E-02	8.39E-02	8.85E-01	1.70E-09	0.00E+00	0.00E+00	0.00E+00	0.00E+00	0.00E+00	0.00E+00	0.00E+00	0.00E+00
34	4.16E-01	1.03E+00	3.30E+01	6.58E-01	3.41E-01	3.08E-02	1.23E-01	8.47E-01	6.08E-09	0.00E+00	0.00E+00	0.00E+00	0.00E+00	0.00E+00	0.00E+00	0.00E+00	0.00E+00
35	2.23E-01	5.41E+00	8.37E+01	8.30E-01	1.69E-01	2.54E-02	5.02E-01	4.72E-01	2.12E-09	0.00E+00	4.12E-01	0.00E+00	3.53E-01	0.00E+00	0.00E+00	0.00E+00	0.00E+00
36	5.36E-02	4.44E-01	3.49E+01	8.82E-01	1.11E-01	3.32E-02	1.18E-01	8.49E-01	2.07E-09	0.00E+00	0.00E+00	0.00E+00	0.00E+00	0.00E+00	0.00E+00	0.00E+00	0.00E+00
38	4.89E-08	0.00E+00	8.80E-01	6.10E-02	8.84E-05	1.26E-01	4.33E-01	4.40E-01	1.96E-05	0.00E+00	2.06E-01	0.00E+00	1.96E-01	0.00E+00	0.00E+00	0.00E+00	0.00E+00
39	3.95E-01	1.68E+00	9.68E+00	8.04E-01	1.96E-01	1.57E-01	4.81E-01	3.62E-01	1.85E-07	0.00E+00	9.64E-01	0.00E+00	9.05E-01	0.00E+00	0.00E+00	0.00E+00	0.00E+00
40	6.48E-02	1.56E+00	6.71E+00	5.05E-01	4.94E-01	1.22E-01	5.17E-01	3.61E-01	1.55E-06	0.00E+00	3.04E+00	0.00E+00	3.04E+00	0.00E+00	0.00E+00	0.00E+00	0.00E+00
41	1.84E-02	6.70E-03	1.32E-01	8.39E-01	1.61E-01	2.28E-01	3.50E-01	4.22E-01	1.43E-05	0.00E+00	1.18E-01	0.00E+00	1.03E-01	0.00E+00	0.00E+00	0.00E+00	0.00E+00
42	2.45E-04	7.48E-03	8.46E+00	9.35E-01	4.65E-03	4.20E-02	1.72E-01	7.86E-01	3.83E-08	0.00E+00	2.83E-01	0.00E+00	1.96E-01	0.00E+00	0.00E+00	0.00E+00	0.00E+00
43	3.38E-04	4.33E-06	2.43E+00	6.87E-01	3.12E-01	2.43E-01	5.91E-01	1.66E-01	5.25E-06	0.00E+00	2.50E+00	0.00E+00	2.50E+00	0.00E+00	0.00E+00	0.00E+00	0.00E+00
44	9.04E-02	2.08E+00	4.27E+01	7.32E-01	2.66E-01	3.53E-02	1.50E-01	8.15E-01	3.53E-08	0.00E+00	1.47E-02	0.00E+00	1.47E-02	0.00E+00	0.00E+00	0.00E+00	0.00E+00
45	1.54E-01	2.47E-01	1.90E-01	4.90E-01	5.09E-01	2.35E-01	5.10E-01	2.54E-01	5.73E-05	0.00E+00	2.07E+00	0.00E+00	2.03E+00	0.00E+00	0.00E+00	0.00E+00	0.00E+00
46	3.80E-02	7.59E-01	3.80E+01	9.04E-01	7.77E-02	2.67E-02	6.73E-02	9.06E-01	2.00E-09	0.00E+00	0.00E+00	0.00E+00	0.00E+00	0.00E+00	0.00E+00	0.00E+00	0.00E+00
47	2.73E-01	1.88E+00	2.93E+01	7.51E-01	2.47E-01	3.14E-02	1.15E-01	8.53E-01	3.14E-08	0.00E+00	0.00E+00	0.00E+00	0.00E+00	0.00E+00	0.00E+00	0.00E+00	0.00E+00
49	4.36E-02	1.04E+00	6.70E+01	8.62E-01	1.33E-01	1.36E-02	4.63E-02	9.40E-01	3.13E-09	0.00E+00	0.00E+00	0.00E+00	0.00E+00	0.00E+00	0.00E+00	0.00E+00	0.00E+00
50	8.33E-01	9.28E-01	3.87E+01	6.16E-01	3.83E-01	4.15E-02	2.23E-01	7.35E-01	5.14E-09	0.00E+00	1.47E-02	0.00E+00	0.00E+00	0.00E+00	0.00E+00	0.00E+00	0.00E+00
no.	4.20E+01	4.20E+01	4.20E+01	4.20E+01	4.20E+01	4.20E+01	4.20E+01	4.20E+01	4.20E+01	4.20E+01	4.20E+01	4.20E+01	4.20E+01	4.20E+01	4.20E+01	4.20E+01	4.20E+01
avg	1.74E-01	8.88E-01	2.51E+01	6.30E-01	2.96E-01	1.61E-01	2.66E-01	6.09E-01	2.47E-02	0.00E+00	7.99E-01	0.00E+00	7.69E-01	0.00E+00	0.00E+00	0.00E+00	0.00E+00
s d	2.12E-01	9.69E-01	2.14E+01	2.34E-01	1.84E-01	1.10E-01	1.92E-01	2.76E-01	1.54E-01	0.00E+00	1.24E+00	0.00E+00	1.21E+00	0.00E+00	0.00E+00	0.00E+00	0.00E+00
min	0.00E+00	0.00E+00	1.50E-05	0.00E+00	0.00E+00	0.00E+00	0.00E+00	0.00E+00	7.66E-10	0.00E+00	0.00E+00	0.00E+00	0.00E+00	0.00E+00	0.00E+00	0.00E+00	0.00E+00
max	8.37E-01	5.41E+00	8.37E+01	9.82E-01	6.49E-01	5.79E-01	7.97E-01	9.40E-01	1.00E+00	0.00E+00	3.80E+00	0.00E+00	3.72E+00	0.00E+00	0.00E+00	0.00E+00	0.00E+00
at	50	35	35	13	22	10	30	49	8	1	15	1	15	1	1	1	1

Table A-3 (Page 1 of 2)
SUMMARY OF SELECTED DATA FOR ALL PHASE 1 EXPECTATION CASES

##	1	2	3	4	5	6	7	8	9	10	11	12
1	5.43E-02	6.09E-02	1.14E+02	4.81E+02	5.31E-03	3.32E+01	3.84E+01	1.26E+01	3.55E+00	0.00E+00	5.95E+02	3.32E+01
2	5.89E-02	1.51E-02	1.19E+02	4.49E+02	2.77E-03	0.00E+00	3.86E+01	6.80E+00	1.42E+00	1.96E+00	5.68E+02	2.77E-03
4	6.31E-02	4.37E-02	1.21E+02	4.35E+02	8.83E-03	0.00E+00	3.26E+01	7.99E+00	3.43E+00	2.11E+00	5.56E+02	9.82E-03
6	5.23E-02	4.03E-02	9.01E+01	2.98E+02	2.61E-03	0.00E+00	4.31E+01	1.59E+01	2.50E+00	0.00E+00	3.88E+02	2.61E-03
7	7.11E-02	6.14E-04	6.01E+01	7.44E+00	2.35E-02	0.00E+00	7.69E+00	2.05E+00	6.08E+00	5.10E+00	6.75E+01	2.35E-02
8	0.00E+00	0.00E+00	0.00E+00	2.67E-04	0.00E+00	0.00E+00	2.60E-01	0.00E+00	0.00E+00	6.67E+00	2.67E-04	0.00E+00
10	1.45E-01	9.36E-05	2.09E+00	2.81E-01	3.01E-02	0.00E+00	9.68E+00	2.31E+00	5.50E+00	6.98E+00	2.37E+00	3.01E-02
11	8.39E-02	4.63E-02	2.02E+02	2.16E+02	1.66E-02	0.00E+00	2.41E+01	1.07E+01	1.60E+00	0.00E+00	4.18E+02	1.66E-02
12	5.11E-02	3.56E-02	9.73E+01	7.25E+02	1.28E-03	0.00E+00	3.69E+01	1.13E+01	1.59E+00	3.44E+00	8.22E+02	1.28E-03
13	3.38E-03	2.18E-02	2.96E+01	4.44E+02	0.00E+00	0.00E+00	4.10E+01	5.76E+00	1.20E+00	1.37E+00	4.74E+02	0.00E+00
15	2.49E-03	1.66E-02	1.26E+01	5.35E+01	0.00E+00	0.00E+00	1.05E+01	0.00E+00	2.82E+00	5.28E+00	6.61E+01	0.00E+00
16	6.44E-02	2.96E-02	8.30E+01	3.36E+02	6.24E+00	0.00E+00	2.15E+01	1.39E+01	1.93E+00	0.00E+00	4.19E+02	6.24E+00
17	6.25E-02	3.09E-02	3.33E+01	5.19E+02	5.89E-03	0.00E+00	3.79E+01	1.83E+01	1.86E+00	6.42E+00	5.52E+02	5.89E-03
18	5.37E-02	8.39E-03	2.17E+01	7.99E+01	1.32E-02	0.00E+00	2.30E+01	6.73E+00	1.49E+00	4.30E+00	1.02E+02	1.32E-02
19	5.31E-02	5.43E-02	6.14E+01	2.26E+02	1.33E-03	4.42E+00	2.73E+01	1.80E+01	2.46E+00	0.00E+00	2.87E+02	4.42E+00
20	6.29E-02	3.91E-03	6.58E+01	4.40E+01	1.81E-02	0.00E+00	1.03E+01	3.40E+00	8.31E+00	6.29E+00	1.10E+02	1.81E-02
22	1.60E-02	3.14E-02	4.44E+01	2.91E+02	0.00E+00	0.00E+00	3.47E+01	2.01E+01	2.20E+00	0.00E+00	3.35E+02	0.00E+00
23	8.03E-02	1.68E-02	1.41E+02	4.35E+02	1.34E-02	0.00E+00	3.46E+01	3.80E+00	9.85E+00	7.04E+00	5.76E+02	1.34E-02
24	5.94E-02	2.16E-02	9.81E+01	2.99E+02	5.90E-03	0.00E+00	3.02E+01	6.43E+00	7.67E+00	1.03E+00	3.97E+02	5.90E-03
25	5.89E-02	6.13E-02	7.99E+01	2.99E+02	5.61E-03	2.54E+01	2.69E+01	1.04E+01	2.85E+00	0.00E+00	3.79E+02	2.54E+01
26	6.68E-02	1.23E-02	5.93E+01	1.57E+02	3.23E-03	0.00E+00	2.19E+01	6.46E-01	2.19E+00	1.03E+00	2.16E+02	3.23E-03
27	9.60E-02	7.19E-02	1.81E+02	2.86E+02	4.61E-02	5.19E+01	2.40E+01	8.25E+00	2.54E+00	2.54E+00	4.67E+02	5.19E+01
28	2.39E-06	3.54E-06	8.38E-03	1.29E-02	0.00E+00	0.00E+00	2.59E-01	0.00E+00	1.52E+00	6.06E+00	2.13E-02	0.00E+00
30	5.54E-02	2.80E-03	1.85E+01	3.14E+01	1.34E-02	0.00E+00	1.26E+01	3.52E+00	8.57E+00	7.57E+00	4.99E+01	1.34E-02
31	6.91E-02	2.61E-04	5.96E+00	3.82E-01	1.70E-02	0.00E+00	9.43E+00	2.18E+00	5.79E+00	6.44E+00	6.34E+00	1.70E-02
32	4.87E-02	3.13E-02	9.01E+01	4.03E+02	0.00E+00	0.00E+00	4.04E+01	7.62E+00	2.77E+00	6.49E+00	4.93E+02	0.00E+00
33	5.71E-02	5.26E-02	7.45E+01	5.48E+02	8.20E-03	7.24E+00	4.67E+01	6.50E+00	1.27E+00	0.00E+00	6.23E+02	7.25E+00
34	6.76E-02	2.78E-02	8.44E+01	3.64E+02	3.48E+00	0.00E+00	3.78E+01	6.42E+00	1.31E+00	0.00E+00	4.48E+02	3.48E+00
35	9.82E-02	6.03E-02	2.35E+02	9.16E+02	5.17E-02	3.35E+01	2.31E+01	7.37E+00	1.30E+00	7.84E+00	1.15E+03	3.36E+01
36	5.42E-02	4.28E-02	7.77E+01	3.91E+02	5.39E-03	0.00E+00	3.53E+01	1.38E+01	2.72E+00	0.00E+00	4.69E+02	5.39E-03
38	3.90E-04	4.54E-04	4.56E+00	9.36E+00	0.00E+00	0.00E+00	1.02E+00	0.00E+00	1.79E+00	7.42E+00	1.39E+01	0.00E+00
39	2.94E-01	5.76E-03	9.91E+01	9.31E+01	2.66E-01	0.00E+00	2.60E+01	7.77E+00	1.44E+00	1.38E+00	1.92E+02	2.66E-01
40	5.49E-02	5.27E-03	9.07E+01	7.42E+01	4.12E-03	0.00E+00	1.29E+01	3.96E+00	9.18E+00	6.63E+00	1.65E+02	4.12E-03
41	1.36E-02	1.18E-04	9.22E+00	1.38E+00	0.00E+00	0.00E+00	3.55E+00	0.00E+00	1.45E+00	2.12E+00	1.06E+01	0.00E+00
42	1.16E-01	8.25E-03	2.86E+01	9.43E+01	1.99E-02	0.00E+00	2.98E+01	5.26E+00	3.48E+00	6.22E+00	1.23E+02	1.99E-02
43	2.33E-03	2.91E-03	1.58E+01	2.08E+01	0.00E+00	0.00E+00	5.08E+00	0.00E+00	1.22E+00	4.32E+00	3.66E+01	0.00E+00
44	1.26E-01	2.21E-02	2.27E+02	4.67E+02	3.71E-02	0.00E+00	2.34E+01	8.52E+00	3.66E+00	8.73E+00	6.94E+02	3.71E-02
45	7.65E-02	3.32E-04	2.33E+01	3.74E+00	2.54E-02	0.00E+00	8.08E+00	2.27E+00	6.28E+00	6.17E+00	2.70E+01	2.54E-02
46	1.01E-01	4.46E-02	9.02E+01	4.19E+02	7.67E-03	0.00E+00	2.72E+01	1.45E+01	2.91E+00	0.00E+00	5.09E+02	7.67E-03
47	5.92E-02	2.66E-02	8.65E+01	3.21E+02	8.48E-03	0.00E+00	3.92E+01	7.13E+00	2.29E+00	1.35E+00	4.08E+02	8.48E-03
49	1.11E-01	5.33E-02	1.35E+02	7.40E+02	2.96E-02	7.31E+00	4.86E+01	1.04E+01	2.01E+00	4.05E+00	8.75E+02	7.34E+00
50	6.32E-02	2.53E-02	1.14E+02	4.23E+02	9.09E-03	0.00E+00	4.04E+01	6.65E+00	1.58E+00	2.68E+00	5.37E+02	9.09E-03
no.	4.20E+01	4.20E+01	4.20E+01	4.20E+01	4.20E+01	4.20E+01	4.20E+01	4.20E+01	4.20E+01	4.20E+01	4.20E+01	4.20E+01
avg	6.50E-02	2.47E-02	7.68E+01	2.71E+02	2.48E-01	3.88E+00	2.49E+01	7.12E+00	3.23E+00	3.50E+00	3.48E+02	4.13E+00
s d	4.99E-02	2.13E-02	6.01E+01	2.33E+02	1.09E+00	1.11E+01	1.40E+01	5.45E+00	2.46E+00	2.94E+00	2.77E+02	1.11E+01
min	0.00E+00	0.00E+00	0.00E+00	2.67E-04	0.00E+00	0.00E+00	2.59E-01	0.00E+00	0.00E+00	0.00E+00	2.67E-04	0.00E+00
max	2.94E-01	7.19E-02	2.35E+02	9.16E+02	6.24E+00	5.19E+01	4.86E+01	2.01E+01	9.85E+00	8.73E+00	1.15E+03	5.19E+01
at	39	27	35	35	16	27	49	22	23	44	35	27

Maximum Individual Dose, rem
- Column 1 - Short Term
- Column 2 - Long Term

Population Dose, person-rem
- Column 3 - Short Term (w/o Di Minimus)
- Column 4 - Long Term (w/o Di Minimus)
- Column 5 - Short Term (w Di Minimus)
- Column 6 - Long Term (w Di Minimus)

Area Exceeding Surface Contamination of 0.2 uCi/m2, km2
- Column 7 - on Dry Land
- Column 8 - on Swamp
- Column 9 - on Inland Water
- Column 10 - on Ocean

Total Population Dose, person-rem
- Column 11 - Short and Long Term (w/o Di Minimus)
- Column 12 - Short and Long Term (w Di Minimus)

Total Population Dose by Population Groups, person-rem
- Column 13 - Workers (w/o Di Minimus)
- Column 14 - Spectators (w/o Di Minimus)
- Column 15 - Residents (w/o Di Minimus)

Total Population Dose Fraction to Each Pathway
- Column 16 - Direct Inhalation by Workers
- Column 17 - Re-Suspension by Workers
- Column 18 - Direct Inhalation by Residents
- Column 19 - Re-Suspension by Residents
- Column 20 - Vegetable Consumption by Residents
- Column 21 - Seafood Consumption by Residents

Dry Land Area Exceeding Long Term Dose of 25 mrem, km2
- Column 22 - On-Site 0-70 year Time Interval
- Column 23 - Off-Site 0-70 year Time Interval
- Column 24 - On-Site 0-1 year Time Interval
- Column 25 - Off-Site 0-1 year Time Interval
- Column 26 - On-Site 1-2 year Time Interval
- Column 27 - Off-Site 1-2 year Time Interval
- Column 28 - On-Site 2-3 year Time Interval
- Column 29 - Off-Site 2-3 year Time Interval

Table A-3 (Page 2 of 2)
SUMMARY OF SELECTED DATA FOR ALL PHASE 1 EXPECTATION CASES

	13	14	15	16	17	18	19	20	21	22	23	24	25	26	27	28	29
1	2.55E+00	1.54E+01	5.77E+02	7.80E-01	2.19E-01	1.27E 01	1.51E-01	6.82E 01	2.27E 09	3.29E 01	5.02E+00	3.14E-01	3.21E+00	0.00E+00	0.00E+00	0.00E+00	0.00E+00
2	4.17E+00	4.56E+01	5.18E+02	8.83E-01	1.15E-01	1.35E-01	1.58E-01	7.07E-01	6.39E-09	2.80E-01	5.40E-02	2.80E-01	4.42E-02	0.00E+00	0.00E+00	0.00E+00	0.00E+00
4	3.28E+00	8.13E+01	4.72E+02	6.99E-01	3.00E-01	7.89E 02	9.19E 02	8.30E-01	3.80E-08	1.96E-01	4.54E+00	1.96E 01	3.48E+00	0.00E+00	0.00E+00	0.00E+00	0.00E+00
6	1.97E+00	1.49E+01	3.72E+02	9.04E-01	9.24E-02	1.98E 01	1.11E 01	6.91E 01	3.45E 09	3.44E 01	1.10E+00	3.44E 01	1.10E+00	0.00E+00	0.00E+00	0.00E+00	0.00E+00
7	5.08E+00	4.55E+01	1.70E+01	7.79E-01	2.21E-01	6.29E 01	1.22E 01	2.49E-01	6.50E 06	1.07E 01	3.85E+00	1.03E-01	3.82E+00	0.00E+00	5.46E-01	0.00E+00	0.00E+00
8	1.12E-09	0.00E+00	2.67E-04	0.00E+00	0.00E+00	0.00E+00	0.00E+00	0.00E+00	1.00E+00	0.00E+00	2.55E-01	0.00E+00	2.50E-01	0.00E+00	0.00E+00	0.00E+00	0.00E+00
10	8.44E-01	1.50E+00	3.15E-02	6.83E-01	3.13E-01	5.77E 01	2.90E 01	1.24E-01	9.43E-03	0.00E+00	3.61E+00	0.00E+00	3.57E+00	0.00E+00	4.42E-02	0.00E+00	0.00E+00
11	5.69E+00	3.23E+01	3.80E+02	8.83E-01	1.16E-01	4.33E-01	2.58E-01	3.09E-01	1.77E-09	2.41E-01	2.35E+00	2.26E-01	1.98E+00	0.00E+00	0.00E+00	0.00E+00	0.00E+00
12	1.62E+00	3.35E+01	7.87E+02	7.28E-01	2.71E-01	7.95E-02	1.91E 01	7.30E 01	1.15E-09	3.24E-01	9.71E-01	3.24E-01	5.74E-01	0.00E+00	0.00E+00	0.00E+00	0.00E+00
13	2.82E-01	6.96E+00	4.66E+02	9.82E-01	1.44E-02	4.79E-02	1.11E-01	8.41E-01	1.40E-08	1.77E-01	2.17E+00	1.77E-01	2.17E+00	0.00E+00	0.00E+00	0.00E+00	0.00E+00
15	4.14E-03	5.03E-03	6.61E+01	8.60E-01	1.38E-01	1.90E-01	1.89E-01	6.21E 01	3.20E-08	0.00E+00	8.65E+00	0.00E+00	8.40E+00	0.00E+00	9.03E-01	0.00E+00	0.00E+00
16	9.96E+00	4.45E+01	3.64E+02	8.67E-01	1.32E-01	8.22E-02	1.20E-01	7.97E-01	3.35E-09	2.45E-01	5.58E-01	2.45E-01	1.89E-01	0.00E+00	0.00E+00	0.00E+00	0.00E+00
17	1.18E-01	7.97E-01	5.51E+02	8.60E-01	1.32E-01	5.88E-02	1.51E-01	7.90E-01	1.98E-09	4.03E-01	2.94E-01	3.83E-01	2.94E-01	0.00E+00	0.00E+00	0.00E+00	0.00E+00
18	2.63E+00	1.46E+01	8.44E+01	7.49E-01	2.51E-01	6.06E-02	6.47E-01	2.93E-01	1.85E-06	1.13E-01	3.98E+00	1.13E-01	3.85E+00	0.00E+00	1.48E-01	0.00E+00	0.00E+00
19	6.90E+00	3.23E+01	2.48E+02	6.63E-01	3.36E-01	9.87E-02	1.20E-01	7.61E-01	4.20E-09	3.09E-01	3.25E+00	3.09E-01	2.53E+00	0.00E+00	0.00E+00	0.00E+00	0.00E+00
20	3.37E+00	4.20E+01	6.44E+01	8.17E-01	1.83E-01	3.27E-01	5.07E-01	1.66E-01	2.75E-06	1.52E-01	3.04E+00	1.52E-01	3.00E+00	0.00E+00	2.70E-01	0.00E+00	0.00E+00
22	1.16E+01	2.40E+01	3.00E+02	5.66E-01	4.34E-01	4.60E-02	1.31E-01	8.23E-01	4.14E-09	3.19E-01	5.94E+00	3.19E-01	2.07E+00	0.00E+00	0.00E+00	0.00E+00	0.00E+00
23	9.46E-01	1.48E+01	5.60E+02	6.90E-01	3.09E-01	2.23E-01	2.34E-01	5.42E-01	5.86E-09	3.93E 01	1.22E+00	3.93E-01	1.21E+00	0.00E+00	0.00E+00	0.00E+00	0.00E+00
24	2.15E+00	2.13E+01	3.73E+02	8.77E-01	1.23E-01	2.01E-01	2.78E-01	5.21E-01	1.09E-08	2.95E 01	7.99E 01	2.95E 01	7.94E-01	0.00E+00	0.00E+00	0.00E+00	0.00E+00
25	2.45E+00	3.01E+01	3.47E+02	8.35E-01	1.63E-01	1.38E-01	1.33E-01	7.29E-01	3.86E-09	3.09E-01	2.62E+00	2.95E-01	2.24E+00	0.00E+00	0.00E+00	0.00E+00	0.00E+00
26	2.52E+00	1.87E+01	1.96E+02	7.85E-01	2.15E-01	1.90E 01	4.08E-01	3.95E 01	9.79E-08	2.36E-01	3.79E+00	2.36E-01	3.47E+00	0.00E+00	0.00E+00	0.00E+00	0.00E+00
27	5.57E+01	4.88E+01	3.62E+02	9.48E-01	5.23E-02	2.18E-01	1.59E-01	6.23E-01	2.88E-08	8.34E-02	4.13E+00	8.34E-02	3.70E+00	0.00E+00	0.00E+00	0.00E+00	0.00E+00
28	0.00E+00	0.00E+00	2.13E-02	0.00E+00	0.00E+00	3.94E 01	2.73E-01	3.20E-01	1.24E-02	0.00E+00	2.55E-01	0.00E+00	2.40E-01	0.00E+00	0.00E+00	0.00E+00	0.00E+00
30	3.24E+00	1.25E+01	3.42E+01	7.51E-01	2.49E-01	1.05E-01	7.95E-01	9.94E-02	9.12E-06	1.18E-01	3.44E+00	1.18E-01	3.41E+00	0.00E+00	0.00E+00	0.00E+00	0.00E+00
31	1.91E+00	4.36E+00	8.25E-02	8.20E-01	1.79E-01	5.22E 01	3.35E 01	1.40E 01	3.27E-03	7.36E-02	4.18E+00	7.36E-02	4.18E+00	0.00E+00	1.35E+00	0.00E+00	0.00E+00
32	8.32E+00	5.79E+01	4.27E+02	6.01E-01	3.99E-01	6.37E-02	2.10E 01	7.26E-01	3.06E-08	2.16E-01	1.60E+00	2.16E-01	1.60E+00	0.00E+00	0.00E+00	0.00E+00	0.00E+00
33	1.88E+01	2.19E+01	5.82E+02	7.65E-01	2.35E 01	6.56E-02	8.60E-02	8.48E-01	2.82E-09	2.21E-01	8.22E+00	2.11E-01	6.73E+00	0.00E+00	0.00E+00	0.00E+00	0.00E+00
34	2.12E+01	3.77E+01	3.89E+02	8.81E-01	1.18E-01	7.18E 02	1.22E-01	8.06E-01	7.49E-09	2.01E-01	2.99E+00	2.01E-01	0.00E+00	0.00E+00	0.00E+00	0.00E+00	0.00E+00
35	5.38E+00	1.88E+02	9.57E+02	9.11E-01	8.85E-02	4.36E 02	4.91E-01	4.65E-01	3.19E-09	1.13E-01	2.91E+01	1.13E-01	2.40E+01	0.00E+00	0.00E+00	0.00E+00	0.00E+00
36	2.38E+00	1.65E+01	4.50E+02	8.86E-01	1.12E-01	1.31E-01	1.18E-01	7.51E-01	2.74E-09	2.95E-01	1.51E+00	2.95E-01	9.45E-01	0.00E+00	0.00E+00	0.00E+00	0.00E+00
38	1.45E-02	1.48E-09	1.39E+01	9.81E-01	1.91E-02	3.27E-01	3.33E-01	3.40E-01	2.18E-05	0.00E+00	1.02E+00	0.00E+00	1.01E+00	0.00E+00	7.36E-02	0.00E+00	0.00E+00
39	1.19E+01	5.08E+01	1.29E+02	9.16E-01	8.43E-02	2.88E-01	4.07E-01	3.04E-01	1.89E-07	5.89E-02	2.20E+00	5.40E-02	2.08E+00	0.00E+00	1.18E-01	0.00E+00	0.00E+00
40	1.68E+00	6.15E+01	1.02E+02	7.27E-01	2.73E-01	2.75E-01	4.19E-01	3.06E-01	1.69E-06	2.01E-01	3.89E+00	2.01E-01	3.81E+00	0.00E+00	4.38E-01	0.00E+00	0.00E+00
41	1.42E+00	7.71E+00	1.48E+00	8.33E-01	1.67E-01	2.28E-01	3.53E-01	4.19E-01	1.63E-05	9.33E-02	7.88E-01	9.33E-02	7.53E-01	0.00E+00	0.00E+00	0.00E+00	0.00E+00
42	9.05E-02	8.33E-02	1.23E+02	8.77E-01	1.20E-01	2.32E-01	1.53E-01	6.15E-01	4.94E-08	4.76E-01	2.82E+00	3.73E-01	1.40E+00	0.00E+00	0.00E+00	0.00E+00	0.00E+00
43	3.78E-03	4.83E-05	3.66E+01	6.89E-01	3.10E-01	4.33E-01	4.42E-01	1.25E-01	6.13E-06	0.00E+00	4.37E+00	0.00E+00	4.30E+00	0.00E+00	8.84E-01	0.00E+00	0.00E+00
44	3.65E+00	1.45E+02	5.46E+02	8.96E-01	1.03E 01	1.45E 01	1.39E-01	7.16E-01	3.49E-08	1.77E 01	6.35E-01	1.77E 01	6.35E-01	0.00E+00	0.00E+00	0.00E+00	0.00E+00
45	4.64E+00	1.32E+01	9.19E+00	7.78E-01	2.22E-01	7.06E-01	1.94E-01	1.01E-01	2.07E-05	9.82E-02	2.80E+00	9.82E-02	2.68E+00	0.00E+00	1.47E-02	0.00E+00	0.00E+00
46	1.65E+00	4.47E+01	4.63E+02	9.13E-01	8.24E-02	9.50E-02	6.91E-02	8.36E-01	2.83E-09	3.24E-01	5.87E+00	3.24E-01	4.80E+00	0.00E+00	0.00E+00	0.00E+00	0.00E+00
47	4.21E+00	6.28E+01	3.40E+02	7.99E-01	2.00E-01	5.98E-02	1.15E-01	8.25E-01	3.44E 08	2.06E-01	9.54E-01	2.06E-01	1.62E-01	0.00E+00	0.00E+00	0.00E+00	0.00E+00
49	2.43E+00	9.91E+01	7.73E+02	9.26E-01	7.24E-02	4.29E 02	4.75E-02	9.09E-01	4.49E-09	1.87E-01	1.93E+01	1.87E-01	1.53E+01	0.00E+00	0.00E+00	0.00E+00	0.00E+00
50	1.08E+01	7.42E+01	4.52E+02	6.62E-01	3.37E 01	7.17E-02	2.18E-01	7.10E-01	8.34E-09	1.96E-01	1.37E+00	1.87E-01	5.90E-01	0.00E+00	0.00E+00	0.00E+00	0.00E+00
no.	4.20E+01	4.20E+01	4.20E+01	4.20E+01	4.20E+01	4.20E+01	4.20E+01	4.20E+01	4.20E+01	4.20E+01	4.20E+01	4.20E+01	4.20E+01	4.20E+01	4.20E+01	4.20E+01	4.20E+01
avg	5.42E+00	3.49E+01	3.08E+02	7.73E-01	1.79E-01	2.02E-01	2.35E-01	5.38E-01	2.44E-02	1.93E 01	3.80E+00	1.88E-01	3.11E+00	0.00E+00	1.14E-01	0.00E+00	0.00E+00
s d	9.28E+00	3.89E+01	2.50E+02	2.01E-01	1.08E-01	1.74E-01	1.67E-01	2.69E-01	1.54E-01	1.24E-01	5.16E+00	1.18E-01	4.28E+00	0.00E+00	2.91E-01	0.00E+00	0.00E+00
min	0.00E+00	0.00E+00	2.67E-04	0.00E+00	0.00E+00	0.00E+00	0.00E+00	0.00E+00	1.15E-09	0.00E+00	5.40E-02	0.00E+00	0.00E+00	0.00E+00	0.00E+00	0.00E+00	0.00E+00
max	5.57E+01	1.88E+02	9.57E+02	9.82E-01	4.34E-01	7.06E-01	7.95E-01	9.09E-01	1.00E+00	4.76E 01	2.91E+01	3.93E-01	2.40E+01	0.00E+00	1.35E+00	0.00E+00	0.00E+00
at	27	35	35	13	22	45	30	49	8	42	35	23	35	1	31	1	1

and Graphite Impact Shells (GIS, Phase 5), and release of PuO_2 particulates at ground level. Since these releases occur at unspecified worldwide locations (Africa in Phase 2; between 33°N. and 33°S. latitudes in Phases 3 and 4; and worldwide in Phase 5), the use of site-specific, time-varying meteorology in the atmospheric transport and dispersion calculations, as in the cases of Phases 0 and 1, was inappropriate. Accordingly, KSC-EMERGE was used in the calculations for the ground-level releases in Phases 2 through 5, but the meteorology was based on a study of worldwide meteorology presented in Reference A-3 and summarized in Appendix G. The use of average, uniform population densities in the calculations, dependent on the region affected (see Appendix G), implied the results were independent of wind direction. Therefore, time-independent meteorological conditions were assumed. Based on the information in Appendix G, the meteorological conditions used in the most probable and expectation cases consisted of D atmospheric stability conditions and a 5 m/s wind speed. The meteorological conditions used in the maximum cases consisted of F atmospheric stability conditions and a 1 m/s wind speed.

A.2.2 LOPAR

The transport of small particles (less than or equal to 10 microns) released at high altitude has been modeled by LOPAR based on considerations of Sr-90 fallout resulting from high altitude atmospheric nuclear weapons tests. The latitudinal distribution of Sr-90 at the end of 1965 for both the northern and southern hemispheres has been fitted with Gaussian-type curves (Reference A-7). The distribution was found to be a function of the latitude where the material was released (injection latitude). The distribution of Sr-90 is skewed toward the mid-latitudes of the northern hemisphere corresponding to where such tests were conducted.

In assessing the distribution of material released from a variety of injection latitudes, a generalization is made from the Sr-90 data. It is assumed the distribution will be Gaussian in each hemisphere with a null point at the equator and the maximum skewed towards the hemisphere in which the release occurs. A symmetrical bimodal distribution is assumed for an equatorial release. The resulting distributions as a function of injection latitude is then shown in Figure A-7 (Reference A-7). Using this approach, the fraction of source term in each of 20 equal area latitude bands (see Appendix G) can be used to determine the average time-integrated airborne and ground concentrations using the terminal fall velocity of each particle size range below 10 microns.

A.2.3 HIPAR

The atmospheric transport and dispersion of large particles (greater than 10 microns) released above the troposphere are treated using the HIPAR model (References A-7 and A-13).

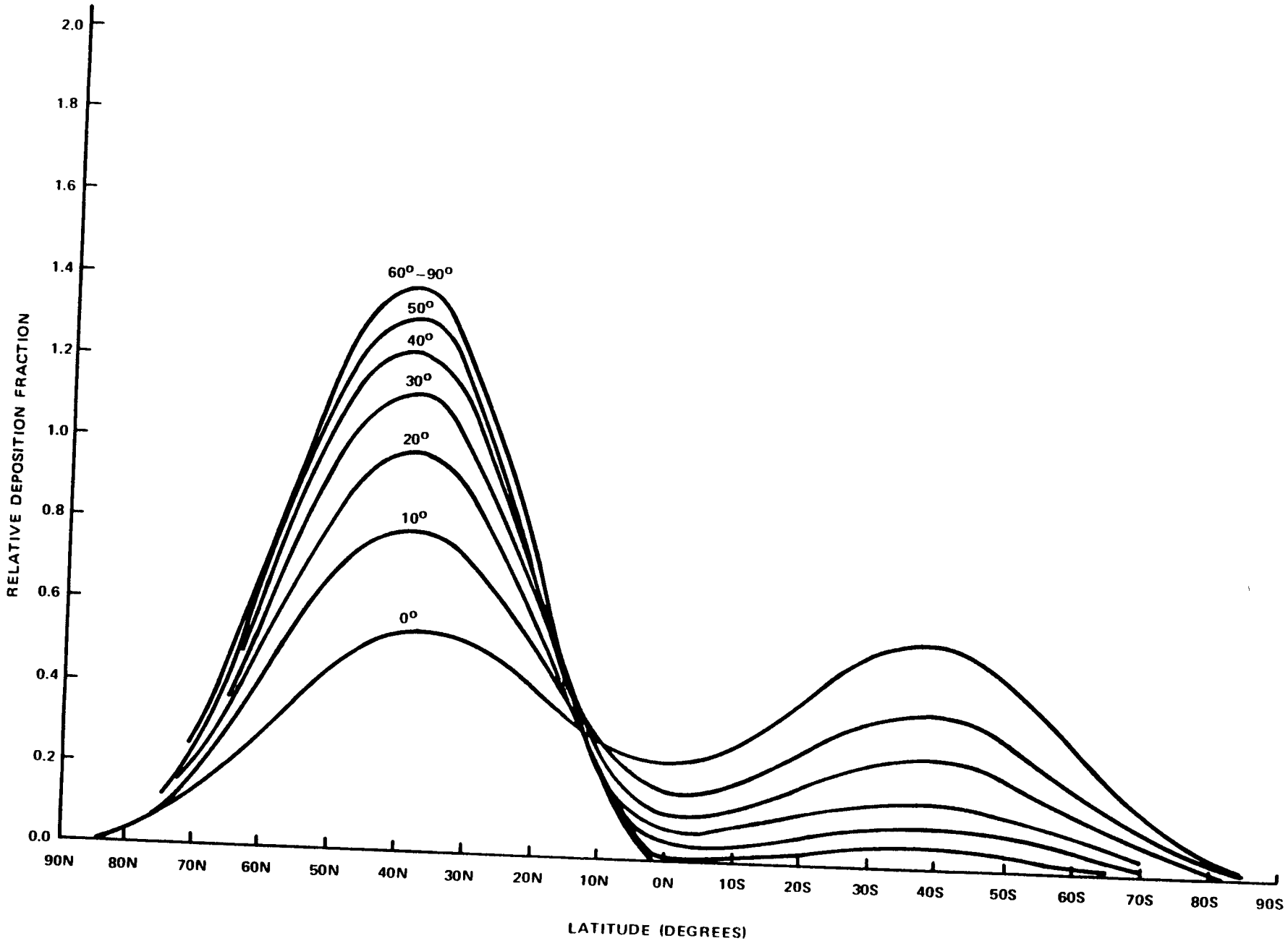

Figure A-7
LOPAR MATERIAL DISTRIBUTION VERSUS RELEASE LATITUDE

In HIPAR the trajectories of individual particle size groups are obtained by numerical integration of ordinary differential equations for the rates of colatitude, longitude, and altitude, using local wind speed components and terminal velocity of particles. HIPAR assumes that the horizontal particle velocity equals the horizontal air velocity and the particle vertical velocity equals the sum of the particle fall velocity and the vertical air velocity.

The wind speed and direction as a function of latitude, longitude and altitude have been modeled as being representative of worldwide atmospheric circulation patterns through the use of data fits using spherical harmonic polynomials.

In addition to particle characteristics (mass density) and wind patterns, the particle trajectory will depend on dynamic properties of the atmosphere (density, speed of sound, viscosity, and the mean free path of air molecules) as functions of temperature and pressure, and, therefore, altitude. HIPAR assumes standard atmospheric properties as a function of altitude fitted by polynomials.

Based on these considerations, HIPAR requires as input the latitude, longitude, altitude, and particle size distribution of the PuO_2 release, and then calculates surface concentrations resulting from particle trajectories and deposition, accounting for the rotation of the earth; variations in wind speed and direction with latitude, longitude, and altitude; and variations in particle terminal fall velocity with altitude.

A.2.4 Exposure Pathway Parameters

The calculation of short- and long-term doses with the atmospheric transport and dispersion models described above and outlined in Section A.1.1 involve a number of assumptions and parameter values related to the exposure pathways considered. Each model (KSC-EMERGE, LOPAR, and HIPAR) calculates the following:

Ψ_i = Time integrated airborne concentration of PuO_2 in particle size range i, Ci-s/m^3

ω_i = Total ground concentration of PuO_2 in particle size range i, Ci/m^2

The short-term dose to individuals due to inhalation of PuO_2 particles during the initial plume passage is determined from:

$$D_s = \sum_i \Psi_i I_i$$

where

D_s = Total short-term dose, rem

I_i = Inhalation dose conversion factor for particle size range i, rem/C_i-s/m^3

Note that the contribution to short-term dose due to external exposure during plume passage is not included because it is orders of magnitude lower than the inhalation dose. The reported dose is in terms of "effective dose equivalent" as defined by ICRP-30 (Reference A-14). The internal dosimetry model used to determine the inhalation dose conversion factors, I_i, is described in Section A.3.

The exposure pathways considered in the calculation of long-term doses include inhalation of resuspended PuO_2 particles initially deposited on the ground, ingestion of contaminated vegetation, and direct external exposure to ground deposited material. Since drinking water supplies in the vicinity of KSC are derived from deep aquifers, contamination of such water supplies is unlikely. Deposition of PuO_2 particles on the surfaces of inland waters and the Atlantic Ocean in Phases 0 and 1 could result in the contamination of fish and seafood, and additional ingestion doses. Other ingestion pathways such as ingestion of milk and meat from grazing cattle have not been considered because they represent secondary, less direct, ingestion pathways which contribute very little due to the low solubility of PuO_2. Basic features, assumptions, and exposure pathway parameters associated with the calculation of long-term doses are presented below.

The total long-term dose to individuals is determined by

$$D_L = D_1 + D_2 + D_3 + D_4$$

where

D_L = Total long-term dose, rem

D_1 = Contribution due to resuspension, rem

D_2 = Contribution due to vegetable ingestion, rem

D_3 = Contribution due to external exposure, rem

D_4 = Contribution due to seafood ingestion, rem

Each of these dose contributions is determined as a function of the total ground/surface concentration, Ψ_i. The formulation of the time-dependent exposure pathway models used in the analysis was based on Reference A-15. Basic features of the analysis include the following:

1. Resuspension

   Resuspension inhalation doses, D_1, were based on an initial resuspension factor of 10^{-5} that decreases exponentially to 10^{-9} after two years, and remains at 10^{-9} thereafter (References A-15 through A-17). Only PuO_2 particles less than 30 microns in diameter were subject to resuspension. Internal dose factors based on continuous inhalation over long time periods were used in this calculation, as described in Section A.3.

   In this analysis, depletion of the initial deposition accounted for the radioactive decay of Pu-238 with an 87.6 year half-life and weathering with a 50-year removal half-time.

2. Vegetable Ingestion

   In the calculation of vegetable ingestion doses, four mechanisms of vegetable contamination were taken into account as described below. The pathway parameter values indicated are derived from References A-16 and A-17 except as noted.

   - Initial deposition immediately following the accident. The analysis assumed a removal half-time of 14 days for leaf-deposited material, a leaf interception fraction of 0.5, and a vegetable density of 2 kg/m^2. Assuming two growing seasons per year, one-half the vegetable production would be affected by the initial deposition. Harvesting and consumption are assumed to take place continuously during the 30-day period immediately following the release, such that the average vegetable contamination level would be the average of the 30-day period.

   - Continuous re-deposition on vegetables due to resuspension over the 70 year period following the accident. The deposition rate is determined from the air concentrations derived from the resuspension model, assuming an effective deposition velocity of 0.01 m/s.

   - Root uptake. A bioaccumulation factor of 2.4×10^{-4} and an aerial soil density of 240 kg/m^2 were assumed (References A-16 and A-17)

- Rain splashup. (See Reference A-18). The contamination due to rain splashup was assumed to consist of 95 percent of that due to root uptake and rain splash-up combined. That is, the contamination due to rain splash-up was estimated as 19 times the amount calculated due to root uptake.

In the calculation of vegetable contamination due to resuspension, root uptake, and rain splash up over the 70-year period following release, deposition source depletion due to weathering and radioactive decay were taken into account.

The calculation of doses due to vegetable ingestion assumed an annual adult vegetable intake of 285 kg, which was obtained by every individual in the affected offsite residential population from a co-located vegetable garden. A wash-off factor of 0.5 is assumed just prior to ingestion. The ingestion dose conversion factors used are those presented in Section A.3.

3. External Radiation

Dose conversion factors used in the calculation of external dose, D_3, are based on Reference A-19. External dose are calculated over a 70 year period following an accident. A shielding factor of 0.5 is used, and deposition source depletion due to weathering and radioactive decay is taken into account.

4. Seafood and Fish Pathway

These doses result from the bioaccumulation of PuO_2 deposited on the surfaces of inland waters and ocean. In calculating water concentration, a mixing depth of 20 m was assumed in theKSC region and 75 m in worldwide regions. The densities of "caught" seafood and fish in Florida waters, based on Reference A-7, and associated bioaccumulation factors and ingestion rates used in the analysis are summarized in Table A-3. The pathway doses are calculated for a 70 year period, accounting for radioactive decay of the deposition source and a K_d of 10^5 (ratio of sediment concentration to water concentration). The ingestion dose conversion factors are those discussed in Section A.3.

A.3 Internal Dosimetry Model

A.3.1 Background

The internal dosimetry model used in the radiological consequence analyses performed in the NRAD is based on concepts developed in the Internal Commission on Radiological Protection (ICRP) Publication 30 (Reference A-14) with modifications

Table A-4

Parameter Values Used in the Analysis of Seafood/Fish Pathway Doses

Seafood/Fish	Mass Density kg/m^3-yr[a]	Bioaccumulation Factor	Adult Consumption Rates, kg/yr
Freshwater Fish	8.61×10^{-6}	40	0.4
Saltwater Fish	8.61×10^{-6}	40	4.0
Crustaceans	1.39×10^{-6}	300	1.8
Mollusca	2.48×10^{-6}	3000	

a. Mass density of "caught" seafood/fish in waters based on Reference A-7

reflected in the specific internal dosimetry model for Pu-238 in the form of PuO_2 presented in Reference A-20. In order to provide background for the internal dosimetry model used in this analysis, the original concepts developed in ICRP-30 are presented as applied to plutonium compounds.

The retention of PuO_2 particles within the respiratory system following inhalation will be a function of breathing rate and particle size, density, and solubility. For the purpose of internal dosimetry, the respiratory system, represented schematically in Figure A-8, consists of three regions that include the nasopharyngeal (N-P), tracheobronchial (T-B) and pulmonary (P) regions where initial deposition occurs. The deposition of particles as functions of the activity median aerodynamic diameter (AMAD) particle size and respiratory region is shown in Figure A-9. The actual physical diameter of a given particle has an equivalent AMAD that represents the diameter of a spherical particle of unit density (1.0 g/cm^3) that has the same terminal fall velocity. For example, particle sizes of 1, 10, and 100 μm AMAD correspond to PuO_2 particle sizes 0.32, 3.2, and 32 rem with a density of 10 g/cm^3 (see Appendix D).

Once initial lung deposition occurs, particles will be cleared from the respiratory system to either the lymph nodes, the blood, or the gastrointestinal system, and then to other organs of the body. The clearance of material from the respiratory system depends on the particle solubility. For the purpose of internal dosimetry, compounds have been classed as Y, W. or D solubility representing clearance half-times on the order of years, weeks, and days, respectively. The ICRP-30 recommended clearance parameters for plutonium compounds corresponding to the three solubility classes are also presented in Figure A-8. Material cleared to the gastrointestinal tract can be subsequently absorbed by the blood. The fraction absorbed, f_1, is 10^{-4} for W class plutonium compounds and 10^{-5} for Y class plutonium compounds.

Radiation dose is a measure of the energy transfer to organ tissue resulting from radioactive decay. The committed dose equivalent, H_{50}, to any organ due to a given radionuclide is discussed in ICRP Publication 30. The committed dose equivalent is defined as the dose to a given organ integrated over 50 years following the initial exposure. For alpha emitters, such as Pu-238, the Quality Factor is 20. The ICRP recommended system for limiting exposure is based on the principle that the limit on risk should be equal whether the whole body is irradiated uniformly or whether there is a non-uniform irradiation. Accordingly, a committed effective dose equivalent is calculated as follows:

Region	Compartment	Class D T day	D F	W T day	W F	Y T day	Y F
N P ($D_{N\ P}$ - 0 30)	a	0 01	0 5	0 01	0 1	0 01	0 01
	b	0 01	0 5	0 40	0 9	0 40	0 99
T B ($D_{T\ B}$ = 0 08)	c	0 01	0 95	0 01	0 5	0 01	0 01
	d	0 2	0 05	0 2	0 5	0 2	0 99
P (D_P = 0 25)	e	0 5	0 8	50	0 15	500	0 05
	f	n a	n a	1 0	0 4	1 0	0 4
	g	n a	n a	50	0 4	500	0 4
	h	0 5	0 2	50	0 05	500	0 15
L	i	0 5	1 0	50	1 0	1000	0 9
	j	n a	n a	n a	n a	∞	0 1

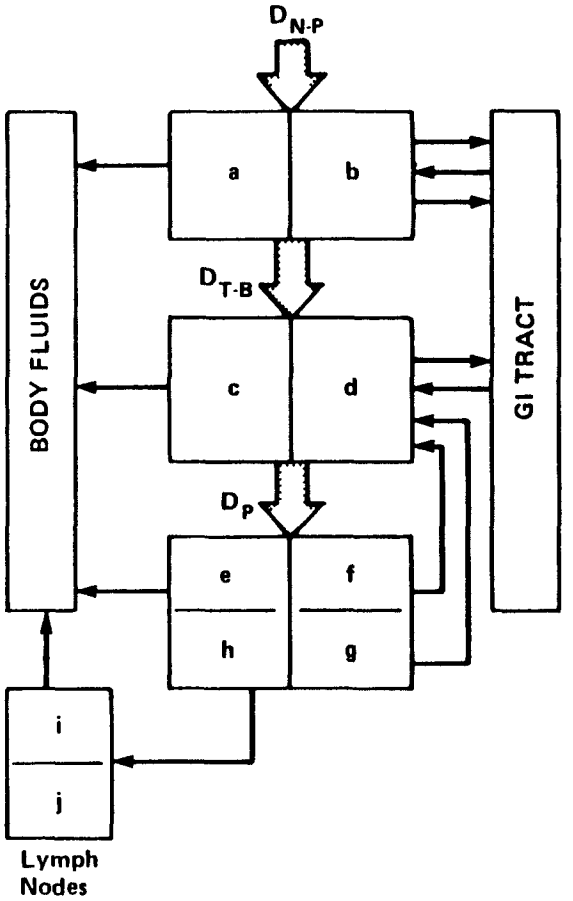

The values for the removal half-times, T_{a-l} and compartmental fractions, F_{a-l} are given in the tabular portion of the figure for each of the three classes of retained materials The values given for $D_{N\ P}$, $D_{T\ B}$ and D_P (left column) are the regional depositions for an aerosol with an AMAD of 1 μm The schematic drawing identifies the various clearance pathways from compartments a-l in the four respiratory regions, N-P, T-B, P and L

n a = not applicable

From ICRP Publication 30, Part 1

Figure A-8
MATHEMATICAL MODEL USED TO DESCRIBE CLEARANCE FROM THE RESPIRATORY SYSTEM

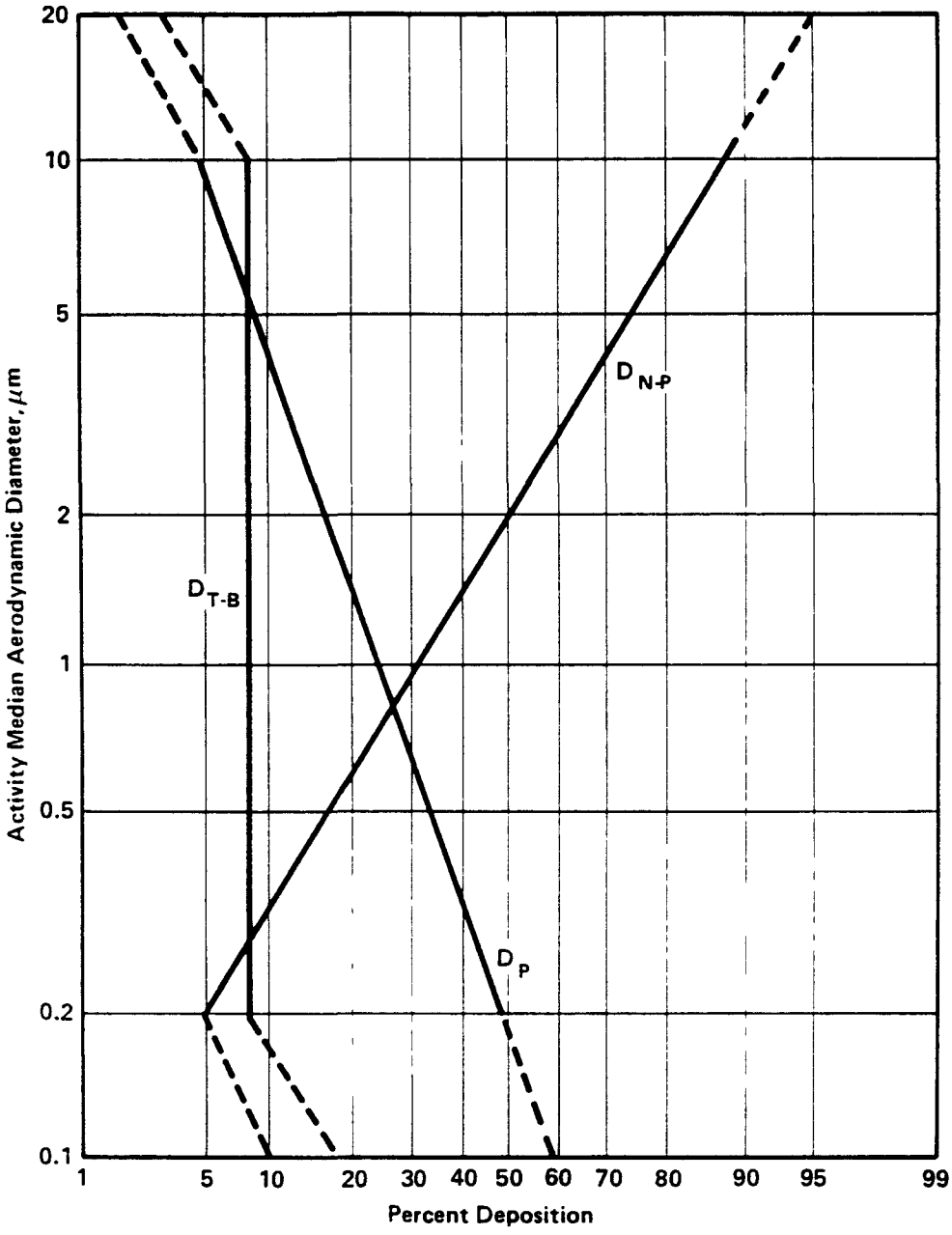

The percentage of activity or mass of an aerosol which is deposited in the N-P, T-B, and P regions is given in relation to the Activity Median Aerodynamic Diameter (AMAD) of the aerosol distribution The model is intended for use with aerosol distributions with AMADs between 0.2 and 10 μm and with geometric standard deviations of less than 4.5 Provisional estimates of deposition further extending the size range are given by the dashed lines For an unusual distribution with an AMAD of greater than 20 μm, complete deposition in N-P can be assumed The model does not apply to aerosols with AMADs of less than 0 1 μm

From ICRP Publication 30, Part 1

Figure A-9
DEPOSITION OF PARTICLES IN THE RESPIRATORY SYSTEM

$$H_{50,WB} = \sum_T W_T H_{50,T}$$

where

$H_{50,WB}$ = Committed effective dose equivalent, rem

$H_{50,T}$ = Committed dose equivalent to organ (tissue) T, rem

W_T = Weighting factor representing the stochastic risk resulting from organ (tissue) T to the total risk when the whole body is irradiated uniformly.

The weighting factors W_T recommended by ICRP are shown in Table A-5.

The ICRP 30 internal dosimetry model for ingested activity is the gastrointestinal portion of the inhalation model.

A.3.2 Revised Internal Dosimetry Model

The ICRP-30 internal dosimetry model uses three solubility classes to represent a large range of radionuclide chemical forms, as well as average transfer factor values for each class. The ICRP recognized this and states "The classification scheme and the clearance constants and regional fractions are to be used when no comparable information is available." Comparable information for inhaled 238-PuO_2 is now available based on extensive inhalation toxicological studies conducted at the Lovelace Inhalation Toxicology Research Institute and the Pacific Northwest Laboratory sponsored by the U.S. Department of Energy. This information is summarized in Reference A-20. Principal features of the revised internal dosimetry model are as follows:

- The inhalability of particulates (fraction inhaled) is that recommended by the American Conference of Governmental Industrial Hygienists (ACGIH) in Reference A-21 for particles up to 100 microns AMAD, given by:

  $F_i = 0.5(1 + e^{-0.06d_i})$

  where

  F_i = Fraction inhaled of particle size i, dimensionless

  d_i = Diameter of particle size i, microns AMAD

  For particles in the size range of 100 to 1500 microns AMAD, F_i decreases linearly from 0.5 to 0.0.

- Deposition of inhaled particulates in the respiratory system follows that recommended by ICRP-30 as presented

Table A-5
ORGAN WEIGHTING FACTORS, W_T

Tissue	Weighting Factors
Gonads	0.25
Breast	0.15
Red bone marrow	0.12
Lungs	0.12
Thyroid	0.03
Bone surfaces	0.03
Each of up to 5 organs with the next highest dose equivalent	0.06

in Figure A-10, with complete deposition occurring in the NP region for particles larger than 20 microns AMAD.

- A rapid initial transfer of PuO_2 from the NP region to the flood is estimated to be represented by a region transfer factor of 3.0×10^{-3}.

- The transfer fraction from the GI tract to the blood, f_i, during the first year is estimated to be 10^{-5}, increasing to 10^{-4} thereafter, reflecting a more rapid transfer observed than originally recommended in ICRP-30.

- Although in the past, as in ICRP-30, 238-PuO_2 has been treated as a Y solubility compound, research evidence cited above indicates clearance from the pulmonary region is better characterized by a fast-clearing portion ($T_{1/2}$ = 50 days) and a slow clearing portion ($T_{1/2}$ = 500 days). The associated region fractions and transfer half-times reflecting this feature, as well as those identified above, are summarized in Figure A-10.

- The clearance half-times from the bone and liver are the same as those in ICRP-30, being 100 and 40 years, respectively.

Based on Reference A-20, NUS incorporated calculated particle-size-dependent internal dose conversion factors for inhalation exposure based on the fraction inhaled, deposition fractions within the respiratory regions, clearance half-times, and region transfer fractions. The dose commitment period was extended from the ICRP-30 value of 50 years to 70 years. The 70-year dose commitment period is used to account for the age span of the population and because the internal dosimetry model used in the analysis is not age dependent. Two types of inhalation dose conversion factors were developed as follows:

- Short-term inhalation dose conversion factors where all material is inhaled at time t = 0, f_1 is initially 10^{-5}, and increases to 10^{-4} after the first year. The resulting internal dose factors for lung, bone, and liver are presented in Table A-6. These results are in terms of "committed dose equivalents" as defined by ICRP-30 except for the extension of the dose commitment period from 50 to 70 years. In addition, the "committed effective dose equivalent" is presented, representing the application of the organ weighting factors presented in Table A-6 to the "committed dose equivalents", as described earlier in this section.

- Long-term inhalation dose conversion factors. These factors involve continuous inhalation of resuspended material. Two sets are required:

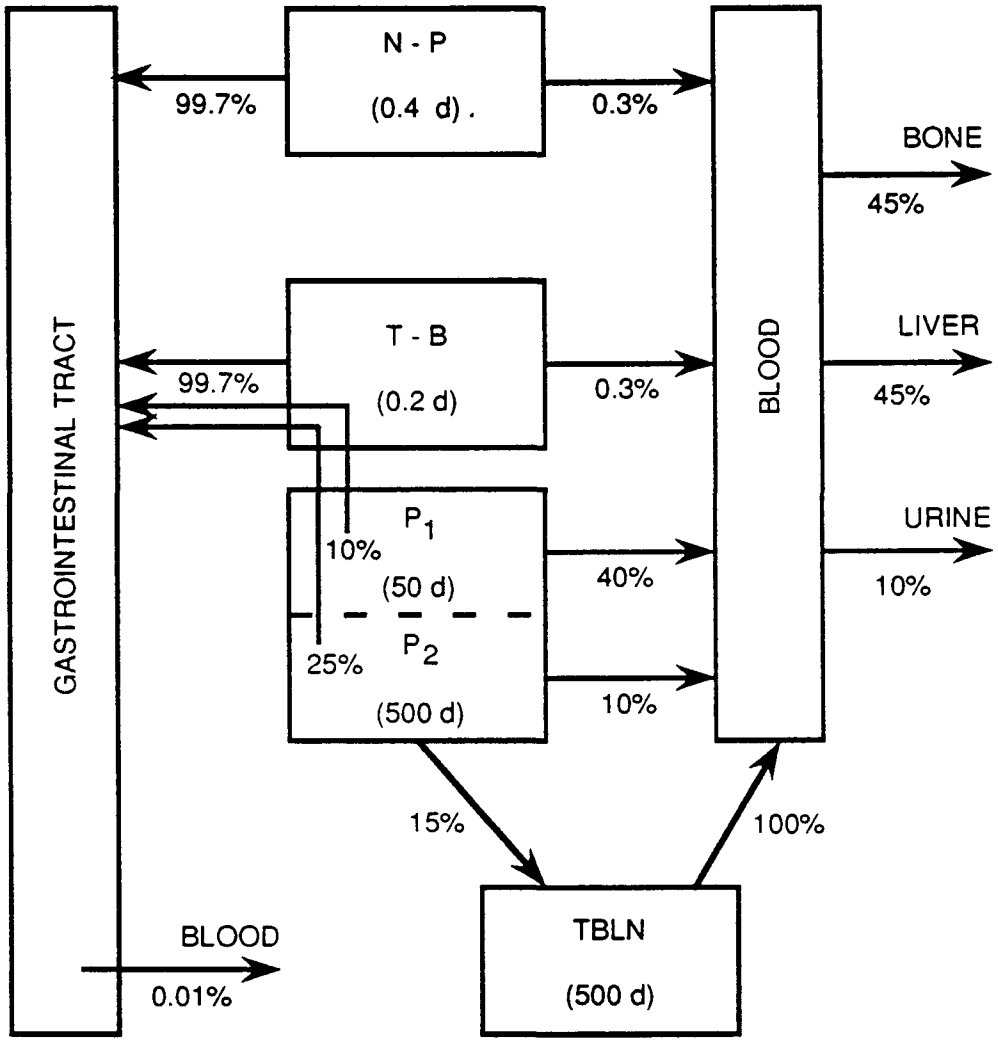

Figure A-10
INSRP-RECOMMENDED INTERNAL DOSIMETRY MODEL

Table A-6
Short-Term Inhalation Dose Conversion Factors

Physical Particle Size Range, μm	Activity Median Particle Size, μm	AMAD Particle Size, μm	Inhalation DCF, rem/μCi Inhaled			Depletion Fraction, α	Inhalation DCF, rem/μCi-s/m³			
			Lung	Bone Surface	Liver		Lung	Bone Surface	Liver	EWBCDE
2000-6000										
840-2000										
420-840	694									
177-420	341	1000	0.0	3.00E+02	6.01E+01	0.167	0.0	9.39E-03	1.88E-03	3.94E-04
125-177	155	620	0 0	3.00E+02	6.01E+01	0.314	0.0	1.77E-02	3.54E-03	7.43E-04
74-125	106	470	0.0	3.00E+02	6.01E+01	0.368	0.0	2.07E-02	4.15E-03	8.70E-04
44-74	63	265	0 0	3.00E+02	6.01E+01	0.441	0.0	2.48E-02	4.97E-03	1.04E-03
30-44	38	135	0.0	3.00E+02	6.01E+01	0.488	0.0	2.74E-02	5.50E-03	1.15E-03
20-30	26	82	0.0	3.00E+02	6.01E+01	0.5	0.0	2.81E-02	5.63E-03	1.18E-03
10-20	16.5	52	0.0	3.00E+02	6.01E+01	0.5	0.0	2.81E-02	5.63E-03	1.18E-03
9-10	9.5	30	0.0	3.00E+02	6.01E+01	0.5	0.0	2.81E-02	5.63E-03	1.18E-03
8-9	8.5	26	0.0	3.00E+02	6.01E+01	0.605	0.0	3.40E-02	6.82E-03	1.43E-03
7-8	7.5	24	0.0	3.00E+02	6.01E+01	0.618	0.0	3.48E-02	6.96E-03	1.46E-03
6-7	6.5	20	0.0	3.00E+02	6.01E+01	0.651	0.0	3.66E-02	7.34E-03	1.54E-03
5-6	5.5	17	0.0	3.00E+02	6.01E+01	0.680	0.0	3.95E-02	7.66E-03	1.61E-03
4-5	4.6	15	0.0	3.00E+02	6.01E+01	0.703	0.0	3.95E-02	7.92E-03	1.66E-03
3-4	3.6	12	0.0	3.00E+02	6.01E+01	0.743	0.0	4.18E-02	8.37E-03	1.76E-03
2-3	2.6	8.4	2.98E+01	9.41E+02	2.27E+02	0.802	4.48E-03	1.42E-01	3.41E-02	6.84E-03
1-2	1.6	5.2	2.88E+02	6.68E+03	1.71E+03	0.866	4.68E-02	1.08E+00	2.78E-01	5.47E-02
0-1	0.79	3	5.73E+02	1.30E+04	3.35E+03	0.918	9.86E-02	2.24E+00	5.77E-01	1.14E-01
0.02	0.02	0.12	6.51E+02	1.46E+04	3.38E+03	0.996	1.22E-01	2.73E+00	6.31E-01	1.34E-01

$$DCF\left[\frac{rem}{\mu Ci-s/m^3}\right] = DCF\left[\frac{rem}{\mu Ci\ inhaled}\right] x \frac{BR\,[m^3/s]\ \psi\left[\frac{\mu Ci-s}{m^3}\right] x\ \alpha}{\psi\left[\frac{\mu Ci-s}{m^3}\right]}$$

$$BR = (750\ cm^3/resp)(15\ resp/min)(1\ min/60\ s)(10^{-6}\ m^3/cm^3)$$

$$= 1\ 875\ E-04\ m^3/5$$

Table A-7
Long Term Inhalation Dose Conversion Factors

Continuous Exposure Conversion Factors (Inhalation)

Physical Particle Size Ranges, μm	Physical Median Size, μm	AMAD Size, μm	Inhalation Dose Factors for Continuous Exposure, Rem/μCi-s/m³ Per Year											
			Exposure 0 1 yr[a]				Exposure 1-70 yr[b]				Exposure 0-70 yr[c]			
			Lung	Bone Surface	Liver	EWBCDE	Lung	Bone Surface	Liver	EWBCDE	Lung	Bone Surface	Liver	EWBCDE
177 420	341	1000	0 0	9 39E-03	1 88E 03	3 94E 04	0 0	3 88E 01	8 55E 02	1 68E-02	0 0	3 97E-01	8 74E-02	1 72E-02
125 177	155	620	0 0	1 77E-02	3 54E 03	7 43E 04	0 0	7 30E-01	1 61E-01	3 16E-02	0 0	7 48E-01	1 65E-01	3 23E-02
74 125	106	470	0 0	2 07E-02	4 15E 03	8 70E-04	0 0	8 56E-01	1 88E-01	3 70E 02	0 0	8.77E-01	1 92E-01	3 79E-02
44 74	63	265	0 0	2 48E-02	4 97E 03	1 04E-03	0 0	1 03E+00	2 26E-01	4 44E-02	0 0	1.05E+00	2.31E-01	4.54E-02
30 44	38	135	0 0	2 74E-02	5 50E 03	1 15E-03	0 0	1 04E+00	2 29E-01	4 51E-02	0.0	1 07E+00	2.34E-01	4.62E-02
20-30	26	82	0 0	2 81E-02	5 63E-03	1 18E-03	0 0	1 16E+00	2 56E-01	5 03E-02	0 0	1.19E+00	2.62E-01	5.15E-02
10-20	16 5	52	0 0	2 81E-02	5 63E-03	1 18E-03	0 0	1 16E+00	2 56E-01	5.03E-02	0 0	1.19E+00	2.62E-01	5.15E-02
9-10	9 5	30	0 0	2 81E-02	5 63E-03	1 18E-03	0 0	1 16E+00	2 56E-01	5 03E-02	0.0	1 19E+00	2.62E-01	5.15E-02
8-9	8 5	26	0.0	3 40E-02	6 82E-03	1 43E-03	0 0	1.41E+00	3 10E-01	6 09E-02	0 0	1.44E+00	3.17E-01	6.23E-02
7-8	7.5	24	0 0	3 48E-02	6 96E-03	1 46E-03	0 0	1 44E+00	3 16E-01	6 22E-02	0.0	1 47E+00	3 23E-01	6 37E-02
6-7	6 5	20	0 0	3 66E-02	7 34E-03	1 54E-03	0 0	1 51E+00	3 33E 01	6 55E-02	0 0	1.55E+00	3 40E-01	6.70E-02
5 6	5 5	17	0 0	3 83E-02	7 66E-03	1 61E-03	0 0	1 58E+00	3 48E-01	6 85E-02	0 0	1.62E+00	3 56E-01	7 01E-02
4-5	4 6	15	0 0	3 95E-02	7 92E-03	1 66E 03	0 0	1 63E+00	3 60E-01	7 08E 02	0 0	1 67E+00	3 68E-01	7.25E-02
3 4	3 6	12	0 0	4 18E 02	8 37E 03	1 76E 03	0 0	1 73E+00	3 80E 01	7 48E-02	0 0	1 77E+00	3 88E-01	7 66E-02
2-3	2 6	8 4	4 48E 03	1 42E-01	3 41E 02	6 84E-03	3 05E 01	5 76E+00	1 52E+00	2 99E-01	3 09E-01	5 90E+00	1 55E+00	3 06E 01
1-2	1 6	5.2	4 68E 02	1 08E-02	2 78E 01	5 47E-02	3 18E+00	4 37E+01	1 22E+01	2 44E+00	3 23E+00	4 48E+01	1 25E+01	2 49E+00
0-1	0.79	3	9 86E-02	2 24E+00	5 77E 01	1 14E 01	5 87E+00	9 07E+01	2 55E+01	5 04E+00	5 97E+00	9.29E+01	2 61E+01	5.15E+00
0 02	0 02	0.12	1.22E-01	2 73E+00	6 31E-01	1 34E-01	8 27E+00	1 10E+02	3 06E+01	6 14E+00	8.39E+00	1.13E+02	3 12E+01	6.27E+00

a. $f_1 = 10^{-5}$ during first year of exposure and internally becomes 10^{-4} after one year
b $f_1 = 10^{-4}$ during entire exposure period
c. $f_1 = 10^{-5}$ during first year and 10^{-4} thereafter for all material

- Set 1 is for continuous inhalation during the first year when $f_1 = 10^{-5}$ and is applied to the average resuspended airborne concentration during the first year. Set 1 is presented in Table A-7.

- Set 2 is for continuous inhalation during the period 1 to 70 years when $f_1 = 10^{-4}$ and is applied to the average resuspended air concentration during the same period. Set 2 is also presented in Table A-7.

In addition, ingestion dose conversion factors were developed by NUS using the ingestion portion of the internal dose model presented in Reference A-20. In this case, assuming continuous ingestion, two dose factor sets result: one for vegetable ingestion with $f_1 = 10^{-4}$ (the first year and 10^{-3} thereafter); and one for seafood ingestion with $f_1 = 10^{-3}$ (initially and constant thereafter). The results are summarized in Table A-7.

A.4 PLUME CONFIGURATION MODEL

The radiological consequences resulting from accidental releases of PuO_2 at low altitude in the launch pad vicinity will be significantly influenced by the initial distribution of material in the resulting plume, and the configuration of the plume. Two types of plume configurations of interest include those associated with ground level releases outside a thermal environment and those associated with liquid propellant explosions and after fires.

For ground level releases outside the thermal environment, the puff of released fuel following impact has been taken to be a spherical puff 10 m in diameter and a center height of 5 m. The material within the puff has a Gaussian distribution with a standard deviation of $\sigma_y = \sigma_z = 2.5$ m. The puff diameter of $4\sigma_y = 4\sigma_z = 10$ m encloses 95 percent of the released fuel within the spherical puff so defined.

For postulated accidents involving liquid propellant explosions, an initial fireball is formed that lifts off from the ground after approximately 10 seconds and continues growing to a maximum diameter of approximately 300 m, as described in Reference A-14. The fireball represents the luminous visible volume of gas following the explosion. A stem extends below the fireball to ground level. However, further expansion, cooling, and mixing with ambient air, followed by condensation of water vapor at higher elevations, results in a stabilized cloud much larger than the fire ball. Furthermore, the stabilized cloud would have a stem extending from the cloud bottom to ground level containing material entrained by the post-explosion residual fire, as well as material spread out from the cloud bottom as the cloud rose vertically to its stabilized height.

Reference A-15 provides information relating cloud dimensions and the energy released in explosions appropriate to current

Table A-8
Ingestion Dose Conversion Factors

Continuous Exposure Dose Conversion Factors (Ingestion)

	Ingestion Dose Factor for Continuous Exposure Periods, rem/μCi per year ingested							
Organ	Exposure 0-70 yr[a]	Exposure 0-1 yr[a]	Exposure 0-70 yr[a]	Exposure 0-1 yr[b]	Exposure 0-70 yr[c]	Exposure 0-1 yr[d]	Exposure 0-70 yr[d]	Exposure 0-1 yr[e]
Lung	-	-	-	-	-	-	-	-
Bone Surface	3.47E+02	8.36E+00	3.39E+02	8.36E-01	3.40E+02	8.36E+01	3.39E+03	6.61E-01
Liver	7.61E+01	1.67E+00	7.44E+01	1.67E-01	7.46E+01	1.67E+01	7.44E+02	1.48E-01
EWBCDE	1.50E+01	3.51E-01	1.46E+01	3.51E-02	1.46E+01	3.51E+00	1.46E+02	2.89E-02

a. $f_1 = 10^{-4}$ (Small intestine to blood transfer factor)
b. $f_1 = 10^{-5}$
c. $f_1 = 10^{-5}$ Over first year and then increases to f1 = 10^{-4} thereafter
d. $f_1 = 10^{-3}$ Applicable to seafood pathway
e. Used in FSAR (1985)

application. The plume configuration resulting from the explosion of liquid propellants that include 1.55×10^6 lbs in the External Tank, 4.35×10^4 lbs in the Centaur, and 2.25×10^4 in the Orbiter has been estimated based on results of high-explosive field tests involving both liquid and solid high explosives. The cloud dimensions were estimated by the following equation:

$$C_c = \text{height to cloud center (m)} = 500\ W^{0.25}$$

$$C_d = \text{diameter of cloud (m)} = 335\ W^{0.25}$$

where

W = Explosive charge TNT equivalent weight, tons

The thermal release associated with the complete combustion of liquid propellants is estimated to be 2.78×10^{12} calories. It is estimated that approximately 50 percent of this heat will be radiated away from the initial fireball resulting in a thermal input to cloud development of 1.39×10^{12} calories. This was taken to be equivalent to 1.39 kilotons of TNT, where one kiloton of TNT has an associated thermal release of 10^{12} calories.

Using these values, the resulting height to the cloud center is 3053 m and the associated cloud diameter is 2045 m. The cloud stem would stretch from ground level to the cloud bottom at a height of 2045 m. The diameter of the stem is taken to be on the order of the maximum fireball diameter, or 300 m.
From a radiological consequences viewpoint, the smaller and lower in height the initial cloud of released radioactive material is, the higher the ground level air concentrations and the resulting radiological consequences. Therefore, for the most probable release cases considered in the NRAD, the cloud and cloud stem dimensions calculated above have been used. For the maximum cases (those maximizing radiological consequence) plume dimensions have been estimated based on 10 percent of the thermal release used in the most probable case. This resulted in a cloud center height of 1717 m, a cloud diameter of 1150 m, and a stem extending from ground level to the cloud bottom height of 1150 m. The stem diameter was again taken to be on the order of the maximum fireball diameter, or 300 m. This is within the range of observed cloud behavior.

The distribution of material in the cloud and cloud stem was taken to be Gaussian about its defined center with the following standard deviations in the horizontal and vertical directions, representing one fourth of the dimensions stated above:

Most probable release case:

Cloud: $\sigma_y = \sigma_z = 511$ m

Stem: $\sigma_z = 511$ m
$\sigma_y = 75$ m

Maximum case:

Cloud: $\sigma_y = \sigma_z = 288$ m

Stem: $\sigma_z = 288$ m
$\sigma_y = 75$ m

The distribution of released fuel in the vertical direction has been based on measurements of air concentrations of debris as a function of height following high explosive field tests described in Reference A-15. For the purpose of the NRAD analyses, 80 percent of PuO_2 released in the fireball has been put in the cloud and 20 percent in the stem. Uncertainties related to the plume configuration, vertical distribution of material, and particle stratification are addressed further in Appendix H, Uncertainty Analysis.

Diagrams showing the resulting distribution of material with height for the most probable release case and the maximum case are presented in Figure A-11.

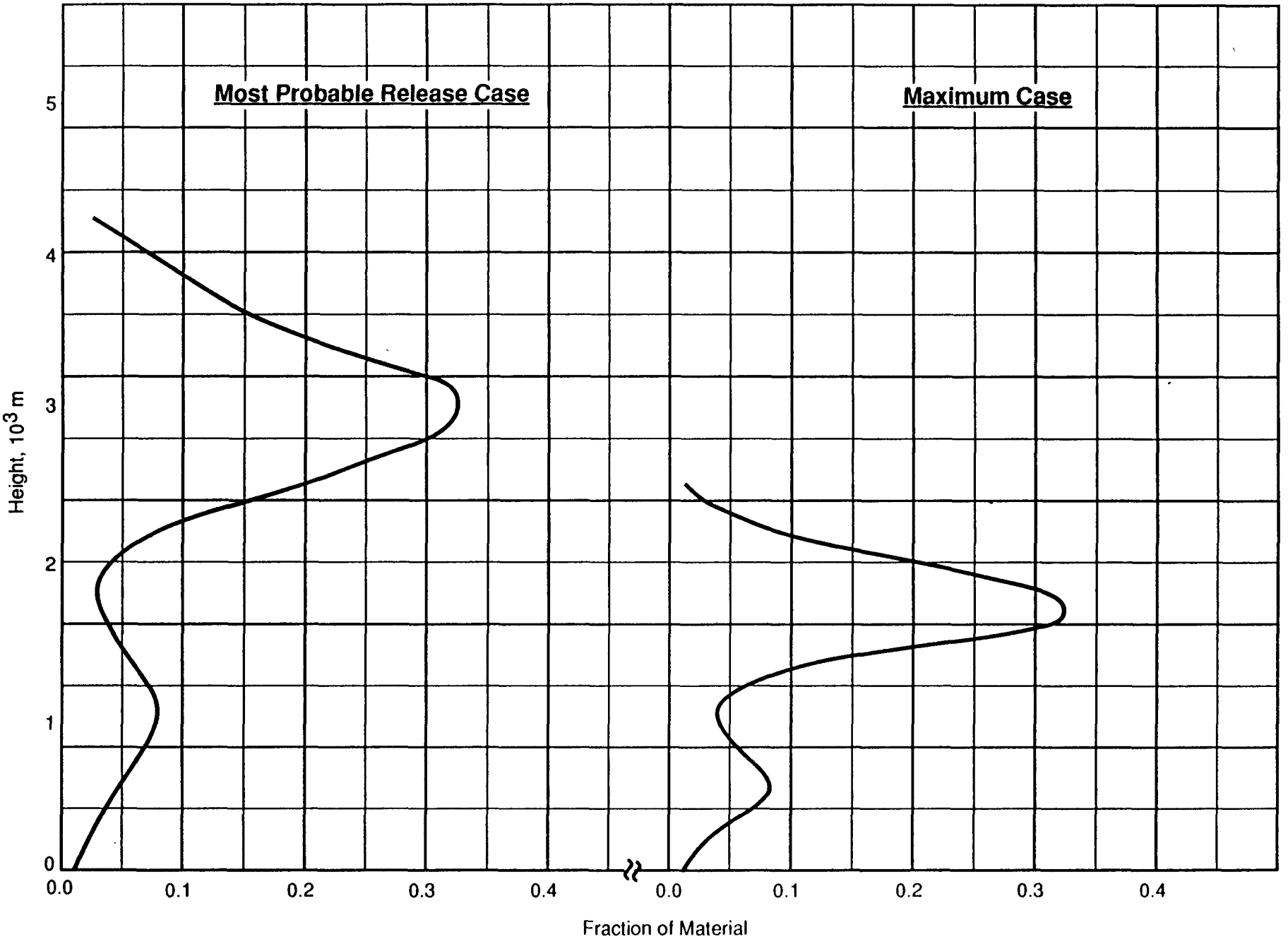

Figure A-11
PLUME CONFIGURATION MODELS

A.5 REFERENCES

A-1 National Council on Radiation Protection and Measurements, Recommendations on Limits for Exposure to Ionizing Radiation, NCRP Report 91 (June 1, 1987)

A-2 U.S. Environmental Protection Agency, Interim Recommendations on Doses to Persons Exposed to Transuranium Elements in the General Environment, Summary Report Discussion Draft (October 31, 1984).

A-3 Person Communication between A. Wallo of the U.S. Department of Energy and R. Englehart/B. Bartram of NUS Corporation (December 1988).

A-4 U.S. Department of Energy, Guidelines for Residual Radioactive Material at Formerly Utilized Sites Remedial Action Program and Remote Surplus Facilities Management Program Sites, Rev. 2, Appendix A (March 1987).

A-5 Firstenberg, H., EMERGE: An Accident Assessment Program for the Galileo and Ulysses Missions, NUS Corporation, NUS-5076 (1988).

A-6 Bartram, B.W. et al, Application of EMERGE to Launch Window Assessments and Safety Analyses for the Galileo and Ulysses Missions, NUS-4931, NUS Corporation (1986).

A-7 NUS Corporation, Overall Safety Manual, Prepared for U.S. Department of Energy (1982).

A-8 Garrett, A.J., and C.E. Murphy, A Puff-Plume Atmospheric Deposition Model for Use at SRP in Emergency Response Situations, Savannah River Laboratory, E.I. du Pont de Nemours and Company, DP-1595 (May 1981).

A-9 Luna, R.E., and H.W. Church, DIFOUT: A Model for Computation of Aerosol Transport and Diffusion in the Atmosphere, Sandia National Laboratories, SC-RR-68-555 (1969).

A-10 Rodrigues, P., et al, User's Guide to the MATHEW/ADPIC Models, Lawrence Livermore National Laboratory, UASG 82-16 (1982).

A-11 Dickerson, M. and R. Orphan "Atmospheric Release Advisory Capability", Nuclear Safety, Vol. 17, No. 3 (May-June 1976).

A-12 NUS Corporation, Validation of the ATMOS Atmospheric Dispersion Model Used in the [1985 Nuclear Risk Analysis of the Galileo and Ulysses Missions, NUS-4783 (1986).

A-13 Huge, K.D., et al, A Computer Model for the Fall and Dispersion of Particles in the Atmosphere, Prepared for Sandia Corporation by Travellers Research Corporation, SC-CR-67-2530 (1967).

A-14 International Commission on Radiological Protection, Limits for Intakes of Radionuclides by Workers, ICRP Publication 30 (1979).

A-15 Bartram, B.W. and D.K. Dougherty, A Long-Term Radiological Risk Model for Plutonium-Fueled and Fission Reactor Space Nuclear Systems, NUS Corporation, NUS-3845 (1982).

A-16 Momeni, M.H., Y. Yuan, and A.J. Zielen, The Uranium Dispersion and Dosimetry (UDAD) Code, Prepared for U.S. Nuclear Regulatory Commission by Argonne National Laboratory, NUREG/CR-0553 (May 1979).

A-17 Strenge, D.L. and T.J. Bander, MILDOS-A Computer Program for Calculating Environmental Radiation Doses from Uranium Recovery Operations, Prepared for U.S. Nuclear Regulatory Commission by Pacific Northwest Laboratory NUREG/CR-2011 (March 1981).

A-18 Dreker, M., T.E. Hakonson, G.C. White, and F.W. Whicker, "Rainsplash as a Mechanism for Soil Contamination of Plant Surfaces", Health Physics, Vol. 46, No. 1 (January 1984).

A-19 Kocher, D.C., "Dose Rate Conversion Factors for External Exposure to Photon and Electron Radiation from Radionuclides Occurring in Routine Releases from Nuclear Fuel Cycle Facilities", Health Physics, Vol. 38, No. 4 (April 1980).

A-20 Cuddihy, R., Recommended Respiratory Tract Dosimetry Model for Inhaled 238-PuO_2, Prepared for Interagency Nuclear Safety Review Panel (November 19, 1985).

A-21 ACGIH Technical Committee on Air Sampling Procedures, Particle Size-Selective Sampling in the Workplace, American Conference of Governmental Industrial Hygienists (1985).

A-22 National Aeronautics and Space Administration Space Shuttle Data for Planetary Mission Radioisotope Thermoelectric Generator Safety Analysis, NSTS-08116, Draft, Rev. A (June 2, 1987).

A-23 Gould, K.E., High-Explosive Field Tests, Explosion Phenomena and Environmental Impacts, Prepared for Defense Nuclear Agency by Kaman Tempo, DNA-6187F (1981).

APPENDIX B

BIOMEDICAL CONSIDERATIONS OF PLUTONIUM 238 OXIDE

B.1 INTRODUCTION AND SUMMARY

The purpose of this Appendix is to present relevant radiological/biomedical information, the use of which may help in interpreting the dosimetric results of accident scenario analyses. This includes justification for analyses of 238-PuO_2 doses only (since the contribution of other isotopes is small), a discussion of important pathways for dose to persons relative to mission phases and their relative radiological significance, and a section on biomedical effects of high doses to individuals and of population doses (usually low doses to larger population groups).

The dominant dose pathway to man is direct inhalation exposure to initial cloud passage for most postulated accidents. Resuspension inhalation of ground deposited material over extended periods is the second most important pathway. Although resuspended air concentrations are much smaller than initial plume air concentrations, the time of exposure considered in this assessment (up to 70 years) is much longer than to the initial plume exposure. Therefore, resuspension inhalation doses can be a significant contributor to total dose. Particle size is extremely important in delivery of dose since particles above 10 microns activity median aerodynamic diameter (AMAD) are very inefficiently deposited and retained in the lung.* Ingestion pathways are much less significant because of inefficient uptake by plants and animals and a very low fraction for adsorbtion in the human digestive tract.

It is recognized that there are age differences for dose-conversion factors, but these are not significantly different to justify reporting separately. As a result of the dosimetry proposed by the INSRP Biomedical and Environmental Effects Subpanel for the 1986 SER, the bone is the critical organ, instead of lung.

For the magnitudes of doses to the public calculated in this report, a few potential statistical lung, bone, and liver cancers in large exposed populations are the mode of health effect delivery which might occur in the event of an accident releasing fuel.

The AMAD is the diameter of a spherical particle of unit density having the same terminal fall velocity as the real particle with its real physical diameter. Ten microns AMAD is equivalent to 3.2 microns physical diameter for PuO_2.

B.2 GPHS-RTG AND LWRHU FUEL DESCRIPTION

The energy source (fuel) of the GPHS-RTGs and the LWRHUs is the alpha decay of the Pu-238 nucleus. The form of the material incorporated in these devices is plutonium dioxide (PuO_2). The physical properties and characteristics of the fuel are described in Appendix A of FSAR Volume I, Reference Design Document. From a biomedical standpoint, the isotopic content of the fuel is of significance because of the differing dosimetric characteristics of the various nuclides involved. A detailed quantification of the radionuclides in the RTGs and LWRHUs is contained in Reference B-1, and presented in Table B-1.

Because of the dominance of 238-PuO_2 in Curie content and the similar magnitudes of the dose conversion factors of the nuclides (see Table B-2), it is sufficient to characterize risk in terms of plutonium-238 oxide alone, especially given the uncertainties of the accident environments, probabilities, and GPHS-RTG and LWRHU response, associated with source-term estimates and the uncertainties of the probability estimates. The combination of the other isotopes compared to Pu-238 represents less than one percent of the total dose.

Plutonium oxide that has been heated to more than 1000°C is very difficult to dissolve in the common acids (Reference B-3) which is evidence of its chemical stability. Since the material has been high fired to in excess of 1500°C, it is expected to remain predominantly in oxide form if released into the environment.

B.3 PATHWAYS TO MAN

Launch-pad or near-launch-pad ascent accidents may involve releases to the atmosphere; the predominant concern would be atmospheric transport of particulates inland and subsequent inhalation doses to people, both during initial cloud passage and from resuspension of ground-deposited material (long term).

Later ascent accidents could involve atmospheric releases and also the possibility of the exposure of fuel to seawater. If Fueled Clads are not ruptured by fragments or the clad is not melted during reentry, the fuel and clad materials (iridium for the GPHS-RTG and platinum-rhodium for the LWRHU) are sufficiently impervious to corrosion so as not to release fuel to the seawater for a long time. Exposure of GPHS Fueled Clads in seawater have been tested for up to 48 months (Reference B-4). These studies indicate that the heat generated promotes encrustation which effectively seals Fueled Clads and enhances encapsulation. The encapsulation phenomena would apply only to Fueled Clads existing in shallow seawater. However, even when fuel is exposed to seawater, the dissolution rate is very small (on the order of 3.0 X 10^{-12}ng/m^2-s, Reference B-5), resulting in very low water concentrations. The primary mode of subsequent exposure to humans would be through the consumption of contaminated seafood.

Table B-1 - Initial Assay of Radionuclides[a]
Typical Content

	GPHS-RTG (F-1 Unit)		LWRHU	
Radioisotope	Curies	Percent	Curies	Percent
Pu-236	2.46E-02	1.74E-05	8.61E-04	2.52E-05
Pu-238	1.37E+05	97.3	3.32E+03	97.2
Pu-239	8.01E+01	5.69E-02	2.01E+00	1.43E-03
Pu-240	4.13E+01	2.93E-02	1.02E+00	2.99E-02
Pu-241	3.73E+03	2.65	9.27E+01	2.71
Pu-242	4.65E-02	3.30E-05	1.18E-03	3.45E-05
Am-241	3.27E+00	2.32E-03	2.33E-01	6.82E-03
Np-237	5.63E-03	4.00E-05	3.81E-05	1.12E-06
U-234	2.76E-02	1.96E-05	1.03E-02	3.02E-04
Th-232	9.25E-07	6.57E-10	6.78E-09	1.98E-10

a. Additional radionuclides are present at launch time by virtue of the decay chains of the parent radionuclides listed above. However, since the parent nuclides are long half-lived isotopes, the daughter nuclide curie strengths are small compared to the parent. Dose conversion factors are comparable. Ingrowth of Am-241 at mission times corresponding to VEEGA maneuver could increase to on the order of 3000 curies.

Source: Reference B-1.

Table B-2 - Dose Conversion Factor Comparison for 1.0 micron AMAD Particles[a]

Radioisotope	DCF, Rem/μCi Inhaled Translocation Class	
	Y (Lung)	W (Bone)
Pu-238[b]	5.1E+02	1.4E+03
Pu-239	4.8E+02	1.6E+03
Pu-240	4.8E+02	1.6E+03
Pu-241	8.5E-01	2.9E+01
Pu-242	4.6E-01	1.5E+03
Am-241	5.2E+02	8.8E+02

a. Lung doses are listed for Y compounds and bone doses for W compounds since Y implies slow translocation from the lung while W implies relative rapid translocation to other organs (bone is dominant for those included). This particle size is representative of the radiologically most significant particle size range (to 10 micron AMAD).

b. The 238 PuO2 dose conversion factors used in the NRAD based on the INSRP Biomedical and Environmental Effects Subpanel model proposed to the 1986 SER are presented in Appendix A. The dose factors presented above are for relative comparison only.

Source: Reference B-2

Reentry of GPHS modules is expected to result in intact reentry impact of the modules. This could result in an atmospheric release only if a module were to fail upon impact on a rock surface with hardness comparable to granite. A VEEGA reentry could result in free Graphite Impact Shells (GISs) releasing fuel on rock impact and both vaporization and bare fuel from LWRHUs.

Besides inhalation doses, atmospheric releases also involve the ingestion pathway, either from direct ingestion of foodstuffs contaminated by deposition or by ingestion of material through uptake of PuO_2 by vegetation or animals and subsequent consumption by man. Finally, atmospheric releases result in ground deposition of material, which results in groundplane radiation, transport of material into soils, or in rainwater runoff.

B.4 RADIOLOGICAL SIGNIFICANCE OF DOSE DELIVERY PATHWAYS

B.4.1 Direct Inhalation

This pathway is the primary focus of the mission risk assessment because it is the one potentially involving the highest dose to individuals (as differentiated from highest population dose). It also is a mode of dose delivery which cannot be avoided unless evacuation in the projected path of cloud transport is undertaken. The inhalation dose model associated with the INSRP Biomedical and Environmental Subpanel 1986 SER, as applied to potential mission accidents is described in Appendix A. Particle size is an important consideration in this evaluation, since the smaller size ranges are more susceptable to direct and resuspension inhalation.

B.4.2 Resuspension Inhalation

This pathway results when particulates are deposited on the ground and are later resuspended in the atmosphere by surface disturbance (i.e., by wind or plowing). It is the second most significant pathway.

Material deposited on the ground by cloud spreading (vertically) and settling (the action of gravity) is less concentrated in the area of a person (his immediate environment) than during the initial cloud passage. In addition, the resuspension factor, an empirical parameter factor relating air concentration to ground concentration, is fairly small, (10^{-5} M^{-1}) initially, and decreases with time because of weathering (penetration into the soil with rain, etc.) to 10^{-9} M^{-1} (See Appendix A). However, unless the material is removed or immobilized or persons are restricted from access, inhalation of material continues during the lifetime of individuals existing in that environment.

In areas of deposition of large particles, there is the potential for breakdown of these into smaller inhalation-important particulates. It is also possible for smaller particulates to agglomerate to less significant (larger) particle sizes. Finally, it has been demonstrated that fuel chunks, large enough to be thermally warm, undergo spallation, producing inhalable particulates. These phenomena should be considered in the event of an accident in decision making for cleanup operations, etc., but they are not considered sufficiently significant to alter the mission risk assessment based on the original particle size data.

B.4.3 Ingestion

Ingestion of environmentally released PuO_2 can occur from consumption of 1) vegetation contaminated by direct deposition, splash-up of material on the ground to leaf surfaces by rain, or by root uptake, of 2) animals which have consumed contaminated foodstuff or of 3) fish and seafood which are caught in contaminated waters. Because of the low root uptake and fish/seafood concentration factors, the dominant ingestion pathways would be through swallowing material cleared following inhalation and direct consumption of externally contaminated foodstuffs. However, the transfer of this material to the organs of the body is very inefficient. As noted in Appendix A, the INSRP 1986 SER model has a GI tract to transfer factor of 10^{-3} to 10^{-4}.

Because of the factors described here, transport of plutonium through the foodchain and subsequent ingestion is generally of lesser importance than inhalation (Reference B-6), as confirmed by analyses for the NRAD.

B.5 CHRONIC HEALTH EFFECTS OF RADIATION

The health effects which are thought to be caused by radiation exposure of the type and in the range of doses analyzed for RTG accidents can be divided into three categories - cancer, genetic effects, and mental retardation.

Within each category, two types of radiation are discussed: high-LET and low-LET. LET means linear-energy-transfer and refers to the spatial density at which the energy from radiation is deposited in human tissue. High-LET radiation includes neutrons, protons, and alpha particles, while low-LET radiation includes x-rays, gamma rays, and electrons. The doses and resulting health impacts are different from these two types of radiation.

In all scientific disciplines, especially those concerning medical statistics, numerical estimates involve some level of uncertainty. In the study of radiation-induced health effects, the major source of uncertainty stems from the method selected to extrapolate observed radiation effects in humans and animals

at high doses (ranging up to 1000 rem) down to the much lower doses (less than 1 rem). Other sources of uncertainty include statistical errors, errors in diagnosis, and others.

Many scientists believe that there are no health effects from radiation below 1 rem. In fact, many believe that the small amount of radiation that we are exposed to daily (0.2 rem/yr) is actually beneficial. Further, no one has ever demonstrated any health effects from radiation at these levels. For these reasons, the lower end of uncertainty in all of the estimates present here is zero. That is to say, there is a small possibility that no health effects would result from exposure of up to 1 rem in any one year. The risk estimators presented here are the upper end of the risk range.

For each category of health effect, the best or central estimate of the upper end of the risk range is provided. To characterize the uncertainty associated with this best estimate, an upper and lower bound is provided. In the NRAD, health effect calculations are based on the central estimate.

B.5.1 Cancer Induction

Cancer is the most readily recognized and best understood health effect of radiation. Epidemiological studies of the survivors of the atomic bomb detonations at Hiroshima and Nagasaki at the end of World War II have provided a basis for estimating the cancer risk from radiation. Data from uranium miners exposed to radon and its daughters, from patients who received large doses of radiation in the early 1900s, and from animal experiments, are also used in estimating cancer risk.

High-LET Radiation - Most of the cancer risk from an accident releasing PuO_2 would result from human exposure to alpha particles from transuranic isotopes in the GPHS-RTG and LWRHUs. This radiation is high-LET. The Committee on the Biological Effects of Ionizing Radiation (BEIR) of the National Research Council (National Academy of Sciences) has compiled the most recent data in this area. Their report entitled Health Risks of Radon and Other Internally Deposited Alpha-Emitters is commonly referred to as BEIR IV (Reference B-9).

BEIR IV identified three types of cancer which can be caused by internally deposited transuranic radionuclides - lung, bone, and liver. Cancer in other tissues has not been demonstrated in either humans or animals from this type of exposure.

Human data on lung cancers associated with transuranic radionuclides are too sparse to use in estimating risks. BEIR IV evaluated three alternative data sets for quantifying these risks:

1. Animal experiment data;
2. Human data for low-LET radiation; and,
3. Human data for radon exposure.

BEIR IV selected Alternative 3 (Radon Exposure) mainly due to weaknesses in the other alternatives but also because radon exposure to the lungs is high-LET radiation. The committee used a "method of ratios" to extrapolate data from four miner studies. This is essentially a relative-linear model. The resulting risk factor is 700 lung cancer deaths/million person-rad. Assuming a quality factor of 20 is used in the lung dose model, this would translate to 35 lung cancer deaths/million person-rem.

The uncertainty of this value was not strictly quantified by the committee. However, they suggested, as an example, that each of the six sources of uncertainty in the model could have a multiplicative standard error of 30%. If each were treated as independent additive errors, the uncertainty range (at the 95% confidence interval) would be 10 to 127 lung cancer deaths/million person-rem.

The committee used data from animal studies to quantify bone cancer risks. They used a statistical technique referred to as Bayesian methodology to combine the linear extrapolations of observed risk levels in a variety of studies involving dogs and mice. The resulting risk factor is 300 bone cancer deaths/million person-rad (15 bone cancer deaths/million person-rem assuming a quality factor of 20). The Bayesian method provides an uncertainty range at the 95% confidence interval of 4 to 55 bone cancer deaths/million person-rem.

Liver cancer associated with transuranic exposure has not been demonstrated in humans. However, liver cancer has occurred with Thorotrast injections of humans and in animal studies with transuranics. Patients with liver and other diseases were given Thorotrast (colloidal Thorium-232-oxide) as a contrast medium in diagnostic radiology in the 1930s. The committee selected the data from follow-up studies of these patients to estimate liver cancer risk from transuranics. Using a linear-absolute model, BEIR predicts 300 liver cancer deaths/million person rad (15 liver cancer deaths/million person-rem).

BEIR did not provide an estimate of the uncertainty associated with this estimate. However, the results of two other studies probably bound the uncertainty. An analysis of thorotrast patient data by Faber (Reference B-10) gave an estimate of 170 liver cancer deaths/million person-rad. Dogs injected with transuranics have exhibited liver cancer mortality rates as high

as 920/million-rad (Reference B-11). These two studies would form a range of 9 to 46 liver cancer deaths/million person-rem (assuming a quality factor of 20).

Low-LET Radiation - The previous BEIR report (BEIR III) was published in 1980 and has formed a basis for most low-LET radiation risk estimates since then. This report provided two models for the projection of future health effects among Japanese bomb survivors (relative and absolute) and three models for extrapolating risks to lower doses (linear, linear quadratic, and quadratic). However, the BEIR III report failed to identify a preferred model. The various models have generally been used to establish the range of potential health effects. The quadratic model should generally predict zero health effects from low doses of low-LET radiation. The combination of the linear and relative models would predict the highest risk.

More recent epidemiological studies have indicated that the relative risk model better explains the observed cancer risk data than the absolute model. These reports have been issued which reflect this change: the radioepidemiological tables published by the National Institutes of Health (Reference B-12), an updated United Nations report on the effects of ionizing radiation (Reference B-13), and Nuclear Regulatory Commission models for reactor accidents (Reference B-14). The models and results reported by the NRC are most representative of a potential RTG accident. The risk factors are shown in Table B-3. The risk factors were obtained using life table methods and the summed site approach. Central estimates are based on the combination of projection and extrapolation models most appropriate for each cancer type. Other models were selected to provide an upper and lower estimate. The models used for each risk factor are shown in Table B-4. These factors are considerably higher than previous estimates (see Table B-5). This is primarily due to a preference for the relative risk model.

The original dose estimates for the survivors of the Japanese bombs were referred to as "T65D" and formed a basis for the cancer risk estimates for low-LET radiation discussed above. In 1981, Loewe and Mendelsohn published a preliminary revision to these estimates (Reference B-15). The revised analysis shows a lower neutron dose component at both bomb sites, a higher gamma component at Hiroshima, and a lower gamma component at Nagasaki. This report prompted a major new analysis of the Hiroshima and Nagasaki dosimetry by the Radiation Effects Research Foundation (RERF). The new dosimetry system will be called "DS86". The DS86 data are not yet fully available, and their impacts on cancer risk factors have not been analyzed. Others have postulated that the net effect of the new analysis on risk factors should be no more than a factor of 2 (References B-15 and B-16).

Table B-3 - Risk Factors for Low-LET Radiation

Type of Cancer	Cancer Deaths/Million Person-Rem		
	Lower Estimate	Central Estimate	Upper Estimate
Leukemia	5	14	48
Bone	0.2	1	2
Breast	4	60	87
Lung	5	20	138
Gastrointestinal	9	57	189
Thyroid	0.7	2	7
Other	5	29	96
In-Utero	2	2	6
Total	31	185	573

Table B-4 - Models Used in Low-LET Risk Factors*

Type of Cancer	Lower Estimate	Central Estimate	Upper Estimate
Leukemia	ABS-LQ'	ABS-LQ	ABS-L
Bone	ABS-LQ'	ABS-LQ	ABS-L
Breast	ABS-LQ'	REL-L'	REL-L
Lung	ABS-LQ'	REL-LQ'	REL-L
Gastrointestinal	ABS-LQ'	REL-LQ	REL-L
Thyroid	ABS-L"	ABS-L'	ABS-L
Other	ABS-LQ'	REL-LQ	REL-L
In-Utero	ABS-L"	ABS-L'	ABS-L

*ABS = Absolute
REL = Relative
L = Linear
LQ = Linear Quadratic
' and " indicate the use of a reduced risk coefficient.

Table B-5 - Comparison of Cancer Risk Factors From Various Sources

Type of Cancer	Central Estimate of Cancer Deaths/Million Man-Rem Low-LET		
	NRC	BEIR III[1]	ICRP.26
Leukemia	14	20	20
Bone	1	-[2]	5
Breast	60	10	25
Lung	20	28	20
Gastrointestinal	57	16	-
Thyroid	2	7	5
Liver	-	7	-
Pancreas	-	8	-
Urinary	-	3	-
Other	29	19	50
In Utero	2	-	-
Total	185	118	125[3]

[1]Based on average of relative and absolute projections with linear quadratic model.
[2]Combined with leukemia
[3]Rounded by ICRP to 100

It should be noted that this increase would impact only those risk factors based primarily on data on the survivors of the Japanese bombings. It would not impact the estimates for high-LET radiation presented previously. Also, recent preference for the relative risk model in an attempt to better explain the observed effects may not be necessary once the new analysis is complete. In any case, the new risk factors will be well within the range of uncertainty of the risk factors presented here.

B.5.2 Genetic Effects

Genetic effects of radiation result from damage to the reproductive, or germ, cells of the human body. The effects are manifested in the future generations of those exposed to the radiation. Genetic risk estimates have been based mainly on animal experiment data and have remained largely unchanged since BEIR III. The BEIR III estimates applied to low-LET radiation and were expressed in units of rem. However, for high-LET radiation, such as doses resulting from internally deposited transuranics, BEIR IV presents genetic risk estimates on a per Rad basis. The relative biological effectiveness (RBE), a factor similar to the quality factor, for genetic damage of alpha particles ranged from 2.5 to 15. Dose models generally use a quality factor of 20 for alpha particles. In order to avoid "mixing" of quality factors, all alpha particle doses must be converted to Rad and combined with the BEIR IV genetic risk estimators. The BEIR III and BEIR IV risk estimators are given in Table B-6.

In previous application of the BEIR III genetic risk factors, a simplistic approach has been used which overestimates genetic risks. An equilibrium population is one in which the birth rate is equal to the death rate, or in which each person is "replaced" by one offspring. The simplistic approach was to assume that all individuals in an exposed population have yet to be replaced - that is, no one in the exposed population would have reproduced at the time of exposure. The BEIR III risk estimates would be converted to a usable form as follows:

$$\frac{\text{X Genetic Effects}}{\text{Million Offspring}} \times \frac{\text{1 Generation}}{\text{1 Rem (or Rad)}} \times \frac{\text{1 Offspring/Person}}{\text{Generation}} = \frac{\text{X Genetic Effects}}{\text{Million Person-Rem (or Rad)}}$$

The value of X was taken as the geometric mean of the range of risks in Table B-6.

In a recent application of the BEIR III risk estimates, a life table method was used assuming a birth rate of 16,000 live births/year (480,000 live births/30 year generation) in a population of one million (Reference B-17). The results are given in Table B-7.

Table B-6 - BEIR Genetic Risk Estimators for Low-LET and High-LET Radiation

Genetic Disorder	Effects Per Million Live Born Offspring,1 Rem or Rad per Generation*	
	BEIR III - Low-LET (Rem)	BEIR IV - High-LET (Rad)
Single Gene		
Autosomal Dominant	-	
X-Linked	-	
Subtotal	40-200	100-500
Irregularly Inherited	20-900	50-2,250
Chromosomal Aberrations	-	15-135
Total	60-1,100	165-2,885
Geometric Mean	257	690

*Risk factors are for an equilibrium population.

Table B-7 - Genetic Risk Estimators for Low-LET and High-LET Radiation From RTG Accidents

Genetic Disorder	Genetic Effects Per Million Person-Rem or Rad	
	Low-LET (Rem)	High-LET (Rad)
Single Gene		
Autosomal Dominant	70 (12-210)	175 (30-525)
X-Linked	30 (5-120)	75 (13-300)
Subtotal	100 (17-330)	250 (43-825)
Irregularly Inherited	70 (45-887)	175 (113-2,218)
Chromosomal Aberrations		
Numerical	5 (0-15)	75 (0-225)
Structural	10 (6-25)	150 (90-375)
Subtotal	15 (6-40)	225 (90-600)
Total	180 (68-1,257)	650 (246-3,643)

B.5.3 Mental Retardation

Mental retardation resulting from in-utero exposure is the only serious radiation-induced health effect, other than cancer and genetic effects, which is believed not to exhibit a threshold dose. A threshold dose is a dose below which no ill effects would be expected. Otake and Schull (1984) have observed severe mental retardation among surviving fetuses of the Japanese atomic bombs. Their work suggests that the fetus is most susceptible to central nervous system damage during weeks 5 to 18 of gestation. The increased risk of mental retardation during this period, at doses less than 10 Rad, is 0.4% per Rad. In a population of 1 million there are 16,000 live births per year. For external whole body exposures, where the dose is delivered over a short period, only those fetuses in the 8-15 weeks of gestation would be affected. This would be about 2500 fetuses in a population of 1 million. The resulting risk factor is 10 cases of mental retardation/million person-rem. This risk factor cannot be used with internal exposures, especially to high-LET radiation, because the dose models do not provide an estimate of doses to any part of the central nervous system.

B.6 ACTIVE HEALTH EFFECTS OF RADIATION

At very high doses, the biological effects of plutonium inhalation have been characterized as shown in Figure B-1 and Table B-8 from Reference B-7. The threshold for destruction of lung tissue and function is estimated at 4000 rem (200 rad, using the ICRP alpha quality factor of 20). If the animal data of Table B-8 are applied to man (1000 g lung), a body burden on the order of 2000 to 10000 nCi would be required to clinically observe cancer in the lung or bone in specific individuals.

B.7 SUMMARY AND CONCLUSIONS

The following conclusions and positions for the FSAR analyses are taken, based on the information presented in this Appendix:

1) Radiation dose and radiological impact to persons from a potential accident leading to an RTG fuel release can be characterized using the dose from Plutonium-238 dioxide along, since the dose contribution of all other isotopes is about one percent of total.

2) Radiological impact of calculated population doses is expressed only in terms of potential cancer deaths. Generic and mental retardation effects are not calculated since Plutonium-238 dioxide does not significantly deposit in the involved organs. The health risk estimator used for potential cancers is 185 per million person rem which was derived from Low-LET radiation studies. Since an effective whole body dose equivalent is calculated, an effective whole body health risk estimator is appropriate. An alternative approach would have been to calculate organ

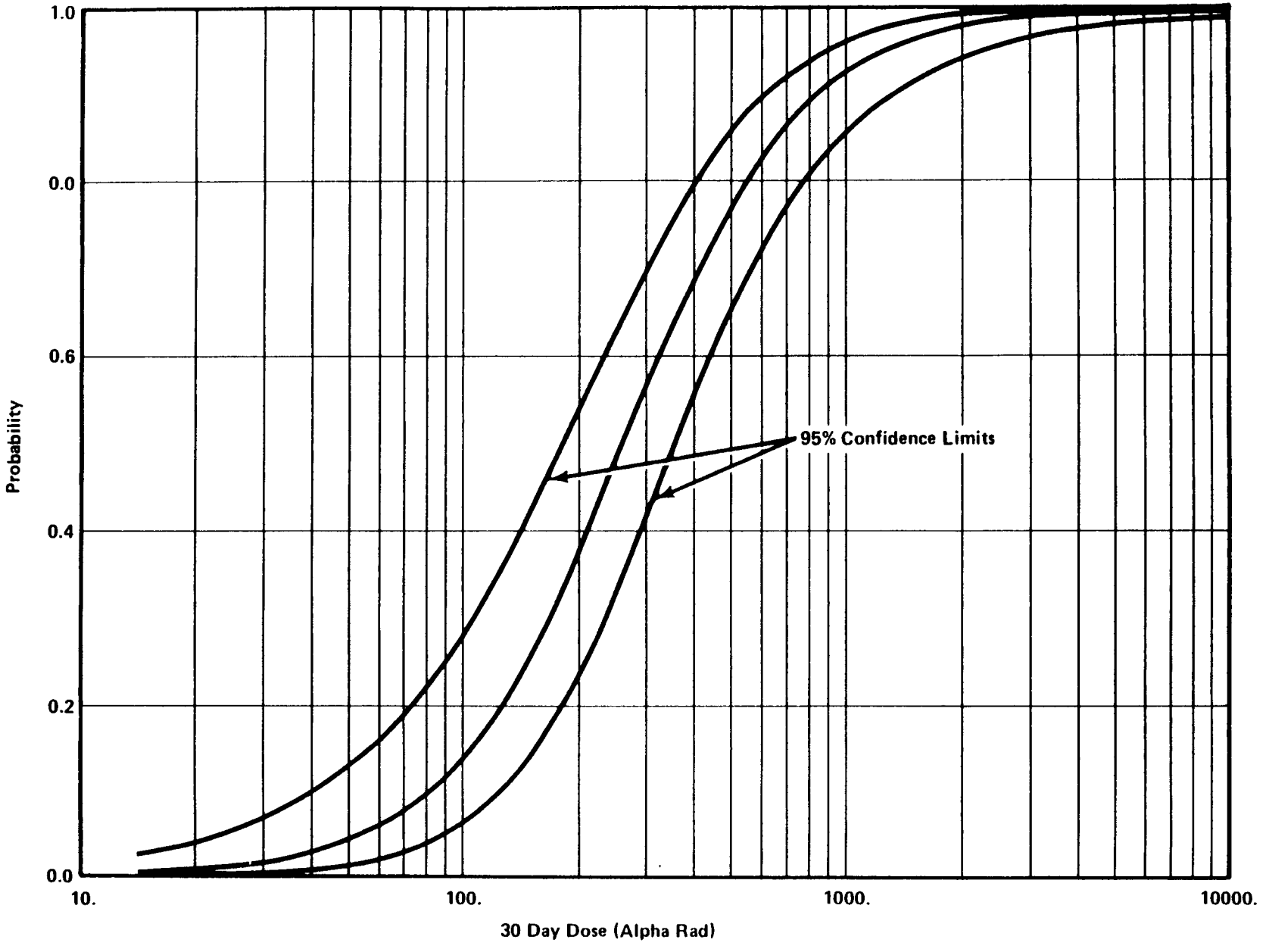

From PNL 3257 RH

Figure B-1
PROBABILITY OF DEATH FROM PULMONARY INJURY CAUSED BY ALPHA RADIATION

Table B-8 - Clinical Responses to Inhaled Plutonium in Experimental Animals

Biological Effect	Approximate Minimal Dose Observed to Cause the Effect: Inhaled Dose (μCi/g of Lung)	Approximate Minimal Dose Observed to Cause the Effect: Radiation Dose to Critical Tissue or organ (Rad)
Lung Hemorrhage and Edema	0.5	15,000
Respiratory Insufficiency	0.02	1,800
Lung Fibrosis	0.005	200
Lymphopenia	0.001	(Critical tissue not known)
Lung Cancer	0.002	10 (rats) 1,000 (dogs)
Bone Cancer	0.01	3.6 (rats) 78 (dogs)

Source: Reference B-7

doses separately and apply the high-LET organ dose health effect estimators. The former approach (effective whole body dose equivalent) was selected in order to provide a more commonly known comparison level (natural radiation background).

B.8 REFERENCES

B-1 B.R. Kokenge (MRC-Mound), letter to J.A. Morley (DOE), dated July 23, 1985.

B-2 P.O. Strom and E.C. Watson, "Calculated Doses from Inhaled Transuranium Radionuclides and Potential Risk Equivalence to Whole-Body Radiation," in the Proceedings of Transuranium Nuclides in the Environment Symposium, sponsored by USERDA and IAEA, November 1975.

B-3 George M. Matlack, "The Chemistry of Plutonium in Relation to Its Behavior in Biological and Environmental System," in the Proceedings of the Plutonium Information Meeting for an Ad Hoc Subcommittee of the Advisory Committee on Reactor Safeguards, Los Alamos, New Mexico, January 4 and 5, 1974. (Conf 740115).

B-4 Naval Ocean Systems Center, Informal Quarterly Progress Report, Fourth Quarter 1985, NOSC/DOE Environmental Test Program, October 3, 1985.

B-5 Heaton, R.C., et. al., "Long-Term Exposure of Pressed Plutonium Oxide Heat Sources to Aquatic Environments," LA-10197-MS, Los Alamos National Laboratory, November 1984.

B-6 USEPA, "Interim Recommendations on Doses to Persons Exposed to Transuranium Elements in the General Environment," Summary Report Discussion Draft, October 31, 1984.

B-7 "A Mathematical Model for Predicting the Probability of Acute Mortality in a Human Population Exposed to Accidentally Released Radionuclides," Battelle Pacific Northwest Laboratory, NUREG/CR-1261, May 1980.

B-8 International Commission of Radiological Protection, Nonstochastic Effects of Ionizing Radiation. ICRP Publication 41. Peragamon Press, (1984).

B-9 Committee on the Biological Effects of Ionizing Radiation, 1988. Health Risks of Radon and Other Internally Deposited Alpha-Emitters, National Academy Press, Washington, (1988).

B-10 Faber, M. 1979. "Twenty-Eight Years of Continuous Followup on Patients Injected With Thorotrast for Cerebral Angiography", Environmental Research, 19:37-43.

B-11 Muggenburg, B. A., B. B. Buecker, F. F. Hahn, W. E. Griffith, and R. O. McClellan, 1976. "The Risk of

Liver Tumors in Dogs and Man From Radioactive Aerosols", Proceedings of the 22nd Annual Life Science Symposium. Conf.-830951, 556-a563 (1976).

B-12 National Institutes of Health, Report on the NIH Ad Hoc Working Group to Develop Radioepidemiological Tables. NIH Publication #85-2748, U. S. Public Health Service, Washington, (1985).

B-13 United Nations Scientific Committee on the Effects of Ionizing Radiation, Genetic and Somatic Effects of Atomic Radiation, United Nations, New York (1986).

B-14 U.S. Nuclear Regulatory Commission, Health Effects Model for Nuclear Power Plant Accident Consequences analysis, NUREG/CR-42141 (1985).

B-15 Loewe, W. E., and E. Mendelsohn, 1981. "Revised Dose Estimates at Hiroshima and Nagaski". Health Physics, Volume 41, No. 4, PP. 663-666.

B-16 U. S. Department of Energy, Health and Environmental Consequences of the Chernobyl Nuclear Power Plant Accident. DOE/ER-0032, Washington, (1987).

APPENDIX C

KSC METEOROLOGY

C.1 INTRODUCTION

Meteorological data collected at Cape Canaveral and West Palm Beach, Florida were summarized for input in the evaluation of potential radiological impacts of aborted shuttle launches involving nuclear systems. Since the launch window is October 7 through November 25, only historical meteorological data collected during this period were analyzed. Wind speed, wind direction and atmospheric stability data were summarized for input to atmospheric dispersion assessments (see Appendix A). Data from meteorological towers were used to analyze near ground level conditions and data from balloon launched instruments (rawinsondes) were used to analyze meteorological conditions aloft. Tower and rawinsonde data collected during the 1980-1984 period were available and used for analysis.

Summaries of various meteorological parameters for the data collected are provided in the following sections. For reasons of data availability and recovery, tower and rawinsonde data for the combined 1982 and 1984 launch window periods were used to generate launch window meteorological summaries. These summaries represent data necessary to characterize meteorological conditions during the range of launch times and during periods when the potential exists for accidental atmospheric releases prior to the launch and during post-accident periods when pollutants may still be transported toward receptors. The specific meteorological sequences used as direct input to atmospheric dispersion assessments are discussed in Appendix A.

Launch window data collected over the entire 1980-1984 period were used to generate climatological summaries. These summaries provide long-term averages that may be used for comparison to the launch window meteorological summaries.

C.2 METEOROLOGICAL DATA SOURCES

C.2.1 SURFACE DATA

Surface meteorological data to represent near ground-level releases were available on magnetic tape for the period 1980 through 1984. These data were obtained from Tower 313 of the Weather Information Network Display System (WINDS) at Cape Canaveral. Figure C-1 shows the location of this tower within the current WINDS meteorological tower network. The 1980 and 1981 data sets consist of 30-minute averages of wind speed, wind direction, temperature, and other parameters, while the data sets from 1982 through 1984 are comprised of 5-minute averages. For the analyses discussed in this section, hourly averages were calculated for all data sets. Generally, the WINDS magnetic tapes had hourly data deleted when all parameters were missing.

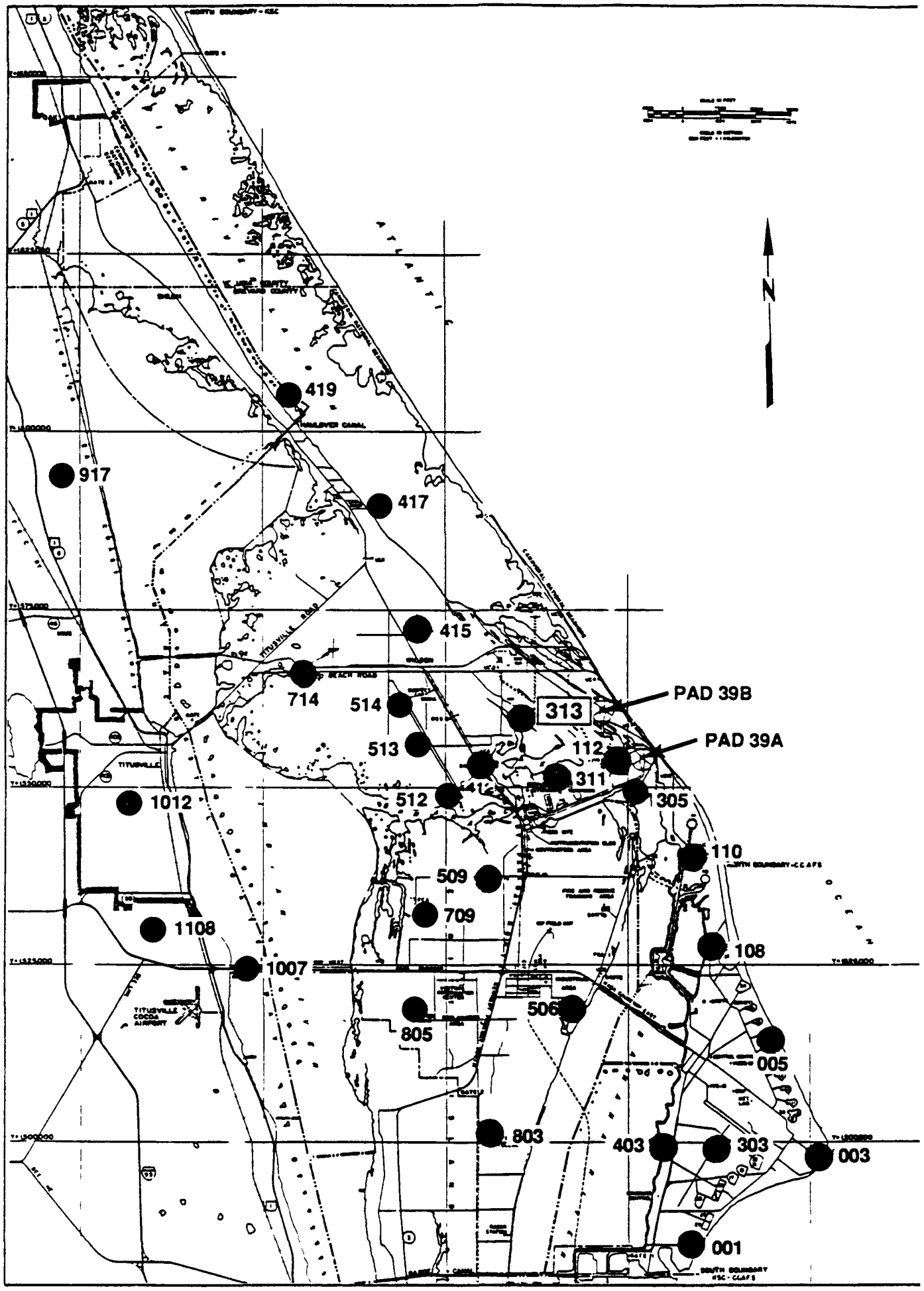

FIGURE C-1
WINDS METEOROLOGICAL TOWER LOCATIONS

However, review of the data set indicated that in some cases data missing for individual parameters had been replaced by a value of zero. This complicated data processing since, for some parameters, differentiating between a valid zero value (e.g., calm wind speed) and the zero missing indicator was difficult. Therefore all zero values were treated as missing.

Tower number 313 was used as a primary source of meteorological data for this assessment. This 500-foot tower is located approximately 3 miles from both the shuttle launch complex and the Atlantic Ocean. The tower has been instrumented at the 6-, 12-, 54-, 204-, 295-, and 492-foot levels. Wind and temperature data used in these analyses were obtained from the 54-, 204-, and 492-foot levels.

C.2.2 UPPER AIR DATA

Upper air meteorological data to represent elevated releases were available on magnetic tape. These data were obtained from rawinsonde balloon measurements taken at Cape Canaveral (KSC) and West Palm Beach (PBI), Florida. The KSC measurements were generally taken once daily between 0900 and 1100 GMT (0400 and 0600 EST) from 1982 through 1984. On some occasions more than one observation was taken in a day. In these cases the observation with the greatest data recovery and closest to 1200 GMT (0700 EST) was used for analysis. The National Climatic Data Center allows a 6-hour tolerance for rawinsonde stations reporting once daily (Reference C-1). Therefore, the KSC data were assumed to be applicable at 1200 GMT. PBI measurements were taken twice daily, 1200 and 0000 GMT (0700 and 1900 EST), from 1980 through 1984. To be consistent with KSC data, only those measurements taken at 1200 GMT were considered in this appendix. The PBI data contained a zero wind direction whenever a zero wind speed was reported. For computational purposes a zero wind direction was considered missing.

As with the surface meteorological data, only data from those dates corresponding to the launch window were analyzed.

C.2.3 DATA RECOVERY

WINDS Tower 313 data were available for the months of October and November from 1980 through 1984 with the exception of October 1983. In addition the October 1981 data month primarily consisted of observations between the hours of 0100 and 1800 EST, with many days that contained extensive periods of missing hourly data. For these reasons the October 1981 data were not included in the data set. Therefore, based on the available data, the total number of possible hourly observations for the launch window was 4800 for the 5-year data period (1980-1984) and 2400 for a combined 1982/1984 data period.

The data recoveries of Tower 313 hourly observations, based on all parameters, were 93 percent for both the 5-year and

1982/1984 data periods. Table C-1 presents data recoveries for the individual Tower 313 parameters analyzed in this appendix.

KSC rawinsonde data were available for the months of October and November from 1982 through 1984. Sufficient data were available for the launch window to allow 100 percent data recovery for the individual parameters analyzed. PBI rawinsonde data were available for the months of October and November from 1980 through 1984. These data had an overall hourly recovery of 98 percent for the launch window period. Table C-2 provides the individual recovery rates for the PBI data discussed in the following sections.

C.3 KSC CLIMATOLOGY

C.3.1 SURFACE CLIMATOLOGY

C.3.1.1 Wind Direction and Speed

The distributions of wind speed and wind direction for the 54-, 204-, and 492-foot levels of Tower 313 are shown in Figures C-2, C-3, and C-4, respectively. These distributions were determined from KSC WINDS Tower 313 data for the 1980 through 1984 launch window period. In accordance with standard meteorological convention, data in this appendix labeled with a wind direction means that the wind is from that direction. The figures show that generally winds from the north through east sectors dominate at all levels. The 54-foot level exhibits a peak wind-direction frequency from the north while the remaining levels show that east winds are predominant. At all levels the predominant winds represent an onshore flow in the vicinity of the shuttle launch pads.

The average wind speeds for the 5-year period examined were 10.0, 14.3, and 17.2 mph for the 54-, 204-, and 492-foot levels respectively. Calm periods (i.e., zero wind speeds) in the Tower 313 data were treated as missing. Previous analyses of data collected at the Cape Canaveral Air Force Weather Station showed an average 4.4 percent calms during the fall season (September-November) based on 8 years of data (1961-1968) (Reference C-2).

C.3.1.2 Wind Direction Persistence

Figure C-5 presents the maximum wind direction persistence periods by direction sector for each of the three tower levels as determined from the 5-year WINDS data set. It can be seen that the longer persistence periods at all levels are generally associated with onshore flows. The maximum persistence period for each level and its year/month of occurrence are listed in Table C-3.

The probability of onshore winds persisting for periods of 1 through 44 hours were calculated for the launch window using

Table C-1
Data Recoveries by Parameter for
WINDS Tower 313 Launch Window Data
(October 7 through November 25)

Parameter	Data recovery (%)	
	Combined 1980-1984*	Combined 1982-1984
Wind Speed		
54 feet	92	94
204 feet	88	86
492 feet	92	94
Wind Direction		
54 feet	92	94
204 feet	89	88
492 feet	92	94
Delta-T (492 feet-54 feet)	92	94

* Excluding the month of October for 1981 and 1983

Table C-2
Data Recoveries by Parameter for
West Palm Beach, Fla. Rawinsonde Launch
Window Data (October 7 through November 25)

Parameter	Data Recovery (%) for Combined 1980-1984
850 mb	
Wind Speed	92
Wind Direction	91
700 mb	
Wind Speed	94
Wind Direction	93
500 mb	
Wind Speed	94
Wind Direction	94
350 mb	
Wind Speed	94
Wind Direction	94

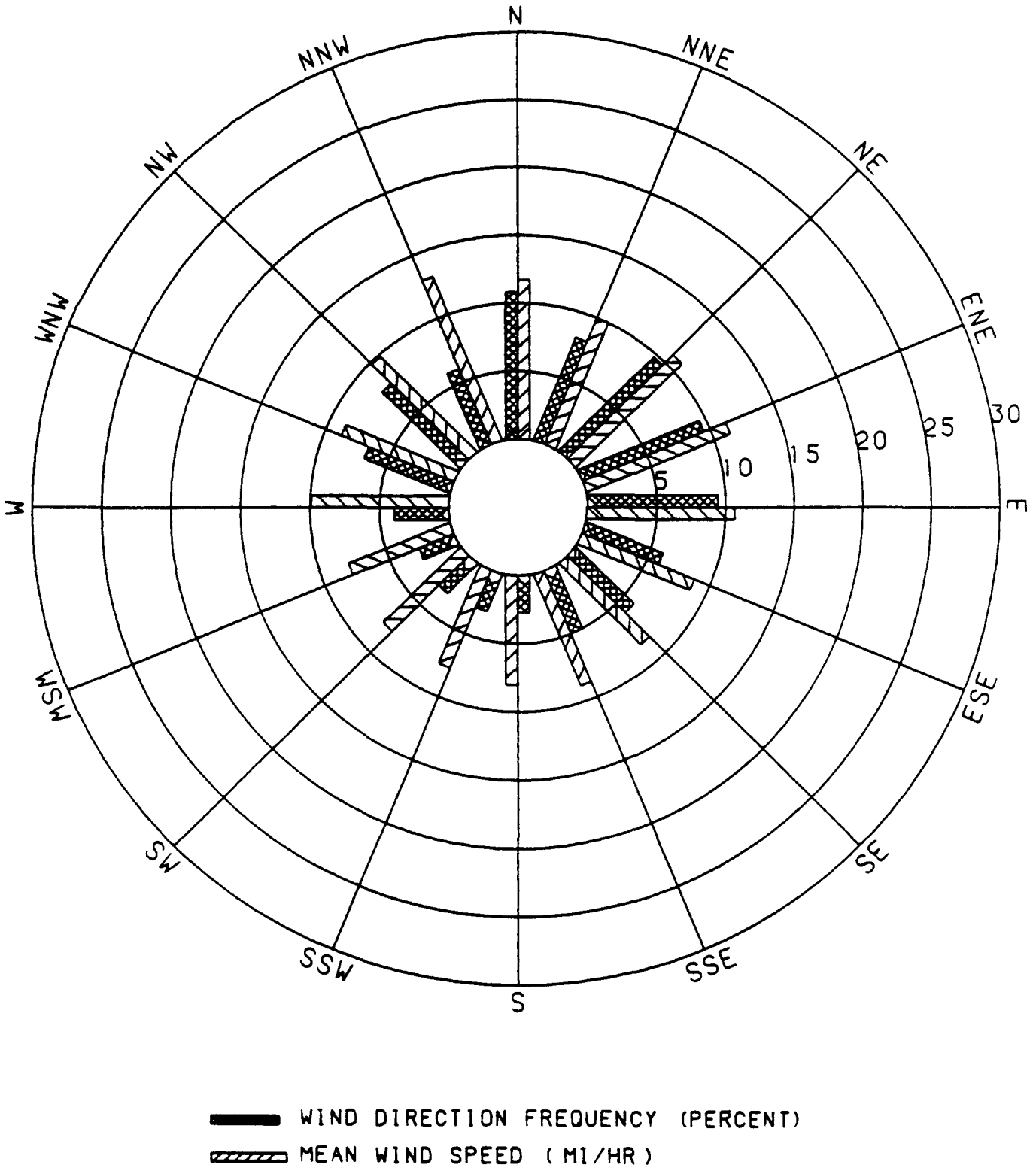

FIGURE C-2
CAPE CANAVERAL 54-FT
5-YEAR WIND ROSE
(OCTOBER 7 THROUGH NOVEMBER 25)

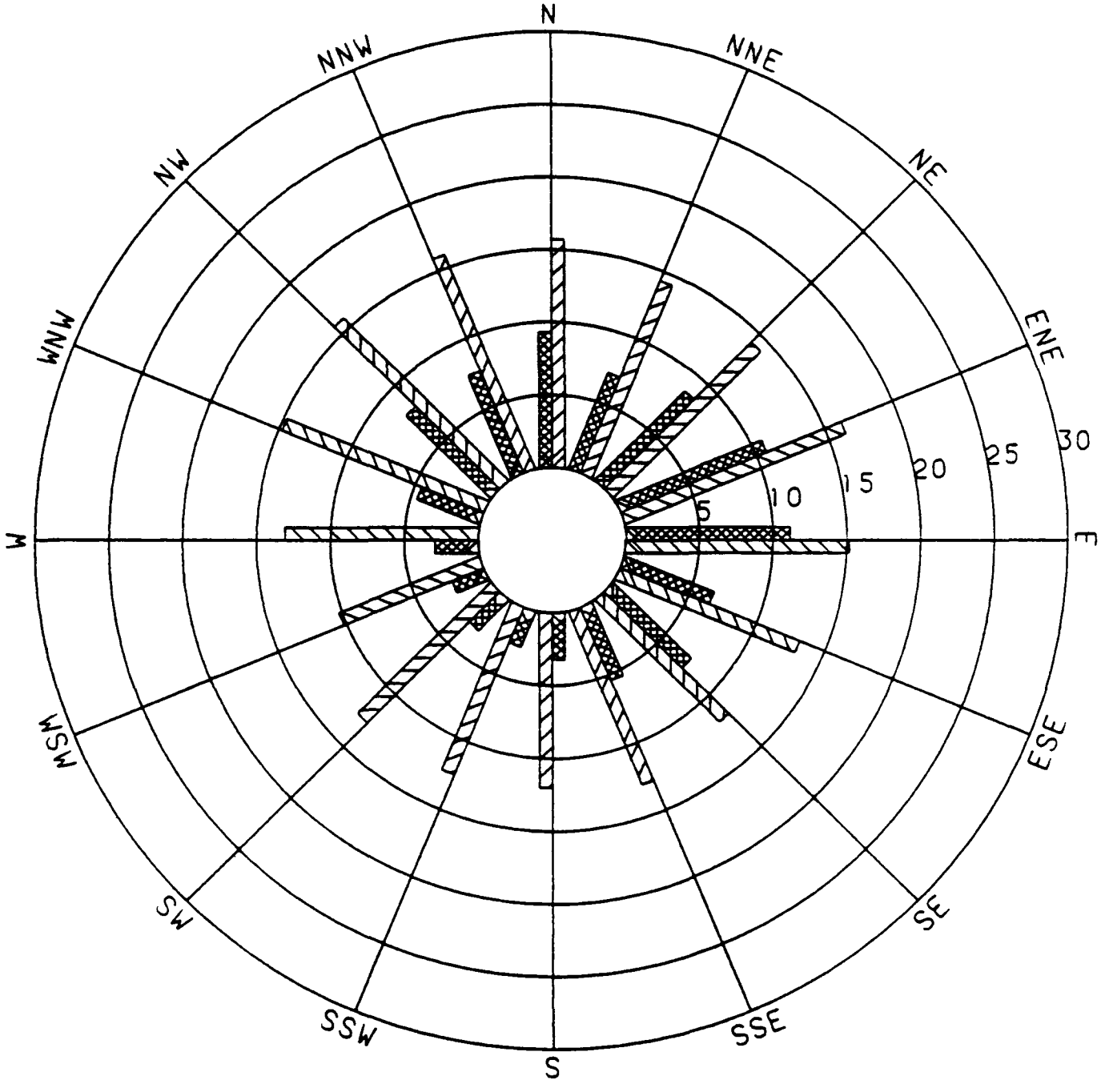

FIGURE C-3
CAPE CANAVERAL 204-FT
5-YEAR WIND ROSE
(OCTOBER 7 THROUGH NOVEMBER 25)

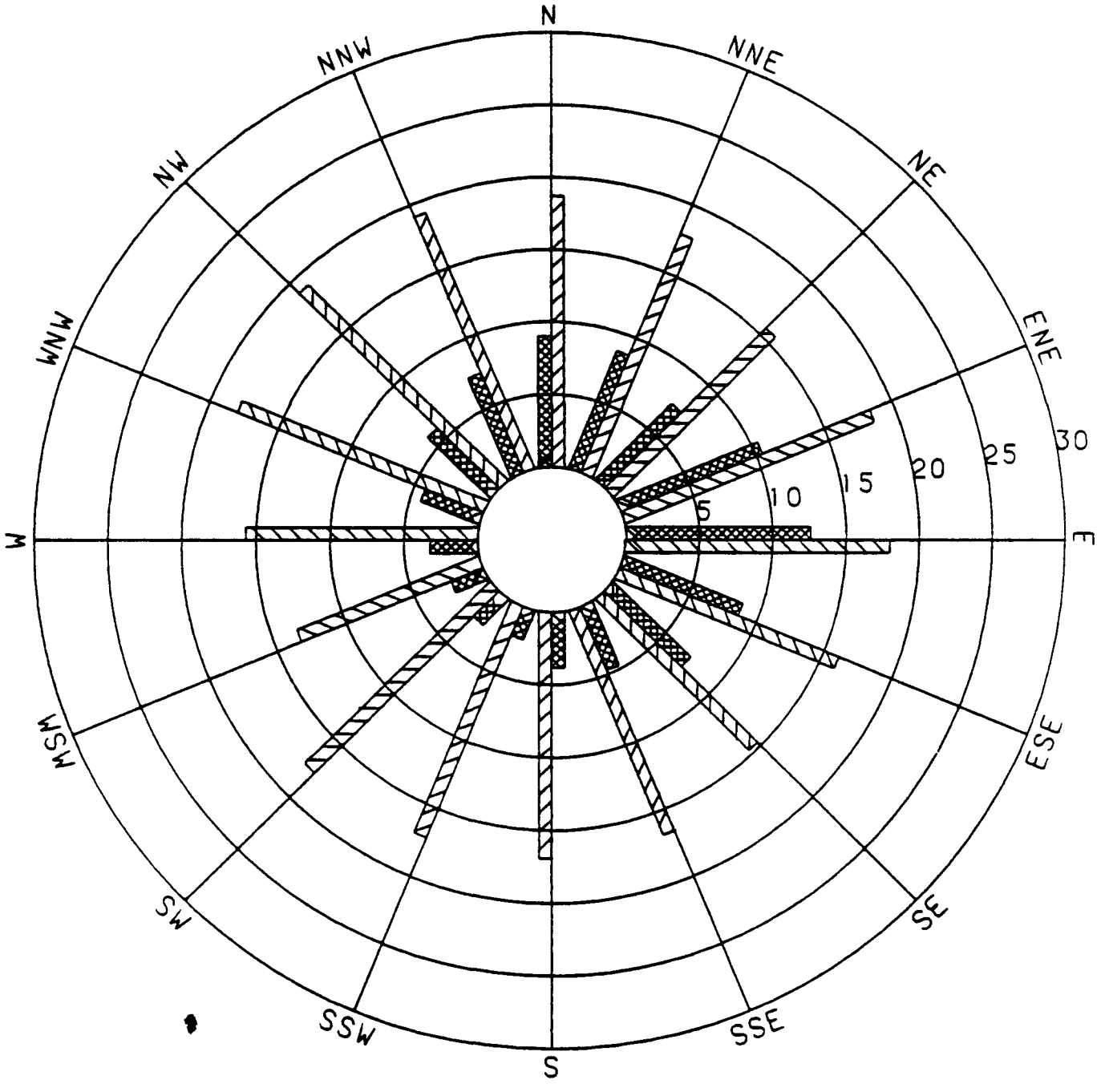

FIGURE C-4
CAPE CANAVERAL 492-FT
5-YEAR WIND ROSE
(OCTOBER 7 THROUGH NOVEMBER 25)

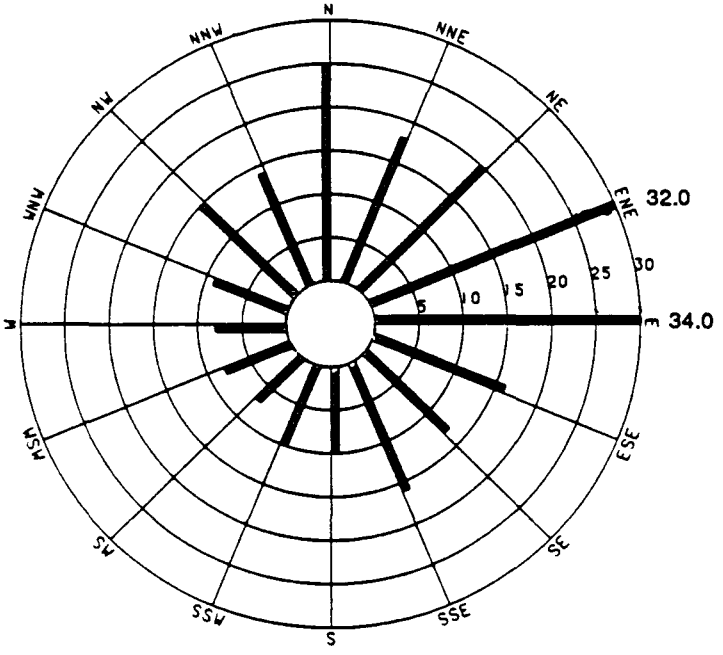

54 Feet

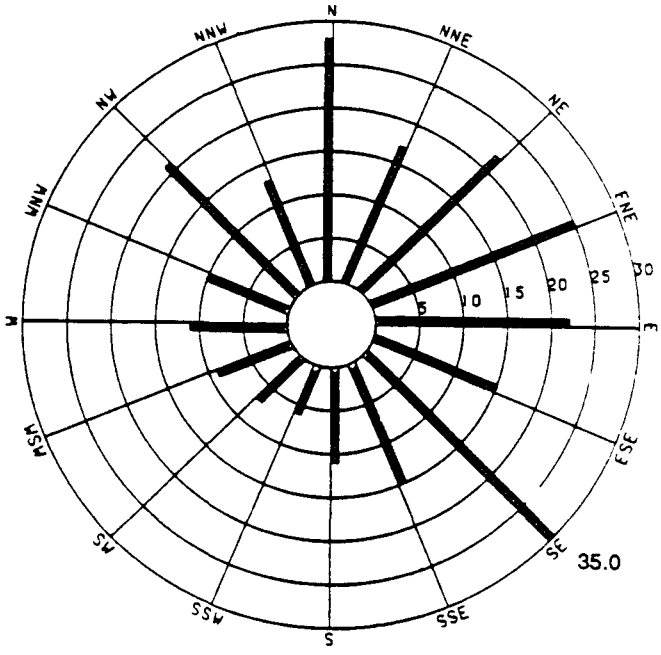

204 Feet

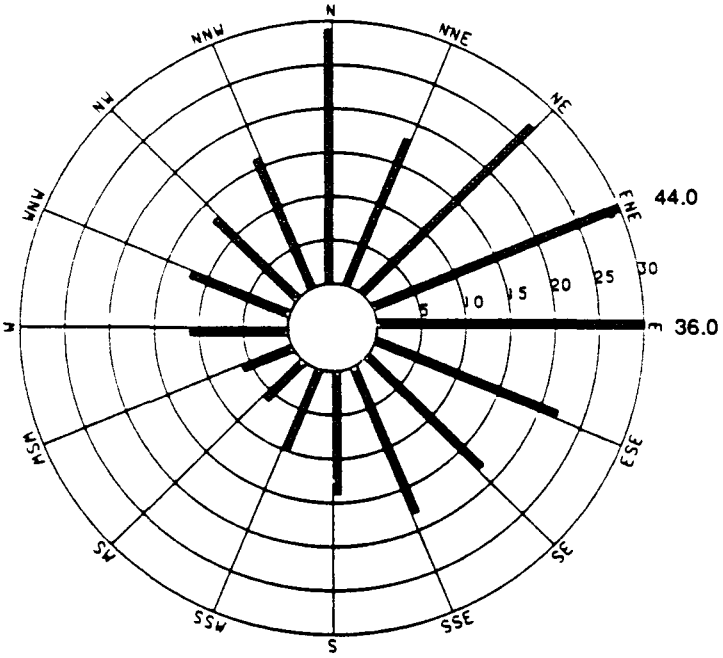

492 Feet

Rings extend to 30 hours only. Persistence periods greater than or equal to 30 hours are indicated by a bar out to 30 and the numerical value at the end of the bar.

FIGURE C-5
CAPE CANAVERAL 5-YEAR
MAXIMUM DIRECTIONAL WIND PERSISTENCE ROSES (HOURS)
(OCTOBER 7 THROUGH NOVEMBER 25)

Table C-3
Maximum Wind Direction Persistence (Hours)
Cape Canaveral WINDS Tower 313
October 7 through November 25 of 1980 through 1984

Level	Month, Year	Sector	Persistence Period (Hours)
54-foot	October 1982	E	34
204-foot	October 1984	SE	35
492-foot	October 1984	ENE	44

492-ft wind data. These probabilities are presented in Figure C-6 which illustrates that persistence periods greater than three hours have less than a 50 percent probability of occurrence. Furthermore, it is seen that the maximum persistence period (44 hours) has only a 0.03 percent probability of occurrence.

C.3.1.3 Atmospheric Stability

Low-level atmospheric stability classifications at Cape Canaveral were determined using the methodology presented in the Nuclear Regulatory Commission (NRC) Regulatory Guide 1.23 (Reference C-3). These stability classifications were based on the temperature differential (delta T) between 492 feet and 54 feet. Table C-4 provides stability distributions for the 5-year launch window period. Class E (slightly stable) conditions are seen to dominate, occurring approximately 55 percent of the time. Class D (neutral) conditions are the next most prevalent occurring about 31 percent of the time. The dominance of Class E and D conditions is reflective of the effects of nearby water bodies on the local meteorology.

C.3.1.4 Sea Breeze and Onshore Gradient Wind Flows

Few detailed studies have been accomplished to determine the specific characteristics of the sea breeze at Cape Canaveral. Limited data during sea breeze events collected at Cape Canaveral and on the west coast of Florida were used to parameterize the sea-breeze module in the EMERGE model (Appendix H). A true sea breeze condition is characterized by the following:

1. Very light synoptic (e.g., gradient) winds usually associated with a high-pressure system over the region

2. Strong insolation

3. Daytime air temperatures rising above sea-surface temperatures

4. A shift of surface winds from offshore (perhaps due to a land breeze) to onshore during the day

5. The presence of a definite front or convergence zone with corresponding rising air separating surface air flows with oversea and overland trajectories

6. The presence of an unstable thermal internal boundary layer (TIBL) which begins at the shoreline and increases in depth with increasing distance inland

7. A discernible, though sometimes weak, return flow layer aloft (i.e., offshore wind flows), and

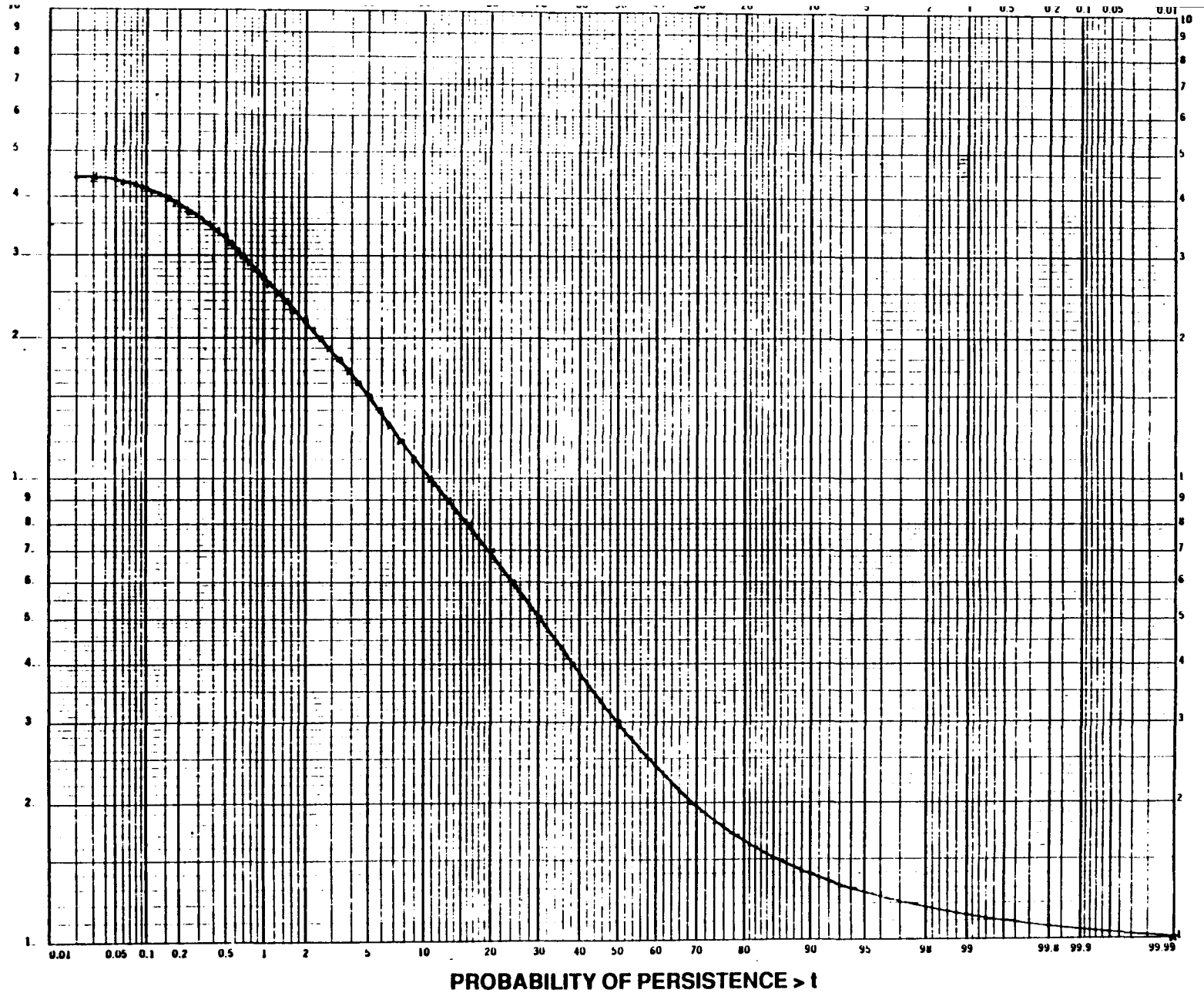

FIGURE C-6
CAPE CANAVERAL 492-FT 5-YEAR ONSHORE WIND PERSISTENCE
(OCTOBER 7 THROUGH NOVEMBER 25)

5-YEAR OCT/NOV CAPE CANAVERAL 492 FT TOWER DATA
SITE IDENTIFIER: TOWER313
DATA PERIOD EXAMINED: 10/ 7/80 - 11/30/84

*** OCTOBER/NOVEMBER ***

STABILITY CLASS A

STABILITY BASED ON: DELTA T BETWEEN 492.0 AND 54.0 FEET
WIND MEASURED AT: 492.0 FEET
WIND THRESHOLD AT: 0.60 MPH

JOINT FREQUENCY DISTRIBUTION OF WIND SPEED AND DIRECTION IN HOURS AT492.00 FEET

SPEED (MPH)	N	NNE	NE	ENE	E	ESE	SE	SSE	S	SSW	SW	WSW	W	WNW	NW	NNW	TOTAL
CALM																	0
0.61- 3.50	0	0	0	0	0	0	0	0	0	0	0	0	0	0	0	0	0
3.51- 7.50	0	1	0	0	0	0	0	0	0	0	0	0	0	0	0	0	1
7.51-12.50	0	2	0	0	2	3	3	0	0	0	0	0	0	0	0	2	12
12.51-18.50	0	0	0	1	1	3	0	0	0	0	0	0	0	0	0	1	6
18.51-24.00	1	0	0	0	11	0	0	0	2	0	0	0	0	0	0	4	18
>24.00	1	0	0	6	20	0	0	0	0	0	0	0	0	0	0	3	30
TOTAL	2	3	0	7	34	6	3	0	2	0	0	0	0	0	0	10	67

STABILITY CLASS B

STABILITY BASED ON: DELTA T BETWEEN 492.0 AND 54.0 FEET
WIND MEASURED AT: 492.0 FEET
WIND THRESHOLD AT: 0.60 MPH

JOINT FREQUENCY DISTRIBUTION OF WIND SPEED AND DIRECTION IN HOURS AT492.00 FEET

SPEED (MPH)	N	NNE	NE	ENE	E	ESE	SE	SSE	S	SSW	SW	WSW	W	WNW	NW	NNW	TOTAL
CALM																	0
0.61- 3.50	0	0	0	0	0	0	0	0	0	0	0	0	0	0	0	0	0
3.51- 7.50	0	0	0	1	0	0	0	0	1	0	0	0	0	0	0	0	2
7.51-12.50	1	2	0	0	0	1	0	1	0	0	1	0	0	0	0	1	7
12.51-18.50	0	0	2	0	3	0	1	1	3	0	0	0	0	0	0	0	10
18.51-24.00	1	0	0	1	4	0	0	1	0	0	0	0	0	0	1	0	8
>24.00	3	1	1	1	3	0	0	0	0	0	0	0	0	0	0	7	16
TOTAL	5	3	3	3	10	1	1	3	4	0	1	0	0	0	1	8	43

TABLE C-4
CAPE CANAVERAL 5-YEAR WIND AND ATMOSPHERIC STABILITY DISTRIBUTIONS
(OCTOBER 7 THROUGH NOVEMBER 25)

5-YEAR OCT/NOV CAPE CANAVERAL 492 FT TOWER DATA
SITE IDENTIFIER: TOWER313
DATA PERIOD EXAMINED: 10/ 7/80 - 11/30/84

*** OCTOBER/NOVEMBER ***

STABILITY CLASS C

STABILITY BASED ON: DELTA T BETWEEN 492.0 AND 54.0 FEET
WIND MEASURED AT: 492.0 FEET
WIND THRESHOLD AT: 0.60 MPH

JOINT FREQUENCY DISTRIBUTION OF WIND SPEED AND DIRECTION IN HOURS AT492.00 FEET

SPEED (MPH)	N	NNE	NE	ENE	E	ESE	SE	SSE	S	SSW	SW	WSW	W	WNW	NW	NNW	TOTAL
CALM																	0
0.61- 3.50	0	0	0	0	0	0	0	0	0	0	0	0	0	0	0	0	0
3.51- 7.50	0	0	1	2	1	0	0	0	1	0	0	0	0	0	0	0	5
7.51-12.50	0	3	2	0	1	0	0	0	0	0	1	0	0	0	0	0	7
12.51-18.50	1	1	3	0	1	1	1	5	1	1	5	1	0	0	1	1	23
18.51-24.00	1	2	3	4	3	1	1	2	0	1	2	0	0	0	5	6	31
>24.00	2	3	0	3	1	0	0	0	0	0	0	0	0	0	1	0	10
TOTAL	4	9	9	9	7	2	2	7	2	2	8	1	0	0	7	7	76

STABILITY CLASS D

STABILITY BASED ON: DELTA T BETWEEN 492.0 AND 54.0 FEET
WIND MEASURED AT: 492.0 FEET
WIND THRESHOLD AT: 0.60 MPH

JOINT FREQUENCY DISTRIBUTION OF WIND SPEED AND DIRECTION IN HOURS AT492.00 FEET

SPEED (MPH)	N	NNE	NE	ENE	E	ESE	SE	SSE	S	SSW	SW	WSW	W	WNW	NW	NNW	TOTAL
CALM																	0
0.61- 3.50	1	2	1	1	0	0	0	3	2	1	0	0	0	0	1	3	15
3.51- 7.50	10	5	14	10	8	5	1	3	3	2	3	4	3	2	6	6	85
7.51-12.50	30	31	33	31	31	29	30	12	9	5	3	11	15	10	6	19	305
12.51-18.50	30	38	24	40	24	41	44	22	11	8	11	8	14	21	9	21	366
18.51-24.00	40	28	28	48	46	31	5	16	11	8	9	2	3	11	23	46	355
>24.00	53	54	23	36	28	5	0	3	1	2	0	0	5	7	10	35	262
TOTAL	164	158	123	166	137	111	80	59	37	26	26	25	40	51	55	130	1388

TABLE C-4 (CONTINUED)
CAPE CANAVERAL 5-YEAR WIND AND ATMOSPHERIC STABILITY DISTRIBUTIONS
(OCTOBER 7 THROUGH NOVEMBER 25)

5-YEAR OCT/NOV CAPE CANAVERAL 492 FT TOWER DATA
SITE IDENTIFIER: TOWER313
DATA PERIOD EXAMINED: 10/ 7/80 - 11/30/84

*** OCTOBER/NOVEMBER ***

STABILITY CLASS E

STABILITY BASED ON: DELTA T BETWEEN 492.0 AND 54.0 FEET
WIND MEASURED AT: 492.0 FEET
WIND THRESHOLD AT: 0.60 MPH

JOINT FREQUENCY DISTRIBUTION OF WIND SPEED AND DIRECTION IN HOURS AT492.00 FEET

SPEED (MPH)	N	NNE	NE	ENE	E	ESE	SE	SSE	S	SSW	SW	WSW	W	WNW	NW	NNW	TOTAL
CALM																	0
0.61- 3.50	1	2	2	3	0	0	0	2	2	0	1	0	0	2	0	0	15
3.51- 7.50	8	12	10	12	9	18	18	10	2	2	6	10	3	6	6	5	137
7.51-12.50	28	40	53	50	68	61	49	29	15	11	8	12	12	10	19	16	481
12.51-18.50	57	68	39	69	129	96	98	49	29	20	8	20	36	29	24	42	813
18.51-24.00	43	41	26	93	90	75	37	18	27	12	8	9	15	28	36	34	592
>24.00	22	29	27	54	53	19	14	34	18	8	23	6	7	24	42	20	400
TOTAL	159	192	157	281	349	269	216	142	93	53	54	57	73	99	127	117	2438

STABILITY CLASS F

STABILITY BASED ON: DELTA T BETWEEN 492.0 AND 54.0 FEET
WIND MEASURED AT: 492.0 FEET
WIND THRESHOLD AT: 0.60 MPH

JOINT FREQUENCY DISTRIBUTION OF WIND SPEED AND DIRECTION IN HOURS AT492.00 FEET

SPEED (MPH)	N	NNE	NE	ENE	E	ESE	SE	SSE	S	SSW	SW	WSW	W	WNW	NW	NNW	TOTAL
CALM																	0
0.61- 3.50	1	0	3	1	0	1	2	0	1	0	0	0	0	0	0	0	9
3.51- 7.50	5	4	2	1	4	0	1	3	2	1	2	6	1	1	3	3	39
7.51-12.50	10	7	8	6	3	1	6	4	6	4	4	8	11	5	14	9	106
12.51-18.50	12	8	2	2	2	0	5	4	5	2	4	2	10	11	12	22	103
18.51-24.00	16	3	1	0	0	1	0	0	4	4	6	0	1	8	12	13	69
>24.00	7	0	0	0	0	1	0	0	7	3	1	1	5	7	13	12	57
TOTAL	51	22	16	10	9	4	14	11	25	14	17	17	28	32	54	59	383

TABLE C-4 (CONTINUED)
CAPE CANAVERAL 5-YEAR WIND AND ATMOSPHERIC STABILITY DISTRIBUTIONS
(OCTOBER 7 THROUGH NOVEMBER 25)

5-YEAR OCT/NOV CAPE CANAVERAL 492 FT TOWER DATA
SITE IDENTIFIER: TOWER313
DATA PERIOD EXAMINED: 10/ 7/80 - 11/30/84

*** OCTOBER/NOVEMBER ***

STABILITY CLASS G

STABILITY BASED ON: DELTA T BETWEEN 492.0 AND 54.0 FEET
WIND MEASURED AT: 492.0 FEET
WIND THRESHOLD AT: 0.60 MPH

JOINT FREQUENCY DISTRIBUTION OF WIND SPEED AND DIRECTION IN HOURS AT492.00 FEET

SPEED (MPH)	N	NNE	NE	ENE	E	ESE	SE	SSE	S	SSW	SW	WSW	W	WNW	NW	NNW	TOTAL
CALM																	0
0.61- 3.50	0	0	0	0	0	0	0	0	0	0	0	0	0	0	0	0	0
3.51- 7.50	1	2	0	0	0	0	0	0	0	0	0	0	0	0	0	0	3
7.51-12.50	1	7	0	0	0	0	0	0	0	0	0	0	0	0	0	1	9
12.51-18.50	1	2	0	0	0	0	0	0	0	0	0	0	0	4	0	0	7
18.51-24.00	0	0	0	0	1	0	0	0	0	0	0	0	0	1	1	0	3
>24.00	0	0	0	0	0	0	0	0	0	0	0	0	0	0	0	0	0
TOTAL	3	11	0	0	1	0	0	0	0	0	0	0	0	5	1	1	22

STABILITY CLASS ALL

STABILITY BASED ON: DELTA T BETWEEN 492.0 AND 54.0 FEET
WIND MEASURED AT: 492.0 FEET
WIND THRESHOLD AT: 0.60 MPH

JOINT FREQUENCY DISTRIBUTION OF WIND SPEED AND DIRECTION IN HOURS AT492.00 FEET

SPEED (MPH)	N	NNE	NE	ENE	E	ESE	SE	SSE	S	SSW	SW	WSW	W	WNW	NW	NNW	TOTAL
CALM																	0
0.61- 3.50	3	4	6	5	0	1	2	5	5	1	1	0	0	2	1	3	39
3.51- 7.50	24	24	27	26	22	23	20	16	9	5	11	20	7	9	15	14	272
7.51-12.50	70	92	96	87	105	95	88	46	30	20	17	31	38	25	39	48	927
12.51-18.50	101	117	70	112	160	141	149	81	49	31	28	31	60	65	46	87	1328
18.51-24.00	102	74	58	146	155	108	43	37	44	25	25	11	19	48	78	103	1076
>24.00	88	87	51	100	105	25	14	37	26	13	24	7	17	38	66	77	775
TOTAL	388	398	308	476	547	393	316	222	163	95	106	100	141	187	245	332	4417

TABLE C-4 (CONTINUED)
CAPE CANAVERAL 5-YEAR WIND AND ATMOSPHERIC STABILITY DISTRIBUTIONS
(OCTOBER 7 THROUGH NOVEMBER 25)

5-YEAR OCT/NOV CAPE CANAVERAL 492 FT TOWER DATA
SITE IDENTIFIER: TOWER313
DATA PERIOD EXAMINED: 10/ 7/80 - 11/30/84

*** OCTOBER/NOVEMBER ***

STABILITY BASED ON: DELTA T BETWEEN 492.0 AND 54.0 FEET
WIND MEASURED AT: 492.0 FEET
WIND THRESHOLD AT: 0.60 MPH

TOTAL NUMBER OF OBSERVATIONS: 4505

TOTAL NUMBER OF VALID OBSERVATIONS: 4417

TOTAL NUMBER OF MISSING OBSERVATIONS: 88

PERCENT DATA RECOVERY FOR THIS PERIOD: 98.0 %

MEAN WIND SPEED FOR THIS PERIOD: 17.3 MPH

TOTAL NUMBER OF OBSERVATIONS WITH BACKUP DATA: 0

PERCENTAGE OCCURRENCE OF STABILITY CLASSES

A	B	C	D	E	F	G
1.52	0.97	1.72	31.42	55.20	8.67	0.50

DISTRIBUTION OF WIND DIRECTION VS STABILITY

	N	NNE	NE	ENE	E	ESE	SE	SSE	S	SSW	SW	WSW	W	WNW	NW	NNW	CALM
A	2	3	0	7	34	6	3	0	2	0	0	0	0	0	0	10	0
B	5	3	3	3	10	1	1	3	4	0	1	0	0	0	1	8	0
C	4	9	9	9	7	2	2	7	2	2	8	1	0	0	7	7	0
D	164	158	123	166	137	111	80	59	37	26	26	25	40	51	55	130	0
E	159	192	157	281	349	269	216	142	93	53	54	57	73	99	127	117	0
F	51	22	16	10	9	4	14	11	25	14	17	17	28	32	54	59	0
G	3	11	0	0	1	0	0	0	0	0	0	0	0	5	1	1	0
TOTAL	388	398	308	476	547	393	316	222	163	95	106	100	141	187	245	332	0

TABLE C-4 (CONTINUED)
CAPE CANAVERAL 5-YEAR WIND AND ATMOSPHERIC STABILITY DISTRIBUTIONS
(OCTOBER 7 THROUGH NOVEMBER 25)

8. The combination of onshore surface winds, an inland covergence zone, offshore winds aloft, and subsiding air over the sea completes the sea breeze circulation cell.

The KSC WINDS data were reviewed to identify those days during the launch window when sufficient land-sea temperature differential existed to support the potential for a sea breeze. A total of 47 such days were identified out of a possible 200 days in the 5-year launch window data set. Further analysis of wind data showed that 10 of these cases had the potential to be sea-breeze occurrences.

Onshore flows can also occur during gradient wind conditions. In this case, the characteristic sea breeze circulation cell does not occur and significant shears of wind speed or direction in the vertical are normally not present. Of the eight characteristics of the sea breeze noted above, only the occurrence of the TIBL induced by insolation and/or increasing mechanical turbulence may be present. Therefore, the effects on transport and diffusion induced by the TIBL may be present but the effects of the circulation cell will not occur.

C.3.2 UPPER AIR CLIMATOLOGY

C.3.2.1 Wind Direction and Speed

Three years of KSC launch window rawinsonde data (1982-1984) were used to develop the distributions of wind direction and wind speed for the pressure levels of 850, 700, 500, and 350 mb (approximately 4750, 10,000, 18,250 and 26,500 feet, respectively, in the standard atmosphere). These distributions are presented in Figures C-7 through C-10. The figures demonstrate a significant change in wind direction with height. The 4750-ft level, which approximates the gradient wind level, continues to exhibit a high-frequency of onshore flows with winds from the northeast clockwise through east dominating. The high occurrence of northeasterly winds seen at this level is indicative of the influence exerted by the "northeast trade winds" over the tropical and subtropical regions of the North Atlantic (Reference C-4). The minimum value at this level is also noteworthy since, within the 3-year data period, there were no occurrences of a northwest wind. At the 10,000-ft level the distribution becomes slightly more uniform and represents a transition from the low-level trade winds to the upper-level westerlies. The 18,250- and 26,500-ft levels show westerly winds to be highly dominant with easterly winds occurring very infrequently. These frequency distributions are reflective of the westerly winds dominant in the upper tropospheric circulation at this latitude (Reference C-5).

The average wind speeds for the 3-year data period are also seen to change with height. At 4750 ft the average wind speed is 15.7 mph, increasing to 17.6, 25.5, and 37.2 mph at 10,000 18,250 and 26,500 ft respectively. There were no reports of

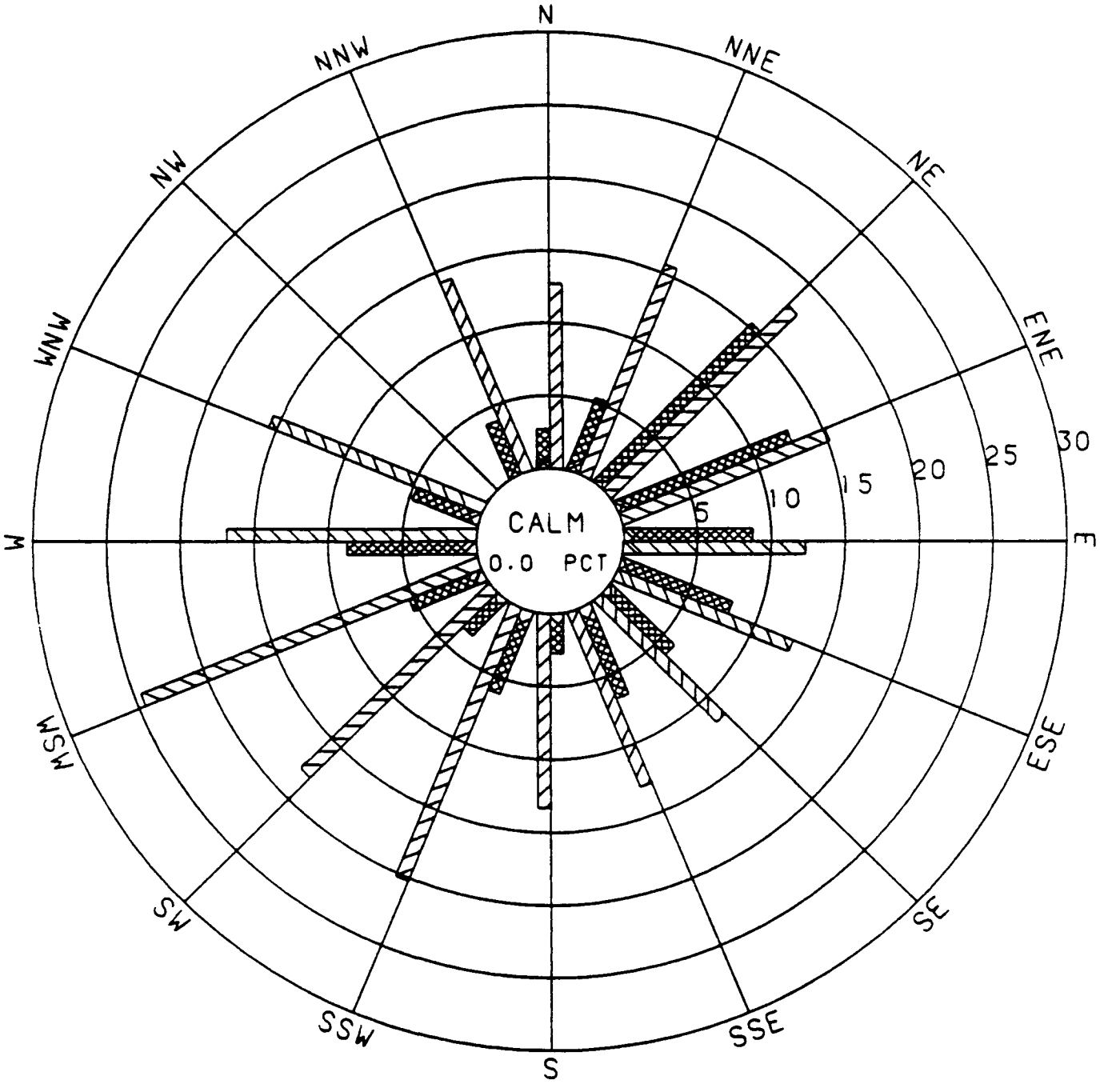

FIGURE C-7
CAPE CANAVERAL 850-MB (4,750-FT)
3-YEAR WIND ROSE
(OCTOBER 7 THROUGH NOVEMBER 25)

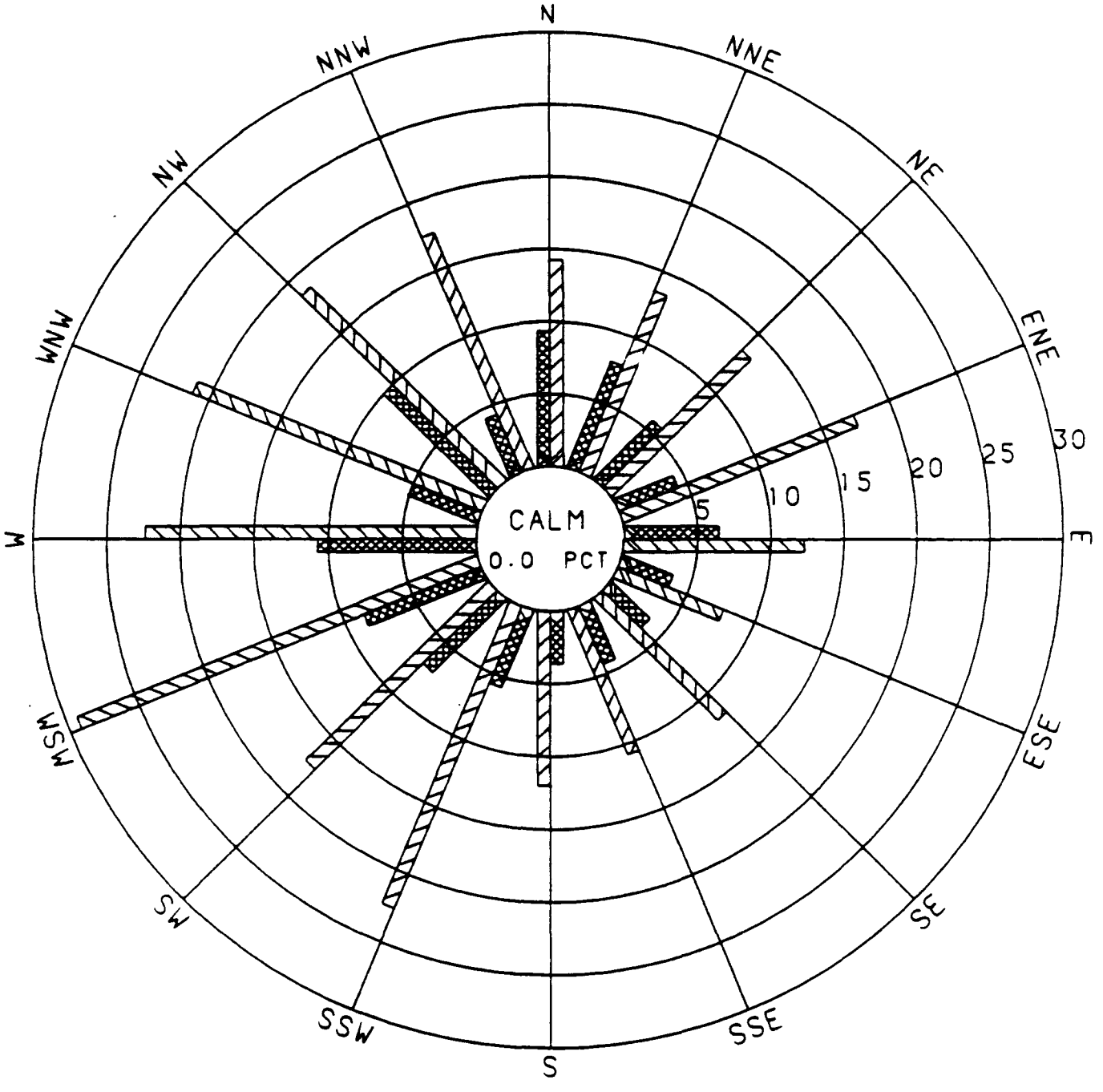

FIGURE C-8
CAPE CANAVERAL 700-MB (10,000-FT)
3-YEAR WIND ROSE
(OCTOBER 7 THROUGH NOVEMBER 25)

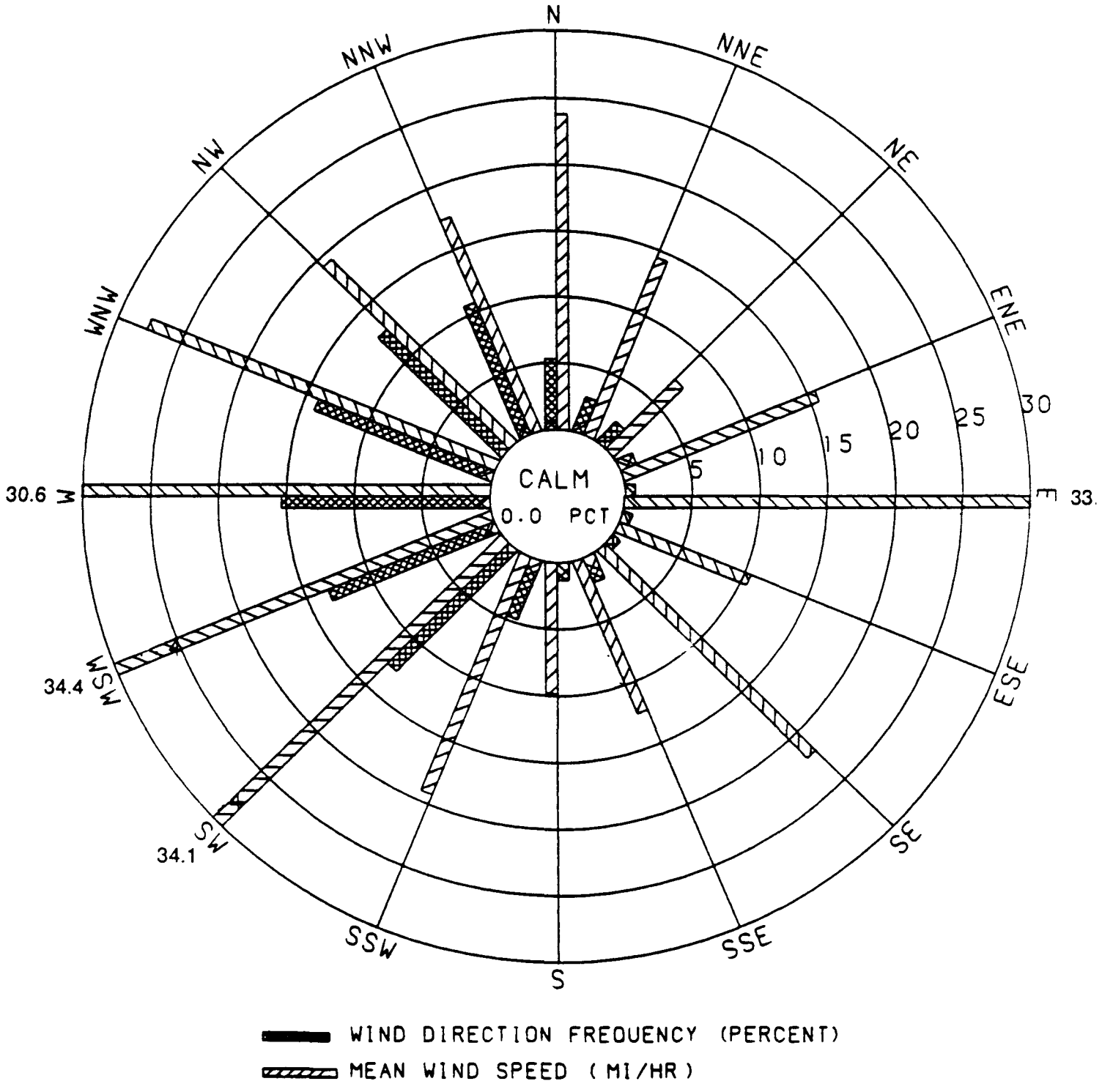

Mean wind speeds greater than 30 mi/hr are indicated by a bar out to 30 mi/hr and the numerical value at the end of the bar.

FIGURE C-9
CAPE CANAVERAL 500-MB (18,250-FT)
3-YEAR WIND ROSE
(OCTOBER 7 THROUGH NOVEMBER 25)

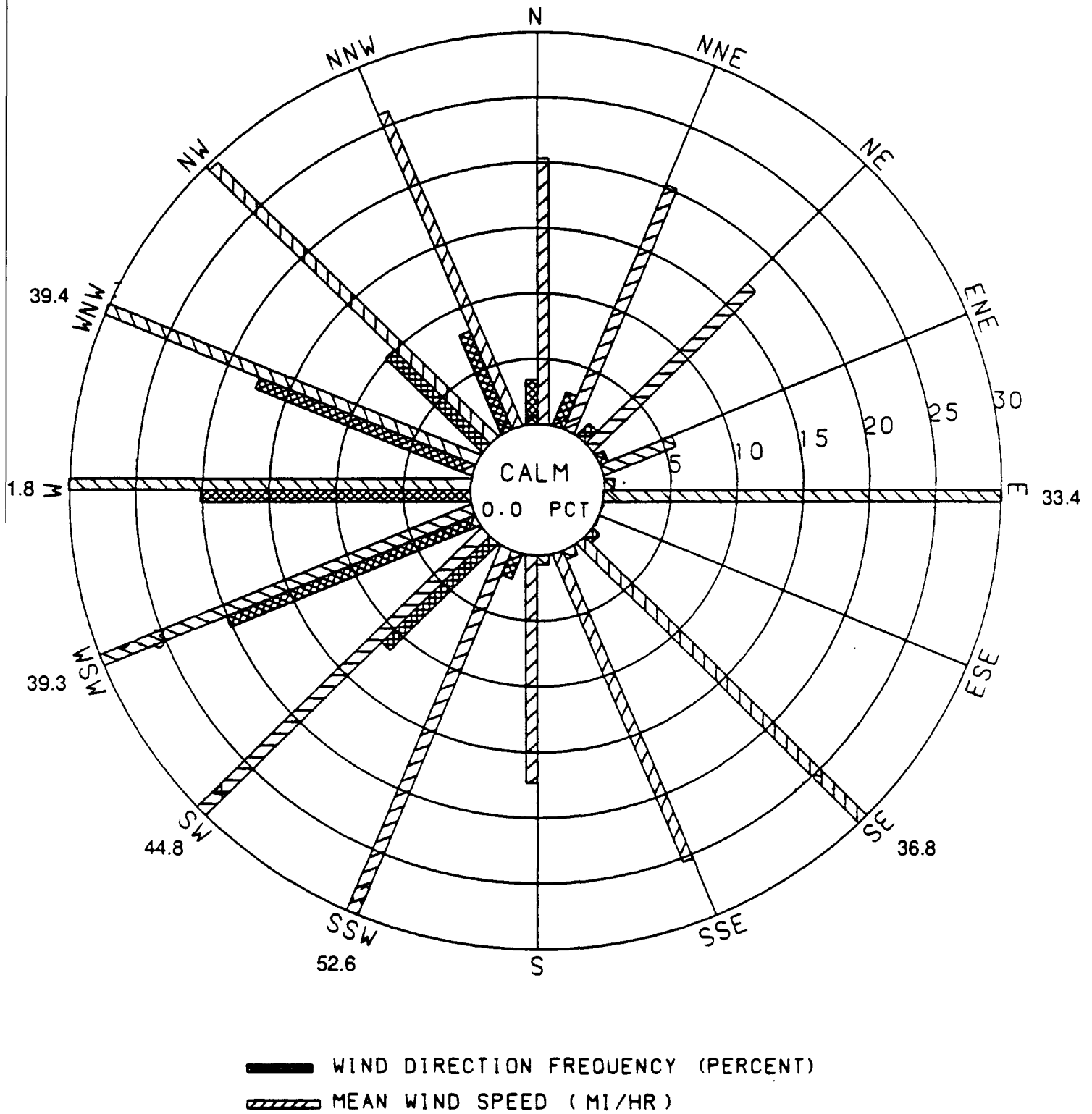

Mean wind speeds greater than 30 mi/hr are indicated by a bar out to 30 mi/hr and the numerical value at the end of the bar.

FIGURE C-10
CAPE CANAVERAL 350-MB (26,500-FT)
3-YEAR WIND ROSE
(OCTOBER 7 THROUGH NOVEMBER 25)

calm winds within the 3-year data period at any of the levels analyzed.

The rawinsonde reporting station at West Palm Beach, Florida (PBI) is the closest routinely reporting station to Cape Canaveral. A 5-year data period (1980-1984) for the launch window dates in October and November was analyzed for a long-term comparison to the 3-year KSC data. Figures C-11, C-12, C-13, and C-14 present wind direction and wind speed distributions at PBI for the 4750-, 10,000-, 18,250-, and 26,500-ft levels respectively. As with the KSC data, a significant change in wind direction is seen to occur with height. The 4750-ft level shows that onshore flows from northeast clockwise through east are dominant with the minimum frequency associated with north winds. The 10,000-ft level again represents a transitional level between the upper and lower wind regimes. At this level a significant decrease in the occurrence of easterly winds is seen with a corresponding increase in westerly winds. At the two upper levels the predominant winds are westerly and it is seen that easterly winds occur very infrequently. These directional distributions are very similar to those seen in the KSC data. In particular, the 26,500-ft frequencies agree very well showing peak occurrences from the west and west-southwest with very few, if any, occurrences of southeasterly winds.

The average wind speeds for the 5-year PBI data also agree well with the KSC data. The 5-year wind speeds are 14.0, 15.1, 23.1 and 36.1 mph from the lowest to highest level respectively. These averages are within 3 mph of the corresponding KSC values. Calm winds were reported only twice in the PBI data. These occurred once each at the 4750- and 10,000-ft levels.

No discussion of wind direction persistence is provided for upper-level winds since rawinsonde data are only available as once- or twice-daily observations.

C.4 DOWNRANGE CLIMATOLOGY

C.4.1 SURFACE CLIMATOLOGY

Streamlines depicting mean surface wind flows and isobars showing mean sea-level pressure are seen in Figures C-15 (July) and C-16 (January). The mean wind flow downrange of Cape Canaveral is seen to be greatly influenced by a sub-tropical high pressure ridge resulting in a predominantly easterly flow. In July the sub-tropical ridge, being fairly strong and well organized, exerts a significant influence on the mean surface winds. South of approximately 25°N the surface winds are seen to maintain an easterly flow. North of this latitude, however, they exhibit an anticylonic curvature northward around the sub-tropical high. By January the ridge becomes relatively weak and

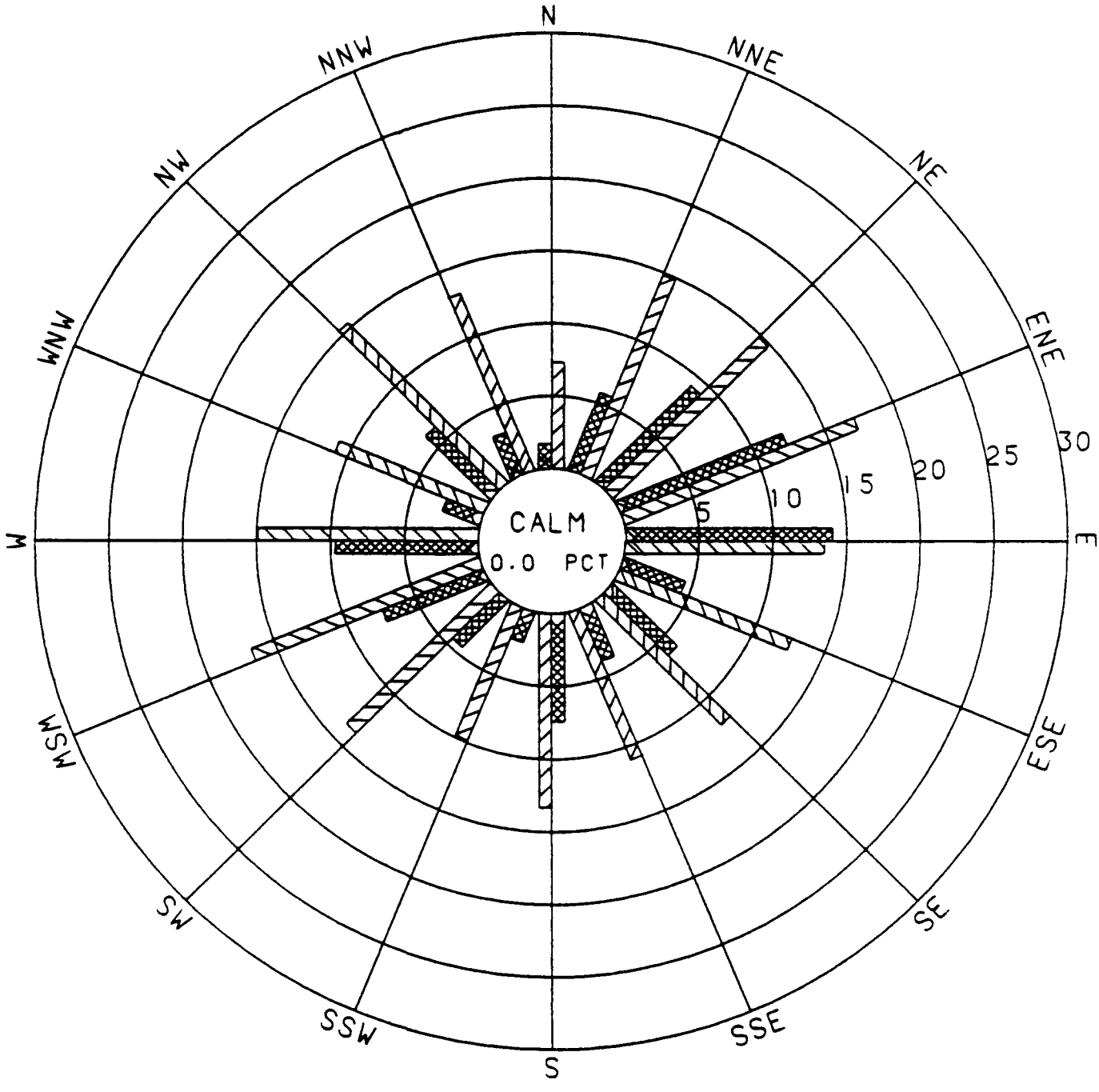

FIGURE C-11
WEST PALM BEACH 850-MB (4,750-FT)
5-YEAR WIND ROSE
(OCTOBER 7 THROUGH NOVEMBER 25)

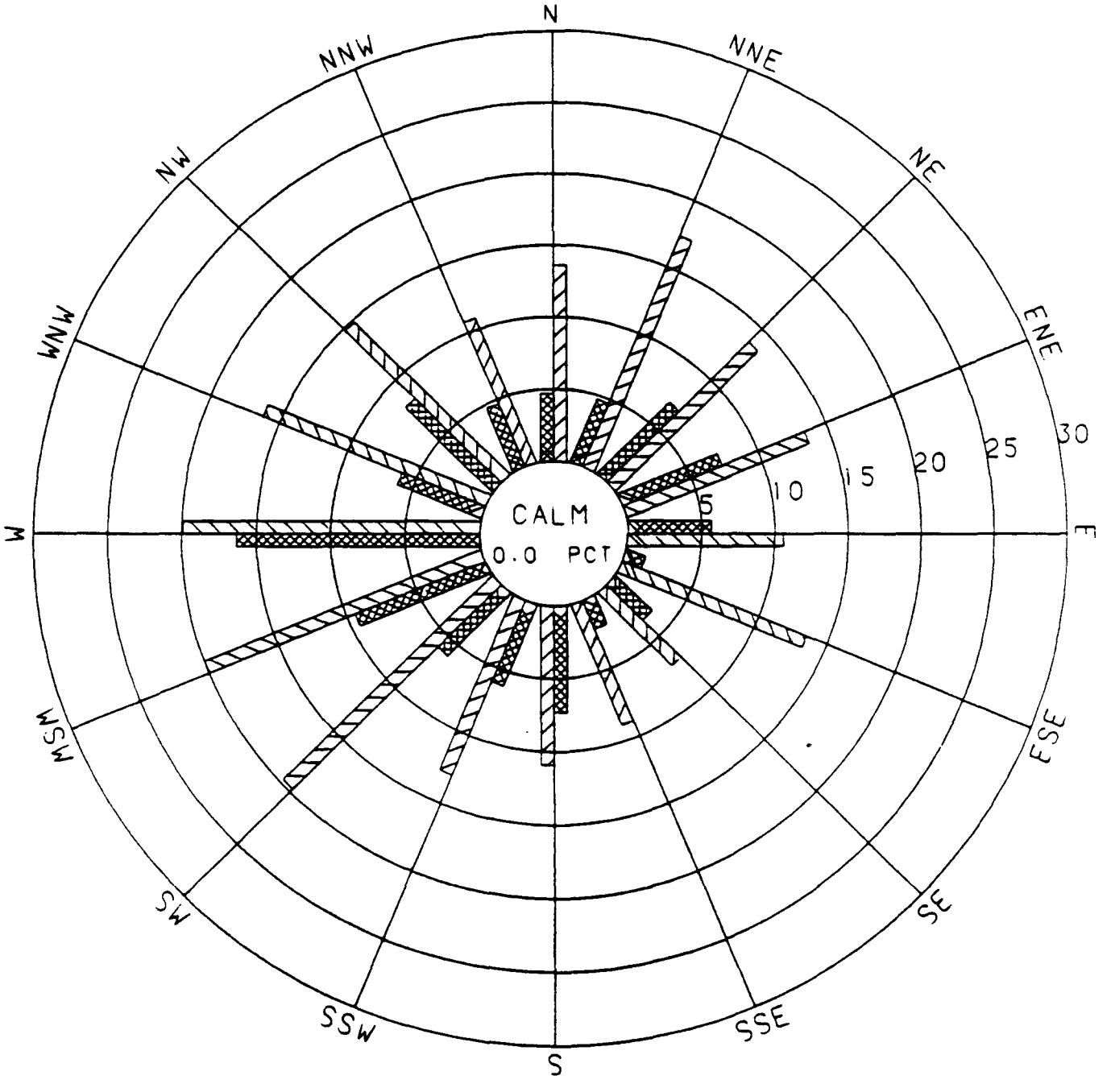

FIGURE C-12
WEST PALM BEACH 700-MB (10,000-FT)
5-YEAR WIND ROSE
(OCTOBER 7 THROUGH NOVEMBER 25)

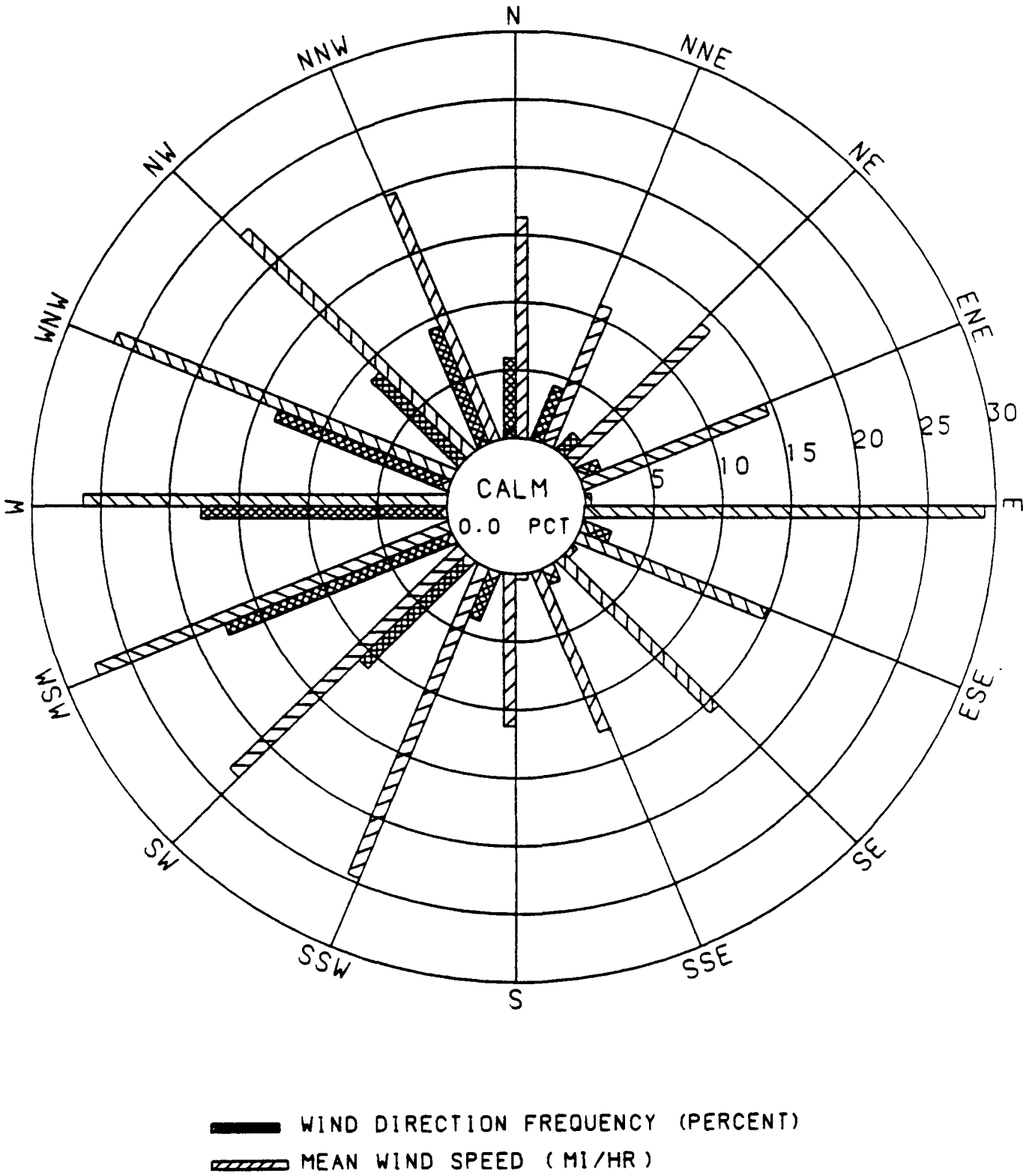

FIGURE C-13
WEST PALM BEACH 500-MB (18,250-FT)
5-YEAR WIND ROSE
(OCTOBER 7 THROUGH NOVEMBER 25)

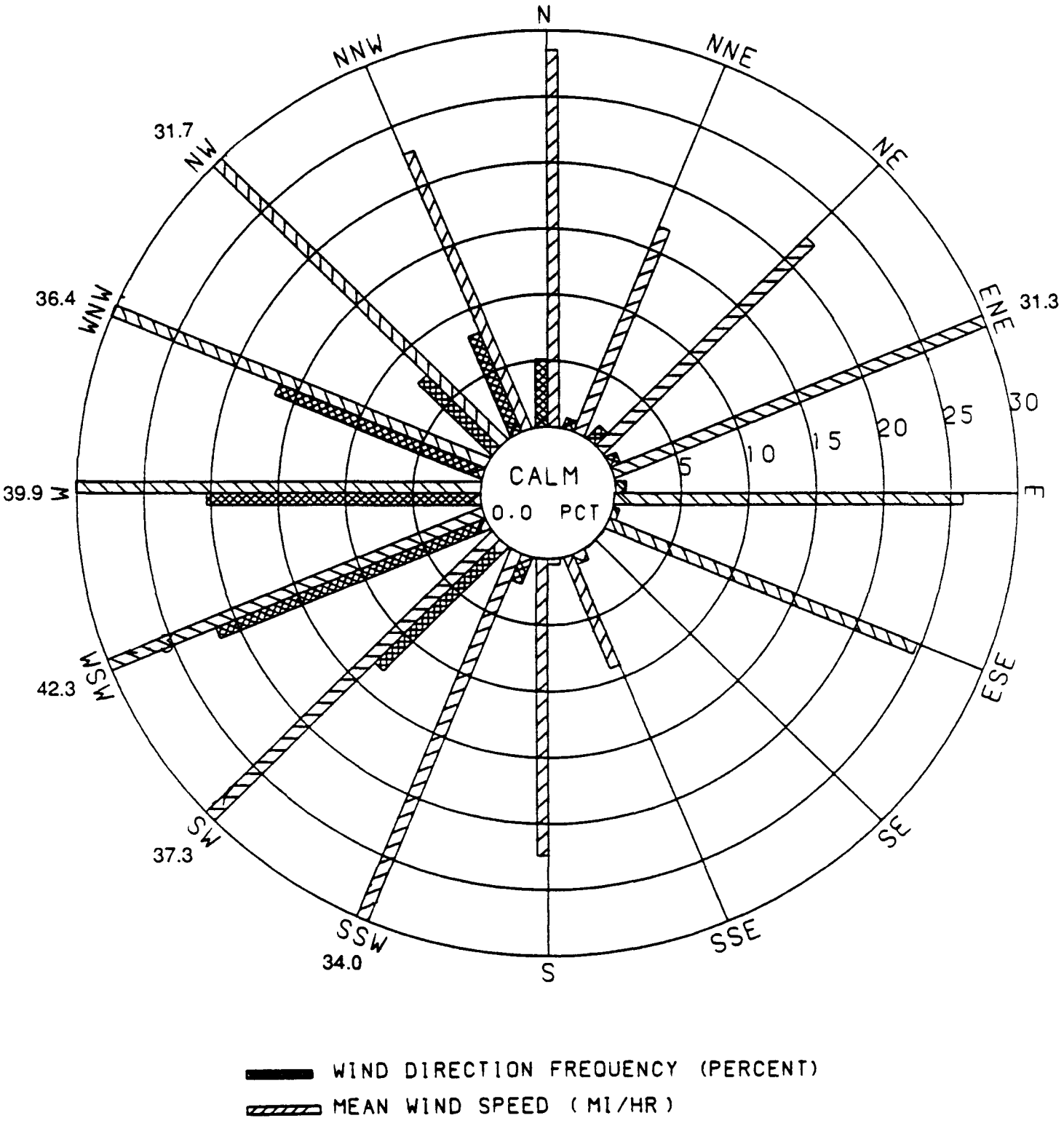

Mean wind speeds greater than 30 mi/hr are indicated by a bar out to 30 mi/hr and the numerical value at the end of the bar.

FIGURE C-14
WEST PALM BEACH 350-MB (26,500-FT)
5-YEAR WIND ROSE
(OCTOBER 7 THROUGH NOVEMBER 25)

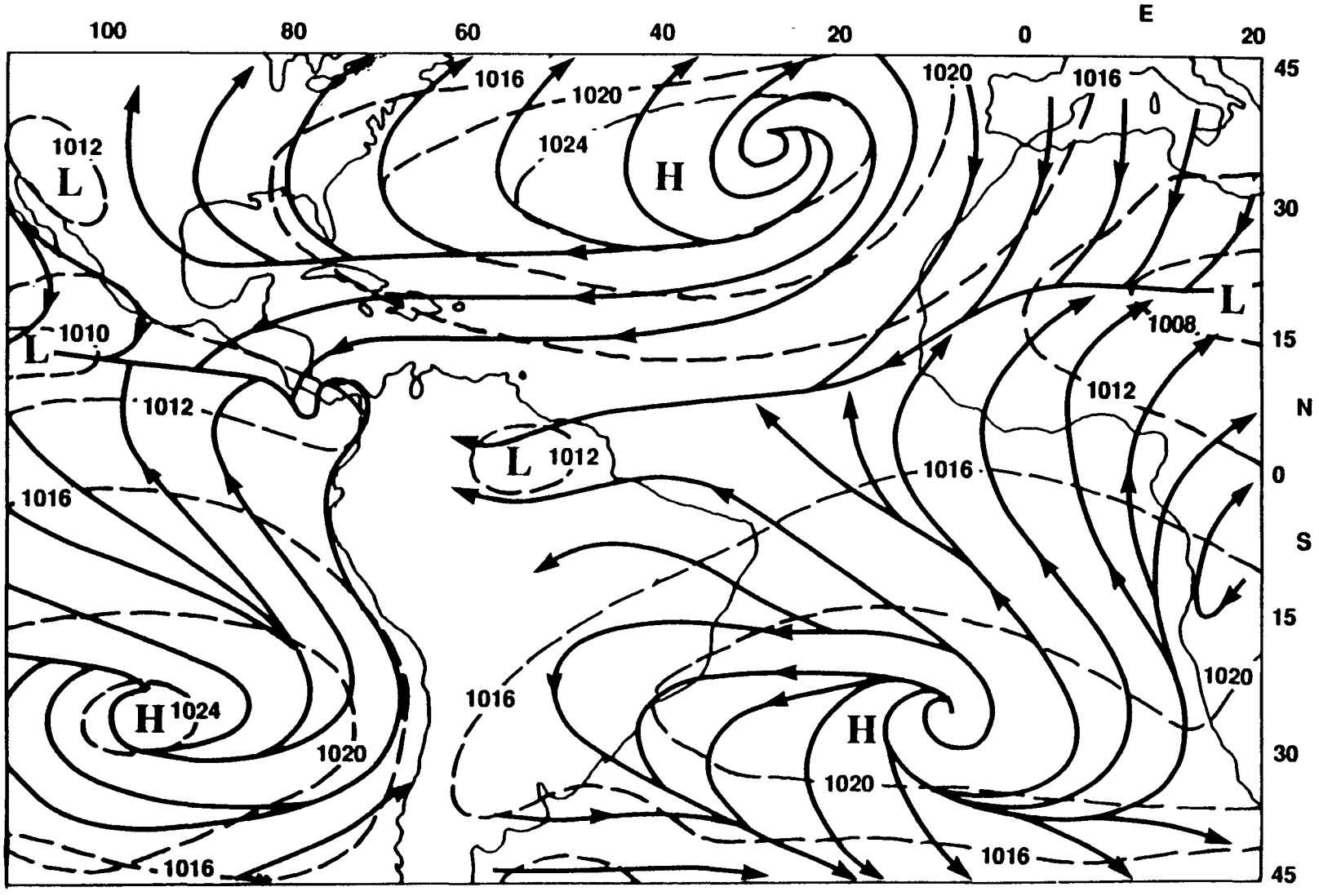

Key:

——— Surface Streamlines

– – – Sea-level Isobars (mb)

Source: Riehl, Herbert, 1974 (Reference C-2)

FIGURE C-15
MEAN SURFACE STREAMLINES AND
MEAN SEA-LEVEL PRESSURE FOR JULY

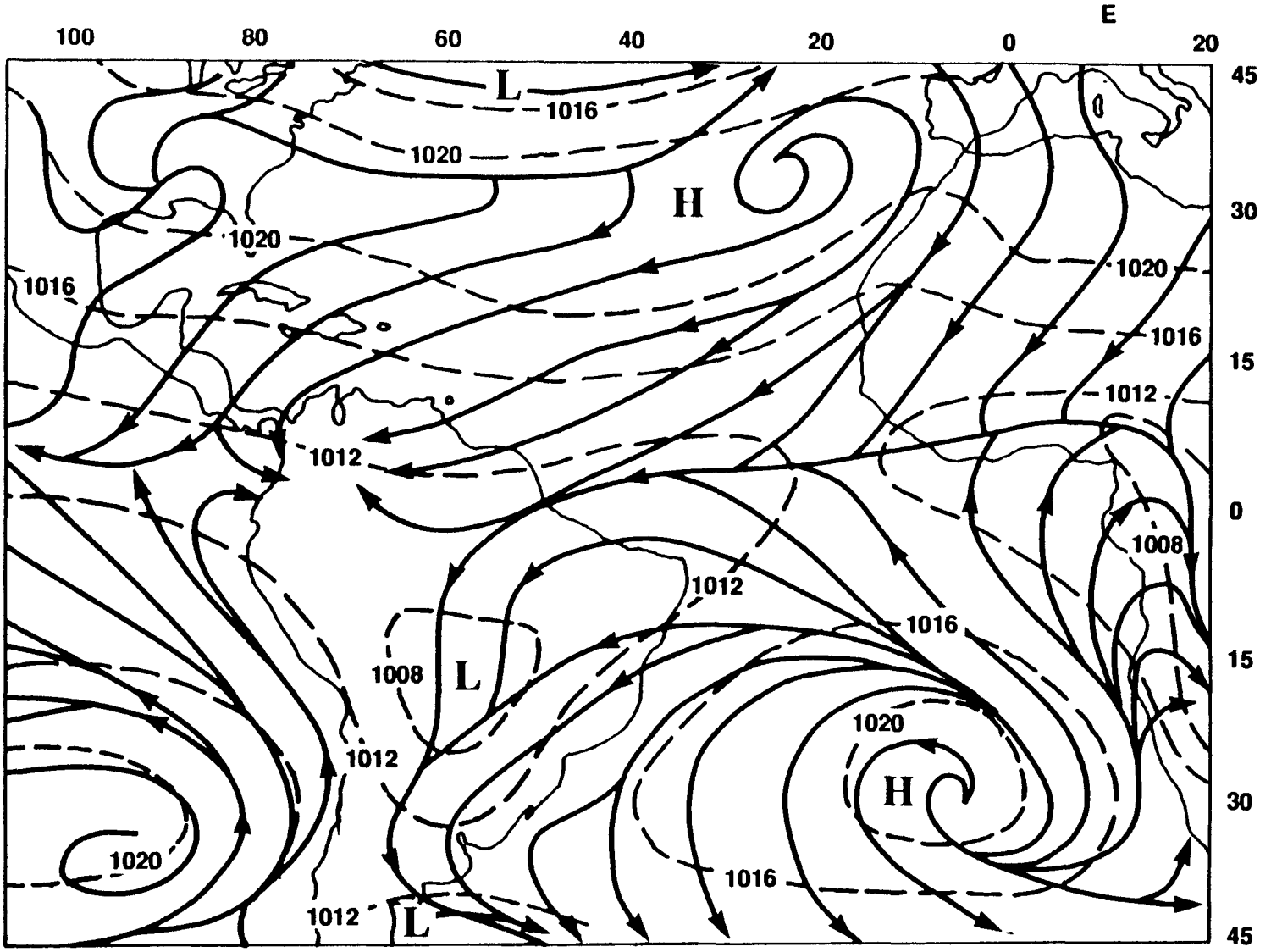

Key:

——— Surface Streamlines

— — — Sea-level Isobars (mb)

Source: Riehl, Herbert, 1974 (Reference C-2)

FIGURE C-16
MEAN SURFACE STREAMLINES AND
MEAN SEA-LEVEL PRESSURE FOR JANUARY

ill-defined with the surface flow from northeast to southwest across the entire downrange Atlantic Ocean.

Surface climatological conditions for the launch window period would represent a transition between the July and January regimes, perhaps being more like January.

C.4.2 UPPER AIR CLIMATOLOGY

Several sources of information can provide climatological analyses of 850 and 200 mb winds on a global scale (References C-4, C-6, and C-7). However, these sources generally provide analyses only for January and July.

At 850-mb during July the North Atlantic Ocean downrange of Cape Canaveral generally lies in a region of transition with polar westerlies to the north and tropical easterlies to the south. This pattern does not change dramatically with height, although, at 200 mb the tropical easterlies tend to prevail from the Florida peninsula to about 50° west longitude and polar westerlies tend to be more prevalent east of 50° west (Reference C-4).

During the fall months this transition region undergoes a southward migration that is more extensive at 200 mb than 850 mb. By January the patterns at both levels over the downrange Atlantic are primarily dominated by the polar westerlies which increase significantly in strength with height (Reference C-4).

C.5 LAUNCH WINDOW METEOROLOGICAL SUMMARIES

Meteorological data collected at Cape Canaveral were summarized for input in the evaluation of potential radiological impacts of aborted shuttle launches. Since the launch window is restricted to the October 7 through November 25 time period, meteorological data collected only during this period were analyzed. Data from 1982 and 1984 were available from WINDS Tower 313 and rawinsondes for analysis of ground-level and elevated sources respectively. The specific meteorological sequences used as direct input to atmospheric dispersion assessments and the potential radiological impacts are discussed in Appendix A. In order to provide more resolution on the relationship of radiological impacts and their corresponding meteorological conditions, mappings in time of upper-level versus low-level wind direction are presented in Figures C-17 and C-18. The upper and lower winds from 8 hours prior up to launch time are seen in Figure C-17 and those from launch up to 16 hours after are seen in Figure C-18.

Summaries of various meteorological parameters for tower and rawinsonde data are provided in the following sections. These summaries represent data necessary to characterize meteorological conditions for the range of launch window dates. Long-

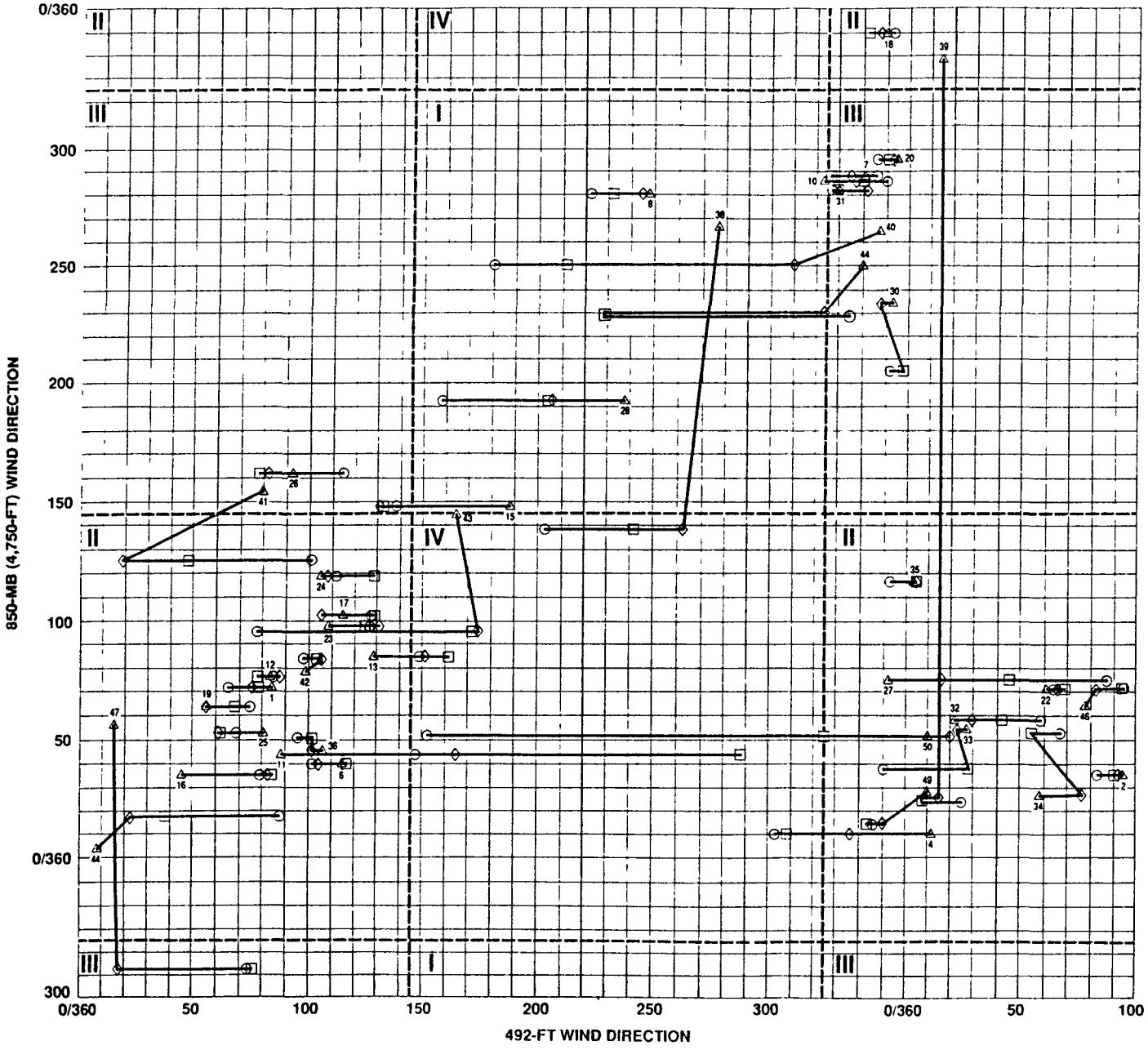

Legend:

- ○ - Wind direction at T-8 hours
- □ - Wind direction at T-4 hours
- ◇ - Wind direction at T-2 hours
- △ - Wind direction at T-0 hours

Arabic numerals denote EMERGE case number

I - Offshore winds at 492 ft and 5000 ft

II - Onshore winds at 492 ft and 5000 ft

III - Onshore winds at 492 ft Offshore winds at 5000 ft

IV - Offshore winds at 492 ft Onshore winds at 5000 ft

Figure C-17

Time History of KSC Upper- and Lower-Level Wind Directions for EMERGE Cases (T-8 to T-0 Hours)

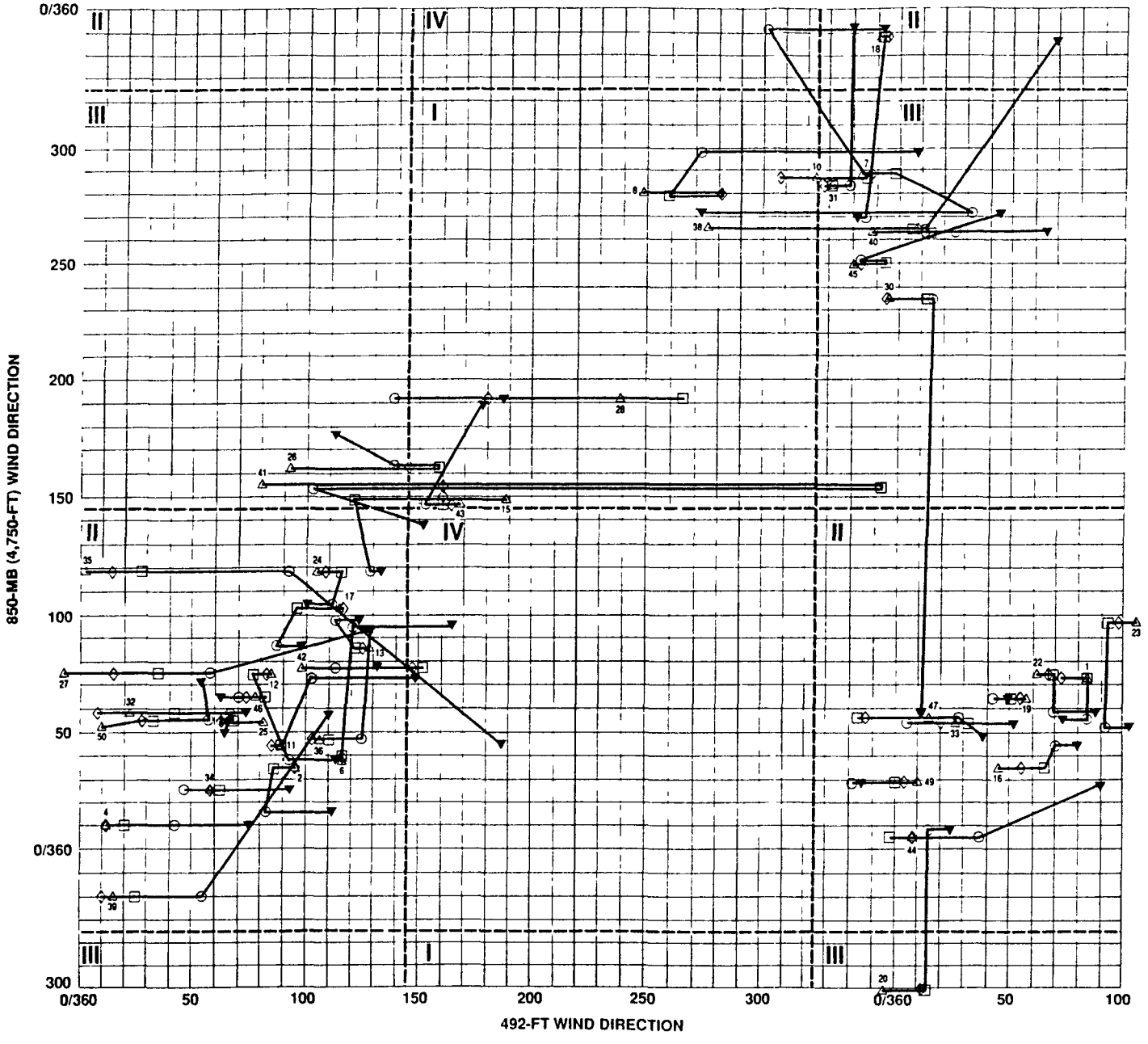

Legend:

△ - Wind direction at T-0 hours

◇ - Wind direction at T+2 hours

□ - Wind direction at T+4 hours

○ - Wind direction at T+8 hours

▼ - Wind direction at T+16 hours

Arabic numerals denote EMERGE case number

I - Offshore winds at 492 ft and 5000 ft

II - Onshore winds at 492 ft and 5000 ft

III - Onshore winds at 492 ft Offshore winds at 5000 ft

IV - Offshore winds at 492 ft Onshore winds at 5000 ft

Figure C-18

Time History of KSC Upper- and Lower-Level Wind Directions for EMERGE Cases (T-0 to T+16 Hours)

term averages provided by the climatological summaries of previous sections may be used for comparison.

C.5.1 LOW-LEVEL WIND DIRECTION AND SPEED

Wind direction and wind speed distributions for the 54-, 204-, and 492-ft levels of Tower 313 are provided in Figures C-19 through C-21. These figures exhibit distributional trends similar to those of the 5-year KSC WINDS data. The directional distribution is dominated by winds from the north clockwise through southeast sectors at all levels. The predominant winds at 54 feet are from the north, while the 204-, and 492-ft levels exhibit predominantly east-northeast winds.

The average wind speeds for the 1982/1984 data period are 9.6, 14.0, and 17.0 mph for the 54-, 204-, and 492-ft levels respectively. These values are all within 0.5 mph of their corresponding 5-year averages.

C.5.2 LOW-LEVEL WIND DIRECTION PERSISTENCE

Maximum wind direction persistence periods by direction sector for the 54-, 204-, and 492-ft levels are presented in Figure C-22. This figure indicates that, like the 5-year data, the longer persistence periods at all levels are associated with onshore flows. Further, it can be seen from Table C-3 that the maximum period for each level is found within the 1982/1984 data.

The probability of onshore winds persisting for periods from 1 through 44 hours were calculated for the launch window using 492-ft wind data. Figure C-23 presents these probabilities. This figure demonstrates that persistence periods of 4 hours or more have less than a 45 percent probability of occurrence.

C.5.3 ATMOSPHERIC STABILITY

Table C-5 presents atmospheric stability distributions for Cape Canaveral based on temperature differential between 492 feet and 54 feet. The stability classifications presented in these distributions were determined from the methodology described in the NRC Regulatory Guide 1.23 (Reference C-3). The most dominant conditions are Class E (slightly stable) and Class D (neutral) which occur nearly 57 and 33 percent of the time, respectively. By comparison the occurrence of unstable (Classes A, B, and C) and extremely stable (Class G) conditions are relatively infrequent. These trends are very similar to those exhibited in the 5-year stability distribution.

C.5.4 UPPER-LEVEL WIND DIRECTION AND SPEED

Distributions of wind direction and wind speed for the 850-, 700-, 500-, and 350-mb levels (approximately 4750, 10,000 18,250, and 26,500 feet, respectively, in the standard

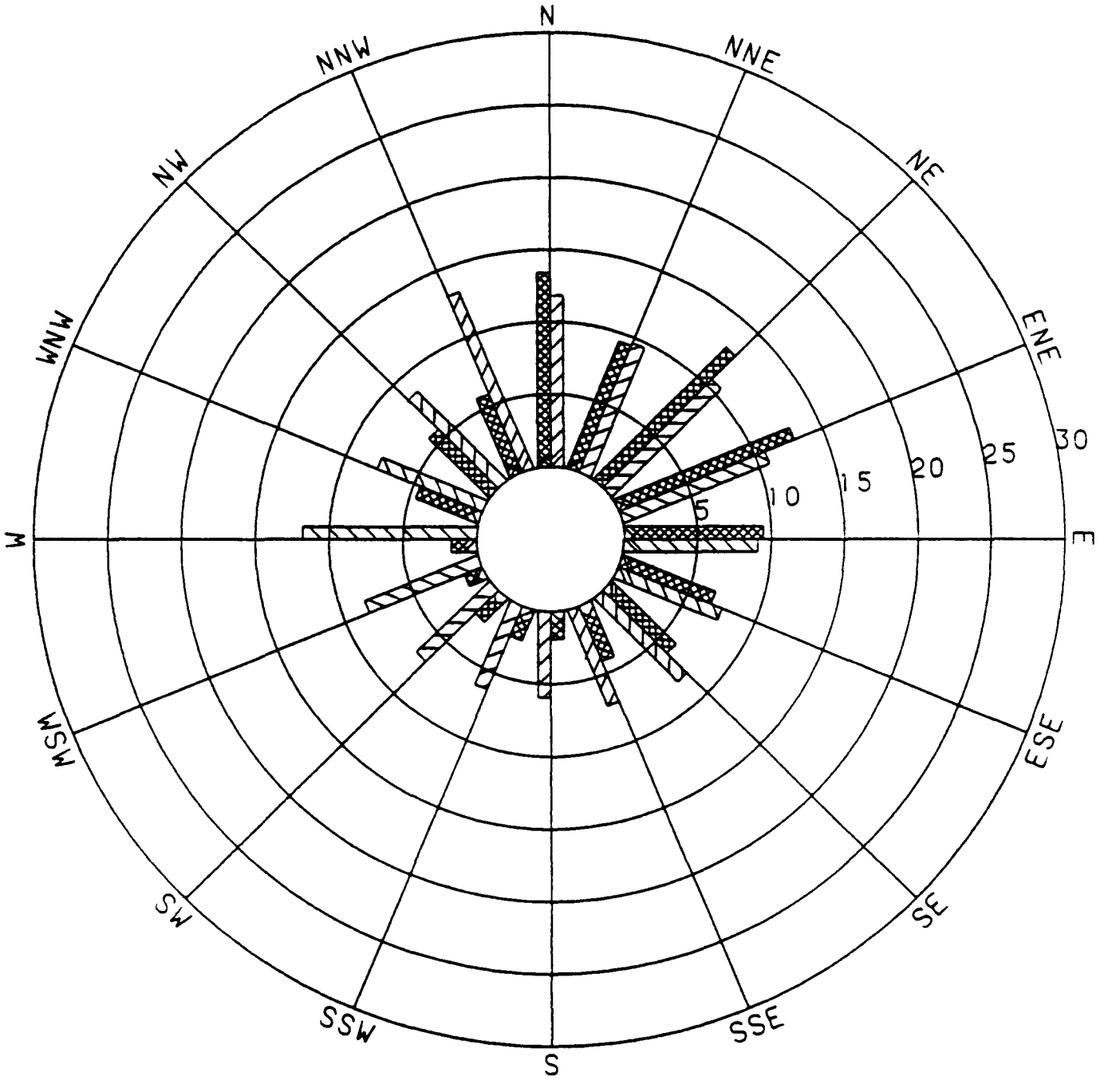

FIGURE C-19
CAPE CANAVERAL 54-FT
1982/1984 WIND ROSE
(OCTOBER 7 THROUGH NOVEMBER 25)

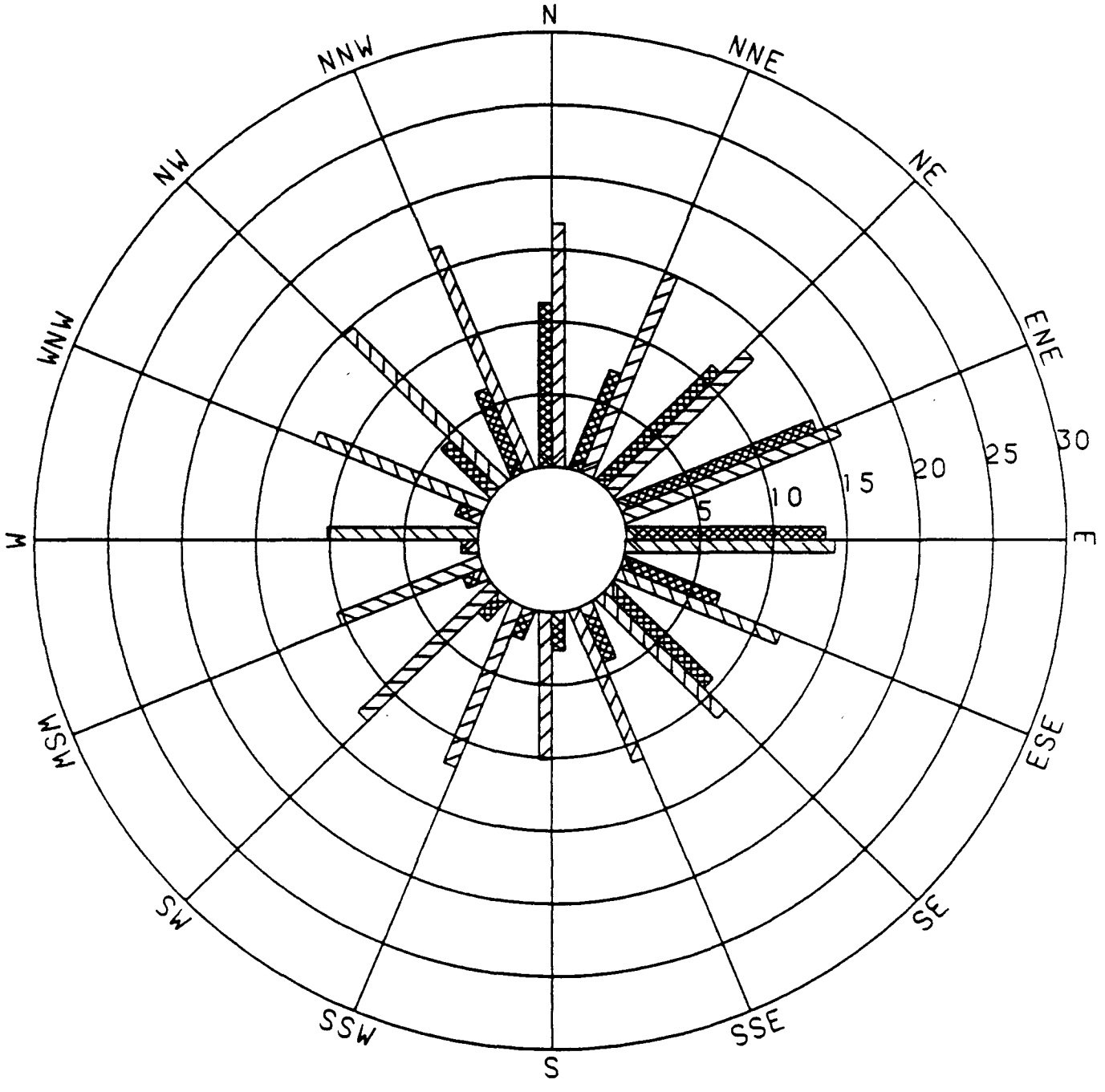

FIGURE C-20
CAPE CANAVERAL 204-FT
1982/1984 WIND ROSE
(OCTOBER 7 THROUGH NOVEMBER 25)

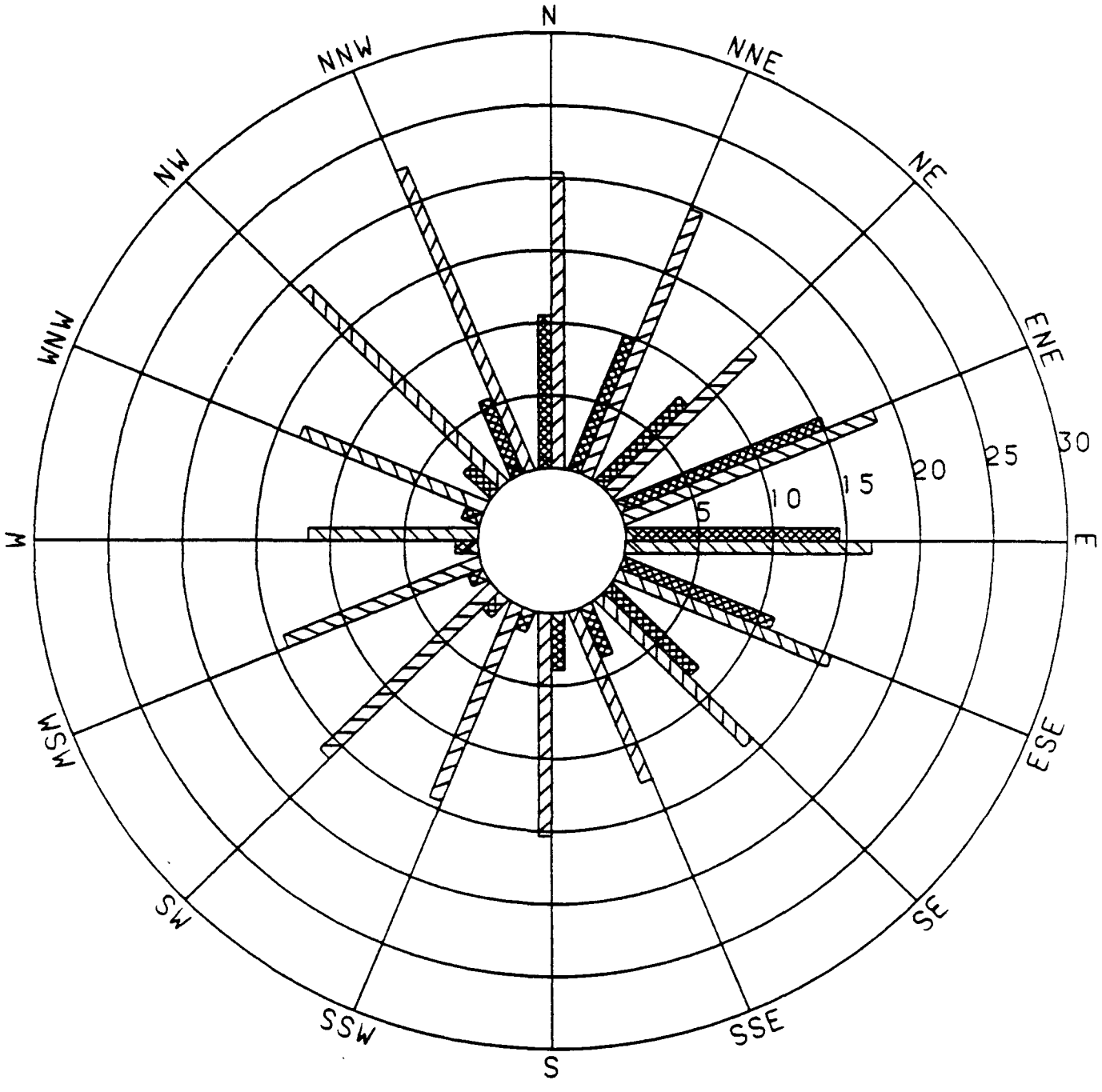

FIGURE C-21
CAPE CANAVERAL 492-FT
1982/1984 WIND ROSE
(OCTOBER 7 THROUGH NOVEMBER 25)

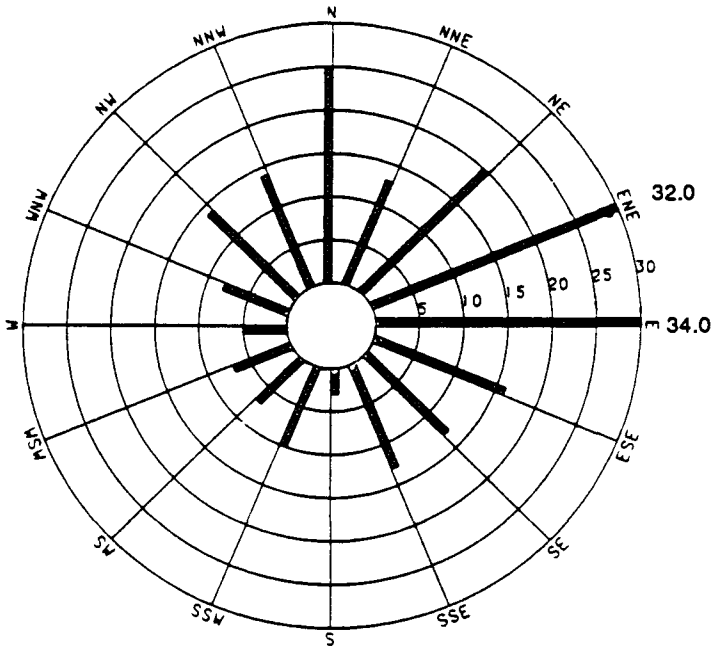

54 Feet

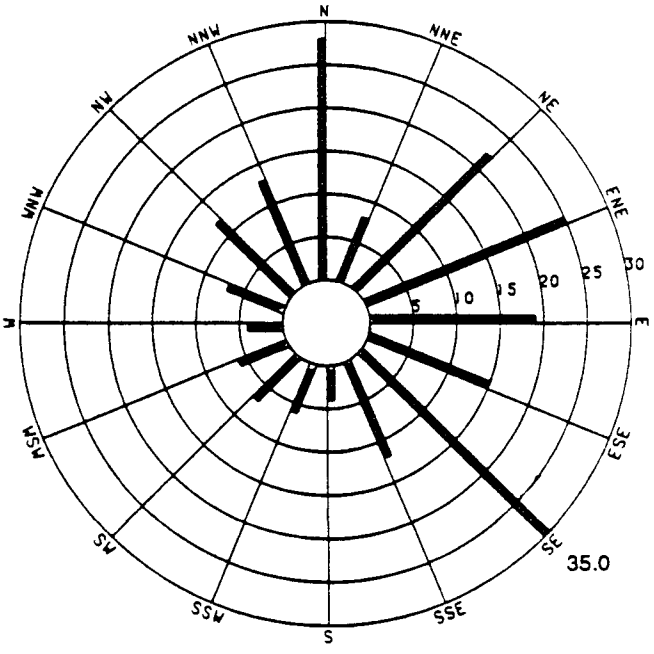

204 Feet

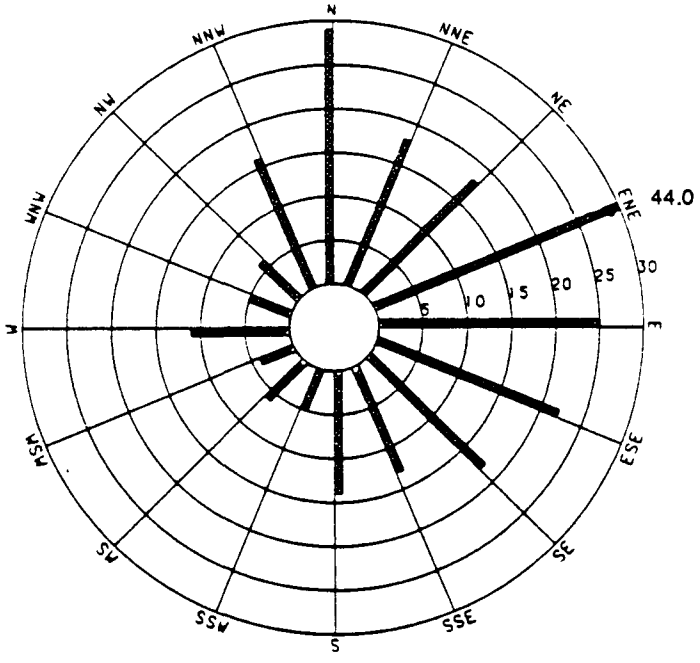

492 Feet

Rings extend to 30 hours only. Persistence periods greater than or equal to 30 hours are indicated by a bar out to 30 and the numerical value at the end of the bar.

FIGURE C-22
CAPE CANAVERAL 1982/1984
MAXIMUM DIRECTIONAL WIND PERSISTENCE ROSES (HOURS)
(OCTOBER 7 THROUGH NOVEMBER 25)

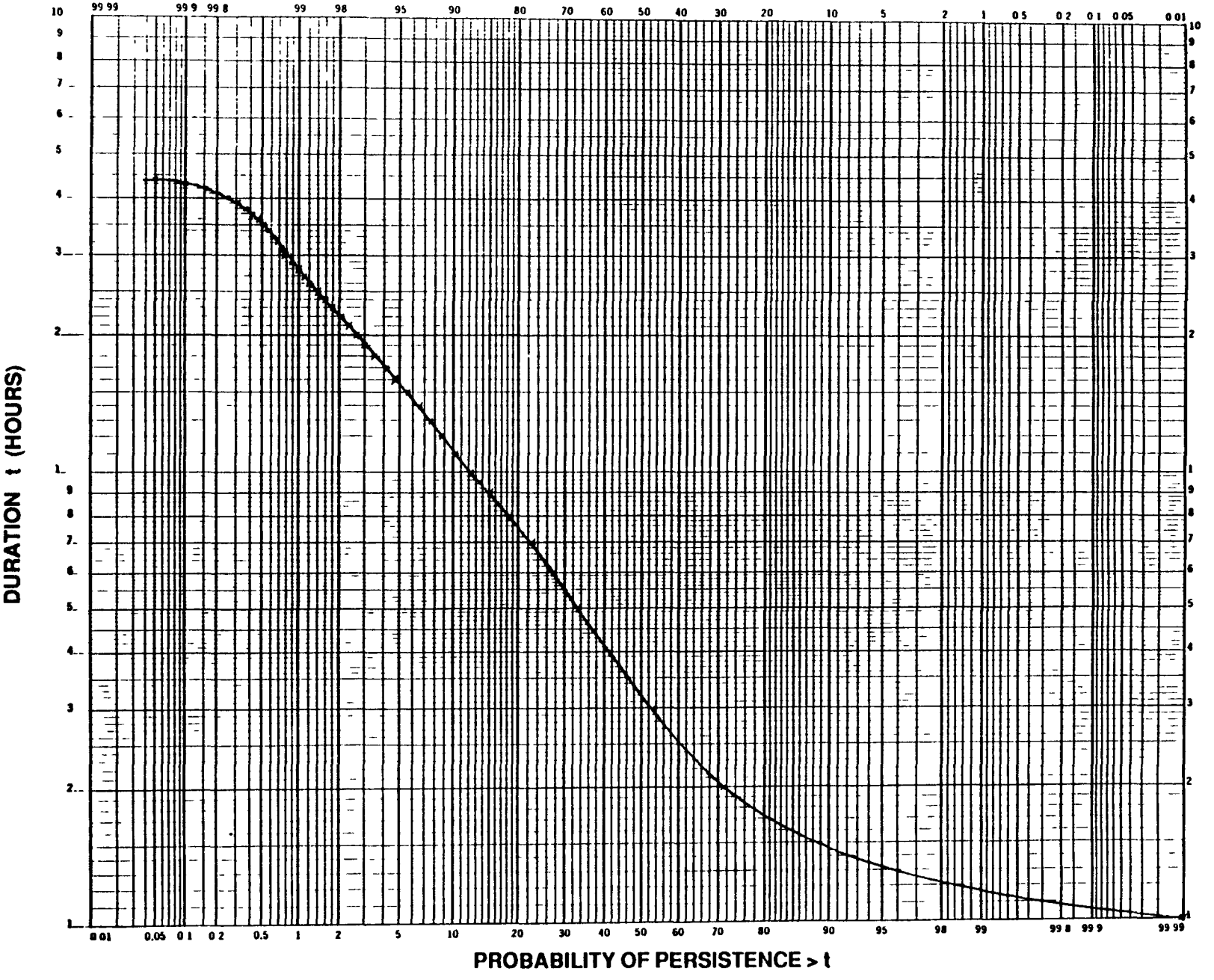

FIGURE C-23
CAPE CANAVERAL 492-FT 1982/1984 ONSHORE WIND PERSISTENCE
(OCTOBER 7 THROUGH NOVEMBER 25)

OCT/NOV 1982/1984 CAPE CANAVERAL 492 FT TOWER DATA
SITE IDENTIFIER: TOWER313
DATA PERIOD EXAMINED: 10/ 7/82 - 11/25/84

*** OCTOBER/NOVEMBER ***

STABILITY CLASS A

STABILITY BASED ON: DELTA T BETWEEN 492.0 AND 54.0 FEET
WIND MEASURED AT: 492.0 FEET
WIND THRESHOLD AT: 0.60 MPH

JOINT FREQUENCY DISTRIBUTION OF WIND SPEED AND DIRECTION IN HOURS AT492.00 FEET

SPEED (MPH)	N	NNE	NE	ENE	E	ESE	SE	SSE	S	SSW	SW	WSW	W	WNW	NW	NNW	TOTAL
CALM																	0
0.61- 3.50	0	0	0	0	0	0	0	0	0	0	0	0	0	0	0	0	0
3.51- 7.50	0	1	0	0	0	0	0	0	0	0	0	0	0	0	0	0	1
7.51-12.50	0	0	0	0	0	0	2	0	0	0	0	0	0	0	0	0	2
12.51-18.50	0	0	0	1	0	0	0	0	0	0	0	0	0	0	0	0	1
18.51-24.00	1	0	0	0	0	0	0	0	0	0	0	0	0	0	0	0	1
≥24.00	1	0	0	1	0	0	0	0	0	0	0	0	0	0	0	0	2
TOTAL	2	1	0	2	0	0	2	0	0	0	0	0	0	0	0	0	7

STABILITY CLASS B

STABILITY BASED ON: DELTA T BETWEEN 492.0 AND 54.0 FEET
WIND MEASURED AT: 492.0 FEET
WIND THRESHOLD AT: 0.60 MPH

JOINT FREQUENCY DISTRIBUTION OF WIND SPEED AND DIRECTION IN HOURS AT492.00 FEET

SPEED (MPH)	N	NNE	NE	ENE	E	ESE	SE	SSE	S	SSW	SW	WSW	W	WNW	NW	NNW	TOTAL
CALM																	0
0.61- 3.50	0	0	0	0	0	0	0	0	0	0	0	0	0	0	0	0	0
3.51- 7.50	0	0	0	1	0	0	0	0	0	0	0	0	0	0	0	0	1
7.51-12.50	0	1	0	0	0	0	0	1	0	0	1	0	0	0	0	0	3
12.51-18.50	0	0	1	0	0	0	1	0	2	0	0	0	0	0	0	0	4
18.51-24.00	1	0	0	1	0	0	0	0	0	0	0	0	0	0	0	0	2
≥24.00	3	0	0	0	0	0	0	0	0	0	0	0	0	0	0	0	3
TOTAL	4	1	1	2	0	0	1	1	2	0	1	0	0	0	0	0	13

TABLE C-5
CAPE CANAVERAL 1982/1984 WIND AND ATMOSPHERIC STABILITY DISTRIBUTIONS
(OCTOBER 7 THROUGH NOVEMBER 25)

OCT/NOV 1982/1984 CAPE CANAVERAL 492 FT TOWER DATA
SITE IDENTIFIER: TOWER313
DATA PERIOD EXAMINED: 10/ 7/82 - 11/25/84

*** OCTOBER/NOVEMBER ***

STABILITY CLASS C

STABILITY BASED ON: DELTA T BETWEEN 492.0 AND 54.0 FEET
WIND MEASURED AT: 492.0 FEET
WIND THRESHOLD AT: 0.60 MPH

JOINT FREQUENCY DISTRIBUTION OF WIND SPEED AND DIRECTION IN HOURS AT492.00 FEET

SPEED (MPH)	N	NNE	NE	ENE	E	ESE	SE	SSE	S	SSW	SW	WSW	W	WNW	NW	NNW	TOTAL
CALM																	0
0.61- 3.50	0	0	0	0	0	0	0	0	0	0	0	0	0	0	0	0	0
3.51- 7.50	0	0	0	2	1	0	0	0	1	0	0	0	0	0	0	0	4
7.51-12.50	0	1	0	0	1	0	0	0	0	0	1	0	0	0	0	0	3
12.51-18.50	0	0	3	0	0	0	0	3	0	0	1	0	0	0	0	0	7
18.51-24.00	0	2	1	4	0	0	1	1	0	1	2	0	0	0	0	0	12
>24.00	1	3	0	1	0	0	0	0	0	0	0	0	0	0	0	0	5
TOTAL	1	6	4	7	2	0	1	4	1	1	4	0	0	0	0	0	31

STABILITY CLASS D

STABILITY BASED ON: DELTA T BETWEEN 492.0 AND 54.0 FEET
WIND MEASURED AT: 492.0 FEET
WIND THRESHOLD AT: 0.60 MPH

JOINT FREQUENCY DISTRIBUTION OF WIND SPEED AND DIRECTION IN HOURS AT492.00 FEET

SPEED (MPH)	N	NNE	NE	ENE	E	ESE	SE	SSE	S	SSW	SW	WSW	W	WNW	NW	NNW	TOTAL
CALM																	0
0.61- 3.50	0	1	1	1	0	0	0	3	2	0	0	0	0	0	0	0	8
3.51- 7.50	7	3	12	6	7	3	1	2	3	2	0	2	3	1	0	1	53
7.51-12.50	5	17	24	23	28	19	24	9	5	4	0	0	4	2	4	5	173
12.51-18.50	14	19	22	31	15	32	30	16	5	3	8	4	3	3	1	7	213
18.51-24.00	24	20	11	37	10	16	2	4	0	3	3	2	0	1	0	14	147
>24.00	43	51	2	27	6	1	0	0	0	0	0	0	0	0	0	28	158
TOTAL	93	111	72	125	66	71	57	34	15	12	11	8	10	7	5	55	752

TABLE C-5 (CONTINUED)
CAPE CANAVERAL 1982/1984 WIND AND ATMOSPHERIC STABILITY DISTRIBUTIONS
(OCTOBER 7 THROUGH NOVEMBER 25)

OCT/NOV 1982/1984 CAPE CANAVERAL 492 FT TOWER DATA
SITE IDENTIFIER: TOWER313
DATA PERIOD EXAMINED: 10/ 7/82 - 11/25/84

*** OCTOBER/NOVEMBER ***

STABILITY CLASS E

STABILITY BASED ON: DELTA T BETWEEN 492.0 AND 54.0 FEET
WIND MEASURED AT: 492.0 FEET
WIND THRESHOLD AT: 0.60 MPH

JOINT FREQUENCY DISTRIBUTION OF WIND SPEED AND DIRECTION IN HOURS AT492.00 FEET

SPEED (MPH)	N	NNE	NE	ENE	E	ESE	SE	SSE	S	SSW	SW	WSW	W	WNW	NW	NNW	TOTAL
CALM																	0
0.61- 3.50	1	2	2	2	0	0	0	2	2	0	0	0	0	1	0	0	12
3.51- 7.50	3	7	9	8	6	12	10	8	2	2	4	1	1	3	1	1	78
7.51-12.50	16	11	33	23	55	49	28	17	12	7	2	2	7	1	5	2	270
12.51-18.50	27	26	27	61	84	69	52	12	14	7	3	4	5	2	10	12	415
18.51-24.00	26	14	8	76	67	48	20	7	20	6	4	1	2	2	7	21	329
>24.00	16	29	13	37	36	10	5	2	4	0	2	1	0	2	12	9	178
TOTAL	89	89	92	207	248	188	115	48	54	22	15	9	15	11	35	45	1282

STABILITY CLASS F

STABILITY BASED ON: DELTA T BETWEEN 492.0 AND 54.0 FEET
WIND MEASURED AT: 492.0 FEET
WIND THRESHOLD AT: 0.60 MPH

JOINT FREQUENCY DISTRIBUTION OF WIND SPEED AND DIRECTION IN HOURS AT492.00 FEET

SPEED (MPH)	N	NNE	NE	ENE	E	ESE	SE	SSE	S	SSW	SW	WSW	W	WNW	NW	NNW	TOTAL
CALM																	0
0.61- 3.50	1	0	3	1	0	0	1	0	1	0	0	0	0	0	0	0	7
3.51- 7.50	1	3	0	0	2	0	0	2	0	0	1	2	0	1	0	0	12
7.51-12.50	7	7	2	1	0	0	1	0	2	0	0	4	7	2	2	4	39
12.51-18.50	10	6	2	2	1	0	1	1	2	2	1	1	1	5	1	6	42
18.51-24.00	11	3	0	0	0	1	0	0	1	1	3	0	0	1	5	8	34
>24.00	6	0	0	0	0	0	0	0	6	0	1	0	0	0	2	3	18
TOTAL	36	19	7	4	3	1	3	3	12	3	6	7	8	9	10	21	152

TABLE C-5 (CONTINUED)
CAPE CANAVERAL 1982/1984 WIND AND ATMOSPHERIC STABILITY DISTRIBUTIONS
(OCTOBER 7 THROUGH NOVEMBER 25)

OCT/NOV 1982/1984 CAPE CANAVERAL 492 FT TOWER DATA
SITE IDENTIFIER: TOWER313
DATA PERIOD EXAMINED: 10/ 7/82 - 11/25/84

*** OCTOBER/NOVEMBER ***

STABILITY CLASS G

STABILITY BASED ON: DELTA T BETWEEN 492.0 AND 54.0 FEET
WIND MEASURED AT: 492.0 FEET
WIND THRESHOLD AT: 0.60 MPH

JOINT FREQUENCY DISTRIBUTION OF WIND SPEED AND DIRECTION IN HOURS AT492.00 FEET

SPEED (MPH)	N	NNE	NE	ENE	E	ESE	SE	SSE	S	SSW	SW	WSW	W	WNW	NW	NNW	TOTAL
CALM																	0
0.61- 3.50	0	0	0	0	0	0	0	0	0	0	0	0	0	0	0	0	0
3.51- 7.50	1	2	0	0	0	0	0	0	0	0	0	0	0	0	0	0	3
7.51-12.50	1	7	0	0	0	0	0	0	0	0	0	0	0	0	0	0	8
12.51-18.50	0	0	0	0	0	0	0	0	0	0	0	0	0	1	0	0	1
18.51-24.00	0	0	0	0	1	0	0	0	0	0	0	0	0	0	0	0	1
≥24.00	0	0	0	0	0	0	0	0	0	0	0	0	0	0	0	0	0
TOTAL	2	9	0	0	1	0	0	0	0	0	0	0	0	1	0	0	13

STABILITY CLASS ALL

STABILITY BASED ON: DELTA T BETWEEN 492.0 AND 54.0 FEET
WIND MEASURED AT: 492.0 FEET
WIND THRESHOLD AT: 0.60 MPH

JOINT FREQUENCY DISTRIBUTION OF WIND SPEED AND DIRECTION IN HOURS AT492.00 FEET

SPEED (MPH)	N	NNE	NE	ENE	E	ESE	SE	SSE	S	SSW	SW	WSW	W	WNW	NW	NNW	TOTAL
CALM																	0
0.61- 3.50	2	3	6	4	0	0	1	5	5	0	0	0	0	1	0	0	27
3.51- 7.50	12	16	21	17	16	15	11	12	6	4	5	5	4	5	1	2	152
7.51-12.50	29	44	59	47	84	68	55	27	19	11	4	6	18	5	11	11	498
12.51-18.50	51	51	55	95	100	101	84	32	23	12	13	9	9	11	12	25	683
18.51-24.00	63	39	20	118	78	65	23	12	21	11	12	3	2	4	12	43	526
≥24.00	70	83	15	66	42	11	5	2	10	0	3	1	0	2	14	40	364
TOTAL	227	236	176	347	320	260	179	90	84	38	37	24	33	28	50	121	2250

TABLE C-5 (CONTINUED)
CAPE CANAVERAL 1982/1984 WIND AND ATMOSPHERIC STABILITY DISTRIBUTIONS
(OCTOBER 7 THROUGH NOVEMBER 25)

OCT/NOV 1982/1984 CAPE CANAVERAL 492 FT TOWER DATA
SITE IDENTIFIER: TOWER313
DATA PERIOD EXAMINED: 10/ 7/82 - 11/25/84

*** OCTOBER/NOVEMBER ***

STABILITY BASED ON: DELTA T BETWEEN 492.0 AND 54.0 FEET
WIND MEASURED AT: 492.0 FEET
WIND THRESHOLD AT: 0.60 MPH

TOTAL NUMBER OF OBSERVATIONS: 2318

TOTAL NUMBER OF VALID OBSERVATIONS: 2250

TOTAL NUMBER OF MISSING OBSERVATIONS: 68

PERCENT DATA RECOVERY FOR THIS PERIOD: 97.1 %

MEAN WIND SPEED FOR THIS PERIOD: 17.0 MPH

TOTAL NUMBER OF OBSERVATIONS WITH BACKUP DATA: 0

PERCENTAGE OCCURRENCE OF STABILITY CLASSES

A	B	C	D	E	F	G
0.31	0.58	1.38	33.42	56.98	6.76	0.58

DISTRIBUTION OF WIND DIRECTION VS STABILITY

	N	NNE	NE	ENE	E	ESE	SE	SSE	S	SSW	SW	WSW	W	WNW	NW	NNW	CALM
A	2	1	0	2	0	0	2	0	0	0	0	0	0	0	0	0	0
B	4	1	1	2	0	0	1	1	2	0	1	0	0	0	0	0	0
C	1	6	4	7	2	0	1	4	1	1	4	0	0	0	0	0	0
D	93	111	72	125	66	71	57	34	15	12	11	8	10	7	5	55	0
E	89	89	92	207	248	188	115	48	54	22	15	9	15	11	35	45	0
F	36	19	7	4	3	1	3	3	12	3	6	7	8	9	10	21	0
G	2	9	0	0	1	0	0	0	0	0	0	0	0	1	0	0	0
TOTAL	227	236	176	347	320	260	179	90	84	38	37	24	33	28	50	121	0

TABLE C-5 (CONTINUED)
CAPE CANAVERAL 1982/1984 WIND AND ATMOSPHERIC STABILITY DISTRIBUTIONS
(OCTOBER 7 THROUGH NOVEMBER 25)

atmosphere) are shown in Figures C-24 through C-27. At the 4750-ft level onshore flows from northeast clockwise through southeast are dominant with northeast winds being the most prevalent. At 10,000 ft, easterly winds generally decrease in frequency as a transition is made to the dominance of westerly winds. The upper two levels show that westerly winds dominate and winds from the east sectors are very infrequent. These figures illustrate the change in wind direction with height from the low-level northeast trade winds to the upper-level prevailing westerlies seen in the longer-term KSC and PBI data.

Average wind speeds based on the 1982/1984 data are 14.8, 16.4, 24.1, and 35.4 mph for 4750, 10,000, 18,250, and 26,500 feet respectively. These values are in close agreement with the corresponding long-term data.

No discussion is provided on wind direction persistence for upper-level winds since rawinsonde data are only available as once- or twice-daily observations.

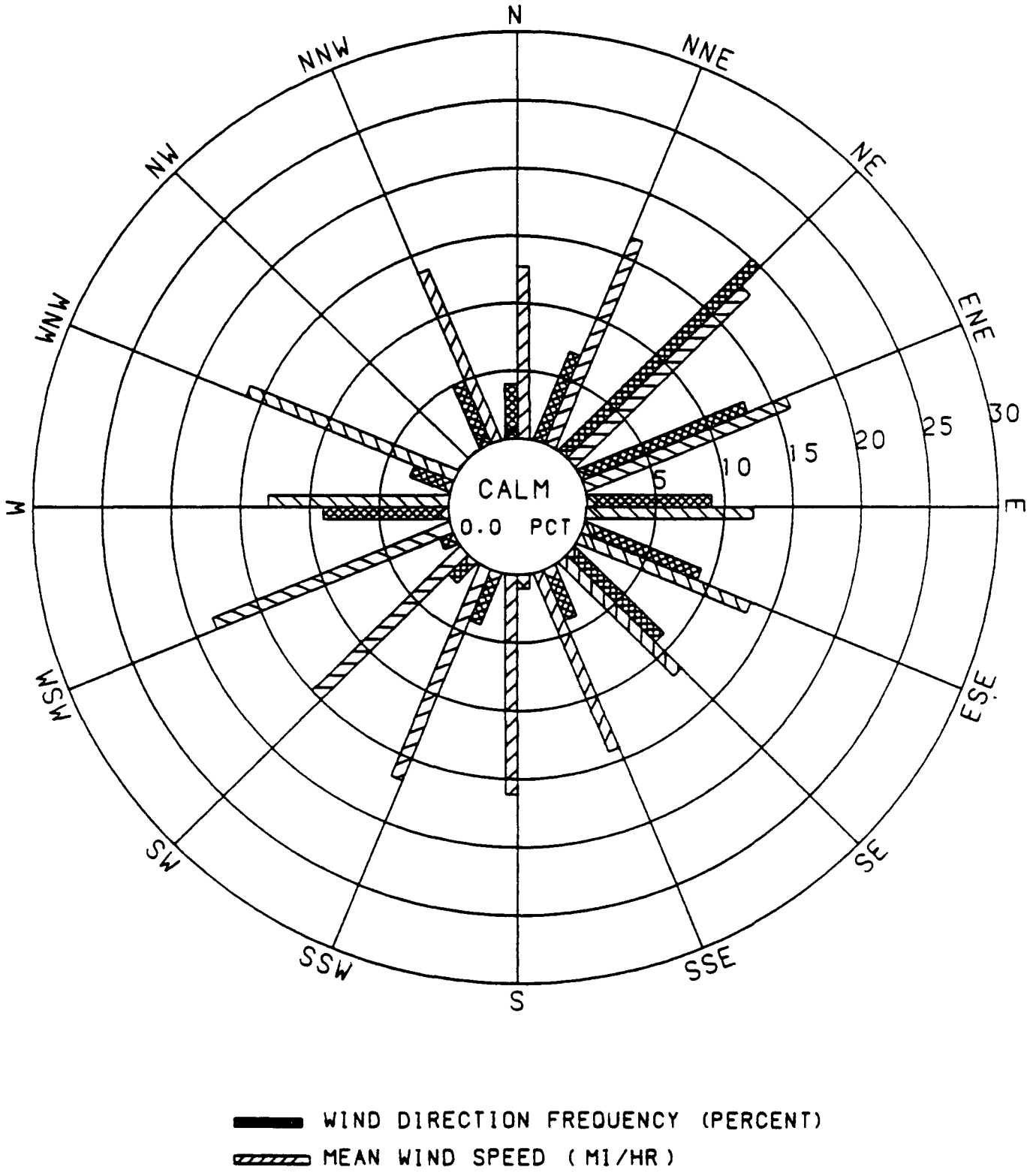

FIGURE C-24
CAPE CANAVERAL 850-MB (4,750-FT)
1982/1984 WIND ROSE
(OCTOBER 7 THROUGH NOVEMBER 25)

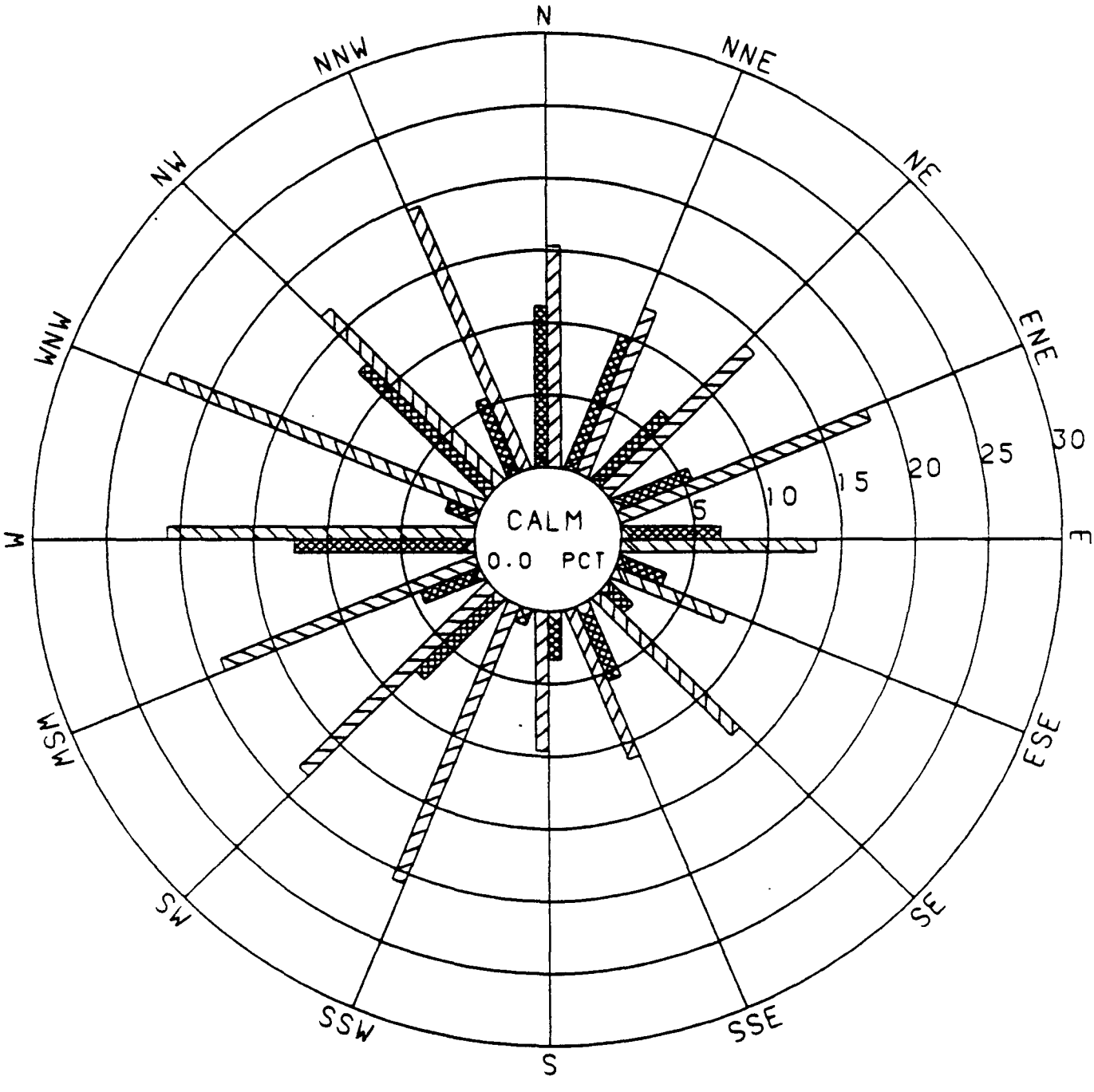

FIGURE C-25
CAPE CANAVERAL 700-MB (10,000-FT)
1982/1984 WIND ROSE
(OCTOBER 7 THROUGH NOVEMBER 25)

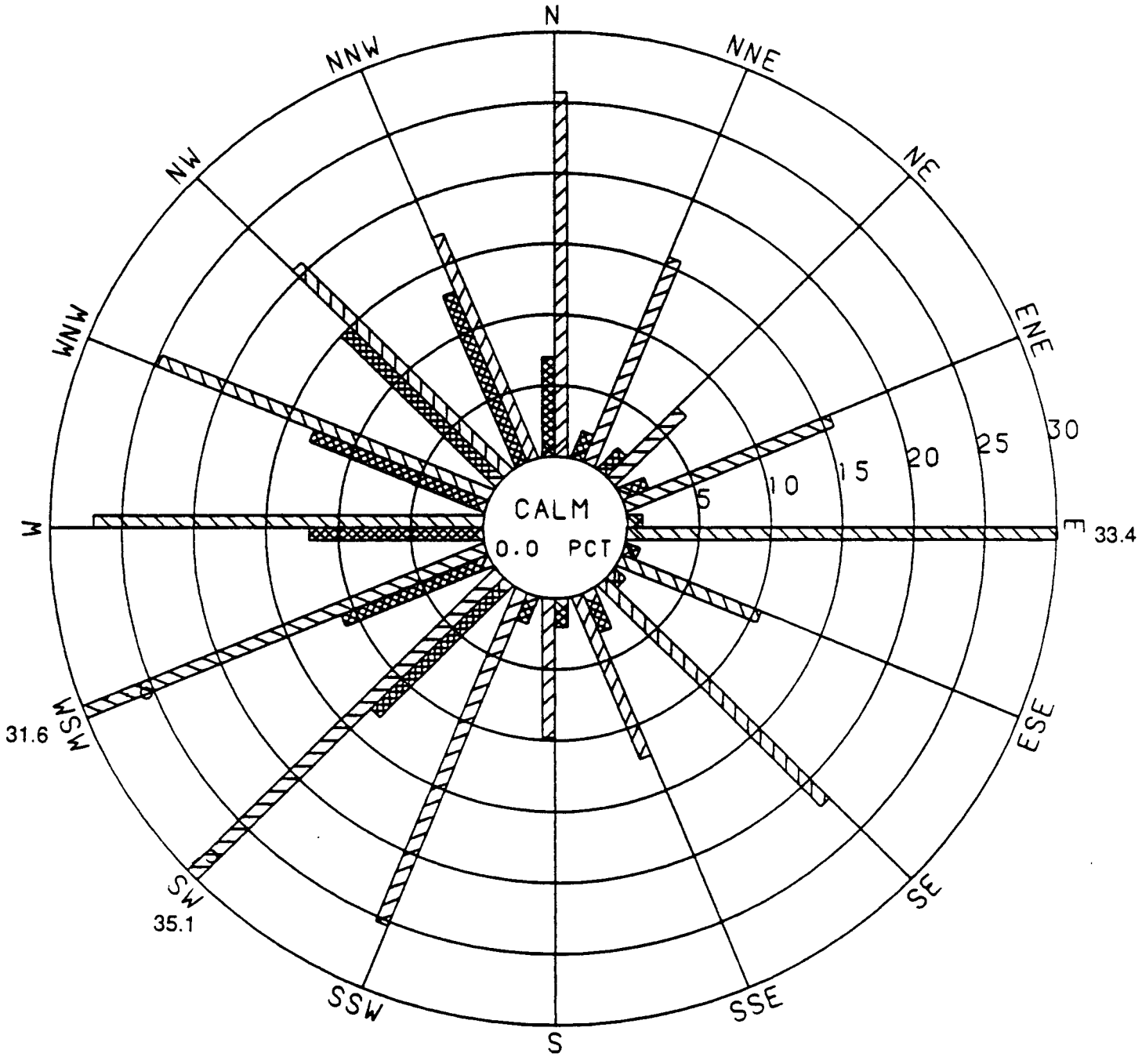

Mean wind speeds greater than 30 mi/hr are indicated by a bar out to 30 mi/hr and the numerical value at the end of the bar.

FIGURE C-26
CAPE CANAVERAL 500-MB (18,250-FT)
1982/1984 WIND ROSE
(OCTOBER 7 THROUGH NOVEMBER 25)

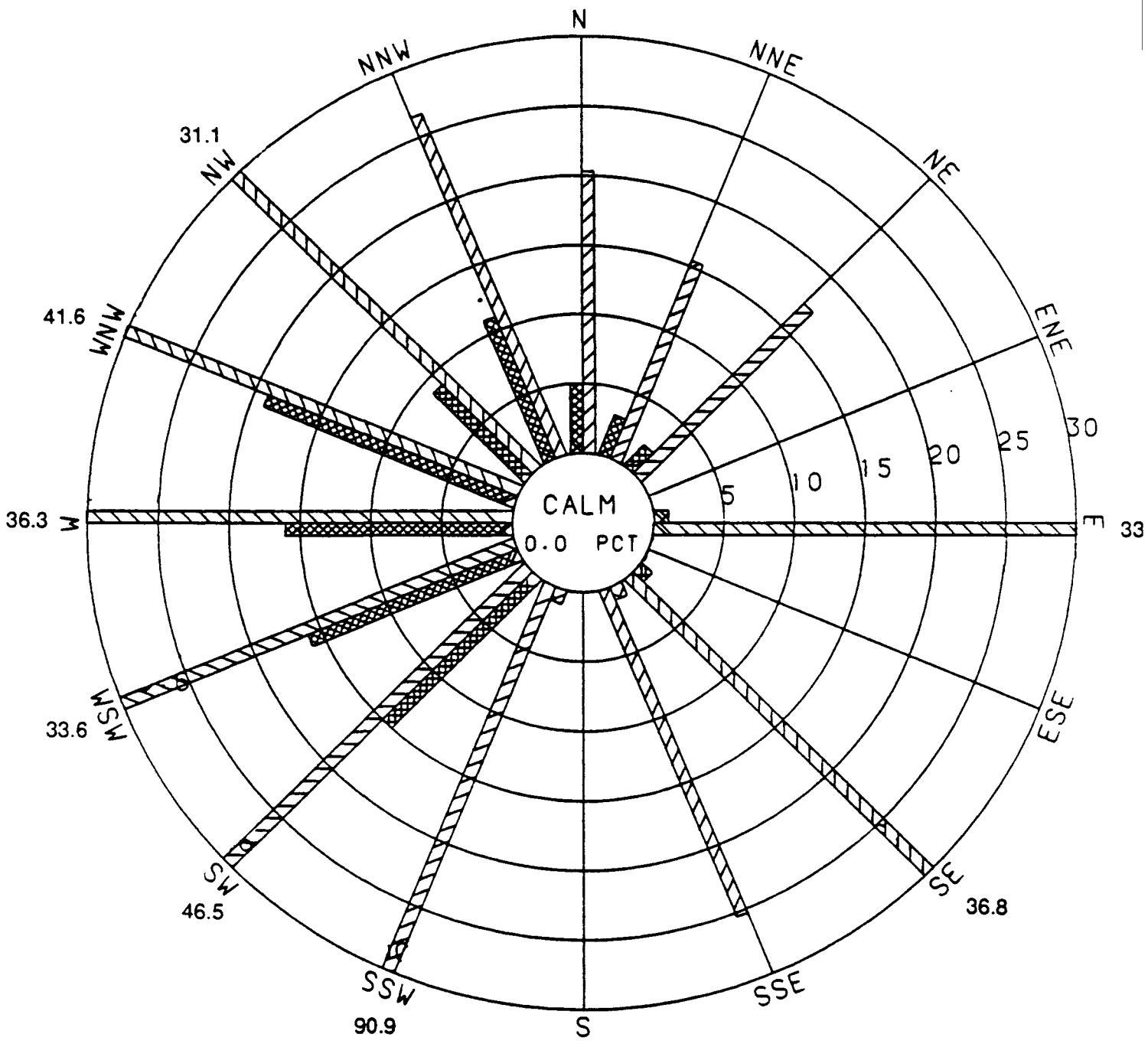

Mean wind speeds greater than 30 mi/hr are indicated by a bar out to 30 mi/hr and the numerical value at the end of the bar.

FIGURE C-27
CAPE CANAVERAL 350-MB (26,500-FT)
1982/1984 WIND ROSE
(OCTOBER 7 THROUGH NOVEMBER 25)

References

C-1. National Climatic Data Center (NCDC), TD-6200 Series NCDC Upper Air Digital Files, NCDC, May 1986.

C-2. Parsont, M.A., et al., Environmental and Demographic Data Summary for the Cape Kennedy Florida Vicinity, NUS Corporation, NUS-793, June 1971.

C-3. U. S. Nuclear Regulatory Commission, 1986. Meteorological Measurement Program for Nuclear Power Plants, Second Proposed Revision 1 to Regulatory Guide 1.23, Issued for Comment, April.

C-4. Riehl, Herbert, Climate and Weather in the Tropics, Academic Press Inc., 1979.

C-5. Wallace, John M., and Peter V. Hobbs, Atmospheric Science - An Introductory Survey, Academic Press Inc., 1977.

C-6. Sadler, J.C., The Upper Tropospheric Circulation over the Global Tropics, UHMET-75-05, Department of Meteorology, University of Hawaii, Honolulu, 1975.

C-7. van de Boogaard, H., The Mean Circulation of the Tropical and Subtropical Atmosphere - July, National Center for Atmospheric Research Technical Note TN-118+STR, 1977.

APPENDIX D

PARTICLE SIZE CONSIDERATIONS

D.1 INTRODUCTION

The particle size distribution of any PuO_2 release resulting from accidents will strongly influence the atmospheric transport and dispersion, deposition, resuspension, and internal dosimetry of such a release. This appendix documents the basis for the particle size distributions used in FSAR, Vol. III, Nuclear Risk Analysis Document (NRAD), discusses mechanisms that could alter the particle size distribution following release, and summarizes the results of a particle size effects analysis. The latter represents a sensitivity analysis designed to show the effects of particle size distribution on the NRAD results. It also provides a basis for incorporation of particle size variability into the NRAD uncertainty analysis, presented in Appendix H.

D.2 PARTICLE SIZE DISTRIBUTIONS

Particle size distributions were identified in FSAR, Vol. II, Accident Model Document (AMD) for all source terms (See AMD, Section 3.0, Tables 3-4 and 3-5). The approach taken in the AMD in the development of particle size distributions was as follows:

- The Launch Accident Scenario Evaluation Program (LASEP-2) used by GE in Phases 0 and 1 calculates source terms based on a correlation of Fueled Clad deformation and release quantity derived from PuO_2-fueled and urania-simulant Bare Clad Impact (BCI) tests and PuO_2-fueled module Safety Verification Tests (SVT) series conducted by Los Alamos National Laboratory (See AMD, Appendix G). Another correlation based on the same test data relates Fueled Clad distortion and crack size.

- Two base particle size distributions are used in LASEP-2 corresponding to steel and concrete impacts, respectively. These particle size distributions were derived from PuO_2-fueled and urania-simulant BCI tests by fitting the particle size distributions of contained material for respective impact surfaces by Weibull functions. The assumptions are then made that 1) the retained and released fuel have the same base particle size distribution, and 2) the maximum diameter of particle released is one-half the maximum crack size. The particle size distribution of the release is then determined by cutting off the base particle size distribution at a size corresponding to one-half the maximum crack width, and then renormalizing the sum of the remaining fractions in each size range to 1.0. The vaporization model described in the AMD is then applied for any releases into the fireball.

- In Phases 2, 3, 4, and 5 a base particle size distribution corresponding to SVT-1 was used for releases resulting from module (Phases 2, 3, and 4) and GIS

(Phase 5) impacts on rock. Using estimates of crack width based on SVT data for the appropriate reentry conditions, the base particle size distribution was then cutoff and renormalized in a manner similar to that described previously.

The original base particle size distributions for steel and concrete impacts (and the associated Weibull fits) used in LASEP-2 in the Phase 0 and 1 analyses were reviewed along with newly available BCI test data, with the following conclusions:

- Since the LASEP-2 correlations of Fueled Clad distortion with release quantity and crack size were based on all the BCI and SVT test data, NUS reasoned that the particle size distributions should be based on the same test data (not just BCI data). This also reflects both Fueled Clad and module impact configurations considered in LASEP-2.

- An examination of PuO_2-fueled and urania-simulant BCI test data indicated significant differences between the particle size distributions of the two types of material.

- The LASEP-2 output of particle size distributions revealed they were uniquely "fingerprinted" according to the mix of base particle size distributions corresponding to the mix of steel and concrete impacts obtained in the Monte Carlo analysis performed in LASEP-2. This would allow a decomposition of the two base particle size distributions and an identification of the maximum particle size cutoff.

Based on the above rationale, it was concluded that an updating of the base particle size distributions was warranted and feasible. This was accomplished using only the PuO_2-fueled BCI and SVT data for retained fuel. The LASEP-2 particle size distributions were decomposed and the maximum particle size cutoff determined. In generating replacement particle size distributions based on all the PuO_2-fueled BCI and SVT data for retained fuel, two types of particle size distributions were developed. First an "average" particle size distribution was developed by averaging the weight fractions in each size range as presented in the test data. The "average" particle size distribution was used as the base particle size distribution for all the most probable and expectation cases in the NRAD, after application of the particle size cutoff and renormalization. A "maximum" particle size distribution was developed by selecting that particle size distribution among the test data that would maximize radiological consequences (population dose). This was determined to be that of SVT-1 which has the highest fraction less than 10 microns. The "maximum" particle size distribution was used for all maximum cases, after application of the appropriate particle size cutoff and renormalization.

The updated particle size distributions on a source term by source term basis are presented in Table D-1 and Figure D-1 for use in the most probable and expectation cases and in Table D-2 and Figure D-2 for use in the maximum cases. The particle size distributions presented in Tables D-1 and D-2 replace those presented in Table 3-5 of the AMD, with the size code identifiers (1 through 24) corresponding to the same source terms identified in Tables 3-4 and 3-5 of the AMD. Also shown are the unnormalized average and maximum distributions (based on BCI and SVT test data) from which the replacement particle size distributions were developed.

D.3 MECHANISMS ALTERING PARTICLE SIZE

Following release of PuO_2 from Fueled Clads, a number of mechanisms become operative which could alter the released particle size distribution with time. The degree to which these mechanisms are important depends on the accident environment and sequential environments to which the released PuO_2 particles are exposed.

Mechanisms which tend to decrease particle size following release include the following:

- Secondary overpressures
- Secondary impacts (includes both collection and break-up on large fragments)
- Aerodynamic break-up
- Thermal shock
- Erosion (by high speed through fine particle cloud)
- Vaporization of particles in fireball
- Environmental effects (e.g., weathering, spallation, and dissolution)

Of these mechanisms, only vaporization within the fireball associated with accident scenarios during mission Phases 0 and 1 was judged significant, and it has been taken into account. The vaporization model applied is described in the AMD and is reflected in the particle size distributions of released fuel presented in Section D.2. The particles affected by these mechanisms retain their original composition (PuO_2) and mass density (10 g/cm^3) at the reduced size.

Table D-1
UPDATED PARTICLE SIZE DISTRIBUTIONS FOR AMD AVERAGE SOURCE TERMS

Maximum Particle Size, um	Average PSD	Particle Size Code 1	2	3	4	5	6	7	8	9	10	11	12
6000	3.30E-02	-	-	9.65E-02	1.47E-02	1.47E-02	-	-	-	1.87E-01	4.80E-04	4.80E-04	-
2000	2.20E-01	2.04E-01	1.80E-01	3.35E-01	2.64E-01	2.64E-01	2.23E-01	4.85E-01	4.85E-01	3.88E-01	3.39E-01	3.39E-01	1.13E-01
841	9.40E-02	3.76E-01	3.87E-01	2.67E-01	3.40E-01	3.40E-01	3.66E-01	2.43E-01	2.43E-01	2.24E-01	3.12E-01	3.12E-01	4.18E-01
420	5.39E-02	2.16E-01	2.22E-01	1.53E-01	1.95E-01	1.95E-01	2.10E-01	1.39E-01	1.39E-01	1.29E-01	1.79E-01	1.79E-01	2.40E-01
177	9.52E-03	3.81E-02	3.92E-02	2.70E-02	3.45E-02	3.45E-02	3.71E-02	2.46E-02	2.46E-02	2.27E-02	3.16E-02	3.16E-02	4.24E-02
125	1.07E-02	4.29E-02	4.42E-02	3.05E-02	3.89E-02	3.89E-02	4.18E-02	2.77E-02	2.77E-02	2.56E-02	3.56E-02	3.56E-02	4.78E-02
74	8.71E-03	3.48E-02	3.58E-02	2.47E-02	3.15E-02	3.15E-02	3.40E-02	2.25E-02	2.25E-02	2.08E-02	2.89E-02	2.89E-02	3.88E-02
44	6.79E-03	2.72E-02	2.79E-02	1.93E-02	2.46E-02	2.46E-02	2.65E-02	1.75E-02	1.75E-02	1.62E-02	2.25E-02	2.25E-02	3.02E-02
30	6.08E-03	2.43E-02	2.50E-02	1.73E-02	2.20E-02	2.20E-02	2.37E-02	1.57E-02	1.57E-02	1.45E-02	2.02E-02	2.05E-02	2.71E-02
20	5.31E-03	2.12E-02	2.19E-02	1.51E-02	1.92E-02	1.92E-02	2.07E-02	1.37E-02	1.37E-02	1.27E-02	1.76E-02	1.76E-02	2.36E-02
10	0.001268	-	-	3.60E-03	-	4.59E-03	-	-	3.27E-03	3.03E-03	-	4.20E-03	-
9	0.000512	0.005069	0.005218	1.45E-03	4.59E-03	1.86E-03	4.95E-03	3.27E-03	1.32E-03	1.22E-03	4.20E-03	1.70E-03	5.64E-03
8	4.05E-04	2.05E-03	2.11E-03	1.15E-03	1.86E-03	1.47E-03	2.00E-03	1.32E-03	1.05E-03	9.67E-04	1.70E-03	1.34E-03	2.28E-03
7	2.25E-04	-	-	6.39E-04	-	8.15E-04	-	-	5.81E-04	5.37E-04	-	7.46E-04	-
6	3.22E-04	2.52E-03	2.59E-03	9.15E-04	2.28E-03	1.17E-03	2.46E-03	1.63E-03	8.31E-04	7.69E-04	2.09E-03	1.07E-03	2.80E-03
5	2.59E-04	1.29E-03	1.33E-03	7.36E-04	1.17E-03	9.38E-04	1.26E-03	8.31E-04	6.69E-04	6.18E-04	1.07E-03	8.58E-04	1.43E-03
4	2.59E-04	-	-	7.36E-04	-	9.38E-04	-	-	6.69E-04	6.18E-04	-	8.58E-04	-
3	2.28E-04	1.04E-03	1.07E-03	6.48E-04	9.38E-04	8.26E-04	1.01E-03	6.69E-04	5.89E-04	5.44E-04	8.58E-04	7.56E-04	1.15E-03
2	2.21E-04	-	-	6.28E-04	-	8.01E-04	-	-	5.71E-04	5.28E-04	-	7.33E-04	-
1	3.76E-04	-	-	1.07E-03	-	1.36E-03	-	-	9.71E-04	8.98E-04	-	1.25E-03	-
0.02	-	4.33E-03	4.46E-03	-	3.93E-03	-	4.23E-03	2.80E-03	-	-	3.59E-03	-	4.83E-03

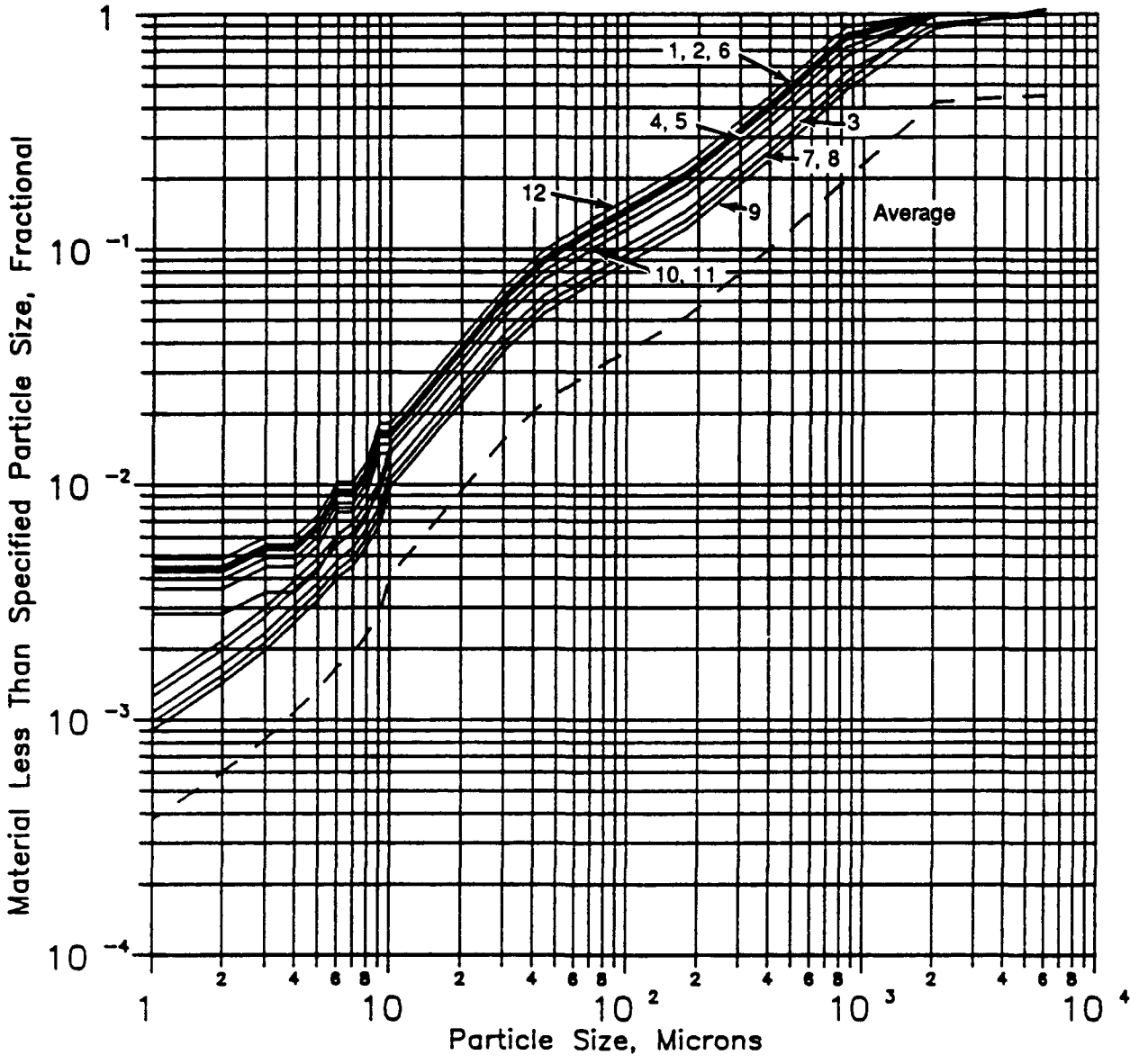

Note: Numbers 1 - 12 refer to
particle size codes in Table D-1.

Figure D-1
UPDATED PARTICLE SIZE DISTRIBUTION FOR AMD AVERAGE SOURCE TERMS

Table D-2
UPDATED PARTICLE SIZE DISTRIBUTIONS FOR AMD MAXIMUM SOURCE TERMS

Maximum Particle Size, um	Maximum PSD	Particle Size Code 16	18	21	23
6000	2.26E-01	-	-	-	-
2000	3.31E-01	3.96E-01	5.17E-01	5.02E-01	4.28E-01
841	1.57E-01	2.94E-01	2.35E-01	2.42E-01	2.79E-01
420	9.57E-02	1.80E-01	1.44E-01	1.48E-01	1.70E-01
177	1.49E-02	2.80E-02	2.24E-02	2.30E-02	2.65E-02
125	1.71E-02	3.21E-02	2.57E-02	2.64E-02	3.04E-02
74	8.40E-03	1.58E-02	1.26E-02	1.30E-02	1.49E-02
44	7.80E-03	1.46E-02	1.17E-02	1.21E-02	1.39E-02
30	6.20E-03	1.16E-02	9.30E-03	9.58E-03	1.10E-02
20	7.00E-03	1.31E-02	1.05E-02	1.08E-02	1.25E-02
10	1.53E-03	-	2.30E-03	2.37E-03	-
9	1.12E-03	2.87E-03	1.67E-03	1.73E-03	2.72E-03
8	7.84E-04	2.10E-03	1.18E-03	1.21E-03	1.99E-03
7	2.63E-04	-	3.95E-04	4.06E-04	-
6	9.92E-04	1.97E-03	1.49E-03	1.53E-03	1.86E-03
5	3.83E-04	1.86E-03	5.75E-04	5.92E-04	1.76E-03
4	4.41E-04	-	6.62E-04	6.82E-04	-
3	5.79E-04	7.19E-04	8.69E-04	8.95E-04	6.81E-04
2	3.98E-04	-	5.97E-04	6.15E-04	-
1	1.59E-03	-	2.39E-03	2.46E-03	-
0.02	-	5.65E-03	-	-	5.36E-03

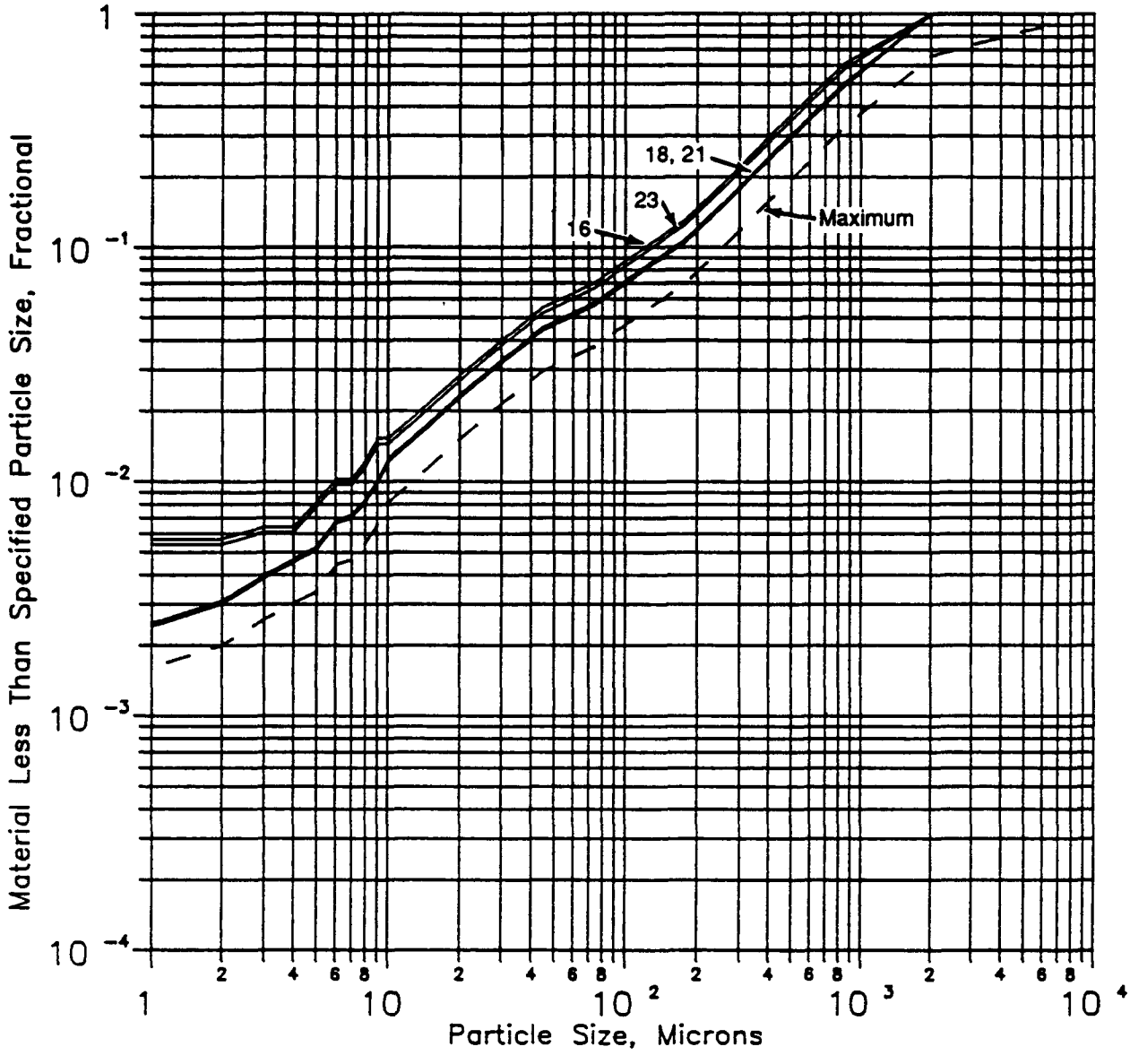

Note: Numbers 18 - 23 refer to
particle size codes in Table D-2.

Figure D-2
UPDATED PARTICLE SIZE DISTRIBUTIONS FOR AMD MAXIMUM SOURCE TERMS

Mechanisms which increase particle size related primarily to agglomeration include the following:

- Condensation (Includes homogeneous and heterogeneous nucleation, and chemical reactions leading to condensation of composite particles)
- Coagulation (Arises from particle collisions. Includes contributions from Brownian motion and turbulence, both of which increase particle collision cross-sections.)
- Scavenging (Gravitational sweeping of small particles by large particles and aerosols)

In accidents involving explosion overpressure and fireball environments, agglomeration mechanisms become operative as the fireball cools, expands, and water vapor condensation occurs as the plume stabilizes. Following condensation, gravitational scavenging continues until particle deposition occurs.

Following fireball development, agglomeration is promoted as a result of the high number density of aluminum oxide (Al_2O_3) particles from the Solid Rocket Booster exhaust and burning aluminum in the after-fire. In addition, the large quantity of water vapor in the plume due to the liquid oxygen/hydrogen explosion of the liquid propellants in the External Tank, as well as the deluge water injected into the flame trench on the launch pad, will result in further condensation and coagulation effects, and some wash-out of material. The number density of PuO_2 particles in the plume will be very small compared to that of Al_2O_3 and water droplets. The very high particle number densities in the developing plume would tend to cause agglomeration of Al_2O_3 particles with PuO_2 particles, resulting in larger particles with lower mass densities. The PuO_2 particles with an initial mass density of 10 g cm^3 would be driven towards larger particles of predominantly Al_2O_3 with a mass density of 2.3 g/cm^3. Condensation of water vapor and scavenging by water droplets would result in still larger particles of lower density.

The overall effect of agglomeration is to increase terminal fall velocity, causing deposition to occur closer to the point of release and to decrease internal doses from inhalation. Since agglomeration was not included in the NRAD analyses, the near-field (within 5 km) ground concentrations are judged to be under-estimated by a factor of 0.5, and the near- and far-field doses and far-field ground concentrations are judged to be over-estimated by a factor of 2.

D.3 PARTICLE SIZE SENSITIVITY ANALYSIS

A sensitivity analysis has been performed to evaluate the effects of particle size distribution and its variability on the NRAD results. The sensitivity analysis also provides a basis

for incorporation of particle size variability into the NRAD uncertainty analysis, presented in Appendix H.

The approach taken in the sensitivity analysis is to establish a base analysis case, and then vary the particle size distribution in a consistent manner in order to observe the effects of the variations.

The base case for analysis consists of the Phase 1, maximum case (see NRAD Book I, Section 3.2.2). This case consists of a 3,096 Ci release into the fireball with the "maximum" particle size distribution identified in Section D.2 (size code 23 in Table D-2). The plume configuration corresponding to the maximum case consists of the maximum plume configuration described in Appendix A.

Cases considered in the sensitivity analysis consisted of the following:

- Case 0 - Base case results (Phase 1, maximum case, using the "maximum" particle distribution).
- Case 1 - Base case decomposition showing contribution by particle size group.
- Case 2 Same as Case 0 but with the representative particle size in each range taken at the low end of each range.
- Case 3 - Same as Case 0 but with the representative particle size in each range taken at the high end of each range.
- Case 4 - Same as Case 0 but the "average" particle size distribution identified in Section D.2.

The particle size distributions used in these cases are summarized in Table D-3.

In presenting the results of the sensitivity analysis, the short- and long-term population doses without de minimis and the land area contaminated above 0.2 $\mu Ci/m^2$ were selected as the bases for comparison. De minimis has not been included because its use introduces a threshold or non-linearly which would make it difficult to determine the contribution by particle size group, as in Case 1.

The first step in the sensitivity analysis focuses only on features of the base case (Case 0) and its decomposition by particle size (Case 1). The results of the sensitivity analysis using Case 1, showing the contribution by particle size group to the results of Case 0, are presented in Table D-4. In conjunction with these results, Table D-5 shows the stratification effects within the plume at various downwind

Table D-3
Particle Size Distributions Used in Sensitivity Analysis

Particle Size Range, μm	Cases 0, 1		Case 2[a]	Case 3[a]	Cases 4	
	Representative Size, μm[b]	Weight Fraction	Representative Size, μm	Representative Size, μm	Representative Size, μm	Weight Fraction
>6000	-	-	-	-	-	-
2000-6000	-	-	-	-	-	-
841-2000	1625	4.28E-01	841	2000	1625	4.45E-01
420-841+	694	2.79E-01	420	841	694	2.62E-01
177-420	341	1.70E-01	177	420	341	1.50E-01
125-177	155	2.65E-02	125	177	155	2.65E-02
77-125	106	3.04E-02	77	125	106	2.99E-02
44-77	62.6	1.49E-02	44	77	62.6	2.43E-02
30-44	38.3	1.39E-02	30	44	38.3	1.89E-02
20-30	26.0	1.10E-02	20	30	26.0	1.69E-02
10-20	16.5	1.25E-02	10	20	16.5	1.48E-02
9-10	9.53	-	9	10	9.53	-
8-9	8.53	2.72E-03	8	9	8.53	3.53E-03
7-8	7.53	1.99E-03	7	8	7.53	1.43E-03
6-7	6.54	-	6	7	6.54	-
5-6	5.55	1.86E-03	5	6	5.55	1.76E-03
4-5	4.55	1.76E-03	4	5	4.55	8.97E-04
3-4	3.57	-	3	4	3.57	-
2-3	2.60	6.81E-04	2	3	2.60	7.22E-04
1-2	1.65	-	1	2	1.65	-
Vapor	0.02	5.36E-03	0.02	0.02	0.02	3.02E-03

a. Weight fraction same as Cases 0 and 1
b. Diameter of average volume within size range

Table D-4
Effects of Particle Size on Radiological Consequences

Particle Size Range, μm	Weight Fraction[a]	Population Dose, Person-rem		Area Above 0.2 μCi/m², km²	Fractional Relative Contribution		
					Population Dose, Person-rem		Area Above 0.2 μCi/m², km²
		Short-Term	Long-Term		Short-Term	Long-Term	
+420	7.07E-01	0.00E+00	1.46E-07	3.63E+00	0.00E+00	1.35E-11	2.28E-02
177-420	1.70E-01	3.50E-06	2.56E-08	2.99E+00	3.62E-09	2.37E-12	1.88E-02
125-177	2.65E-02	8.86E-03	2.96E-09	3.75E+00	9.17E-06	2.74E-13	2.36E-02
77-125	3.04E-02	1.97E+00	7.50E-08	6.39E+00	2.04E-03	6.94E-12	4.02E-02
44-77	1.49E-02	1.37E+00	1.71E-05	6.52E+00	1.42E-03	1.58E-09	4.10E-02
30-44	1.39E-02	3.55E+00	1.97E-04	1.49E+01	3.67E-03	1.82E-08	9.37E-02
20-30	1.10E-02	6.64E+01	1.20E+03	1.56E+01	6.87E-02	1.11E-01	9.81E-02
10-20	1.25E-02	3.07E+01	1.93E+03	1.05E+02	3.18E-02	1.79E-01	6.61E-01
1-10	9.01E-03	2.74E+01	1.91E+02	0.00E+00	2.84E-02	1.77E-02	0.00E+00
0.02	5.36E-03	8.35E+02	7.44E+03	0.00E+00	8.64E-01	6.89E-01	0.00E+00
	1.00E+00	9.66E+02	1.08E+04	1.59E+02	1.00E+00	1.00E+00	1.00E+00

a. Total release: 3096 Ci in fireball

Table D-5
Plume Stratification Versus Time[a]

Plume Segment	Particle Size, μm	Source Fraction	Source Height (m) at Indicated Distance (km)[b]							
			0.0	0.5	1.0	3.0	5.0	10	30	50
Cloud	+841	0.3422	1717	147	-	-	-	-	-	-
	420-841	0.2230	1717	407	-	-	-	-	-	-
	177-420	0.1360	1717	1107	497	-	-	-	-	-
	125-177	0.0212	1717	1469	1221	864	-	-	-	-
	77-125	0.0243	1717	1556	1385	1163	107	-	-	-
	44-77	0.0119	1717	1628	1539	1411	828	-	-	-
	30-44	0.0111	1717	1673	1630	1567	1281	845	-	-
	20-30	0.0088	1717	1697	1676	1647	1513	1309	493	-
	10-20	0.0100	1717	1709	1700	1668	1634	1552	1222	892
	0-10	0.0115	1717	1716	1715	1714	1707	1697	1657	1617
Stem	+841	0.0854	575	-	-	-	-	-	-	-
	420-841	0.0558	575	-	-	-	-	-	-	-
	177-420	0.0340	575	-	-	-	-	-	-	-
	125-177	0.0053	575	327	79	-	-	-	-	-
	77-125	0.0061	575	414	253	21	-	-	-	-
	44-77	0.0030	575	486	397	269	-	-	-	-
	30-44	0.0028	575	531	488	397	139	-	-	-
	20-30	0.0022	575	555	534	488	371	167	-	-
	10-20	0.0025	575	567	558	526	492	410	80	-
	0-10	0.0029	575	574	573	573	565	555	515	475
		Source Fraction Remaining	1.0	0.8248	0.2596	0.1183	0.0880	0.0490	0.0357	0.0332

a. Phase 1, Maximum Case
b. Based on a 5 m/s wind speed
c. Mass fraction of source consisting of particle size groups with center of masses still above ground plane

distances, illustrating the effect of gravitational settling by particle size group. Using Table D-5, the downwind distances at which the center of mass of each particle size group in the upper cloud and stem would deposit can be estimated. Table D-6 presents the number of particles associated with each particle size group corresponding to the source term for Case 0. In addition, the number of particles and associated area required to yield an average surface concentration of 0.2 $\mu Ci/m^2$ is presented.

Based on the results for Case 0 and Case 1 the following conclusions can be made:

- Although the initial plume configuration is assumed to be uniformly mixed with respect to particle size, stratification is very rapid within the first 1 kilometer. Therefore, the results are not sensitive to the assumption of initial uniform mixing.

- The contribution by the vapor (0.02 micron diameter) component of the source term is significant (86.4 percent of the short-term dose and 68.9 percent of the long-term dose).

- The source term component in the 10 to 20 micron range is the primary contributor to the area contaminated above 0.2 $\mu Ci/m^2$.

The results of Cases 2 through 4 compared with Case 0 are presented in Table D-7. Based on these results, the following conclusions can be made:

- The use of the diameter of average volume (or activity) as representative of the size range tends to maximize total population dose and surface concentration areas, as in Case 0, compared to using the low end or high end of the range diameters (as in Cases 2 and 3).

- Although the use of the "average" particle size distribution (as in Case 4) decreases total population dose compared to the "maximum" particle size distribution (as in Case 0), the "average" increases the dry land area contaminated above 0.2 $\mu Ci/m^2$.

Table D-6

Particle Number Composition of Source and Associated Environmental Contamination

Particle Size Range, μm	Representative Size, μm	Weight Fraction[a]	Number of Particles in Source[a]	Number of Particles per m^2 Associated with 0.2 μCi/m^2	Area (m^2) per Particle Associated with 0.2 μCi/m^2
>6000	6000	-	-		
2000-6000	4820	-	-		
841-2000	1625	4.28E-01	4.68E+03	7.06E-07	1.42E+06
420-841	694	2.79E-01	3.92E+04	9.08E-06	1.10E+05
177-420	341	1.70E-01	2.01E+05	7.64E-05	1.31E+04
125-177	155	2.65E-02	3.34E+05	8.14E-04	1.23E+03
77-125	106	3.04E-02	1.20E+06	2.55E-03	3.92E+02
44-77	62.6	1.49E-02	2.85E+06	1.24E-02	8.09E+01
30-44	38.3	1.39E-02	1.16E+07	5.39E-02	1.85E+01
20-30	26.0	1.10E-02	2.94E+07	1.73E-01	5.79E+00
10-20	16.5	1.25E-02	1.31E+08	6.77E-01	1.48E+00
9-10	9.53	-	-	3.50E+00	2.86E-01
8-9	8.53	2.72E-03	2.06E+08	4.89E+00	2.04E-01
7-8	7.53	1.99E-03	2.19E+08	7.11E+00	1.41E-01
6-7	6.54	-	-	1.08E+01	9.23E-02
5-6	5.55	1.86E-03	5.11E+08	1.77E+01	5.63E-02
4-5	4.55	1.76E-03	8.77E+08	3.22E+01	3.11E-02
3-4	3.57	-	-	6.66E+01	1.50E-02
2-3	2.60	6.81E-04	1.82E+09	1.72E+02	5.80E-03
1-2	1.65	-	-	6.75E+02	1.48E-03
Vapor	0.02	5.36E-03	3.14E+16	3.78E+08	2.64E-09

a. Phase 1, Maximum Case (3096 Ci)

Table D-7

Particle Size Sensitivity Analysis Results

Case	Population Dose, Person-rem				Dry Land Area Above 0.2 μCi/m², km²
	Without De Minimis		With De Minimis		
	Short-Term	Long-Term	Short-Term	Long-Term	
0, 1	9.66E+02	1.08E+04	2.78E+00	8.41E+03	1.48E+02
2	9.83E+02	8.57E+03	2.83E+00	7.34E+03	4.11E+01
3	9.26E+02	8.15E+03	5.87E-02	7.04E+03	3.88E+01
4	6.45E+02	8.53E+03	1.26E-02	6.29E+03	1.72E+02

APPENDIX E

DISTRIBUTIONS OF POPULATION IN THE KSC REGION DURING A LAUNCH

DISTRIBUTIONS OF POPULATION IN THE KSC REGION DURING A LAUNCH

E.1 INTRODUCTION

In the calculation of population dose which might result from an environ mental release of plutonium-238 dioxide, it is important to know the geo graphical distribution of people in the vicinity of that release. That dis tribution has been estimated in the launch area; the bases for that estimate, and the population data are presented in this appendix.

E.2 DEMOGRAPHIC DATA

The primary basis for demographic information is a report by NUS Corporation titled Kennedy Space Center Demographic and Land-Use Study, October 7, 1983 (Reference E-1). This report is based on field studies and contains demo graphic and land-use data to a radius of 20 miles (32.5 km) from a point midway between launch pads 38A and 39B. Demographic data were compiled in the categories of residential, KSC/CCAFS (occupational), and launch specta tors. Residential data were not adjusted (downward) to account for possible double counting of KSC/CCAFS employees or spectators.

KSC/CCAFS occupational data were obtained from KSC in 1983 and have been updated with information provided by Joel R. Reynolds, KSC Safety Office, in June 1985 (Reference E-2). Onsite-spectator data were also updated according to recommendations from the same source.

These updates reflect the fact that employment at KSC and CCAFS has increased since the original data were gathered. They also are based on the observation that the number of persons requesting passes to view shuttle launches has been decreasing as those launches become more routine.

Reference E-1 contains estimates of offsite spectators for both day and night launches. These estimates were based on some of the first shuttle launches. They showed significantly more spectators for day launches than for night launches. In order to provide an estimate for offsite spectators for these day launches which took into account the same decrease in specta tor interest, the offsite spectator data were adjusted by taking the average of day and night data. This resulted in a decrease in the number of offsite spectators used for this report than that reported in Reference E-1 for a day launch.

Total population data beyond 30 km were obtained from 1980 census data.

The nearest people to the launch pad during the prelaunch phase are at the edge of the blast danger area, 4485 feet away. The exception to this is the crew and the people associated with the

operation of delivering and assist ing in crew insertion into the Orbiter at approximately three hours before launch. At launch, the nearest people without respiratory protection are at the Launch Impact Limit Line, about three miles from the launch pad at a minimum.

Demographic data used for the radiological impact analyses in the launch area are shown in Table E-1.

Figure E-1 shows the KSC regional area. The area between the coast (Titusville) and the Orlando area is populated very sparsely.

Figure E-2 shows launchtime population density within 20 miles as reported in Reference E-1.

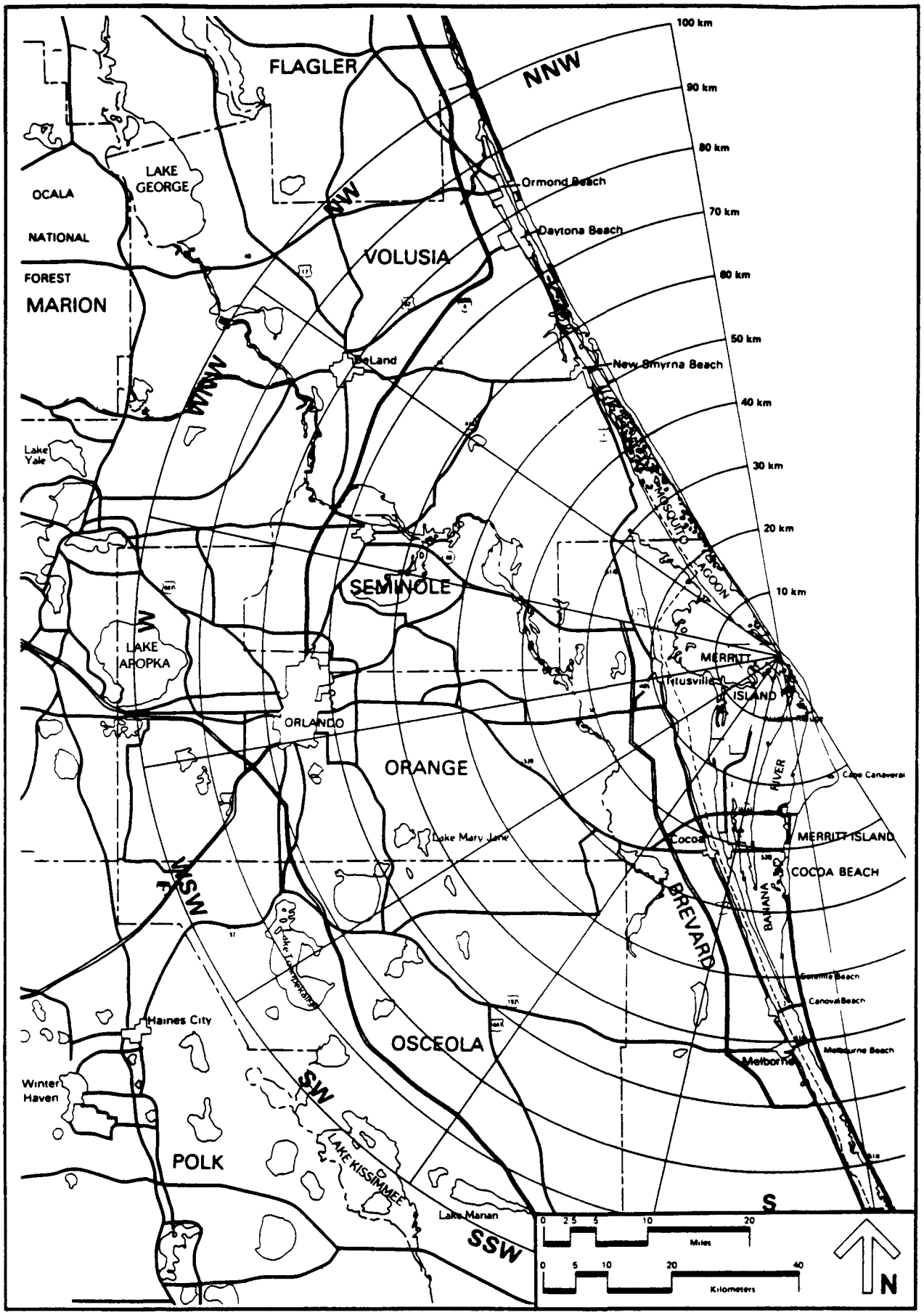

Figure E-1. Kennedy Space Center Vicinity
Map Out to 100 Kilometers

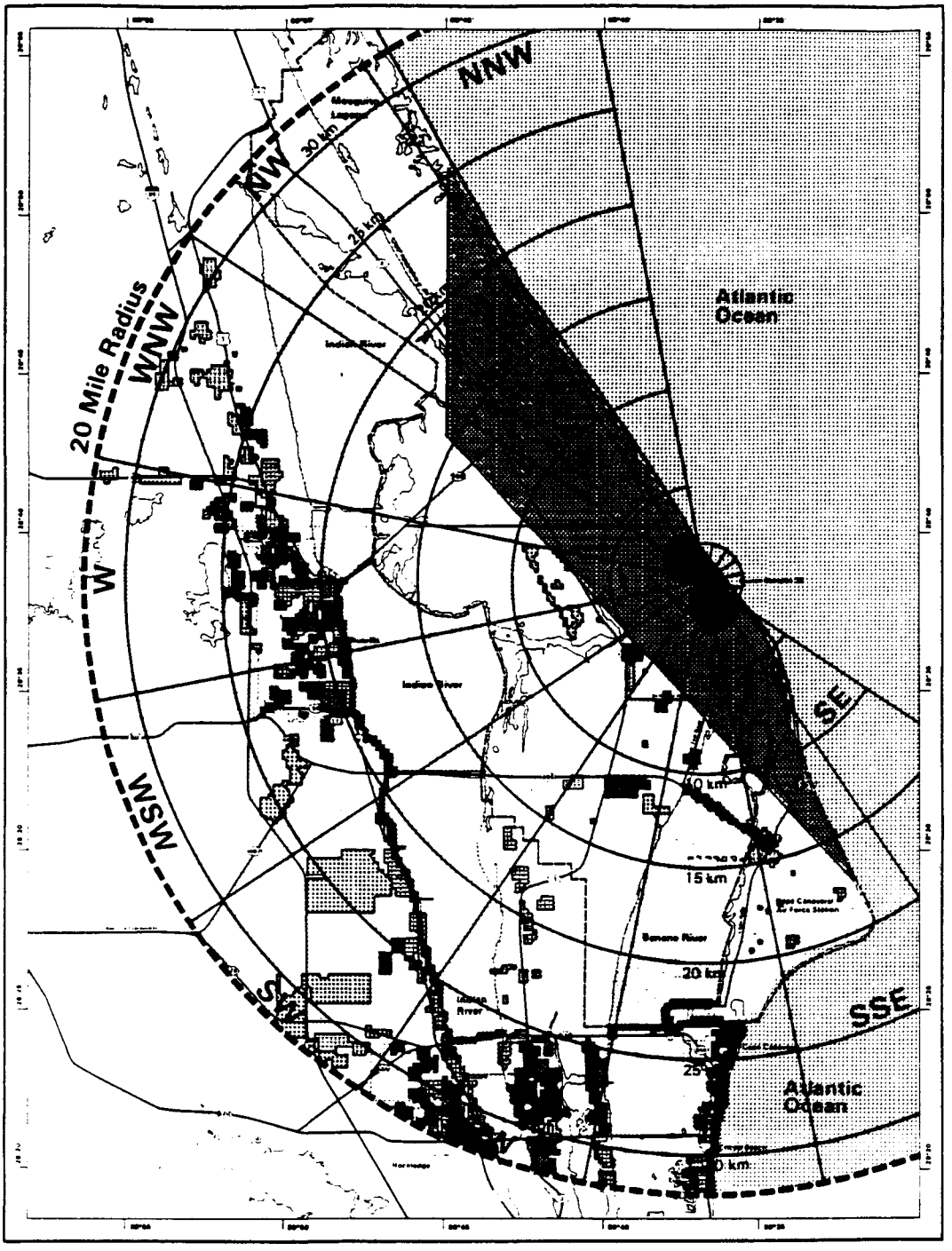

DAY LAUNCH POPULATION DENSITY WITH GRID WHEEL

- Zero Population
- Blast Danger Area (Crew)
- Launch Impact Limit Line (71 People)
- 1 - 10 People Per Square Kilometer
- 11 - 50 People
- 51 - 100 People
- 101 - 500 People
- 501 - 1000 People
- 1001 - 1500 People
- 1501 - 2000 People
- 2001 - 2500 People
- 2501 - 3000 People
- 3001 - 4000 People
- 4001 - 5000 People
- 5001 - 7500 People
- 10,001 - 15,000 People
- 15,001 - 20,000 People
- Greater than 20,000 People

Source: Compilation of NUS Interpreted Data

5760 ACRES
6 SQUARE MILES
2500 HECTARES
25 SQUARE KILOMETERS
N

Kennedy Space Center Study Area

Figure 10

Figure E-2.

REFERENCES

E-1 NUS Corporation, Kennedy Space Center Demographic and Land-Use Study, October 7, 1983.

E-2 Letter and attachments, Reynolds, J. R. to R. W. Englehart dated June 20, 1985, subject: Population Updates to NUS Demographic Study.

Table E1. Launch Population Data

Dis. (km)	-N-	-NNE-	-NE-	-ENE-	-E-	-ESE-	-SE-	-SSE-	-S-	-SSW-	-SW-	-WSW-	-W-	-WNW-	-NW-	-NNW-	-TOTAL-
0-2	0	0	0	0	0	0	0	0	0	0	0	0	0	0	0	0	0
2-5	0	0	0	0	0	0	0	0	0	0	0	0	0	0	0	0	0
5-10	0	0	0	0	0	0	0	0	0	0	0	0	0	0	0	0	0
10-15	0	0	0	0	0	0	0	0	0	0	0	0	0	0	0	0	0
15-20	0	0	0	0	0	0	0	0	0	2800	840	5960	11650	0	0	0	21150
20-25	0	0	0	0	0	0	0	0	5080	2630	11020	10320	35290	4550	0	0	68350
25-30	0	0	0	0	0	0	0	0	16250	48440	5420	190	2640	7000	0	0	79340
30-40	0	0	0	0	0	0	0	0	13242	33103	4027	11371	3990	3693	4318	423	73167
40-50	0	0	0	0	0	0	0	0	18270	7103	10755	22242	17773	7651	8128	659	92587
50-60	0	0	0	0	0	0	0	0	30144	2900	3666	21920	31663	13091	23723	1596	127703
60-70	0	0	0	0	0	0	0	0	62777	4769	1758	16220	40282	35028	9447	19411	189692
70-80	0	0	0	0	0	0	0	0	10200	3812	2545	34650	241304	29665	11199	52811	386186
80-90	0	0	0	0	0	0	0	143	8783	2558	2821	38835	47210	16977	14399	45254	176980
90-100	0	0	0	0	0	0	0	945	17000	2426	2545	10037	57468	6864	5889	2994	106168
TOTAL	0	0	0	0	0	0	0	1088	180746	110607	44397	171645	489270	124519	77103	123148	1322523

Table E1. Launch Population Data (continued)

Dis. (km)	-N-	-NNE-	-NE-	-ENE-	-E-	-ESE-	-SE-	-SSE-	-S-	-SSW-	-SW-	-WSW-	-W-	-WNW-	-NW-	-NNW-	-TOTAL-
0-2	0	0	0	0	0	0	0	0	0	0	0	0	0	0	0	0	0
2-5	0	0	0	0	0	0	2	5	3	3	3	1	2	2	0	0	21
5-10	0	0	0	0	0	0	1	12	7	31	4503	318	650	8	0	2	5532
10-15	0	0	0	0	0	0	0	2084	1046	10466	494	0	0	5	0	2	14097
15-20	0	0	0	0	0	0	0	424	192	0	0	7	0	0	0	2	625
20-25	0	0	0	0	0	0	0	0	52	0	0	0	0	0	0	2	54
25-30	0	0	0	0	0	0	0	0	0	0	0	0	0	0	0	0	0
30-40	0	0	0	0	0	0	0	0	0	0	0	0	0	0	0	0	0
40-50	0	0	0	0	0	0	0	0	0	0	0	0	0	0	0	0	0
50-60	0	0	0	0	0	0	0	0	0	0	0	0	0	0	0	0	0
60-70	0	0	0	0	0	0	0	0	0	0	0	0	0	0	0	0	0
70-80	0	0	0	0	0	0	0	0	0	0	0	0	0	0	0	0	0
80-90	0	0	0	0	0	0	0	0	0	0	0	0	0	0	0	0	0
90-100	0	0	0	0	0	0	0	0	0	0	0	0	0	0	0	0	0
TOTAL	0	0	0	0	0	0	3	2525	1300	10500	5000	326	652	15	0	8	20329

Table E1. Launch Population Data (continued)

SPECTATOR POPULATIONS BY SECTOR

Dis. (km)	-N-	-NNE-	-NE-	-ENE-	-E-	-ESE-	-SE-	-SSE-	-S-	-SSW-	-SW-	-WSW-	-W-	-WNW-	-NW-	-NNW-	-TOTAL-
0-2	0	0	0	0	0	0	0	0	0	0	0	0	0	0	0	0	0
2-5	0	0	0	0	0	0	0	0	0	0	2055	0	0	0	0	0	2055
5-10	0	0	0	0	0	0	0	0	2143	4054	0	0	0	0	0	0	6203
10-15	0	0	0	0	0	0	0	6900	25206	2	27	320	98	0	0	0	32553
15-20	0	0	0	0	0	0	0	0	358	29	3846	41680	22694	0	80	0	68686
20-25	0	0	0	0	0	0	0	0	68000	3115	8438	0	8	0	229	0	85790
25-30	0	0	0	0	0	0	0	0	12222	4471	134	0	0	0	236	0	17063
30-40	0	0	0	0	0	0	0	0	0	0	0	0	0	0	0	0	0
40-50	0	0	0	0	0	0	0	0	0	0	0	0	0	0	0	0	0
50-60	0	0	0	0	0	0	0	0	0	0	0	0	0	0	0	0	0
60-70	0	0	0	0	0	0	0	0	0	0	0	0	0	0	0	0	0
70-80	0	0	0	0	0	0	0	0	0	0	0	0	0	0	0	0	0
80-90	0	0	0	0	0	0	0	0	0	0	0	0	0	0	0	0	0
90-100	0	0	0	0	0	0	0	0	0	0	0	0	0	0	0	0	0
TOTAL	0	0	0	0	0	0	0	6900	107935	17670	14500	42000	22800	0	545	0	212350

Table E1. Launch Population Data (continued)

Dis. (km)	-N-	-NNE-	-NE-	-ENE-	-E-	-ESE-	-SE-	-SSE-	-S-	-SSW-	-SW-	-WSW-	-W-	-WNW-	-NW-	-NNW-	-TOTAL-
0-2	0	0	0	0	0	0	0	0	0	0	0	0	0	0	0	0	0
2-5	0	0	0	0	0	0	2	5	3	3	2058	1	2	2	0	0	2076
5-10	0	0	0	0	0	0	1	12	3156	4085	4503	319	650	8	0	2	11735
10-15	0	0	0	0	0	0	0	8584	26252	10468	521	330	98	5	0	2	46650
15-20	0	0	0	0	0	0	0	434	550	2928	4585	47547	34344	0	80	2	90451
20-25	0	0	0	0	0	0	0	0	73132	11805	19458	10320	35298	4550	229	2	154794
25-30	0	0	0	0	0	0	0	0	28472	53911	5554	190	2640	7000	236	0	97003
30-40	0	0	0	0	0	0	0	0	12242	33103	4027	11371	3990	3693	4318	423	73167
40-50	0	0	0	0	0	0	0	0	18270	7109	10755	22242	17773	7651	8128	659	92587
50-60	0	0	0	0	0	0	0	0	30144	2900	2666	21920	31663	13091	23723	1596	127703
60-70	0	0	0	0	0	0	0	0	62777	4769	1758	16220	40282	35028	9447	19411	189692
70-80	0	0	0	0	0	0	0	0	10200	3812	2545	34650	241304	29665	11199	52811	386186
80-90	0	0	0	0	0	0	0	143	8783	2559	2921	38835	47210	16977	14393	45254	176980
90-100	0	0	0	0	0	0	0	945	17000	2426	2545	10037	57468	6864	5889	2994	106168
TOTAL	0	0	0	0	0	0	3	10513	289981	138777	63897	213971	512722	124534	77648	123156	1555202

APPENDIX F

KENNEDY SPACE CENTER AREA OCEANOGRAPHIC, ESTUARINE, GROUND- AND SURFACE-WATER STUDIES

This appendix contains a summary description of certain aspects of the natural environment in the vicinity of the Kennedy Space Center (KSC) as they relate to potential impacts to man that might result from accidents associated with launches of the space shuttle. This discussion is not intended as an exhaustive description of the environment, but rather focuses on those aspects that may influence the exposure of the nearby human populations to radioactive materials in the case of a launch accident. The information contained herein was obtained from scientific articles and reports and from interviews with scientists, regulatory personnel, and others with knowledge of the area.

The discussion is divided according to type of environment: oceanic, estuarine, inland surface waters, and ground water. For each environment, a summary of pertinent physical characteristics is given followed by a brief discussion of the principal potential pathways to man. The final section of this appendix contains a listing of individuals contacted during its preparation.

F.1 OCEANIC ENVIRONMENT

The area of interest for this section is the Atlantic Ocean from the shore line to the edge of the continental shelf about 48 km offshore.

F.1.1 Physical Description

The bathymetry of the offshore areas in the vicinity of KSC is shown in Figure F-1. Out to depths of about 18 meters (approximately 10 to 12 km offshore), sandy shoals dominate the underwater topography (Ref. F-12). The bathymetry of the shoreward portion of this zone out to a depth of about 6 meters is complicated, with many shoals and reefs. The bottom in this area consists of many materials ranging from thick silt to very hard reef formations (Ref. F-16). Seaward of the 18-meter contour, the bottom continues to slope downward out to about 48 km offshore where depths of about 75 meters are reached. Beyond this, the bottom drops away more sharply to the 730 to 915 meter depths of the Blake Plateau (Ref. F-12).

Tides along the east coast of Florida are semi-diurnal and thus have two complete cycles every lunar day. The range of spring tides at Cape Canaveral is about 1.4 meters. Daily range is about 0.5 meters. Tidal range decreases with distance offshore.

There have been few studies of the water movements in the vicinity of Cape Canaveral. Woods Hole Oceanographic Institute and the Chesapeake Bay Institute of Johns Hopkins University carried out some investigations in 1962 for the USAEC (Ref. F-2 and Ref. F-4). The results of the study indicate that, during March and April, a shoreward current at speeds of several kilometers per day for the entire depth (surface to bottom), was

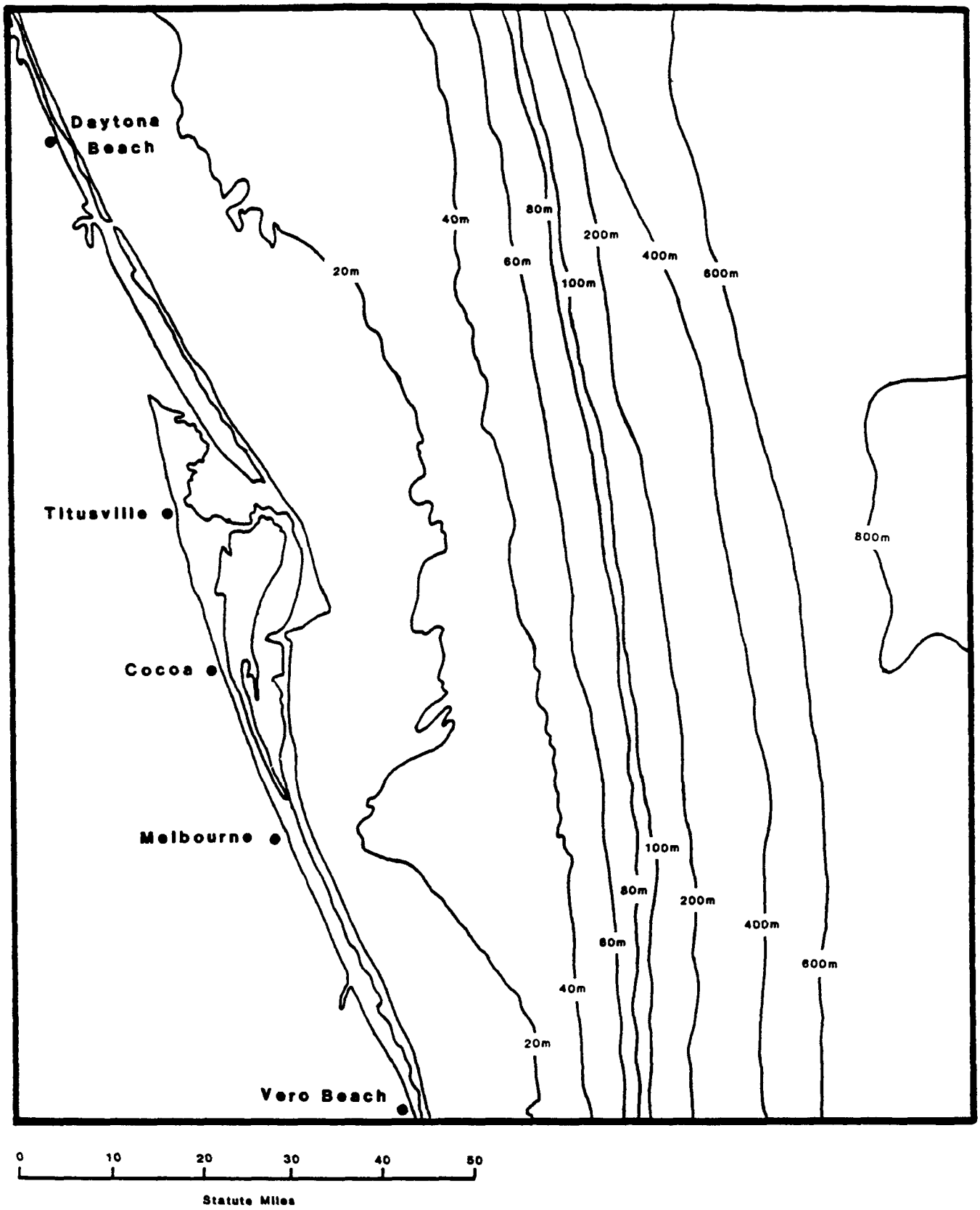

FIGURE F-1

Map of the coastal areas in the vicinity of Cape Canaveral, Florida

present in the region out to depths of about 18 meters. Wind-driven currents generally determined the current flow at the surface. In the region out to the Blake Plateau, the flow was slightly to the north with an eastward reversal when the winds blew to the south. Water over the Blake Plateau flowed to the north most of the time under the influence of the Gulf Stream.

Investigations in the vicinity of the Cape during June and July 1970 indicated that there was present at about the 18-meter depth contour an alternating northwestward and southeastward flow with an apparent periodicity of about 3 to 10 days (Ref. F-10). Typical onshore-offshore velocities in this area were 3 to 4 cm/sec and along-shore flows were 6 to 7 cm/sec. Bumpus (1973) found, as part of a larger study of currents along the Mid-Atlantic Bight, that there was a persistent southward flow at the surface in the inner shelf (water depths: 0 to 20 meters). Local wind forcing and seasonal atmospheric weather fronts also influence water movements in this zone and in the mid-shelf region further offshore (water depths: 21 to 40 meters) (Ref. F-9). Along the outer shelf (depths: 41 to 75 meters), low-frequency flow variability and water exchange is primarily produced by frontal disturbances (eddies and meanders) along the shorward edge of the Gulf Stream (Ref. F-8). The mean northward speed of the Gulf Stream is about 6.4 km per hour.

In nearshore areas, longshore currents continually deposit sand on the beach during summer months (April through September) while during the winter, beach sands are removed and redeposited in offshore sandbars (Ref. F-12). These currents, which are largely confined to the surf zone (i.e., inside the first line of breakers), are caused by waves breaking on the shore, and are responsible for sand transport parallel to the shoreline (Ref. F-16). These currents are distinct from offshore currents and are dependent on wind for direction (Ref. F-12).

The Atomic Energy Commission sponsored an investigation into the movement of coastal sediments in the immediate vicinity of KSC specifically to determine the movement and fate of debris from any launch accident (Ref. F-16). The conclusions of the study indicated that the test particles (with a specific gravity of 2.2) moved rapidly onto the beach from depths of about 6 meters or less and continually moved onshore over a long period of time (up to three years after initial placement). Particles moved considerable distances along the shore (up to 1.6 km or more) and they tended to come onto the beach during times of greatest onshore wave power. No information was obtained on offshore movement, however, other experience indicated particles at depths greater than about 10 meters moved offshore (if at all) in areas of exposed coast (Ref. F-16).

F.1.2 Potential Pathways to Man

The principal potential pathway by which radioactive material in the oceanic environment near KSC could affect man would be

through the consumption of contaminated seafood. Table F-1 lists the principal species of finfish and shellfish that comprised the commercial catch landed in Brevard County during 1983 (the latest year for which statistics are available). These statistics include catches made in the Atlantic Ocean as well as those taken in the estuarine areas (Indian River and Banana River). With the exception of menhadden and sharks, all the species listed are consumed by man.

The following are the principal areas from which the fish are taken. It should be noted that in some cases, species landed in Brevard County (principally at Port Canaveral) are captured in waters some distance from the Cape Canaveral area.

Spot	Indian River
Tilefish	Offshore in waters greater than about 100 meters
Mullet	Indian River and along Atlantic beaches
Grouper/Scamp	Offshore outside the 12-mile limit
King Whiting	Along Atlantic beaches by shrimp trawlers
King Mackerel	Atlantic coastal waters inside 12-mile limit
Calico scallop	Atlantic from Cape Canaveral to New Smyrna Beach from about 25 to 50 meters depth (24 to 40 km offshore)
Blue crabs	Indian River, Banana River
Rock shrimp	Atlantic from south of Cape Canaveral to New Smyrna Beach from about 35 to 65 meters depth (up to about 55 km offshore)
Saltwater shrimp	Pink shrimp: with rock shrimp offshore. White and Brown shrimp: inshore Atlantic and Indian River
Hard clams	Indian River, Banana River

In 1982, the following numbers of commercial fishing craft operated in Brevard County (USCOE 1985, Appendix 1b):

Shrimp vessels	108
Scallop vessels	150
Fishing vessels	165
Undocumented	400

TABLE F-1

Commercial Marine and Estuarine Fishery Landings in Brevard County, Florida in 1983. (Only those species with total landings of 10,000 lbs. or more are listed)

Species	Total Pounds
Spot	725,483
Tilefish	632,731
Black mullet	350,186
Groupers and scamp	325,228
Menhadden	316,260
King whiting	110,876
King mackerel	100,615
Swordfish	83,352
Spotted sea trout	50,098
Bluefish	38,927
Pompano	36,148
Sheepshead	33,301
Sharks	30,922
Red snapper	27,326
Flounders	12,246
Dolphin	10,984
Total Fish (all species)	2,988,460
Calico scallops	8,776,013
Blue crabs	1,616,472
Rock shrimp	1,363,335
Saltwater shrimp	114,495
Hard clams	108,332[1]
Oysters	17,488
Total Shellfish (all species)	12,005,501

Note: 1. Hard clam landings do not include those processed through depuration plants.

Source: National Marine Fisheries Service, Statistical Surveys Branch, Miami

It should be noted that most finfish species are highly mobile and some undergo routine seasonal migrations. Also, many spend different stages of their lives in different environments (e.g., they spawn in the estuaries, pass their juvenile stages there and move offshore as adults). Shrimp and crabs also undergo migrations in response to their spawning cycles. Accordingly, fish captured from an uncontaminated area may in fact have occupied a contaminated area during migrations or at some earlier life stage.

In additional to the commercial fishing activities, Cape Canaveral and surrounding areas support an active saltwater sport fishery. No landing statistics are available specifically for Brevard County or even the entire east coast of Florida (J. Ernest Snell, personal communication). However, almost all fish taken can be presumed to be eaten by the fisherman and their families. Table F-2 lists the principal fish species sought by the recreational fishery.

F.2 ESTUARINE ENVIRONMENT

The principal estuarine areas in the vicinity of KSC are the Indian River, the Banana River, and Mosquito Lagoon (Figure F-2) .

F.2.1 Physical Description

The Indian River is a narrow estuarine lagoon system extending from Ponce de Leon Inlet in Volusia County (about 85 km north of KSC) to Jupiter Inlet in Palm Beach County to the south. The total length of the water body is about 253 km. The width of the lagoon varies from 8.9 km just north of Titusville to a few meters both at the Jupiter Narrows in the south and at New Smyrna Beach to the north. The narrow barrier island that separates the lagoon from the Atlantic Ocean is widest at Cape Canaveral where Merritt Island divides the Indian River lagoon on the west from the Banana River lagoon on the east. The Banana River is directly connected to the Atlantic by an artificial inlet and locks at Port Canaveral. The Indian River is indirectly connected to the Atlantic on the north via Haulover Canal, Mosquito Lagoon and the Ponce de Leon Inlet, and on the south by Sebastian Inlet (about 75 km below KSC). The northern end of the Banana River is separated from the Mosquito Lagoon only by a shallow marsh with waters coming within 0.8 km of a direct connection between the two. To the south, the Banana River communicates with the Indian River through a narrow inlet near Eau Gallie.

The average depth of the Indian River is approximately 1.5 meters with greatest depths occurring in the Intracoastal Waterway which is dredged to an average depth of about 3.7 meters in the Cape Canaveral area. This dredged channel has an average width of 30 meters (Ref. F-7).

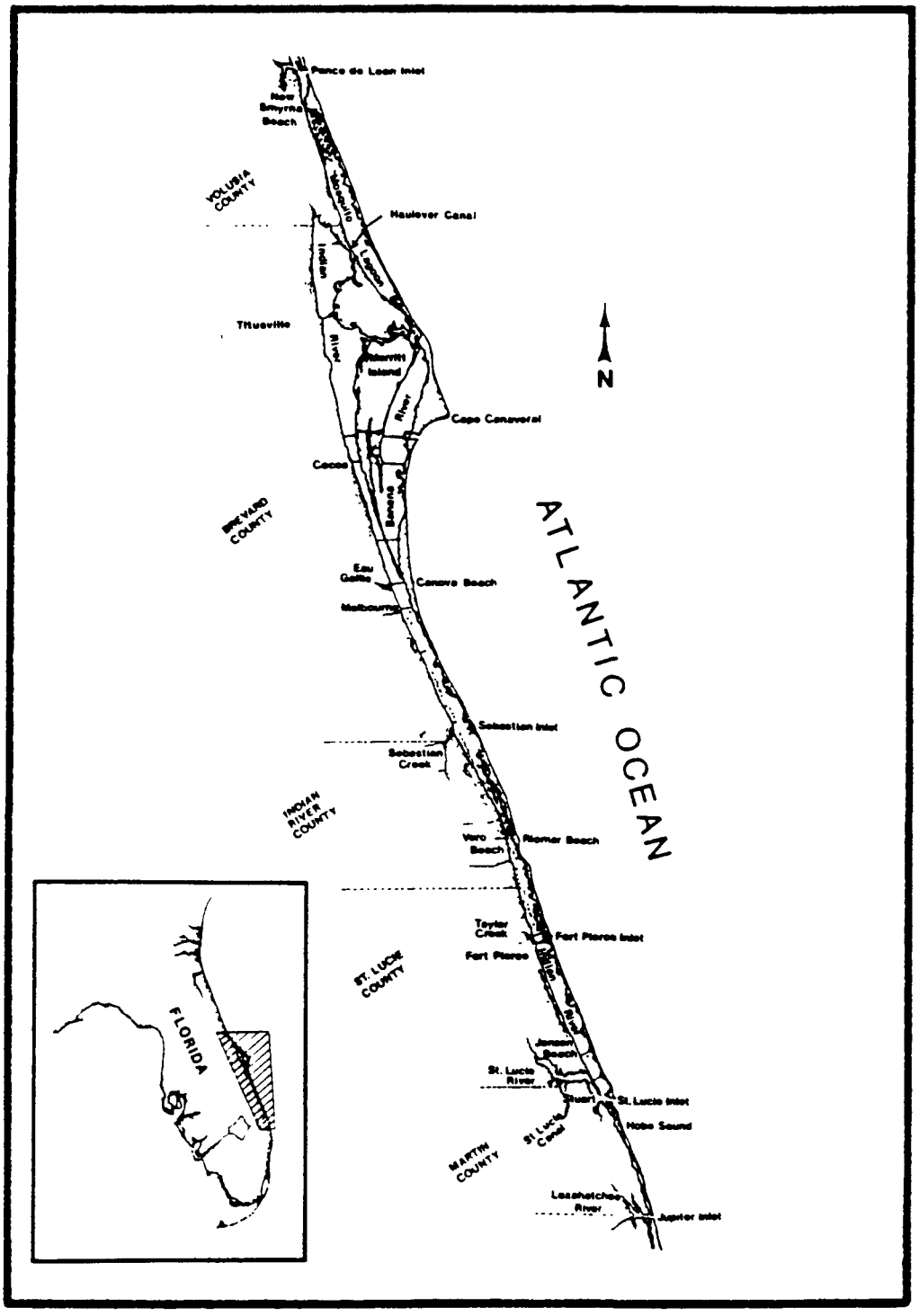

Source: Gilmore et al. 1981

FIGURE F-2

Map of the Indian River coastal lagoon system of the eastern central Florida

TABLE F-2

Principal Species of Marine and Estuarine Fishes Sought by Recreational Fisherman in the Cape Canaveral area

OFFSHORE

king mackerel	Spanish mackerel
blue marlin	red snapper
white marlin	grouper (several species)
sailfish	jewfish
dolphin	greater amberjack
great barracuda	crevalle jack

ESTUARIES, SURF ZONE, INSHORE

tarpon	gafftopsail catfish
bluefish	sea catfish
Spanish mackerel	summer flounder
spotted seatrout	Atlantic croaker
gray snapper	northern kingfish
Florida pompano	Atlantic spadefish
crevalle jack	red drum
snook	black drum
sheepshead	striped mullet
ladyfish	

Source: USCOE 1985.

The lagoonal system in the KSC area is not influenced by lunar tides because of the distance to the ocean and the effects of natural and man-made constrictions. Daily tidal fluctuations in the Banana River are usually less than 5 cm, although the annual range of sea level exceeds 30 cm (Ref. F-17). There are no regular circulation patterns in the lagoon system. Winds are primarily responsible for water movements, although fresh water surges during the wet season have a slight influence on those movements (Ref. F-12).

F.2.2 Potential Pathways to Man

As in the oceanic environment, the principal potential pathway to man would be through the consumption of contaminated finfish and shellfish. The harvesting of seafood both by commercial and recreational fishermen is discussed in Section F.1.2 above. Lists of the species that are exploited in both the oceanic and estuarine areas are given in Tables F-1 and F-2.

The Banana River contains a very fine sport fishery and also is subject to moderate commercial fishing pressure. A survey of recreational and commercial use of the resources in the Banana River conducted by the U.S. Fish and Wildlife Service in 1955 and 1956 indicated that sport fishermen spent about 808,000 man-days annually in this area (Ref. F-17). The landing statistics for 1963 show that the commercial catch from the Banana River was about 28,320 kg (618,800 lbs). The recreational catch around Cape Canaveral was approximately 70,750 kg (156,000 lbs) (USCOE 1985). By 1982, the Brevard County commercial catch of estuarine species was 1,405,590 kg (3,098,795 lbs).

One of the most important food items taken from the estuarine system around Cape Canaveral is the hard clam. Exploitation of this species has increased dramatically in the past few years. It is estimated that, during 1984, as many as one million clams per day were passed through a large processing plant in Grant (Brian Poole, personal communication). Most clams are taken by commercial fishermen from closed areas (i.e., those parts of the estuary contaminated with fecal bacteria) and, prior to marketing, they are either passed through depuration plants or resettled in leased clean-water areas. The principal areas for this type of harvesting are in the Indian River from State Road 528 south to Cape Malibar and from the Pinetta Causeway to about 15 km north. There are also some clean areas from which clams can be taken for direct marketing or consumption. These are in the Indian River in southern Brevard County from Cape Malibar to just north of Long Point Park. Both commercial clammers and private individuals harvest clams in these areas. It has been estimated that as many as 400,000 clams per day were taken from this area during summer 1984 (Brian Poole, personal communication). Exploitation in 1985 has been at a much lower level than previously.

Another important species harvested throughout most of the Indian River lagoon system is the blue crab. Total landings reported by the National Marine Fisheries Service for Brevard County in 1983 were 733,219 kg (1,616,472 lbs). Most of this catch was made in estuarine areas, although some were probably taken in nearshore oceanic areas (Derek Busby, personal communication). There is a recreational as well as commercial fishery for this species in the Indian River.

F.3 INLAND SURFACE WATER ENVIRONMENTS

For the purposes of this analysis, only those bodies of fresh water within about an 80 km radius of KSC have been considered. The St. Johns River is the principal water body in this area (Figure F-3). There are also some fresh water marsh areas that run in a band close to the coast in this part of Florida.

F.3.1 Physical Description

The St. Johns River originates in a broad marshy area about 120 km south of Cape Canaveral in St. Lucie and Indian River counties. It flows northward, running parallel to the coastline, for about 480 km to enter the Atlantic Ocean at Mayport east of the City of Jacksonville. The river forms a series of large shallow lakes along its course. Several of these are located within the 80 km radius of KSC. Lake Washington and Lake Poinsett (both with surface areas of about 17 km^2) and smaller Lake Winder are about 50 km south southwest of the Cape. Lakes Harney and Jessup and Lake Monroe (area: 36 km^2) are located to the northwest and are within about 40 km of KSC. The largest of the St. Johns River lakes is Lake George which has a surface area of about 189 km^2. It is located about 130 km to the northwest of the launch area.

The flow in the river and in most of its larger lakes is regulated by low dams and other control structures. Mean annual discharge of the river near Melbourne (i.e., south of KSC) is about 19.9 cms (703 cfs), near Cocoa it is 30.2 cms (1068 cfs) and at Jacksonville it is 156.2 cms (5515 cfs).

The St. Johns River and the lakes support heavy recreational uses including fishing, boating, water skiing and swimming. They also provide water for domestic use and for irrigation and livestock watering.

This part of the coast of Florida is also characterized by a series of narrow coastal basins that run parallel to the coast between the St. Johns River and the Indian River lagoon. These basins are characterized by numerous marshy areas and are drained by streams and man-made canals that flow directly into the estuarine lagoons. The largest of these basins is Tomaka Creek in Volusia County (about 80 km north of KSC) which drains an area of about 394 km^2 (St. Johns River Water Management

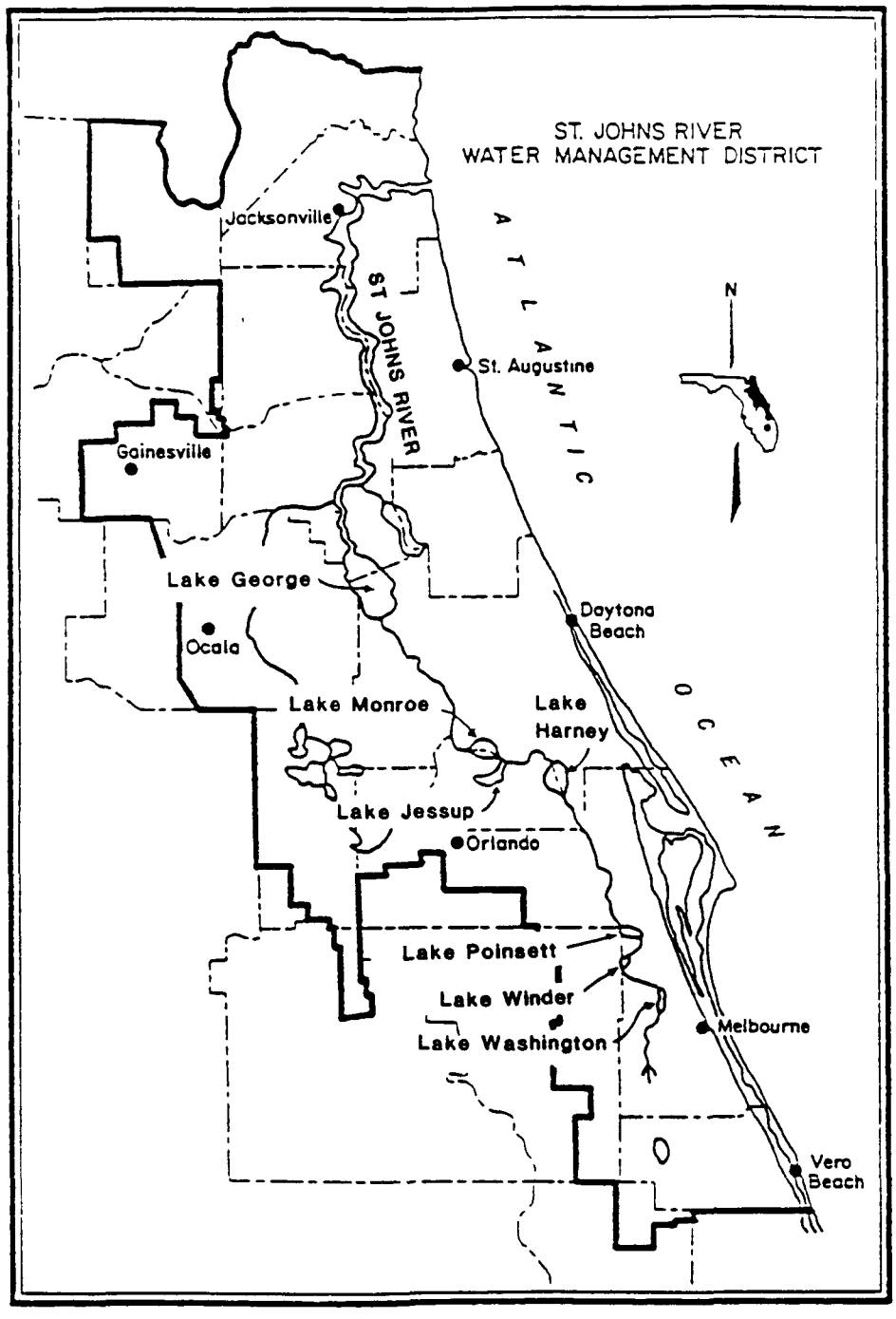

Source: St. Johns River Water Management District 1984a

FIGURE F-3

Map of the major fresh surface water features in the vicinity of Kennedy Space Center

District 1977). These streams and canals are used by sport fishermen.

F.3.2 Potential Pathways to Man

There are two potential pathways by which contaminants in the surface water bodies could reach man: 1) through contaminated fish and 2) through contaminated drinking water.

The lakes, rivers, and streams in east central Florida are heavily used by recreational fishermen. It can be estimated that during the peak months of the year (December through April), as many as 50,000 man-hours are expended by sport fishermen in Lake Washington and Lake Harney alone. Statistics on estimated catch by species are summarized in Table F-3. The large mouth bass is a highly sought-after fish, although actual catches are low. Other popular species are the bream and the black crappie which are caught in greater numbers than the bass. Catfish are also an important sportfish in this area and the American shad is of seasonal importance in Lake Harney.

Surface water is generally not used as a source of drinking water in Florida.

F.4 GROUND WATER

Ground water underlying the area of interest occurs in both the non-artesian and artesian aquifers.

F.4.1 Physical Description

The non-artesian (or unconfined) aquifer is composed mainly of sand and clay-sand deposits. It ranges in thickness along the east coast of central Florida from several centimeters to about 46 meters, in Indian River County south of Cape Canaveral. This aquifer is exposed to the land surface. Its lower limit is the aquaclude (impermeable layer) that forms the upper con fining layer of the Floridian aquifer. The non-artesian aquifer exhibits a wide range of permeability, with the most permeable zones generally occurring in the coastal counties (Ref. F-13). Recharge of the aquifer is by infiltration of local rainfall. Discharge is by several processes: seepage into streams, lakes, or the ocean; downward movement into the artesian aquifer; evapotranspiration; and pumpage.

The unconfined aquifer is not highly utilized in east central Florida except in areas where the Floridan aquifer is highly mineralized (Ref. F-13). During 1975, municipal water suppliers alone pumped over 38 mld (10 mgd) from the non-artesian aquifer in the St. Johns River Water Management District (Ref. F-18). Moderate water supplies may be obtained by controlled pumping in the coastal ridge areas, particularly in northern Brevard County, with lesser supplies available on the barrier islands (Ref. F-1). In eastern St. Johns and Flagler Counties, in

TABLE F-3

Statistics on Fresh Water Sportfish Species Caught in the Upper St. Johns River During Months of Peak Fishing Activity in 1982 and 1983

Lake Washington - Lake Sawgrass
(census period: 1/15/83 to 5/18/83)

Species	Effort (man-hrs)	Harvest (fish caught)
largemouth bass	6,414	4,553
bream	1,797	2,321
crappie	1,103	647
catfish	314	171

Source: Cox et al., 1983

Lake Harney (census period: 12/13/81 to 4/16/82)

Species	Effort (man-hrs)	Harvest (fish caught)
largemouth bass	2,385	953
bream	10,904	10,847
crappie	29,270	44,092
catfish	1,524	2,521
American shad	4,405	4,327

Source: Cox et al., 1982

Seminole County, in western Clay County and in southeastern Alachua County, moderate supplies are obtained for domestic use from wells that draw from sand or coquina aquifers and from permeable limestone beds. Although the amount of water supplied by wells tapping the non-artesian aquifer may be limited by seasonal fluctuations of the water table, it is still a valuable source of water (St. Johns River Water Management District 1977).

The artesian (or confined) aquifer that underlies the area of interest comprises numerous carbonate formations which collectively form a system as much as 729-meters thick called the Floridan aquifer (Ref. F-13). This system extends throughout all Florida and parts of Georgia, Alabama, and South Carolina. The Floridan aquifer is at or near land surface in the central part of Florida. However, toward the east coast (including the area of present interest) it dips to as much as 100 meters below ground surface. The migration of ground water generally follows this trend and flows from the high central areas towards the coast. Artesian conditions are common along the coast and natural springs occur where there are major breaches through the upper confining layer of the aquifer.

Recharge of the Floridan aquifer occurs in the central part of the state, as well as in areas in east central Florida nearer to Cape Canaveral. A map of these generalized recharge areas is shown in Figure F-4. Overall recharge within the east central Florida region is estimated to be about 3875 mld (1,000 mgd).

Discharge from the Floridan aquifer occurs as pumpage from wells, upward seepage to overlying aquifers, seepage or spring flow into water courses, and lake evapotranspiration where the aquifer is at or near land surface, and by underflow to the Atlantic Ocean.

The Floridan aquifer is the preferred water source in the east central parts of the state due to its productivity potential and generally good water quality (Ref. F-13).

F.4.2 Potential Pathways to Man

A possible way for contaminated ground water to affect man is through drinking water. A lesser potential is via a more indirect pathway through livestock watering or irrigation of crops.

Most drinking water in Florida is taken from the artesian aquifer, which is separated from the unconfined aquifer above it by an impermeable layer. Therefore, it has no susceptability to contamination.

Recharge of the unconfined (near surface) aquifer by rainfall has the potential to contaminate the groundwater in the aquifer if plutonium has been deposited on the soil above the aquifer. However, research at Los Alamos National Laboratory indicates

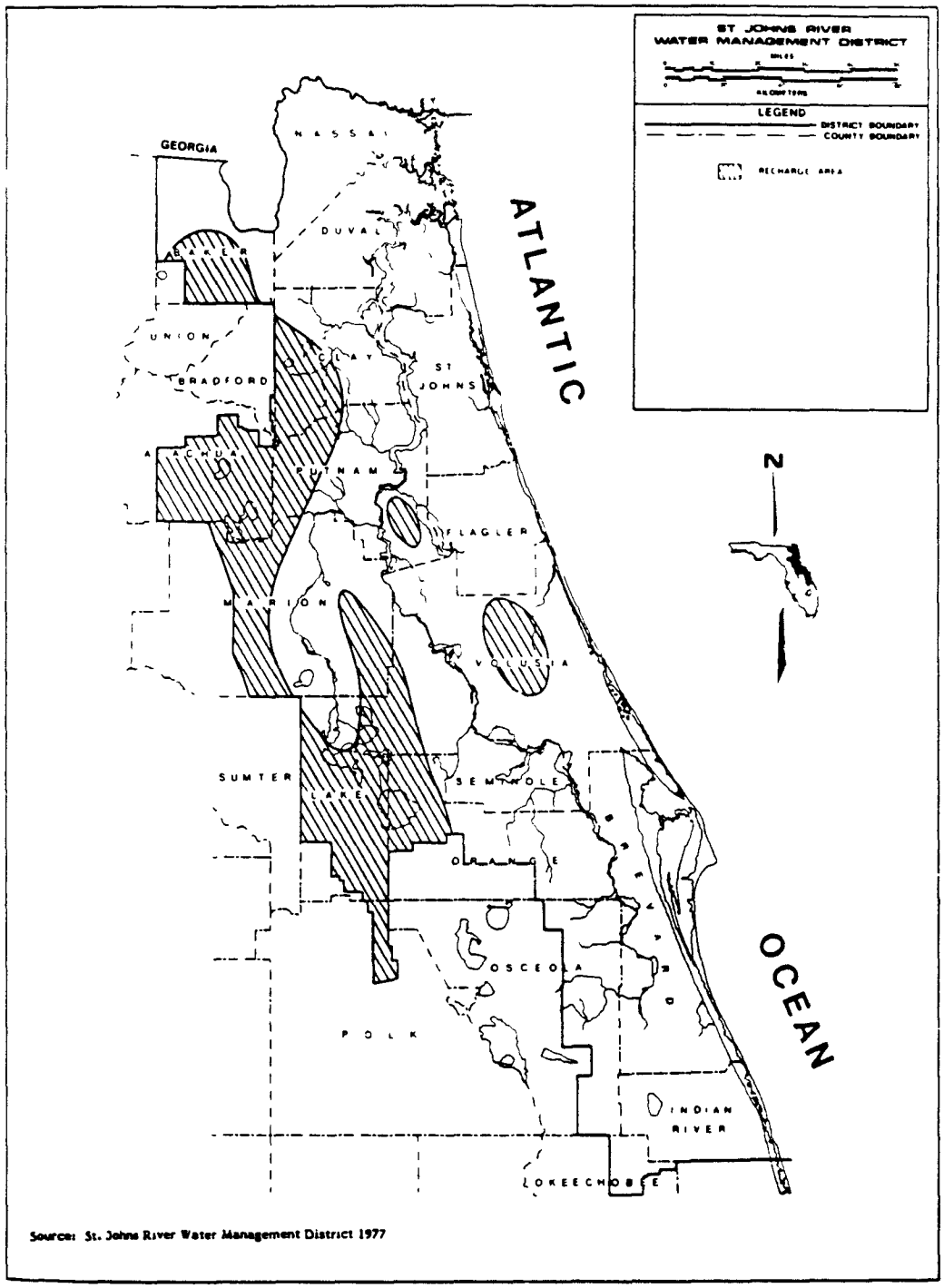

FIGURE F-4

Generalized map of potential ground water recharge areas in eastern central Florida

that plutonium deposited on soil is retained with the soil rather than being transported with soil percolates (Ref. F-11).

Water use statistics for 1983 (the latest year for which data have been published) compiled by the St. Johns River Water Management District (1984b) for east central Florida indicate that Indian River and Brevard Counties used the largest amount of fresh water that year, accounting for 1068.6 mld (282.30 mgd) and 977.4 mld (258.19 mgd), respectively. Orange County (652.2 mld), Lake County (531.0 mld) and Duval County (515.5 mld) were the next three largest fresh water users in 1983.

The largest fresh ground water use county in 1983 was Brevard County which accounted for 873.1 mld (230.64 mgd). Other counties which withdraw more than 378.5 mld (100 mgd) of fresh ground water that year were Orange County (538.0 mld), Duval County (506.8 mld), Lake County (451.0 mld), and Indian River County (403.2 mld).

The county that used the largest amount of fresh surface water in 1983 was Indian River County (661.6 mld; 174.78 mgd). Other counties using substantial amounts of surface water were Putnam (161.4 mld), Orange (114.2 mld), Brevard (104.3 mld), and Lake (80.1 mld).

The largest fresh water use category in the St. Johns River Water Management District during 1983 was Agricultural Irrigation (which includes livestock watering). This category accounted for 44 percent (1894.4 mld) of all ground water used and 82 percent (968.3 mld) of all surface water used in the District. The second largest category was Public Supply which used 25 percent (1076.3 mld) of the total fresh ground water and 4 percent (47.3 mld) of the total fresh surface water. The Domestic Self-Supply category accounted for 7 percent (301.4 mld) of ground water use in 1983.

The water use statistics for Brevard County in 1983 are presented in Table F-4. Among the largest uses of both fresh ground water and surface water were for agricultural irrigation and public water supply. Approximately 274,590 individuals were served by public water supplies within the county and another 33,981 used domestic wells. A total of 147,912 acres were farmed in 1983; of this area, 36,106 acres were irrigated (Ref. F-13).

TABLE F-4

Fresh Water Use in Brevard County, Florida in 1983
(Figures are in millions of liters per day)

	Ground Water Total	Surface Water	Total
Public Supply	27.3	45.1	72.4
Domestic Self-Supplied	16.9	0	16.9
Industrial Self-Supplied	0.6	0	0.6
Agricultural Irrigation	291.4	59.2	350.6
Thermoelectric Power Gen.	1.2	0	1.2
Heat Pump/Air Conditioning	535.6	0	535.6
TOTAL	873.0	104.3	977.3

Source: St. Johns River Water Management District 1984a

F.5 REFERENCES

F-1 Brown, D. W., W. E. Kenner, J. W. Crooks, and J. B. Foster. 1962. Water Resources of Brevard County, Florida. Fla. Bur. Geo. RI 28.

F-2 Bumpus, D. F. 1964. Report on non-tidal drift experiments off Cape Canaveral during 1962. Woods Hole Oceanogr. Inst. Ref. No. 64-6. 15pp.

F-3 Bumpus, D. F. 1973. A description of the circulation on the continental shelf of the east coast of the United States. Progr. Oceanogr., 6:111-158.

F-4 Carter, H. H. and Akira Okubo. 1965. A study of the physical process of movement and dispersion in the Cape Kennedy area. Chesa. Bay Inst., Johns Hopkins Univ., Ref. 65-2. 150pp.

F-5 Cox, D. I., E. D. Vosatka, R. Eisenhauer and S. Moore. 1982. Biological Effects of Water Level Fluctuation in the Upper Reaches of the St. Johns River, Annual Report. Fla. Game Freshwater Fish Commission. DJF-33-6. 53pp.

F-6 Cox, D. I., E. D. Vosatka, R. Eisenhauer and S. Moore. 1983. Biological Effects of Water Level Fluctuation in the Upper Reaches of the St. Johns River, Annual Report. Fla. Game Freshwater Fish Commission, DJF-33-7. 70pp.

F-7 Gilmore, R. G., C. J. Donohoe, D. W. Cooke and D. J. Herrema. 1981. Fishes of the Indian River Lagoon and adjacent waters, Florida. Harbor Branch Foundation, Technical Report No. 41. 64pp.

F-8 Lee, T. N. and D. A. Brooks. 1979. Initial observations of current, temperature and coastal sea level response to atmospheric and Gulf Stream forcing on the Georgia shelf. Geophys. Res. Letter. 6:321-324.

F-9 Lee, T. N. and L. P. Atkinson. 1983. Low-frequency current and temperature variability from Gulf Stream frontal eddies and atmospheric forcing along the Southeast U.S. outer continental shelf. J. Geophys Res. 88(C8):4541-4567.

F-10 Leming, T. D. 1979. Observations of temperature, current and wind variations off the central eastern coast of Florida during 1970 and 1971. National Marine Fisheries Service. NOAA Technical Memorandum, NMFS-SEFG-6. 172pp.

F-11 Los Alamos National Laboratory. 1985. Long-Term Exposure of 238 PuO_2 to a Terrestrial Environment. Report LA-9487-MS, Vol. III.

F-12 National Aeronautics and Space Administration. 1979. Final Environmental Impact Statement for the Kennedy Space Center.

F-13 St. Johns River Water Management District. 1977. Water Resource Management Plan, Phase 1. 368pp.

F-14 St. Johns River Water Management District. 1984a. Annual water use survey: 1983. Technical Publication SJ 84-5. 103pp.

F-15 St. Johns River Water Management District. 1984b. Annual report of hydrologic conditions, 1983 water year. Technical Publication SJ 84-7. 41pp.

F-16 U.S. Atomic Energy Commission. 1970. Tracing of coastal sediments movement at Cape Canaveral. University of Florida. Department of Coastal and Oceanographic Engineering. Report UF/COEL-70/12. 60pp.

F-17 U.S. Corps of Engineers. 1985. Supplement Draft Environmental Impact Statement. Proposed Plan for Navigation Improvement, West Basin and Approach Channel, Canaveral Harbor, Florida.

F-18 U.S. Geologic Survey. 1977. Water use inventory in Florida - 1975. Open File Report 77-577.

APPENDIX G

WORLDWIDE DEMOGRAPHIC, SURFACE-TYPE AND METEOROLOGICAL DATA

G.1 INTRODUCTION

This section summarizes worldwide data on demography, surface characteristics, and meteorology used in the NRAD analyses for accidents in Phases 2 through 5. Section G.2 presents the worldwide meteorological and demographic data base and Section G.3 presents the manner in which surface impact probabilities were calculated as a function of orbital inclination. This information was derived from Reference G-1.

G.2 WORLDWIDE METEOROLOGICAL AND DEMOGRAPHIC MODEL

Worldwide meteorological and demographic characteristics affecting the risk from accidental fuel releases involving random reentry and earth impact have been analyzed on a grid system. The grid system was selected which produced 20 equal area latitude bands. Each of the 20 latitude bands was segmented into 36 equal area cells in 10° longitude increments. Thus, a total of 720 cells are contained within the framework which is presented in Figure G-1. Each equal area cell has an area of 708,435 km^2, and its bounding latitudes are determined from

$$A = R^2 (\sin \theta_2 - \sin \theta_1) (\phi_2 - \phi_1)$$

where

θ = latitude

ϕ = longitude

The latitude bands for both the northern and southern hemispheres are bounded as shown in Table G-1. This grid allows the characteristics of each cell to be normalized to the same area.

G.2.1 Worldwide Meteorological Summary

The evaluation of random reentry impacts and the atmospheric dispersion of released fuel require a knowledge of worldwide meteorological conditions. Worldwide meteorology has been analyzed by assigning the world's land area into 14 categories of climate presented in Table G-2, which represents a condensed version of the Koppen classification. The probability distribution of the categories present in each area latitude band is presented in Table G-3. The meteorological data for a five year period were obtained from up to six stations in each category on magnetic tapes which were then reduced using the NUS WINDIF computer program to yield for each station the annual average frequency of occurrence of the seven stability classes and the wind speed associated with each. The atmospheric stability categories, based on the Turner-Pasquill classification, were summarized previously in Table G-2. An extensive statistical analysis of this data determined the validity of the 14 categories and the data to best represent each (Reference G-1). The probability distribution of stability

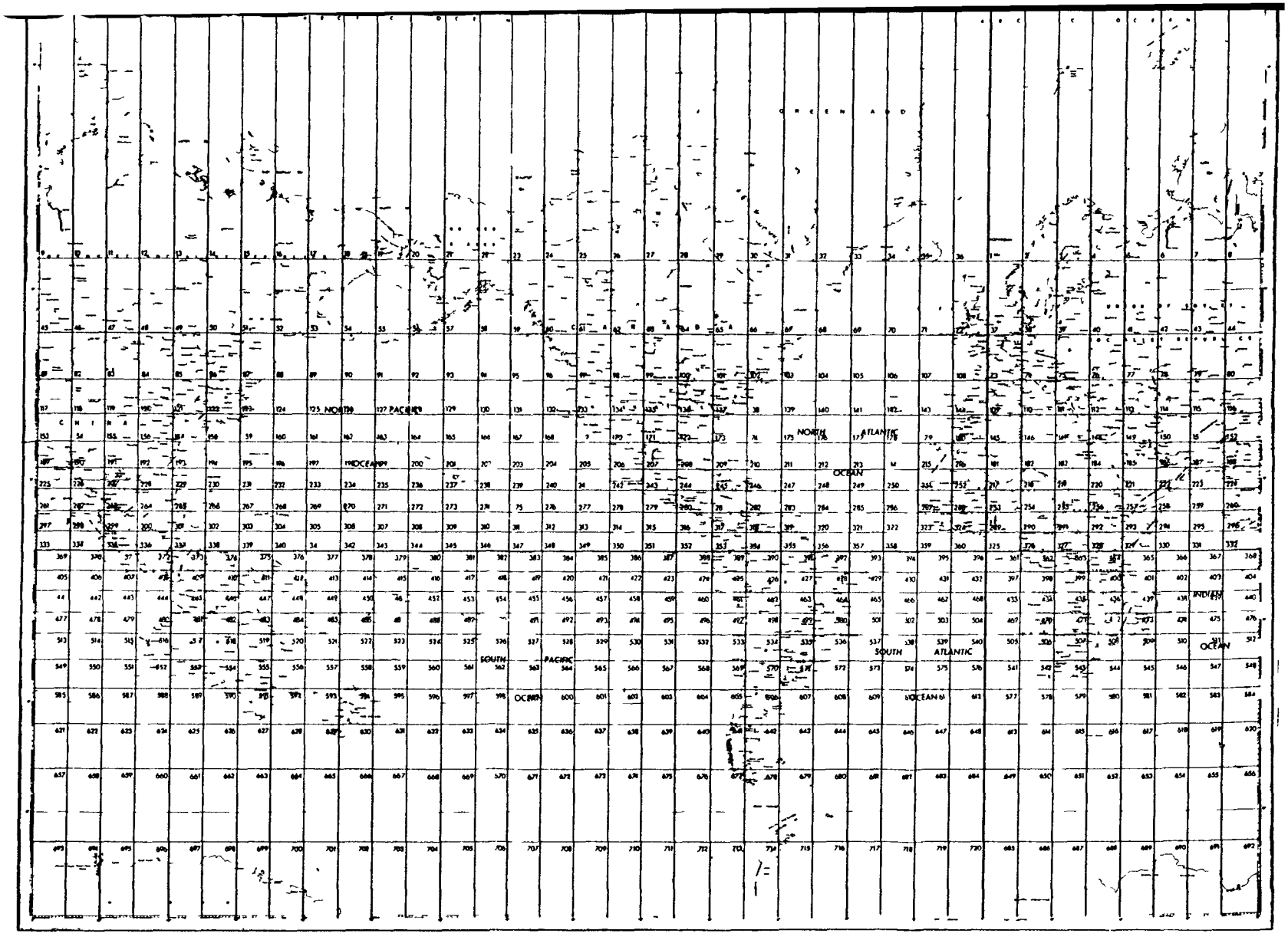

Figure G-1
CELL FRAMEWORK NUMBERING SEQUENCE

Table G-1
EQUAL AREA LATITUDE BAND BOUNDARIES

Number of Band	Latitude Range
1	64° 9' 30" N - 90° N
2	53° 7' 30" N - 64° 9' 30" N
3	44° 26' 30" N - 53° 7' 30" N
4	36° 52' 30" N - 44° 26' 30" N
5	30° 30" N - 36° 52' 30" N
6	23° 35' 30" N - 30° 30" N
7	17° 27' 30"N - 23° 35' 30" N
8	11° 32' 30"N - 17° 27' 30" N
9	5° 44' 30" N - 11° 32' 30" N
10	Equator - 5° 44' 30" N
11	5° 44' 30" S - Equator
12	11° 32' 30" S - 5° 44' 30" S
13	17° 27' 30"S - 11° 32' 30" S
14	23° 35' 30" S - 17° 27' 30" S
15	30° 30" S - 23° 35' 30" S
16	36° 52' 30" S - 30° 30" S
17	44° 26' 30" S - 36° 52' 30" S
18	53° 7' 30" S - 44° 26' 30" S
19	64° 9' 30" S - 43° 7' 30" S
20	90° S - 64° 9' 30" S

Table G-2
FOURTEEN WORLDWIDE METEOROLOGICAL CATEGORIES CONSIDERED IN THE ANALYSIS

Meteorological Category	Köppen Classification
1	Af
2	Aw
3	BSh
4	BSk
5	BWk
6	Caf
7	Cas
8	Cbf
9	Bcf
10	Daf
11	Dbf
12	Daw
13	ET
14	EF

Table G-3
METEOROLOGICAL CATEGORY DISTRIBUTION FOR EACH EQUAL AREA LATITUDE BAND

EQUAL AREA LATITUDE BAND	METEOROLOGICAL CATEGORY 1	2	3	4	5	6	7
1	0.0000	0.0000	0.0000	0.0000	0.0000	0.0000	0.0000
2	0.0000	0.0000	0.0000	.0523	0.0000	0.0000	.0514
3	0.0000	0.0000	0.0000	.2925	.0487	0.0000	.0928
4	0.0000	0.0000	0.0000	.2389	.0833	.1373	.0882
5	0.0000	0.0000	.2377	.0866	.1084	.2163	0.0000
6	0.0000	.0253	.1773	.0250	.4387	.2314	0.0000
7	0.0000	.2391	.1379	0.0000	.4801	.1430	0.0000
8	.0087	.3588	.2507	0.0000	.3033	.0426	0.0000
9	.1836	.6507	.0790	0.0000	0.0000	0.0000	0.0000
10	.5489	.3164	.0532	0.0000	0.0000	.0191	0.0000
11	.4787	.3831	0.0000	0.0000	0.0000	.0479	0.0000
12	.1156	.6711	.0087	0.0000	.0331	.0181	0.0000
13	.0294	.5713	.0652	0.0000	.0554	.1349	0.0000
14	.0057	.1942	.2682	0.0000	.2044	.3160	0.0000
15	0.0000	.0293	.2592	.0125	.4052	.2326	.0034
16	0.0000	0.0000	.2049	.1773	.1923	.2339	.0298
17	0.0000	0.0000	0.0000	.0865	.1731	.1354	.5435
18	0.0000	0.0000	0.0000	.0638	.1595	0.0000	.6085
19	0.0000	0.0000	0.0000	0.0000	0.0000	0.0000	.2934
20	0.0000	0.0000	0.0000	0.0000	0.0000	0.0000	0.0000

EQUAL AREA LATITUDE BAND	METEOROLOGICAL CATEGORY 8	9	10	11	12	13	14
1	0.0000	0.0000	0.0000	.3237	0.0000	.5773	.0991
2	0.0000	0.0000	0.0000	.8213	0.0000	.0699	.0042
3	.0237	.0055	0.0000	.5028	.0097	.0244	0.0000
4	.1046	.0625	.0595	.1343	.0558	.0357	0.0000
5	.0424	.0350	0.0000	.1033	.0130	.1572	0.0000
6	0.0000	.0044	0.0000	.0770	0.0000	.0210	0.0000
7	0.0000	0.0000	0.0000	0.0000	0.0000	0.0000	0.0000
8	0.0000	0.0000	0.0000	0.0000	0.0000	.0319	0.0000
9	0.0000	0.0000	0.0000	0.0000	0.0000	.0857	0.0000
10	0.0000	0.0000	0.0000	0.0000	0.0000	.0624	0.0000
11	0.0000	0.0000	0.0000	0.0000	0.0000	.0903	0.0000
12	0.0000	0.0000	0.0000	0.0000	0.0000	.1534	0.0000
13	0.0000	0.0000	0.0000	0.0000	0.0000	.1438	0.0000
14	0.0000	0.0000	0.0000	0.0000	0.0000	.0115	0.0000
15	0.0000	0.0000	0.0000	0.0000	0.0000	.0578	0.0000
16	.0037	.0658	0.0000	0.0000	0.0000	.0153	0.0000
17	0.0000	.0614	0.0000	0.0000	0.0000	0.0000	0.0000
18	0.0000	0.0000	0.0000	0.0000	.1709	0.0000	0.0000
19	0.0000	0.0000	0.0000	0.0000	0.0000	.7006	0.0000
20	0.0000	0.0000	0.0000	0.0000	0.0000	0.0000	1.0000

classes in each category of climate is presented in Table G-4 and the associated wind speeds are presented in Table G-5.

In the absence of data adequate to determine an average altitude for an inversion base worldwide, the value for the Cape Kennedy area (1500 m) is applied worldwide.

G.2.2 Worldwide Demographic Summary

An extensive compilation of worldwide demographic data is presented in Reference G-1. The worldwide population data is divided into 15 population density classes presented in Table G-6. The land fraction, the total population, and the probability distribution of the population density classes within each equal area latitude band are presented in Table G-7.

An analysis of the surface type distribution for each equal area latitude band was made to determine the land and ocean fractions, and the land fraction was further broken into rock and soil fractions because of their effect on the surface impact characteristics of the space nuclear system. Worldwide ocean depth data was analyzed to determine for each latitude band the fractional distributions of the 75 m and the 500 m average ocean depths which are used in calculating the diffusion of fuel releases in the ocean. These surface fractional distributions are presented in Table G-8.

G.3 RANDOM ORBITAL DECAY PROBABILITY MODEL

The random orbital decay probability model is used to determine the probability of impacting, as a result of orbital decay and random reentry, any worldwide meteorological, demographic, or surface characteristic whose fractional distribution in each of the 20 equal area latitude bands is known.

Using spherical trigonometry, the orbit trace as a function of time is given by

$$t = \frac{1}{\omega} \left| \sin^{-1}\left(\frac{\sin\theta}{\sin\eta} \right) \right| \qquad (1)$$

where

t	=	time measured from an arbitrary zero line
ω	=	orbital angular velocity
θ	=	latitude
η	=	orbital inclination

Table G-4
PROBABILITY FOR EACH STABILITY CLASS IN EACH METEOROLOGICAL CATEGORY

METEOROLOGICAL CATEGORY	STABILITY CLASS						
	A	B	C	D	E	F	G
1	2.82E-02	9.74E-02	1.36E-01	4.42E-01	9.57E-02	1.21E-01	8.07E-02
2	3.71E-02	1.30E-01	1.89E-01	4.53E-01	9.07E-02	6.85E-02	3.27E-02
3	1.17E-02	7.48E-02	1.17E-01	5.47E-01	9.56E-02	8.01E-02	7.33E-02
4	2.87E-02	1.17E-01	1.56E-01	3.02E-01	1.37E-01	1.62E-01	9.77E-02
5	1.54E-02	8.59E-02	1.53E-01	3.56E-01	1.21E-01	1.40E-01	1.28E-01
6	1.48E-02	7.26E-02	1.32E-01	4.62E-01	9.64E-02	1.18E-01	1.04E-01
7	2.00E-02	7.97E-02	1.38E-01	4.11E-01	1.10E-01	1.30E-01	1.11E-01
8	8.89E-03	7.61E-02	1.48E-01	4.52E-01	7.95E-02	1.08E-01	1.27E-01
9	9.07E-03	5.28E-02	1.01E-01	5.87E-01	7.04E-02	9.77E-02	8.21E-02
10	1.14E-02	6.36E-02	1.15E-01	5.30E-01	8.24E-02	1.13E-01	8.39E-02
11	3.99E-03	4.08E-02	1.05E-01	6.23E-01	9.29E-02	8.58E-02	4.79E-02
12	5.89E-02	1.59E-01	1.91E-01	3.46E-01	2.78E-02	7.78E-02	1.39E-02
13	1.72E-04	2.93E-03	1.03E-02	6.40E-01	1.50E-01	1.33E-01	6.40E-02
14	0.	0.	0.	6.61E-01	1.13E-01	1.03E-01	1.23E-01

Table G-5
WIND SPEED (METERS PER SECOND) FOR EACH STABILITY CLASS IN EACH CATEGORY OF CLIMATE STABILITY CLASS

METEOROLOGICAL CATEGORY	STABILITY CLASS A	B	C	D	E	F	G
1	7.68E-02	4.41E-01	1.11E+00	5.05E+00	6.99E-01	4.54E-01	1.15E-01
2	1.12E-01	6.94E-01	1.74E+00	4.76E+00	6.83E-01	3.06E-01	5.45E-02
3	2.43E-02	2.89E-01	8.22E-01	6.98E+00	7.75E-01	3.53E-01	1.04E-01
4	6.37E-02	4.84E-01	1.13E+00	3.47E+00	1.04E+00	7.21E-01	1.41E-01
5	3.42E-02	3.70E-01	1.13E+00	4.10E+00	9.27E-01	5.91E-01	2.92E-01
6	3.09E-02	3.06E-01	8.55E-01	4.41E+00	7.06E-01	4.48E-01	1.60E-01
7	2.80E-02	3.01E-01	1.02E+00	4.47E+00	8.44E-01	5.29E-01	1.16E-01
8	1.60E-02	3.29E-01	1.14E+00	4.31E+00	6.14E-01	4.43E-01	1.19E-01
9	6.83E-03	1.70E-01	4.96E-01	5.32E+00	5.08E-01	3.62E-01	7.20E-02
10	2.48E-02	2.87E-01	7.56E-01	5.02E+00	5.69E-01	4.43E-01	9.32E-02
11	8.33E-03	1.80E-01	7.55E-01	6.59E+00	6.81E-01	3.66E-01	8.02E-02
12	5.88E-02	4.55E-01	8.58E-01	2.06E+00	1.99E-01	2.42E-01	5.98E-02
13	0.	9.85E-03	5.34E-02	7.78E+00	1.14E+00	5.76E-01	6.10E-02
14	0.	0.	0.	1.03E+01	9.54E-01	3.29E-01	6.92E-02

Table G-6
WORLDWIDE POPULATION DENSITY CLASSES

Class	Density (Persons/km^2)
1	0.00
2	1.25
3	3.75
4	7.50
5	17.5
6	37.5
7	75.0
8	175.0
9	375.0
10	750.0
11	1750.0
12	3750.0
13	7500.0
14	17500.0
15	25000.0

Table G-7
POPULATION DENSITY DISTRIBUTION FOR EACH EQUAL AREA LATITUDE BAND

EQUAL AREA LATITUDE BAND	LAND FRACTION	TOTAL POPULATION	DENSITY CLASS 1	2	3	4	5	6	7
1	.4656	30469587	0.0000	.5188	.3966	.0846	0.0000	0.0000	0.0000
2	.5850	161300755	0.0000	.2677	.2015	.2664	.1711	.0727	.0093
3	.5677	432222025	0.0000	.1705	.2000	.2717	.1108	.0832	.1010
4	.4548	543074932	0.0000	.0728	.1995	.1246	.1223	.2020	.1581
5	.4370	691722558	0.0000	.1534	.1112	.0320	.2733	.2232	.0171
6	.3971	605118210	0.0000	.3055	.1023	.0592	.1064	.0763	.1194
7	.3349	387278263	0.0000	.1748	.4190	.0062	.1102	.0353	.0748
8	.2522	199943660	0.0000	.0427	.3934	.0658	.2301	.1052	.0585
9	.2428	203931205	0.0000	.1010	.1619	.1208	.3445	.1381	.0468
10	.2150	76887239	0.0000	.3356	.1410	.2081	.1923	.0646	.0401
11	.2481	69355336	0.0000	.4490	.0796	.1406	.2148	.0742	.0314
12	.2189	132699175	0.0000	.3992	.0722	.2733	.1571	.0495	.0194
13	.2169	43233315	0.0000	.3873	.1580	.1300	.3030	.0161	.0016
14	.2480	58286844	0.0000	.6204	.0359	.0874	.2032	.0273	.0245
15	.2231	44606711	0.0000	.5891	.0067	.1774	.1202	.0997	.0070
16	.1372	37673258	0.0000	.3347	.0409	.3077	.2597	.0493	.0007
17	.0463	7506157	0.0000	.5062	.0884	.0858	.3168	0.0000	.0027
18	.0223	828162	0.0000	.8904	.0145	.0710	.0241	0.0000	0.0000
19	.0036	56392	0.0000	.9989	.0011	0.0000	0.0000	0.0000	0.0000
20	.5438	449	0.0000	1.0000	0.0000	0.0000	0.0000	0.0000	0.0000

EQUAL AREA LATITUDE BAND	DENSITY CLASS 8	9	10	11	12	13	14	15
1	0.0000	0.0000	0.0000	0.0000	0.0000	0.0000	0.0000	0.0000
2	.0082	.0005	.0022	.0004	.0000	0.0000	0.0000	0.0000
3	.0446	.0131	.0044	.0004	.0002	.0000	.0001	0.0000
4	.1050	.0128	.0025	.0002	.0000	.0001	0.0000	0.0000
5	.1179	.0671	.0032	.0009	.0002	.0004	0.0000	0.0000
6	.1741	.0510	.0054	.0002	.0001	0.0000	.0000	0.0000
7	.1591	.0089	.0113	.0000	.0003	.0000	.0000	0.0000
8	.0350	.0071	.0012	.0000	0.0000	0.0000	0.0000	0.0000
9	.0660	.0158	.0051	.0000	0.0000	0.0000	0.0000	0.0000
10	.0173	.0003	.0002	.0004	.0001	.0000	0.0000	0.0000
11	.0103	.0000	.0001	0.0000	0.0000	0.0000	0.0000	0.0000
12	.0034	.0085	.0171	.0001	0.0000	0.0000	.0001	0.0000
13	.0037	0.0000	.0001	.0002	.0001	0.0000	0.0000	0.0000
14	.0005	.0003	0.0000	0.0000	.0004	0.0000	0.0000	0.0000
15	0.0000	0.0000	0.0000	.0000	0.0000	0.0000	0.0000	0.0000
16	.0069	0.0000	0.0000	0.0000	0.0000	0.0000	.0001	0.0000
17	0.0000	0.0000	0.0000	0.0000	0.0000	0.0000	0.0000	0.0000
18	0.0000	0.0000	0.0000	0.0000	0.0000	0.0000	0.0000	0.0000
19	0.0000	0.0000	0.0000	0.0000	0.0000	0.0000	0.0000	0.0000
20	0.0000	0.0000	0.0000	0.0000	0.0000	0.0000	0.0000	0.0000

Table G-8
SURFACE TYPE DISTRIBUTIONS FOR EACH LATITUDE BAND

Latitude Band	Total Land Fraction	Ocean Surface Depth Fraction	Ocean Intermediate Depth Fraction	Land Soil Fraction	Land Rock Fraction
1	0.4739	0.1648	0.1444	0.0*	1.00*
2	0.5845	0.1247	0.0704	0.0*	1.00*
3	0.5665	0.0441	0.0452	0.749*	0.251*
4	0.4580	0.0349	0.0429	0.749	0.251
5	0.4353	0.0357	0.0290	0.847	0.153
6	0.3980	0.0312	0.0365	0.912	0.088
7	0.3391	0.0358	0.0334	0.924	0.076
8	0.2545	0.0214	0.0300	0.942	0.058
9	0.2444	0.0400	0.0368	0.923	0.077
10	0.2211	0.0400	0.0197	0.916	0.084
11	0.2500	0.0326	0.0263	0.956	0.044
12	0.2199	0.0387	0.0299	0.945	0.055
13	0.2169	0.0329	0.0200	0.915	0.085
14	0.2480	0.0128	0.0319	0.911	0.089
15	0.2231	0.0088	0.0155	0.908	0.092
16	0.1372	0.0185	0.0172	0.888	0.112
17	0.0465	0.0191	0.0256	0.704	0.296
18	0.0223	0.0172	0.0427	0.704*	0.296*
19	0.0034	0.0036	0.0115	0.0*	1.00*
20	0.5438	0.0077	0.0850	0.0*	1.00*

* Assumed Values

The period of the orbit is

$$T = \frac{2\pi}{\omega} \tag{2}$$

If it is assumed that the probability of impacting a latitude band is proportional to the fraction of time spent over that latitude band, then the cumulative probability distribution is

$$\begin{aligned} P(\theta,\eta) &= \frac{t}{0.5T} \\ &= \frac{1}{\pi}\left[\sin^{-1}\left(\frac{\sin\theta}{\sin\eta}\right)\right] \end{aligned} \tag{3}$$

Therefore, the probability density function is

$$\begin{aligned} p(\theta,\eta) &= \frac{dP(\theta,\eta)}{d\theta} \\ &= \frac{1}{\pi}\left[\frac{\cos\theta}{(\sin^2\eta - \sin^2\theta)^{\frac{1}{2}}}\right] \end{aligned} \tag{4}$$

where sin $\theta \leq$ sin η. The cumulative probability of impacting a location on the earth's surface between $-\eta$ and θ is

$$\begin{aligned} P(\theta) &= \int_{-\eta}^{\theta} p(\theta',\eta)\, d\theta' \\ &= \tfrac{1}{2}\left\{\frac{2}{\pi}\left[\sin^{-1}\left(\frac{\sin\theta}{\sin\eta}\right)\right] + 1\right\} \end{aligned} \tag{5}$$

The probability of impacting a latitude band i bounded by latitudes θ_i and θ_{i+1}

$$P_i = P(\theta_i) - P(\theta_{i+1}) \tag{6}$$

Using Eqn. (5), the probability of impacting a given worldwide meteorological, demographic, or surface characteristic k, whose fractional distribution f_{ik} in each of the 20 equal area latitude bands is known, is given by

$$\begin{aligned} P_k = \Bigg\{\Big[1 - P(\theta_{j+1})\Big] f_{jk} + P(\theta_{20-j}) f_{19-j,k} + \sum_{i=j+1}^{19-j}\Big[P(\theta_i) - P(\theta_{i+1})\Big] f_{ik}\Bigg\} x \\ (1-\delta_{j,10}) + \tfrac{1}{2}(f_{10k} + f_{11k})\delta_{j,10} \end{aligned} \tag{7}$$

where orbital inclination is in the range $\theta_{j+1} \leq \eta \leq \theta_j$ and

$\delta_{j,m}$ = Kronecker delta function

$$= \begin{cases} 1 \text{ if } j = m \\ 0 \text{ if } j \neq m \end{cases}$$

The form of f_{ik} for various characteristics of interest is presented in Table G-9. Using the data presented in Section 6.2, the probability of impacting each characteristic listed in Table G-10 as a function of orbital inclination is presented in Figures G-2 through G-6.

G.4 REFERENCES

G-1 NUS Corporation, Overall Safety Manual, Prepared by U.S. Department of Energy (1982).

Table G-9
WORLDWIDE CHARACTERISTICS OF INTEREST
IN CALCULATING RANDOM REENTRY IMPACT PROBABILITIES

Characteristic k
Land
Rock
Soil
Fresh Water
Deep Ocean
Intermediate Ocean Depth
Shallow Ocean Depth
Population Density Class j
Mean Pupulation Density
Meteorological Category j
Atmospheric Stability Class j
Mean Wind Speed

Table G-10
IMPACT PROBABILITIES OF EACH METEOROLOGICAL CATEGORY AS A FUNCTION OF ORBITAL INCLINATION (LAND PROBABILITY = 1.0)

Meteorological Category (k)	Orbital Inclination (°)									
	0°	10°	20°	30°	40°	50°	60°	70°	80°	90°
1 (Af)	0.5245	0.3213	0.1574	0.0935	0.0732	0.0594	0.0515	0.0413	0.0372	0.0361
2 (Aw)	0.4191	0.5016	0.3548	0.2094	0.1575	0.1251	0.1078	0.0860	0.0774	0.0751
3 (Bsh)	0.0335	0.0472	0.1354	0.1498	0.1239	0.0866	0.0714	0.0559	0.0499	0.0483
4 (Bsk)	0.0000	0.0000	0.0000	0.0106	0.0946	0.1330	0.0990	0.0676	0.0569	0.0543
5 (Bw)	0.0038	0.0090	0.1973	0.1884	0.1405	0.1175	0.0917	0.0704	0.0625	0.0604
6 (Caf)	0.0334	0.0368	0.1230	0.1691	0.1590	0.1138	0.0902	0.0700	0.0617	0.0596
7 (Cbf)	0.0613	0.0691	0.0263	0.0226	0.0400	0.0588	0.0550	0.0372	0.0311	0.0296
8 (Cas)	0.0000	0.0000	0.0000	0.0000	0.0379	0.0260	0.0186	0.0138	0.0120	0.0116
9 (Cbs)	0.0000	0.0000	0.0000	0.0003	0.0196	0.0122	0.0091	0.0068	0.0060	0.0058
10 (Daf)	0.0000	0.0000	0.0000	0.0003	0.0116	0.0078	0.0054	0.0481	0.0634	0.0671
11 (Dbf)	0.0000	0.0000	0.0000	0.0145	0.0454	0.1381	0.1784	0.1114	0.0886	0.0835
12 (Daw)	0.0000	0.0000	0.0000	0.0000	0.0151	0.0155	0.0101	0.0859	0.1230	0.1195
13 (Et)	0.0052	0.0026	0.0060	0.0220	0.0410	0.0769	0.1862	0.1271	0.1067	0.1023
14 (Ef)	0.0000	0.0000	0.0000	0.0000	0.0000	0.0000	0.0019	0.1604	0.2170	0.2307
Land Impact Probability	0.2315	0.2311	0.2514	0.2749	0.2654	0.2721	0.2760	0.3169	0.3348	0.3395

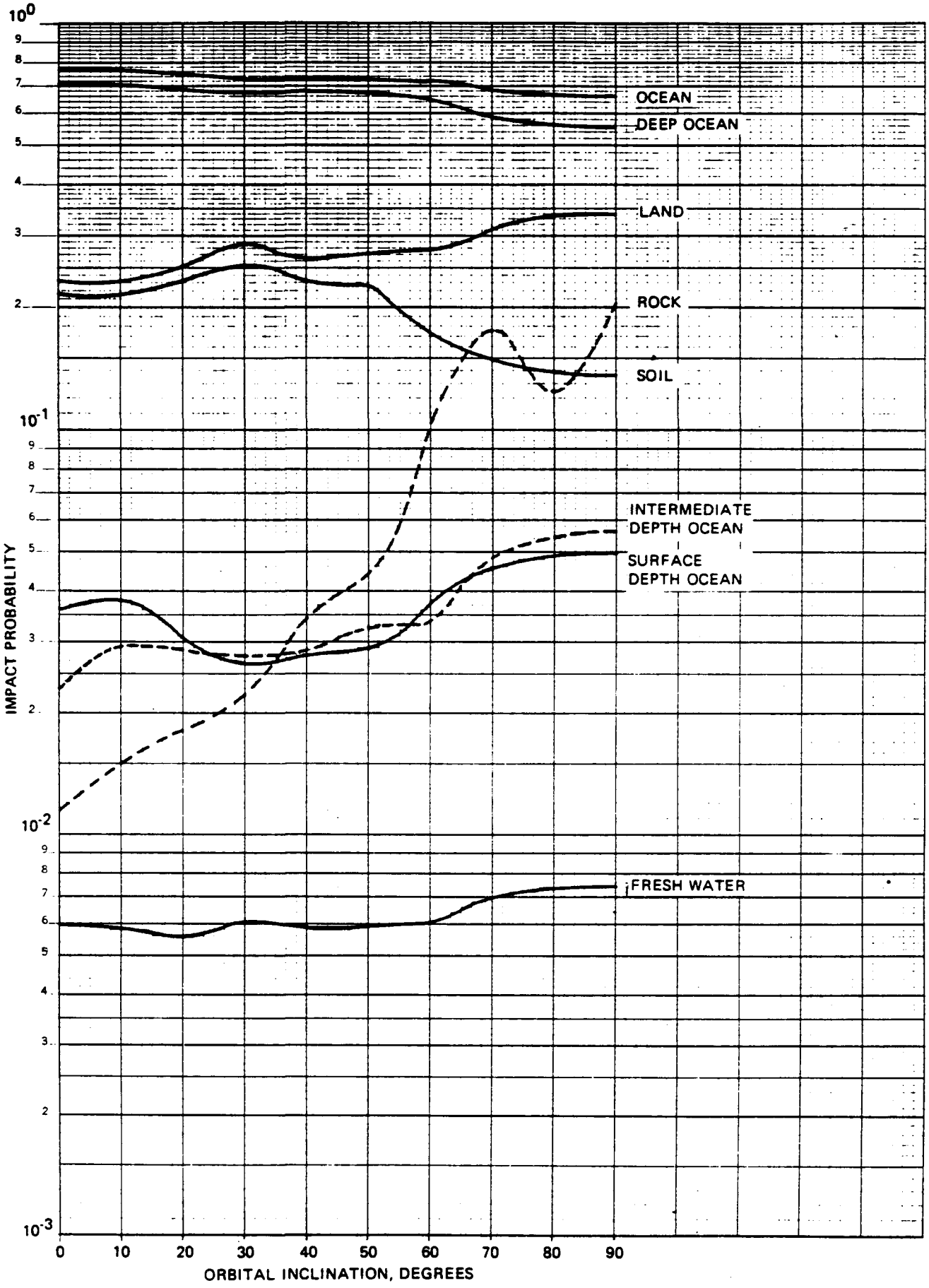

Figure G-2
RANDOM ORBITAL REENTRY IMPACT PROBABILITIES

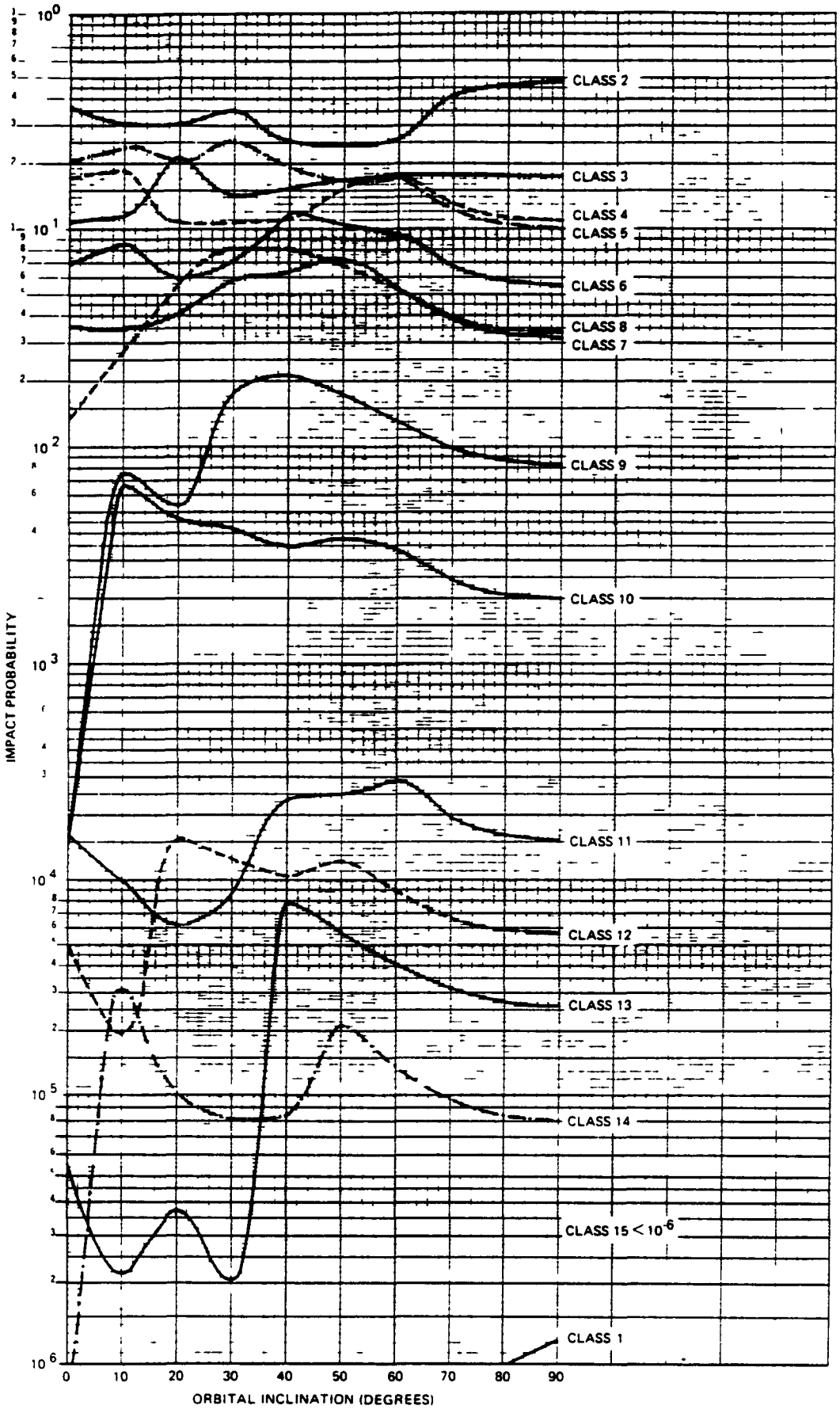

Figure G-3
IMPACT PROBABILITY OF EACH POPULATION DENSITY CLASS VERSUS ORBITAL INCLINATION (LAND IMPACT PROBABILITY = 1.0)

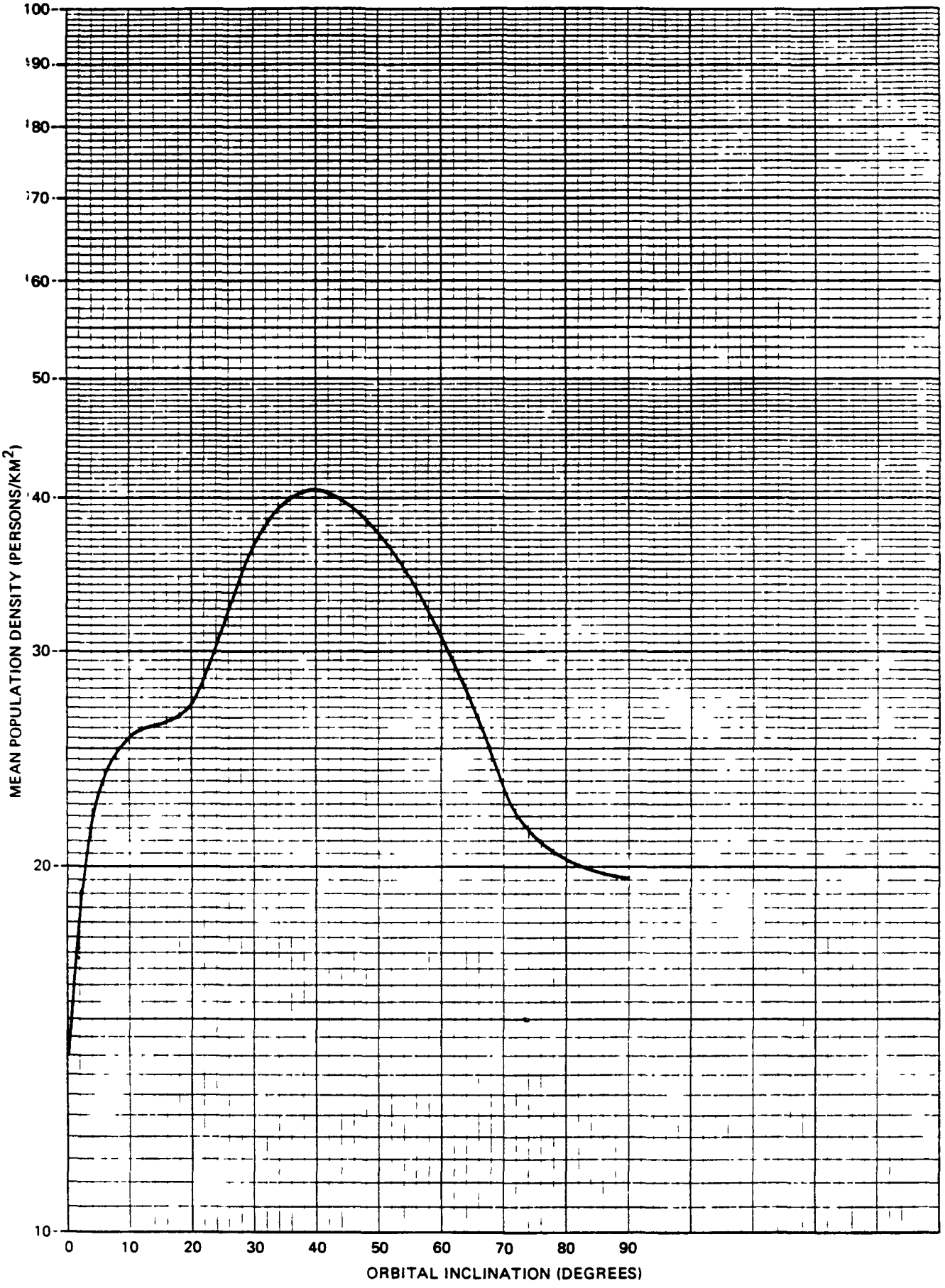

Figure G-4
EXPECTED POPULATION DENSITY IMPACTED VERSUS ORBITAL INCLINATION (LAND IMPACT PROBABILITY = 1.0)

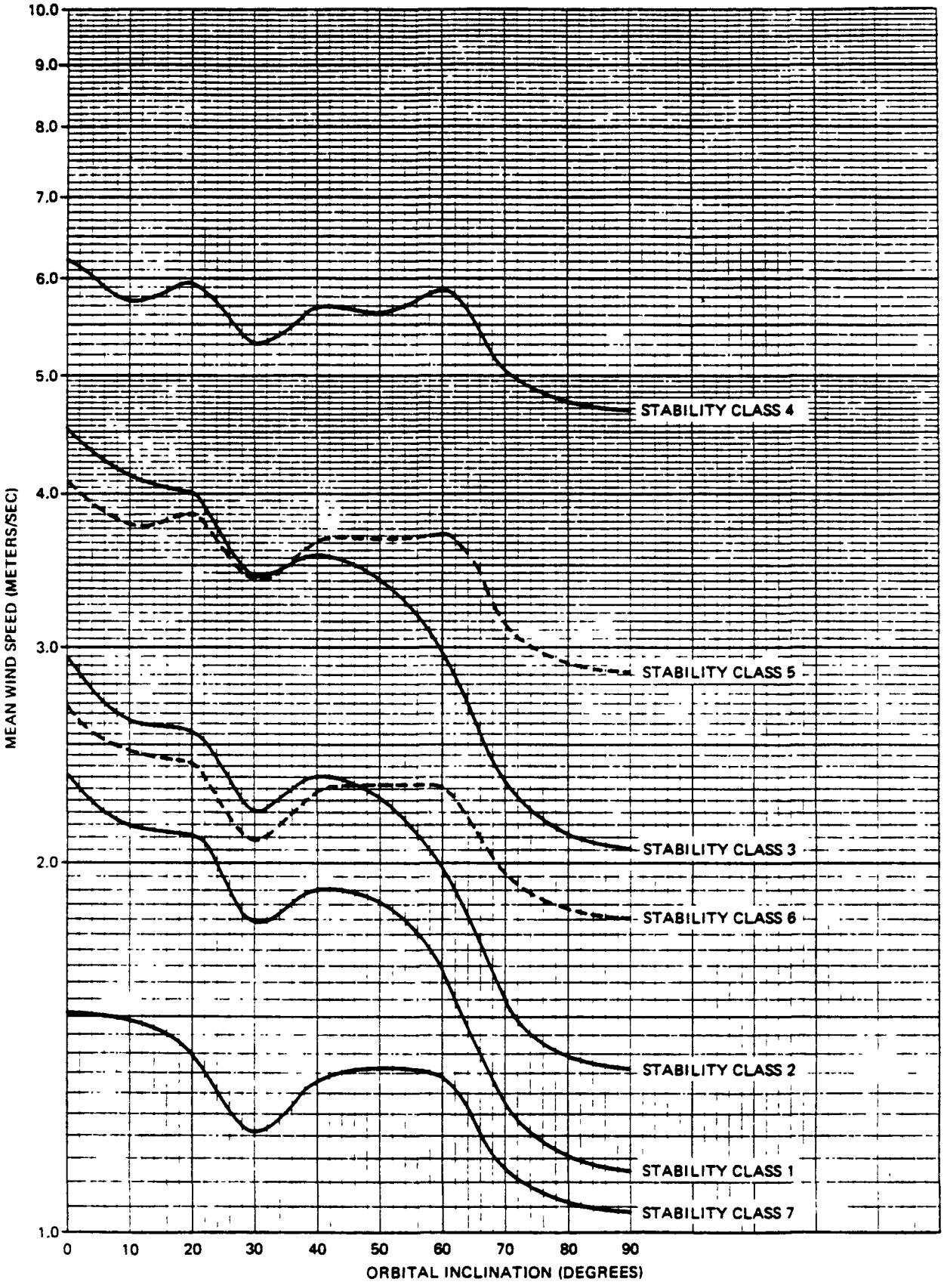

Figure G-5
EXPECTED WIND SPEED AT IMPACT VERSUS ORBITAL INCLINATION AND STABILITY CLASS (LAND IMPACT PROBABILITY = 1.00)

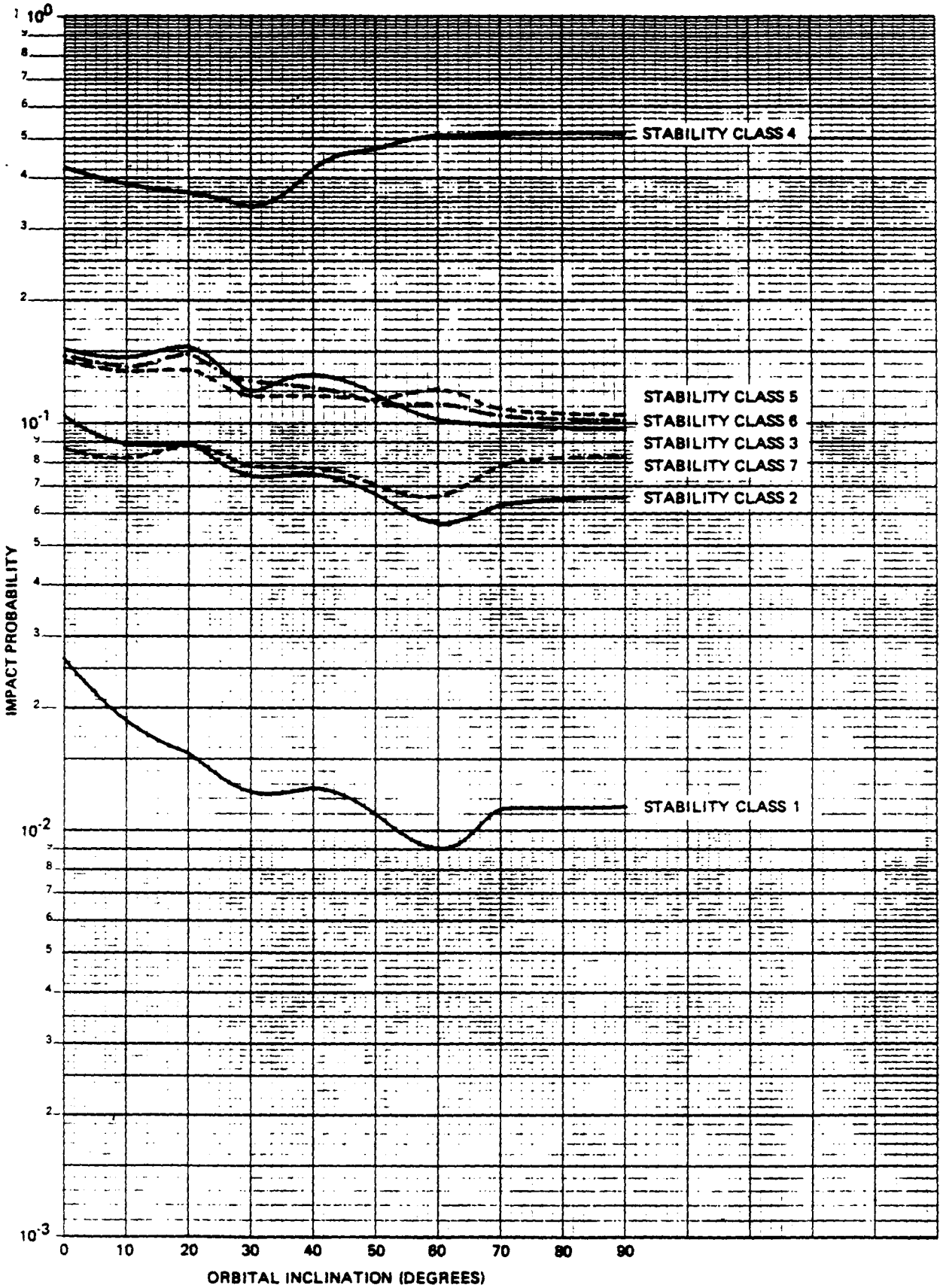

Figure G-6
STABILITY CLASS IMPACT PROBABILITY VERSUS ORBITAL INCLINATION (LAND IMPACT PROBABILITY = 1.0)

APPENDIX H

UNCERTAINTY ANALYSIS

H.1 INTRODUCTION

The radiological consequences of PuO_2 releases following postulated accidents and mission risks have been analyzed using the methodology described in Appendix A, Radiological Assessment Methodology and the results are presented in FSAR, Volume III, Nuclear Risk Analysis Document (NRAD), Book 2. The resulting radiological consequences and mission risks are dependent on characteristics of the models utilized and values selected for key model parameters. Due to the potentially large range of source term release and environmental conditions that could affect the results, an uncertainty analysis has been performed in this appendix to determine what variation from the estimated radiological consequences and mission risks might be expected.

Important parameters or conditions affecting the radiological consequences and mission risks include the following:

- Accident scenario
  - Accident environment
  - Accident probability
- Release characterization
  - Conditional source term probability
  - Source term
  - Source term modifiers
  - Particle size distribution
  - Particle size distribution modifiers
  - Initial cloud dimensions
  - Vertical source term distribution
  - Release location
- Meteorological conditions
  - Atmospheric stability
  - Wind speed and direction
  - Mixing height
  - Sea-breeze recirculation
  - Fumigation
  - Space and time variation
- Exposure pathway parameters
  - Population distribution
  - Resuspension factor
  - Deposition velocity
  - Vegetable ingestion
  - Protective action

- Radiation doses and health effects.
  - Internal dose factors
  - Health effects estimator

Potential variation in these parameters or conditions and their effect on the radiological consequences and mission risks are evaluated in the uncertainty analysis. However, the approach taken will be dependent on the type of radiological consequences under consideration which include the following:

- Short-term population dose (with and without de minimis)
- Long-term population dose (with and without de minimis)
- Surface contamination levels
- Health effects

Population dose health effects, and risk, are the primary types of results considered in the uncertainty analysis. The other measures will be discussed where appropriate, but will be considered as being of secondary importance from an uncertainty viewpoint.

Section H.1 address uncertainties in initiating accident probabilities. Section H.2 addresses uncertainties in the release characterization. Section H.3 and H.4 address uncertainties in the meteorological conditions and the exposure pathways, respectively. Section H.5 outlines the methodology used in combining uncertainty factors to arrive at the overall uncertainties. Finally, Section H.6 provides a summary of the uncertainty analysis results and estimates of the overall uncertainties associated with the estimated radiological consequences and mission risks.

H.2 ACCIDENT SCENARIOS

The accident scenarios and associated accident environments postulated for each phase of the Galileo mission were developed by NASA in the Shuttle Data Book. The probabilities for the accident scenarios were developed by NASA, Code M, in terms of probability ranges. Based on this information, GE evaluated the response of the GPHS-RTG to these accident environments and developed source terms, as documented in FSAR, Volume II, Accident Model Document (AMD). In applying the NASA-provided initiating accident probability ranges to conditional source term probabilities in order to arrive at total probabilities of release, the NASA-provided probability ranges were treated as $\pm 2\sigma$ of log-normal distributions, and the geometric means of the ranges end values were used in the AMD to compute total probabilities of release. The probability ranges, geometric means, conditional source term probabilities , and total probabilities are presented in the AMD.

Within NASA, Code Q Division independently developed a set of accident probabilities, analogous to those developed by Code M. The principal difference between the two sets of probabilities affecting the NRAD results is that the SRB mean failure probabilities in Phase 1. The SRB failure probability range as estimated by NASA Codes M and Q, when combined, result in an overall uncertainty factor range of 0.32 to 9.0.

In reviewing the NASA Code M probabilities, overall ranges in probabilities are on the order of 1 to 10. Treating the ranges as $\pm 2\sigma$ of log-normal distributions, the probability ranges about the geometric means used in the AMD are between factors of 0.32 to 3.2.

In addition to uncertainties in the accident probabilities, there are uncertainties in accident environments. The accident environments were specified in the Shuttle Data Book as distributions of conditions (such as explosion overpressure and fragment velocities). These distributions are factored into the AMD analyses discussed below, and therefore the uncertainties in the accident environments are implicit in the source term distributions determined in AMD analyses.

H.3 RELEASE CHARACTERIZATION

The release source terms for mission phase 0 and 1 accidents were predicted using the LASEP-2 program. LASEP-2 uses a Monte Carlo approach to simulate RTG response to a given accident environment. This is done using 10,000 trials for each scenario or sub-scenario considered, representing variations on accident environment severity and RTG component responses determined by probability distributions of conditions based on the accident environments defined in the Shuttle Data Book, hydrocode modeling, and component test results. The LASEP-2 model directs the calculations to arrive ultimately at Fuel Clad distortion. Correlations based on RTG component test data are then used by LASEP-2 to determine fuel clad crack size, the fuel release quantity, and particle size distribution of the release.

No uncertainty analyses has been performed on the factors within LASEP-2 which affect the source terms. However, LASEP-2 outputs a distribution of source terms for each accident scenario considered. The NRAD analyses uses the average value of the source term distribution in determining values most probable and expectation case. An estimate of the range of these distributions can be made by examining the average and maximum source terms for each accident scenario as reported in the AMD. Examining Table 3-4 of the AMD, the maximum source terms are roughly 10 times the average. Therefore, for the purpose of this uncertainty analysis, the range associated with a given average source term has been taken to be between a factor of 0.1 and 10.

Based on information presented in Appendix D related to particle size, and a review of the variability of test data related to particle size distribution, the uncertainty in results due to variability in particle size distribution is estimated to be a factor of 0.5 to 2.

Subsequent modifications to the source term and particle size distribution not considered in the NRAD results include 1) retention by graphitics or other materials; 2) agglomeration within the fireball, tending to increase effective particle size; 3) erosion by a high flux of particles within the fireball, tending to decrease particle size; and 4) wash-out by plume condensation or rain. Except for erosional effects within the fireball, these effects tend to increase ground concentrations of 238-PuO_2 in the near field (within 5 km), and decrease population exposure in the far-field. Due to those factors, the near field ground concentration are judged to be underestimated by a factor of 2, and the near- and far-field doses and the far-field ground concentrations are judged to be overestimated by a factor of 2. The overall effect of agglomeration is to reduce particulate dispersion and associated areas. The surface areas where contamination levels exceed $0.2\mu Ci/m^2$ are judged to be reduced by a factor of 0.75.

The retention factor associated with the graphitics and other materials is assumed to be between 0.25 and 1.0. The uncertainty analyses assumes the geometric mean of the range for the retention factor, which is 0.5.

The radiological consequences will be sensitive to the release height, initial cloud size, and the vertical distribution of released fuel in the plume. The plume configuration used for the most probable and maximum cases has been described in Section A.2 of Appendix A. However, large initial cloud sizes resulting from the fireball tend to dampen the effect of release height, since material is more spread out in the vertical. The release height and initial cloud size are judged to be uncertain to the extent that the resulting radiological consequences uncertain by a factor ranging from 0.5 to 2.

The vertical distribution of material within the plume for launch area fireball releases was taken to be 80 percent in the cloud and 20 percent in the stem, spread in a Gaussian manner. The particle size distribution within the plume was taken to be homogeneous, and no particle stratification was assumed (i.e., larger particles predominately lower in the plume than smaller particles). However, the atmospheric dispersion model used in evaluating the launch area releases, FSAR-EMERGE, does account for center of mass trajectories of particle size groups resulting from the horizontal wind vector and the vertical terminal fall velocity vector. In order to evaluate how the model treats the various particle size groups, the plume configuration for the Phase 1 maximum case was tracked with time following the initial release, as a function of particle size.

The results were presented in of Appendix D. The results indicate that particle stratification within the plume is rapidly established within 1 km, well before the cloud has travelled one cloud diameter downwind. Therefore, assuming that the particle size distribution is initially homogeneous, or that there initially is particle stratification, does not significantly affect the results. The model allows particle stratification to rapidly develop. Hence, no uncertainty factor is assigned to particle stratification within the plume.

H.4 METEOROLOGICAL CONDITIONS

The atmospheric transport and dispersion model used for launch area accidents in Phases 0 and 1 was the FSAR-EMERGE model. FSAR-EMERGE treats meteorology that varies in time and space (vertically), and accounts for vertical plume configuration; particle-size-dependent transport, deposition, and plume depletion; and sea-breeze recirculation. As described in Section A.2.1 of Appendix A, in applying FSAR-EMERGE to releases in Phases 0 and 1, 42 sets of 24-hour historical meteorological data sequences (in 96 15-minute time steps) were selected as being representative of the 50-day launch window during October-November. The expectation case source term for each of Phases 0 and 1 was modeled using KSC-EMERGE and each of the 42 sequential data sets (i.e., 42 KSC-EMERGE runs for each expectation case). The distribution of results, presented as Tables A-2 and A-3 in Appendix A, reflect the result of variations over the following meteorological conditions:

- Atmospheric stability class
- Wind speed and direction
- Mixing height
- Sea-breeze recirculation
- Fumigation
- Space and time variations

In addition, the results also reflect variations in population and surface-type distributions in the KSC vicinity.

Treating the distributions of results as uncertainties in these factors, and using Phase 1, expectation case results for the distributions as presented in Table A-3 of Appendix A, the uncertainty ranges presented in Table H-1 are established for the collective factors identified above. Similar uncertainties are assumed to hold for worldwide locations in phases 2, 3, 4, and 5.

H.5 EXPOSURE PATHWAY, DOSE, AND HEALTH EFFECTS

The exposure pathways considered in the radiological consequence analysis include short-term exposures (direct inhalation during plume passage) and long-term exposures.

TABLE H-1

Uncertainty Factor Ranges Due to Variations in Meteorological Factors

Radiological Consequence Type	Normalized Mean Value[a]	Uncertainty Range[b]
Population Dose		
Short-term	1.0	0.32-3.1
Long-term	1.0	0.12-8.0
Area with Deposition Above 0.2 $\mu Ci/m^2$		
Dry Land	1.0	0.50-2.0
Swamp	1.0	0.36-2.8
Inland Water	1.0	0.43-2.3
Ocean	1.0	0.27-3.7

a. Represents the geometric mean of the range.

b. The low end of these ranges actually extend to zero. However, they have been arbitrarily set equal to the reciprocal of the upper range. This allows the distribution to be treated as log-normal later in the analysis.

Parameters affecting short-term doses, beyond the factors discussed in Section H-4, include the breathing rate and the internal dosimetry model parameters discussed in Appendix A. The doses calculated using the internal dose model are judged to be uncertain by a factor of 2 due to uncertainties in actual breathing rates, inhalability of particulates, deposition of particulates in the respiratory system, and transfer parameters used in the model.

Secondary exposure pathways potentially could include inhalation of resuspended material, ingestion of contaminated food (vegetables and seafood), and external exposure to ground deposited material.

The doses resulting from inhalation of resuspended material account for approximately 75 percent of the long-term doses resulting from launch area releases. The resuspension doses are based on a resuspension factor of 10^{-5} that decreases to 10^{-9} over two years. Furthermore, particles subject to resuspension have been restricted to those physical diameters of 30 μm and less. Due to variability in actual environmental conditions affecting resuspension, the doses due to resuspension are judged to be uncertain by a factor ranging from 0.1 to 10.

The external doses are several orders of magnitude lower than the other land based long-term doses. No uncertainty factor is assigned to external doses, since even a large uncertainty would not affect the results significantly.

The possible ingestion pathways will be limited by the very insoluble nature of PuO_2. Since drinking water supplies in the KSC region are obtained from deep aquifers, no contamination by PuO_2 releases is postulated. For fuel releases to the ocean or inland waters, the ingestion of contaminated fish or seafood has been considered based on a K_D of 10^{-5} and a density of caught seafood of 1.2×10^{-8} g/cm^3 yr. The K_D of 10^{-5}, representative of plutonium in actual aquatic environments, results in higher water concentrations than would dissolution rates of PuO_2 particles determined by LANL under laboratory conditions. Hence, seafood ingestion may be overestimated. However, since seafood ingestion doses are so low, they could be uncertain by several orders of magnitude up or down without affecting the results. Therefore, no uncertainty factor has been assigned.

The ingestion of vegetables contaminated by direct PuO_2 fallout has been considered based on a 14 day removal half-time for leaf deposited material and a bioaccumulation factor of 2.5×10^{-4}. The calculations are conservative since it was assumed that 1) no protective measures were taken to ban vegetables from consumption in affected areas, and 2) all persons in affected areas were assumed to obtain their entire annual usage of vegetables (285 kg for adults) from a local garden. These assumptions are judged to result in an overestimated of

ingestion doses, accounting for approximately 25 percent of the long-term doses, by a factor of 2.

The health effects resulting from a given calculated population dose has been based on an evaluation of health effects models as described in Appendix B. Due to differences in various health effects models, the resulting estimated health effects are judged to be uncertain by a factor ranging from 0.5 to 2.

The discussion in this section up to this has focused primarily uncertainties in NRAD results for launch area accidents in mission phases 0 and 1. However, the same ranges of uncertainty factors would be expected to occur in mission phases 2 through 5.

H.6 COMBINING UNCERTAINTIES

The uncertainty factors resulting from consideration of accident probabilities release characterization, meteorological conditions, and exposure pathway parameters are summarized in Table H-2. Based on these uncertainty factors, the overall uncertainty associated with various types of radiological consequences and mission phase risk must be determined.

In assessing the overall uncertainty, a methodology is required that combines the uncertainties in each uncertainty area. In developing this methodology, first consider the meaning of the uncertainty factors developed in Section H-5. As an example, if the uncertainty factor is in the range of 0.1 to 10, the mean uncertainty factor is taken as the geometric mean of the range which is 1.0. Furthermore, the uncertainty factor range of 0.1 to 10 is treated as a log-normal distribution with a mean of log (1) = 0 and $\pm$ 2σ values of log (0.1) = -1 and log (10) = 1. The log-normal distribution represents the probability of having a given uncertain factor, with a total probability of approximately 0.95 that the log of the uncertainty factor is between the $\pm$ 2σ limits.

In determining overall uncertainties in results, the log-normal distributions of the individual uncertainty factor ranges were combined,such that the overall mean uncertainty factor was taken as the product of the individual mean uncertainty factors affecting the result type. The standard deviation of the log-normal distribution representing the overall range was determined by square root of the sum of the squares of the standard deviations of the individual ranges.

H.7 UNCERTAINTY ANALYSIS RESULTS

Based on the methodology outlined above, the resulting overall mean uncertainty factors and associated ranges are summarized in Table H-3. The uncertainty factors represent multipliers that should be applied to the results presented in the NRAD.

Table H-2 Radiological Consequences and Risk Analysis Uncertainty Factors

Area of Uncertainty	Uncertainty Factor[a]	Result Type Affected
• Accident scenarios		
- Accident probabilities	0.32 - 9.0	Mission Phase 1 risk
	0.32-3.2	Mission phase risk (Phases 0, 2, 3, 4, and 5)
• Release characterization		
- LASEP-2 source term Distribution	0.1-10	Radiological consequences (Phases 0 and 1)[b]
- Graphitics retention	0.25 - 1	All types and phases[c]
- Particle size distribution	0.5-2	Radiological consequences (all phases)[b]
- Particle size distribution modifiers	2	Near field surface concentrations for all cases[c,d]
	0.5	All doses and far field surface concentrations[c,e]
	0.75	Areas exceeding specified contamination areas (all cases).[c]
- Release height and cloud size	0.5-2	Radiological consequences[b]
- Particle stratification in plume	1	All types
• Meteorological conditions	(See Table H-1)	Radiological consequences[b]

Table H-2 Radiological Consequences and Risk Analysis Uncertainty Factors (continued)

Area of Uncertainty	Uncertainty Factor[a]	Result Type Affected
• Exposure pathway parameters		
- Resuspension	0.1-10	75 percent of long-term doses[c]
- Vegetable ingestion	0.5	25 percent of long-term doses[c]
- Internal dose factors	0.5-2	All doses[c]
- Health effects estimator	0.5-2	Health effects[c]

a. The uncertainty factor is used as a multiplier of the result type affected.
b. The expectation case results are unaffected, since the distribution is taken into consideration in development of the expectation case. The uncertainty range reflects the range of possible radiological consequences that determine the expectation case results.
c. This represents a systematic bias affecting all cases.
d. Near field - less than 5 km from pad
e. Far field - greater than 5 km from pad

Table H-3 Overall Uncertainty Analysis Results

Result Type	Overall Uncertainty Factor	
	Mean[a]	Range[b]
• Radiological consequences[a]		
- Short-term population dose	0.25	0.013 - 4.6
- Long-term population dose	0.22	0.0042 - 1.4
- Total population dose	0.23	0.0067 - 7.9
- Health effects	0.23	0.0063 - 8.5
- Surface contamination area	0.75	0.051 - 5.2
• Mission phase risk[b]		
Phase 1		
- Short-term population dose	0.42	0.061 - 2.9
- Long-term population dose	0.37	0.024 - 5.7
- Total population dose	0.39	0.035 - 4.3
- Health effects	0.39	0.032 - 4.8
- Surface contamination area	1.3	0.22 - 7.8
Phases 0, 2-5		
- Short-term population dose	0.25	0.55 - 1.1
- Long-term population dose	0.22	0.019 - 2.5
- total population dose	0.23	0.029 - 1.8
- Health effects	0.23	0.026 - 2.0
- Surface contamination area	0.75	0.20 - 2.9

a. The mean uncertainty factor for radiological consequences multiplies the expectation case results in the NRAD to yield a best estimate of the expectation case results. The best estimate result for the expectation case should the be multiplied by the uncertainty factor range to yield a best estimate of the 5- and 95-percentile values of the range of radiological consequences that feed into the best estimate for the expectation case results.

b. The mean uncertainty factor for mission phase risk multiplies the mission phase risk results reported in the NRAD to yield a best estimate of mission phase risk (defined as total probability times expectation case results). The best estimate result for mission phase risk should then be multiplied by the uncertainty factor range to yield a best estimate of the 5- and 95-percentile values of the best estimate for the mission phase risk.